Mechanisms of drug response and resistance in *Giardia duodenalis*

Brendan Robert Edward Ansell

Submitted in total fulfillment of the requirements of the degree of
Doctor of Philosophy

March 2017

Faculty of Veterinary and Agricultural Sciences,
University of Melbourne

Abstract

'Metronidazole-susceptible Giardia *are all alike; every resistant line is resistant in its own way.'*

— Ansell, with apologies to Tolstoy

Giardia duodenalis is a parasitic protist and the most common intestinal parasite of humans, causing 200-300 million cases of diarrhoeal disease annually. Metronidazole is a widely administered anti-giardial drug, but treatment failure is relatively common, attributed in part to metronidazole resistance in the infecting parasites. This drug enters parasitic cells as a pro-drug, which is activated to cytotoxic intermediate forms via oxidoreductase enzymes in the parasite's antioxidant system. Metronidazole-resistant lines — defined here as those that exhibit significantly greater tolerance to the drug *in vitro* compared to wild-type cells, show perturbed transcription and activity of various oxidoreductase enzymes. However inconsistencies in these features suggest that yet-undiscovered genes and biochemical mechanisms may also contribute to resistance. Progress in understanding the biology of resistance, and of *Giardia* in general, is further hampered by a lack of functional information for around half of the proteins encoded in the genome.

Therefore in this work, high-throughput protein structure prediction was used to attribute putative functions to hypothetical proteins in *Giardia*, and over-expression of as yet uncharacterized oxidoreductase enzymes was found to increase parasite tolerance to metronidazole. RNA sequencing was used to profile transcriptional changes in parasites over time under standard culture conditions, and in response to sub-lethal concentrations of metronidazole, hydrogen peroxide and thermal stress. Genetically controlled investigation of transcriptional changes in three drug-resistant parasite lines relative to their susceptible parent lines, revealed down-regulation of drug-activating enzymes and of genes that function proximal to pyruvate:ferredoxin oxidoreductase – a nexus of glycolysis and electron transport systems. Changes specific to each resistant line suggested that active drug detoxification and efflux systems may also contribute to metronidazole resistance. In all, this work provides substantial insight into mechanisms of response and resistance to a vital treatment for a major global pathogen.

Declaration

This is to certify that

- the thesis comprises only my original work towards the PhD except where indicated in the Preface,
- due acknowledgement has been made in the text to all other material used,
- the thesis is fewer than 100,000 words in length, exclusive of tables, bibliographies and appendices

Brendan Robert E. Ansell

Preface

The work in this thesis was undertaken at the Faculty of Veterinary and Agricultural Sciences, University of Melbourne, and the Walter and Eliza Hall Institute of Medical Research in the laboratories of A/Prof Aaron Jex and Prof Robin Gasser, and at the Department of Cell & Molecular Biology, Uppsala University, in the laboratory of Prof Staffan Svärd. Stipend support was provided through the Australian Post-graduate Award, the Victorian Life Sciences Computation Initiative, and the Faculty of Veterinary and Agricultural Sciences, University of Melbourne. Travel support was provided by the Overseas Research Experience Scholarship (University of Melbourne), the Dr Sue Newton Travel Award (Faculty of Veterinary and Agricultural Sciences), and the JD Smythe Travel Award (Australian Society for Parasitology).

Publications appear in part and in wholly original format in this thesis. My contribution to these publications is as follows.

Chapter 1: 90%
Chapter 5: 90%
Chapter 6: 90%
Chapter 7: 90%

I acknowledge the contributions of the following individuals to the work in this thesis, as declared in collaborator authorization forms.

Chapter 1. Adapted in part from Ansell et al., 2015, *Biotechnology Advances*
Prof Malcolm McConville Critiqued manuscript
Dr Showgy Ma'ayeh Critiqued manuscript and provided foundational material for Figure 1.1
Dr Michael Dagley Critiqued manuscript
Prof Robin Gasser Critiqued manuscript
Prof Staffan Svärd Critiqued manuscript
A/Prof Aaron Jex Critiqued and helped to structure manuscript

Chapter 5. Ansell et al., 2015, *PLoS Neglected Tropical Diseases*
Prof Malcolm McConville Critiqued manuscript
Dr Louise Baker Assisted with experimental design and optimized cell culture
Dr Pasi Korhonen Provided scripts for bioinformatic analyses and statistical advice
Dr Neil Young Provided scripts for bioinformatic analyses and statistical advice
Mr Ross Hall Provided scripts for bioinformatic analyses
Dr Cristian Alvarez Rojas Assisted with sample generation
Prof Staffan Svärd Critiqued manuscript and provided additional genetic functional information
Prof Robin Gasser Critiqued manuscript
A/Prof Aaron Jex Assisted with experimental design and critiqued manuscript

Chapter 6. Ansell et al., 2016, *Antimicrobial Agents and Chemotherapy*
Prof Malcolm McConville Critiqued manuscript
Dr Louise Baker Assisted with experimental design and sample generation
Dr Pasi Korhonen Provided scripts for bioinformatic analyses
Dr Samantha Emery Critiqued manuscript
Prof Staffan Svärd Critiqued manuscript
Prof Robin Gasser Critiqued manuscript
A/Prof Aaron Jex Assisted with experimental design and critiqued manuscript

Chapter 7. Ansell et al., 2017, *Frontiers in Microbiology*
Dr Louise Baker Assisted with experimental design and sample generation
Dr Samantha Emery Critiqued manuscript and provided additional cell lines
Prof Malcolm McConville Critiqued manuscript
Prof Staffan Svärd Critiqued manuscript
Prof Robin Gasser Critiqued manuscript
A/Prof Aaron Jex Assisted with experimental design and critiqued manuscript

Chapter 3.
Prof. Wang Zhang (MIT) generously provided an academic license for I-TASSER
Prof Robin B Gasser assisted with licensing I-TASSER
Dr Pasi K Korhonen provided assistance running InterProScan and orthoMCL
Mr Ross S Hall assisted with implementing I-TASSER
Victorian Life Sciences Computation Initiative staff assisted with implementing I-TASSER

Chapter 4.
Dr Luboš Voleman Assisted with cloning for experiments
Dr Elin Einarsson Cloned and transfected parasite lines used as controls
Mr Ásgeir Ástvaldsson Assisted with cloning and transfection for experiments
Dr Jon Jerlström-Hultqvist Provided reagents and technical advice for experiments
Dr Showgy Ma'ayeh Performed IC_{50} assays and microscopy
Ms Karin Sköld Assisted with IC_{50} assays

General contributions
Dr Saskia Freytag Provided statistical advice
Mr Andreas Stroehlein Provided scripts for bioinformatic analyses
Mr Stefano Mangiola Provided scripts for bioinformatic analyses

Acknowledgements

The opportunity to embark on a PhD is a fantastic privilege— a confluence of good luck, hard work, and some measure of naivety. Although the PhD is now essentially a pre-requisite for a career in science, I have long viewed it as an opportunity to explore, and ideally to defy the perceived limits of one's potential. This body of work is the culmination of that personal and intellectual journey, which has plumbed some emotional nadirs but mostly yielded deep satisfaction as challenges were overcome and insight gained on a daily basis. It has been an utterly engrossing and fulfilling PhD project for which I must firstly thank A/Prof Aaron Jex, whose academic guidance, support, optimism and trust in my capability allowed me to venture into so many aspects of biological and computer science— from protein structure analysis to automated imaging, and deep sequencing to reverse genetics. Aaron it has been great to work on this project under your guidance, and to see your success in establishing your lab.

To Dr Louise Baker, you have been a fantastic colleague and friend from the conception of this project. Thank you for being so accommodating and positive, day-in and day-out. I also thank Prof Robin Gasser for hiring me at the Vet faculty, and then encouraging me to work on a transcriptomics project via which I could begin learning the skills that I applied during the PhD. Prof Jean-Peirre Scheerlinck has been a most supportive mentor and chair of my PhD committee. Thank you for squeezing me into your packed supervision roster, and for generously allowing us to use your lab space! Prof Malcolm McConville generously included me in his lab meetings and provided great insight into experimental design and the fundamental biology of *Giardia*. Thank you Malcolm. Thank you also to Prof Staffan Svärd for organizing accommodation and hosting me in the lab at Uppsala University in Sweden, where I conducted reverse genetics experiments. It was wonderful to work and party with an entire lab of disciples of the 'poop parasite.' To Dr Neil Young and Dr Pasi Korhonen, I can't thank you enough for your willingness to field questions, at any time, from the painful minutia of coding problems to broad issues of experimental design and statistics. I will not forget your generosity and receptiveness, despite your formidable workloads. Thanks also to Ross Hall, for whom no request was too big or small, and whose scripts allowed me to wade beyond my depth in the early days. I thank the Australian Society for Parasitology and the team at GiardiaDB for supporting and my work and helping to publicize the data. To my neighbours in the cave at Vet Science, Sarah, Cla[i]r[e]s Kaufman and Anstead, Bert, Stefano, Tom and Evan, and Sam E and Nijoy at WEHI, thank you for your delightful company, consolation and camaraderie. To the other Vet research students, especially Andreas, Paola, Alistair, Mauricio, Jana and Reza, thank you for your friendship and positivity. May we all graduate soon. To the fantastic team in Uppsala, especially Elin, Showgy, Luboš, Ulf, Bork, Livia, Asgeir, Dimitra, Jon and Feifei: thanks for welcoming me into the lab and into your lives, and for your generosity with technical assistance and reagents. Would that I could have stayed longer! I would like to pay particular tribute to my very close friends and some-time mentors Kevin Placek and Dominic Dwyer. Kev, our Friday lunch fixture was generally the highlight of my week, a chance to catch up and to revel in topics far from science, for which everything else could wait. Your determination and perseverance is simply indomitable, an inspiration. Dom, the importance of our conversations when I was just starting in science is still revealing itself to me. Your encouragement set me on this path, and your insight and integrity are the marks to which I aspire. To Matto, we have led

parallel lives to this point. Your friendship, caustic wit and casual intellectual brilliance over so many loose nights out and contrite breakfasts, has sustained me. Marra, you saved me from a hovel and shepherded me into the best share house I've ever lived in. Your unbridled enthusiasm, love of a terrible gag, fine taste in puerile television, and culinary prowess made those Page St days simply fantastic. To my great house-mates Gil, Leena and Felicity, music buddies Don, Terry, Keaney and Eds Smith and Sharp-Paul, and breakfast bud Bridie. Thanks for your great friendship and support. Finally I thank my wonderful parents, my sister Tess, grandparents and extended family who have supported me in so many ways throughout my protracted student life. And to my amazing partner ViAnh, I can't imagine how I would have made it through the PhD and everything in between without your incredible love and support. Thank you.

Personal bibliography

Brendan R E Ansell, Louise Baker, Samantha J. Emery, Malcolm J. McConville, Staffan G. Svärd, Robin B. Gasser, Aaron R. Jex. Transcriptomics indicates active and passive metronidazole resistance mechanisms in three seminal *Giardia* lines. *Frontiers in Microbiology* 02/2017; 8(398). DOI: 10.3389/fmicb.2017.00398

Brendan R E Ansell, Malcolm J McConville, Louise Baker, Pasi K Korhonen, Samantha J Emery, Staffan G Svärd, Robin B Gasser, Aaron R Jex. Divergent transcriptional responses to physiological and xenobiotic stress in *Giardia duodenalis*. *Antimicrobial Agents and Chemotherapy* 07/2016; 60(10). DOI: 10.1128/AAC.00977-16

Brendan R E Ansell, Malcolm J McConville, Louise Baker, Pasi K Korhonen, Neil D Young, Ross S Hall, Cristian A A Rojas, Staffan G Svärd, Robin B Gasser, Aaron R Jex. Time-Dependent Transcriptional Changes in Axenic *Giardia duodenalis* Trophozoites. *PLoS Neglected Tropical Diseases* 12/2015; 9(12). DOI: 10.1371/journal.pntd.0004261

Brendan R E Ansell, Malcolm J McConville, Showgy Y Ma'ayeh, Michael J Dagley, Robin B Gasser, Staffan G Svärd, Aaron R Jex. Drug resistance in *Giardia duodenalis*. *Biotechnology Advances* 04/2015; 33(6 Pt 1). DOI: 10.1016/j.biotechadv.2015.04.009

Brendan R E Ansell, Dominic B Dwyer, Stephen J Wood, Emre Bora, Warwick J Brewer, Tina M Proffitt, Dennis Velakoulis, Patrick D Mcgorry, Christos Pantelis. Divergent effects of first-generation and second-generation antipsychotics on cortical thickness in first-episode psychosis. *Psychological Medicine* 02/2014; 45(3). DOI: 10.1017/S0033291714001652

Brendan R E Ansell, Manuela Schnyder, Peter Deplazes, Pasi K Korhonen, Neil D Young, Ross S Hall, Stefano Mangiola, Peter R Boag, Andreas Hofmann, Paul W Sternberg, Aaron R Jex, Robin B Gasser. Insights into the immuno-molecular biology of *Angiostrongylus vasorum* through transcriptomics—Prospects for new interventions. *Biotechnology Advances* 07/2013; 31(8). DOI: 10.1016/j.biotechadv.2013.07.006

Sarah Preston, Pasi K Korhonen, Laurent Mouchiroud, Matteo Cornaglia, Sean L Mcgee, Neil D Young, Rohan A Davis, Simon A Crawford, Cameron J Nowell, Brendan Robert E Ansell … Robin B Gasser. Deguelin exerts potent nematocidal activity via the mitochondrial respiratory chain. *The FASEB Journal* 07/2017; in press. DOI: 10.1096/fj.201700288R

Cristian A. Alvarez Rojas, Jean-Pierre Scheerlinck, Brendan R E Ansell, Ross S Hall, Robin B Gasser, Aaron R Jex. Time-Course Study of the Transcriptome of Peripheral Blood Mononuclear Cells (PBMCs) from Sheep Infected with *Fasciola hepatica*. *PLoS ONE* 07/2016; 11(7). DOI: 10.1371/journal.pone.0159194

Wai-Hong Tham, Nicholas T Y Lim, Greta E Weiss, Sash Lopaticki, Brendan R E Ansell, Megan Bird, Isabelle Lucet, Dominique Dorin-Semblat, Christian Doerig, Paul R Gilson, Brendan S Crabb, Alan F Cowman. *Plasmodium falciparum* Adhesins Play an Essential Role in Signalling and Activation of Invasion into Human Erythrocytes. *PLoS Pathogens* 12/2015; 11(12). DOI: 10.1371/journal.ppat.1005343

Cristian A Alvarez Rojas, Brendan R E Ansell, Ross S Hall, Robin B Gasser, Neil D Young, Aaron R Jex, Jean-Pierre Y Scheerlinck. Transcriptional analysis identifies key genes involved in metabolism, fibrosis/tissue repair and the immune response against *Fasciola hepatica* in sheep liver. *Parasites & Vectors* 12/2015; 8(1). DOI: 10.1186/s13071-015-0715-7

Clare A Anstead, Pasi K Korhonen, Neil D Young, Ross S Hall, Aaron R Jex, Shwetha C Murali, Daniel ST Hughes, Siu F Lee, Trent Perry, Andreas J Stroehlein, Brendan R E Ansell, Bert Breugelmans, Andreas Hofmann et al. *Lucilia cuprina* genome unlocks parasitic fly biology to underpin future interventions. *Nature Communications* 06/2015; 6. DOI: 10.1038/ncomms8344

Bert Breugelmans, Brendan R E Ansell, Neil D Young, Parisa Amani, Andreas J Stroehlein, Paul W Sternberg, Aaron R Jex, Peter R Boag, Andreas Hofmann, Robin B Gasser. Flatworms have lost the right open reading frame kinase 3 gene during evolution. *Scientific Reports* 05/2015; 5(5). DOI: 10.1038/srep09417

Sarah Preston, Abdul Jabbar, Cameron Nowell, Anja Joachim, Baerbel Ruttkowski, Jonathan Baell, Tony Cardno, Pasi K Korhonen, David Piedrafita, Brendan R E Ansell, Aaron R Jex, Andreas Hofmann, Robin B Gasser. Low cost whole-organism screening of compounds for anthelmintic activity. *International Journal for Parasitology* 03/2015; 45(5). DOI: 10.1016/j.ijpara.2015.01.007

Aaron R Jex, Anson V Koehler, Brendan R Ansell, Louise Baker, Harin Karunajeewa, Robin B Gasser. Getting to the guts of the matter: The status and potential of 'omics' research of parasitic protists of the human gastrointestinal system. *International journal for parasitology* 07/2013; 43(12-13). DOI: 10.1016/j.ijpara.2013.06.005

Cali F Bartholomeusz, Sarah L Whittle, Alice Montague, Brendan Ansell, Patrick D McGorry, Dennis Velakoulis, Christos Pantelis, Stephen J Wood. Sulcogyral patterns and morphological abnormalities of the orbitofrontal cortex in psychosis. *Progress in Neuropsychopharmacology and Biological Psychiatry* 02/2013; 44. DOI: 10.1016/j.pnpbp.2013.02.010

Abbreviations

%	Percent
° C	Degrees Celsius
ATP	Adenosine triphosphate
DNA/RNA	Deoxy-/ribose nucleic acid
bp	Base pairs
nt	Nucleotides
mL	Millilitre
µL	Microlitre
nM	Nanomolar
mmol	Nanomoles
PBS	Phosphate-buffered saline
BSA	Bovine serum albumin
v/v	Volume per total volume
min	Minute
sec	Second
h	Hour
IC_{50}	Half-maximal inhibitory concentration

Table of Contents

Abstract i

Declaration ii

Preface iii

Acknowledgements v

Personal bibliography vii

Abbreviations ix

Chapter 1. Literature Review 1

- **Disease burden** 2
- **Life cycle** 2
- **Taxonomy and zoonotic potential** 3
- ***Giardia* culture systems** 4
  - Experimental infection 4
  - Co-culture and axenic culture 4
- **Genome and transcription** 5
- **Giardia-specific gene families** 6
  - NEK kinases and type E annexins 6
  - Cysteine-rich membrane proteins 6
- **The microaerophilic lifestyle of *Giardia duodenalis*** 7
  - The antioxidant system 8
  - Electron transport cofactors and the energetic advantage of oxygen 10
- **Treatment and clinical resistance** 10
- **Nitroheterocyclic resistance in *Giardia duodenalis*** 11
  - Metronidazole chemistry, cytotoxicity and metabolism 12
  - Metronidazole resistance markers and cross-resistance 13
  - Mechanisms of action and resistance to other nitroheterocyclics 14
- **Nitroheterocyclic resistance in other pathogens** 16
  - *Trichomonas vaginalis* 16
  - *Entamoeba histolytica* 17
  - *Helicobacter pylori* 17
- **Biotechnology and informatics for investigating drug response and resistance** 18
  - RNA sequencing and differential transcription analysis 18
  - Experimental and computational investigation of gene function 19
- **Aims** 20

Chapter 2. Materials and Methods 29

Chapter 3. Annotation of the *Giardia* proteome through structure-based homology and machine learning 30

- **Abstract** 31
- **Introduction** 32
- **Materials and Methods** 35
- **Results** 36
- **Discussion** 39

Ch 4. Characterization of two oxygen-insensitive nitroreductases from *Giardia duodenalis* 53

- **Abstract** 54
- **Methods** 56

Protein domain searching, structure prediction and comparison 56
Cloning and transfection of over-expression vectors 57
Immunolocalization of recombinant gene products 58
Metronidazole susceptibility and intracellular NAD(P)H assays 59
Statistical analyses 60
Results 61
Sequence identification and predicted structure analysis 61
Expression and localization of putative nitroreductases 62
Effect of hNR, NTR1 and VSP over-expression on Mtz susceptibility 62
Effect of hNR, NTR1 and VSP over-expression on intracellular NAD(P)H concentrations 62
Discussion 63
Conclusion 64

Chapter 5. Time-dependent transcriptional changes in axenic *Giardia duodenalis* trophozoites 73

Chapter 6. Divergent transcriptional responses to physiological and xenobiotic stress in *Giardia duodenalis* 106

Chapter 7. Transcriptomics indicates active and passive metronidazole resistance mechanisms in three seminal *Giardia* lines 128

Chapter 8. General discussion 157
Informatic and experimental characterization of oxidoreductases 158
Transcriptional responses to nutrient depletion and exogenous stress 159
A model of drug-oxygen interactions 161
Resistance drivers and constraints 162
Redox-responsive epigenetic regulators and cofactor supply 164
Clinical infections and resistance 165
Prospects for metronidazole combination therapies 166
Systems biology and future directions 167

Bibliography 172

Appendix I: Ansell et al. (2015) *Biotechnology Advances* 189

Chapter 1. Literature Review

This chapter includes some figures, text and tables published in Brendan R. E. Ansell, Malcolm J. McConville, Showgy Y. Ma'ayeh, Michael J. Dagley, Robin B. Gasser, Staffan G. Svärd, Aaron R. Jex. 'Drug resistance in *Giardia duodenalis*' *Biotechnology Advances* 2015;33:888-901.
See preface for author contributions, and Appendix I for full text.

Disease burden

Giardia duodenalis (syn. *G. lamblia* or *G. intestinalis*) is a parasitic, gastrointestinal protist that infects approximately one billion people world-wide and causes 200-300 million cases of disease (giardiasis) each year (Lane and Lloyd, 2002; McCormick, 2014). Infection may be acute or chronic, and symptoms include nausea, vomiting, diarrhea and dehydration (Farthing, 1996; Jeelani et al., 2010; Kosek et al., 2003; Robertson et al., 2010; Savioli et al., 2006). *G. duodenalis* infection has been reported in approximately 15% of children aged 0-24 months in the developing world (McCormick, 2014) and contributes to the global burden of diarrhoeal diseases that collectively constitute the second-leading cause of death in children under five years of age (Kosek et al., 2003; Savioli et al., 2006). Infection can also cause malabsorption syndrome and failure to thrive. Indeed, as few as 3 episodes of chronic (> 2 week duration) diarrhoeal disease per year in the first 24 months of life, is associated with significant reductions in height (approximately 10 cm) and IQ (10 points) by 7-9 years of age (Guerrant et al., 2012). *G. duodenalis* infection induces physical stunting and modified gut physiology in laboratory animals (Bartelt et al., 2013). In humans, pathophysiological changes in the gut may persist long after *G. duodenalis* infection is cleared (Halliez, 2013), and so this parasite is also implicated in the etiology of major non-communicable diseases such as irritable bowel syndrome, chronic fatigue, obesity and type II diabetes (Mørch et al., 2013; Verdu and Riddle, 2012).

Life cycle

G. duodenalis has a relatively simple life cycle, comprising the vegetative trophozoite that colonizes the intestinal tract, and the infective cyst stage (reviewed in Bittencourt-Silvestre et al., 2010). Trophozoites are tear-shaped cells characterized by two diploid nuclei, four pairs of flagella, which originate from basal bodies that bisect the cell, a filamentous median body that runs perpendicular to the basal body, and a large ventral disc via which parasites adhere to the intestinal lumen. Once an infection is established, a proportion of trophozoites differentiate into cysts in a process termed 'encystation', which involves the synthesis and export of cyst-wall proteins (CWPs) and the N-acetylgalactosamine (Gal-Nac) homopolymer. Together these molecules form the cyst wall. During encystation, the flagella are also internalized and the encysting parasite undergoes mitosis without cytokinesis to yield four diploid nuclei. Cysts are resistant to hypotonic lysis and conventional water sanitation methods including chloride

treatment (Haas and Aturaliye, 1999) and can survive for months in cool environmental conditions (Erickson and Ortega, 2006). Upon ingestion by a new host, cysts are exposed to a sudden increase in temperature, stomach peptidases and low pH. These stimuli, followed by the relative alkalinity of the small intestine, trigger the emergence of the nascent 'excyzoite' from one end of the cyst, leaving a glycoprotein husk. The excyzoite then undergoes cytokinesis to produce two binucleate trophozoites, completing the life cycle (Adam, 2001).

Taxonomy and zoonotic potential

There is considerable genetic diversity and differential host-specificity within *Giardia*. There are currently six accepted *Giardia* species, infecting mammals (*G. duodenalis*), amphibians (*G. agilis*), rodents (*G. muris*, *G. microti*) and birds (*G. ardeae*, *G. psittacie*) (Monis et al., 2009). Within *G. duodenalis* there are at least eight genetically distinct 'assemblages,' termed A-H. Assemblage A and B show low host-specificity, whereas assemblage E infects cattle another hooved animals, and assemblages C/D and F infect dogs and cats respectively. Assemblage A is further divided into four clades, of which A-II have been reported to infect humans only, and A-III and A-IV are not recorded to infect humans at all (Feng and Xiao, 2011; Monis et al., 2009). Nonetheless, zoonotic *G. duodenalis* (primarily assemblages A and B) can infect a range of mammals, (Feng and Xiao, 2011; Isaac-Renton et al., 1993), and therefore the reservoir of parasites that are potentially pathogenic to humans is vast.

As *Giardia* generally replicates asexually, defining species is conceptually difficult, however the host specificity observed within/among *G. duodenalis* together with genetic diversity evidenced in genotyping studies (Lasek-Nesselquist et al., 2010; Nolan et al., 2011) have led to calls for the classification of assemblages as separate species (Cacciò and Sprong, 2011). Further support for re-classification is provided in the genomic diversity reported between three *G. duodenalis* assemblages that are published to date, specifically strains WB (Assemblage A — the most well-characterized assemblage; Morrison et al., 2007), GS (Assemblage B; Franzén et al., 2009) and P15 (Assemblage E; Jerlström-Hultqvist et al., 2010). However, *G. duodenalis* assemblages are not broadly recognized as distinct species at present. Therefore, for simplicity, the current 'assemblage' nomenclature for the *G. duodenalis* species complex will be used in this thesis.

Giardia culture systems

G. duodenalis can be adapted to continuous *in vitro* culture, and passaged through encystation and excystation, which allows controlled investigation of *Giardia* biology over the life cycle. Certain culture-adapted lines also remain infective in experimental animals.

Experimental infection

The infectivity and pathogenesis of laboratory lines can be tested by infecting laboratory animals. Infecting mice with trophozoites via oral gavage obviates the requirement for infectious cysts. The assemblage B strain GS is the only strain yet reported to be capable of infecting adult mice (Galkin et al., 2014). Suckling mice (5-7 days old) are however susceptible to infection with certain assemblage A trophozoite lines (Tejman-Yarden et al., 2011). Alternatively, the natural murine pathogen *Giardia muris* is a useful model for vaccination experiments. Unlike *G. duodenalis*, *G. muris* trophozoites encyst within mice and cyst shedding occurs for several weeks (Larocque et al., 2003).

Co-culture and axenic culture

To model host-parasite interactions *in vitro*, trophozoites can be co-cultured in open-capped flasks with murine intestinal epithelial cells, HT-29 or colon cancer (CaCo2) cells. Dulbecco's Modified Eagle Medium supports the growth of host cells under under 5% carbon dioxide in air, however *G. duodenalis* trophozoites can only survive short periods under these conditions (Ma'ayeh, 2013; Ringqvist et al., 2008). However trophozoites are reported to survive for up to 21 days in a 9:1 mixture of DMEM and TYI-S-33 (Fisher et al., 2013). TYI-S-33 supports continuous passage of trophozoites in the absence of host cells. This media contains cysteine, glucose and ammonium ferric citrate, as well as casein digest, yeast extract, bovine serum and bovine bile (Davids and Gillin, 2011). As the latter constituents are undefined, work is yet required to completely define the requirements for continuous trophozoite culture. For routine passage, cells are inoculated into 10 mL tubes containing 9 mL of media, and cultured for four days with close caps fitted. As media is prepared under normal atmospheric conditions, it is expected to contain some dissolved oxygen. Encystation can be induced by exposing trophozoites to bile salts and increased pH. Incubating cysts, including clinically isolated cysts,

in low pH to mimic the stomach environment, followed by a more alkaline solution to mimic pancreatic secretions, induces trophozoite excystation (Boucher and Gillin, 1990; Davids and Gillin, 2011).

Genome and transcription

The *G. duodenalis* genome is approximately 12 KB and encodes some 6000 genes (Morrison et al., 2007), including 4,175 shared as one-to-one orthologs, that vary in sequence and expression level between different assemblages (Franzén et al., 2013). The genome is highly condensed, with many overlapping genes. Each trophozoite contains two diploid nuclei (i.e., 4N) both of which are transcriptionally active (Franzén et al., 2013; Kabnick and Peattie, 1990). Although *Giardia* is not known to replicate sexually, the low allelic heterozygosity in strains such as Assemblage A WB, challenges the assumption that the parasite is asexual (Morrison et al., 2007). In WB cysts, the contents of different nuclei have been shown to mix via nuclear envelope fusion, termed 'diplomixis' (Poxleitner et al., 2008), and may account for lower-than-expected allelic heterozygosity in this assemblage (Morrison et al., 2007). Accordingly, the GS strain exhibits greater allelic heterozygosity suggestive of less recombination (Ankarklev et al., 2012; Franzén et al., 2009).

Transcriptional regulation in *G. duodenalis* differs from higher eukaryotes. The protist has short 5' un-translated regions (UTRs) with redundant AT-rich initiator regions (Teodorovic et al., 2007; Tolba et al., 2013); and unusually long 3' UTRs (Franzén et al., 2013). Transcription of heterozygous alleles in Assemblage B tends to mirror allele dosage (Franzén et al., 2013), indicating little bias in allelic transcription. Despite these features, certain DNA elements have been shown to modulate transcription of genes associated with protein unfolding stress (Spycher et al., 2013), encystation (Wang et al., 2007) and central metabolism (Yee et al., 2000). An abundance of sterile transcripts (antisense to coding domains) in *G. duodenalis* is attributed to bidirectional transcription, which may occur due to a lack of directional activator proteins, or loosely defined promoter motifs (Teodorovic et al., 2007). Such non-coding RNA (Li et al., 2008; Saraiya and Wang, 2008) may play important biological roles, however, as is clearly demonstrated by RNA interference-mediated suppression of surface antigens (Prucca et al., 2008; Saraiya et al., 2014).

Giardia-specific gene families

NEK kinases and type E annexins

Although *G. duodenalis* lacks many core eukaryotic genes (Adam, 2001; Morrison et al., 2007), several gene families are vastly expanded in the genome. *G. duodenalis* features a minimized kinome, which lacks canonical kinases associated with DNA repair, stress response, transcriptional regulation, and the cell cycle in higher eukaryotes (Manning et al., 2011). Interestingly however, the NEK (Never in Mitosis Gene A-Related Kinase) family is expanded to some 200 genes, of which only 25% are predicted to be catalytically active (Manning et al., 2011). The expansion of this gene family may relate to the absence of myosin and thus of microfilaments in *G. duodenalis*. Instead, microtubules provide the scaffold for the parasite cytoskeleton, adhesive disc and flagellar system (Dawson and House, 2010; House et al., 2011). Catalytically inactive NEKs and actin appear to associate with microtubules to facilitate key processes such as nuclear division (Manning et al., 2011; Moniz et al., 2011; Paredeza et al., 2011). *G. duodenalis* also has an expanded repertoire of E-type annexins (aka α-Giardins), which are calcium-binding proteins that associate with phospholipids. Interestingly, a number of α-Giardins are found to associate with the cytoskeleton and may work in concert with NEKs during cell division and encystation (Einarsson et al., 2015; Pathuri et al., 2009; Weiland et al., 2005).

Cysteine-rich membrane proteins

The two major membrane-associated protein families are the variant-specific surface proteins (VSPs) and the high-cysteine membrane proteins (HCMPs). VSPs have highly variable sequence in the extracellular domain and a conserved cytoplasmic tail (Ankarklev et al., 2015; Nash, 2002). Unlike the surface antigens of other parasites (Kyes et al., 2007; Pays et al., 2004), sequence variation is not generated through differential gene splicing and translocation (Ankarklev et al., 2010), but instead each VSP is though to be transcribed *in toto* from a specific gene, of which ~250 are encoded in the WB strain (Morrison et al., 2007). VSPs in other assemblages are less well characterized, however recent data suggest that strains GS and P13 have fewer VSP genes with lower sequence variability than WB (Franzén et al., 2009; Jerlström-Hultqvist et al., 2010). The full complement of VSP transcripts have been reported in a WB population (Franzén et al., 2013), however each trophozoite expresses only a single VSP gene product on its surface at any time. Both epigenetic modification (Kulakova et al., 2006) and

post-transcriptional down-regulation via RNA interference (Prucca and Lujan, 2009), are known to control VSP expression. In mouse and human infection studies, the VSP of the clonal infecting trophozoites is barely detectable 2-3 weeks after infection, which is thought to be due to immune elimination (Nash et al., 1990). Instead, trophozoites expressing a variety of other VSPs are found (Gottstein et al., 1990), which suggests that VSP turnover may be a mechanism of immune evasion within an individual host. It remains to be determined, however, whether antigenic variation in this context is due to stochastic VSP turnover followed by clonal selection, or a direct response to cognate antibody binding (Nash, 2002; Touz et al., 2008).

Besides immune recognition, antigenic variation in an infecting population may depend on the sensitivity of certain VSPs to stomach peptidases (Nash et al., 1991). Interestingly, excysted daughter trophozoites display a different VSP to the pre-encysted parent (Svärd et al., 1998). As such, VSP turnover during transmission may partly account for the high rates of reinfection reported in the field (Gilman et al., 1988). Similarly, the VSP repertoires of different strains may relate to host specificity. For example, the B6 and H7 strains express different VSPs, with the former being less infective in experimental human studies (Nash et al., 1990). In summary, the VSPs expressed by the infecting population may determine the efficacy of initial infection, while subsequent VSP turnover (prior to or after immune recognition) can contribute to immune evasion and transmissibility**.**

Around 60 HCMPs are encoded in the WB genome (Davids et al., 2006; Morrison et al., 2007). These membrane proteins are highly transcribed during encystation and lack the conserved cytoplasmic domain characteristic of VSPs. Further, HCMPs feature numerous CxC motifs, which are rare among VSPs. A single member of the HCMP family has been localized to the nuclear membrane in trophozoites, and translocates to the plasma membrane within cysts (Davids et al., 2006).

The microaerophilic lifestyle of *Giardia duodenalis*

Giardia duodenalis is a 'microaerophilic' protist that thrives in environments with dissolved oxygen (dO_2) concentrations in the range of 5-80 μM, but cannot survive under atmospheric dO_2 conditions (~300 μM) (Lane and Lloyd, 2002). This microaerophillic metabolism appears to have been shaped by the commensal bacteria, and fluctuating oxygen levels in the host intestine. In natural infections, *G. duodenalis* trophozoites attach to the intestinal mucosa, and detach periodically, especially during division. Concentrations of dO_2 in this environment fluctuate from 0-80 μM depending on the level of blood perfusion of the intestinal wall; the oxygen affinity of other commensal microbes (Espey, 2013); the antioxidant richness of host bile, and proximity to the anoxic luminal mid-point (Espey, 2013; Mastronicola et al., 2011).

Products of lateral gene transfer (LGT) from anaerobic bacteria allow *G. duodenalis* to maximize energy production under low dO_2 conditions (Morrison et al., 2007; Nixon et al., 2002; Pal et al., 2009). For example, the remnant mitochondria of *G. duodenalis* lack a tricarboxylic acid cycle and oxidative phosphorylation (Leger et al., 2017), but the organism has acquired enzymes of likely LGT origin that support fermentative glycolysis (Lindmark, 1980), the arginine dihydrolase pathway (Schofield et al., 1990; 1992) and substrate-level ATP generation (Adam, 2001; Han and Collins, 2012; Mendis et al., 1992) (Figure 1.1). Many LGT-derived *G. duodenalis* enzymes contain catalytic iron, which renders them liable to inactivation under higher dO_2 concentrations (Dan et al., 2000; Gillin and Reiner, 1982; Lloyd, 2004; Lloyd et al., 2002). Notable among these oxygen-sensitive enzymes are two pyruvate:ferredoxin oxidoreductases (PFOR-1 and -2) that decarboxylate pyruvate to acetyl-CoA and shuttle the resultant electrons to ferredoxin via iron-sulfur clusters (Chabriere, 2001; Nixon et al., 2002; Townson et al., 1996) (Figure 1.2). Oxidation of PFOR iron-sulfur clusters in other pathogens is associated with enzyme inactivation and the generation of reactive oxygen species (ROS) (Pineda et al., 2010), which in *G. duodenalis*, can lead to disruption of the plasma membrane potential and parasite death (Lloyd et al., 2000). In contrast, other iron-dependent enzymes in the antioxidant system of *G. duodenalis* appear more resistant to oxidative inactivation, and may therefore be involved in detoxification (Mastronicola et al., 2010; Müller et al., 2013; Nixon et al., 2002; Pal et al., 2009; Rafferty et al., 2010; Testa et al., 2011b; Vicente et al., 2009).

The antioxidant system

Giardia duodenalis lacks superoxide dismutase, catalase (Brown et al., 1995; Morrison et al., 2007), and glutathione cycling (Brown et al., 1993), but expresses a number of bacterial-like enzymes that detoxify dO_2 and reactive oxygen species. A 46 kDa enzyme termed 'NADH oxidase' that reduces dO2 to water, was the first of these enzymes to be identified (Brown et al., 1996b) (see Table 1. 1 for gene identifiers). More recently a NADH-dependent flavodiiron protein was reported to perform a similar function (Di Matteo et al., 2007; Mastronicola et al., 2011). Complete reduction of dO_2 to water limits the production of superoxide and hydrogen peroxide ROS (resulting from uni- and divalent reduction of dO_2, respectively). However, these systems appear to be saturated at dO_2 concentrations above ~25 μM (Lloyd et al., 2002). In addition to inhibiting PFORs, excessive dO_2 accumulation can result in enzymatic production of ROS. For example, DT-diaphorase (aka NAD(P)H:menadione oxidoreductase) catalyses the partial reduction of dO_2 to superoxide and hydrogen peroxide, and is therefore proposed to contribute substantially to oxygen sensitivity in *G. duodenalis* (Li and Wang, 2006; Lindmark,

1980; Paget et al., 2004; Sánchez et al., 2001). Superoxide accumulation may be managed by an iron-dependent superoxide reductase (SOR) that converts superoxide to hydrogen peroxide without regenerating molecular oxygen (Testa et al., 2011b). Hydrogen peroxide can then be reduced to water by peroxiredoxins 1a and 1b (Mastronicola et al., 2014). If these peroxiredoxins are overwhelmed, hydrogen peroxide may react with divalent cations (e.g., Fe^{2+}, Cu^{2+}) to form the hydroxyl radical (Edwards, 1993a; 1993b; Pacher et al., 2007), which is proposed to be the most cytotoxic ROS.

In addition to endogenous ROS, *G. duodenalis* may be exposed to exogenous ROS and reactive nitrogen species (RNS) produced by epithelial cells, macrophages and granulocytes in the host intestinal wall. These cells release superoxide, hydrogen peroxide and nitric oxide (NO) in response to gastrointestinal parasites (Arbo et al., 2006; Nathan and Shiloh, 2000; Tako et al., 2013). Superoxide can react with NO to form peroxynitrite, which decomposes to form the hydroxyl radical (Pacher et al., 2007) (Figure 1.2). Cysteine-rich variant-specific surface proteins (VSPs) anchored to the parasite plasma membrane, and other high-cysteine membrane proteins (HCMPs) may absorb extracellular ROS and RNS as a first line of defense (Adam et al., 1992; Gillin et al., 1990; Ringqvist et al., 2011). Within the trophozoite, NO may be detoxified through conversion to nitrate by an oxygen-dependent flavohaemoglobin, or to an amine by a ferredoxin-nitroreductase chimera termed NR-2 (Mastronicola et al., 2010; Müller et al., 2013; 2007b; Rafferty et al., 2010). Conversely, another ferredoxin-nitroreductase, NR-1, is implicated in the production of endogenous NO through partial reduction of nitrate/nitrite. This is based on the finding that both the NO and DNA-damage responses are elicited in *E. coli* reporter strains when transfected with the *G. duodenalis* enzyme (Müller et al., 2013). Recent evidence suggests that NR-1 and NR-2 can reduce a range of other substrates including menadione, and act in concert as an enzyme complex (Müller et al., 2015). A canonical nitroreductase that lacks a ferredoxin domain, termed NTR-1, may perform similar functions but is little studied to date (Nixon et al., 2002; Pal et al., 2009). As a further line of defense against RNS, peroxiredoxins may detoxify peroxynitrite (Mastronicola et al., 2014) to prevent formation of the hydroxyl radical (Ma'ayeh and Brook-Carter, 2012; Testa et al., 2011a) (Figure 1.2) (Table 1.1).

Intracellular hydroxyl radicals can be scavenged by cysteine (Brown et al., 1993), cysteine thioglycolate (a non-protein thiol) (Brown et al., 1998; Tekwani and Mehlotra, 1999), and pyruvate (Biagini et al., 2001). In addition, a thioredoxin cycling system may repair oxidized biomolecules (Mustacich and Powis, 2000). An NADPH-dependent thioredoxin reductase

(TrxR), whose activity is enhanced in the presence of an unidentified low molecular weight protein, has been identified (Brown et al., 1996a). While early reports demonstrated that glutathione could act as an electron acceptor for TrxR (Brown et al., 1996a; Smith et al., 1988), it is likely that the endogenous electron acceptor is a yet unidentified thioredoxin (Brown et al., 1996a; Leitsch et al., 2011). Other likely substrates of TrxR are protein disulfide isomerases, which contain thioredoxin domains (Lundström and Holmgren, 1990; McArthur et al., 2001) and are important components of the cellular protein-folding machinery. Thioredoxin is also likely to provide electrons to peroxiredoxins, which are suggested to neutralize peroxidized lipids, in addition to ROS and RNS (Brown et al., 1995; 1998; Mastronicola et al., 2014) (Figure 1.2) (Table 1.1).

Electron transport cofactors and the energetic advantage of oxygen

The nicotinic cofactors NAD and NADP, and their reduced analogues NADH and NADPH (collectively NAD(P)H), are essential electron transporters in *Giardia.* Glycolysis and other core metabolic processes reduce NAD(P) to NAD(P)H, which must be re-oxidized to drive continued energy generation. Under microaerobic conditions, antioxidant enzymes regenerate NAD(P) in the process of reducing oxygen and ROS. Under anaerobic conditions, however, acetyl-coA must be reduced to ethanol in order to maintain the NAD(P) pool. The latter conditions prevent conversion of acetyl-coA to acetate and deprive *G. duodenalis* of additional ATP (Figure 1.2). Therefore *G. duodenalis* derives an energetic advantage from tolerating micromolar oxygen concentrations, as demonstrated by enhanced growth under microaerobic, compared to anoxic (i.e., nitrogen-sparged) conditions (Gillin and Diamond, 1981).

Treatment and clinical resistance

Treatment for *G. duodenalis* infections is largely limited to two drug classes: nitroheterocyclic compounds (e.g., metronidazole, nitazoxanide and furazolidone) and benzimidazoles (e.g., albendazole and mebendazole) (Escobedo and Cimerman, 2007; Wright et al., 2003). Benzimidazoles are antihelminthic compounds that target microtubule polymerization (Diawara et al., 2013). That *G. duodenalis* relies heavily on microtubules may be the basis for its susceptibility to this drug class (Jiménez-Cardoso et al., 2009; Upcroft et al., 1996). Paromomycin and quinacrine are less widely used due to their low efficacy and high toxicity, respectively. Meteronidazole (Mtz) is generally well tolerated, but is not approved for antigiardial therapy by the US Federal Drug Administration due to teteragenic concerns

(Escobedo and Cimerman, 2007). Protracted use is also associated with neurological side effects (Woodruff et al., 2002). Treatment efficacy with this drug ranges from 70-100%, and reports of increased Mtz tolerance in isolates from treatment-refractory patients, indicate that clinical resistance contributes to treatment failures (Abboud et al., 2001; Adagu et al., 2001; Lemée et al., 2000; McIntyre et al., 1986). Despite these short-comings, Mtz remains the mainstay of antigiardial therapy world-wide. Although Mtz has been used clinically since the 1960s, its cytotoxicity against *G. duodenalis*, and mechanisms of resistance, remain incompletely understood.

Metronidazole drug is thought to enter *G. duodenalis* via passive diffusion as a pro-drug, and to be reduced to cytotoxic intermediates by glycolytic and antioxidant enzymes within the parasite. Trophozoite lines resistant to a drug of interest can be created through chronic exposure of wild-type parasites to sub-lethal drug concentrations (Townson et al., 1992). In addition to studies of clinical isolates, much understanding of Mtz resistance has been gained through genetically controlled comparisons of laboratory-derived resistant lines and their susceptible parents. The following sections will detail current understanding of the *G. duodenalis* antioxidant system, and its interactions with Mtz in drug-susceptible and –resistant parasites.

Nitroheterocyclic resistance in *Giardia duodenalis*

The highly reduced (i.e., electron-rich) intracellular environment that *G. duodenalis* maintains in order to manage oxidative stress, is the basis of its susceptibility to Mtz and other nitroheterocyclic drugs. This drug class features a nitro group extending from a heterocyclic backbone, and includes the nitroimidazoles Mtz, ornidazole (ORN), tinidazole (TIN), and a novel compound termed C17 (Crozet et al., 2009; Dunn et al., 2010); as well as the nitrothiazolide nitazoxanide (NTZ), and the nitrofuran furazolidone (FUR) (Figure 1.3). As suppliers of reducing power, glycolytic and antioxidant enzymes are strongly implicated in the activation and detoxification of these drugs (Leitsch et al., 2011; Müller et al., 2013; 2008; 2007a; Tejman-Yarden et al., 2011). Accordingly, differential regulation of multiple oxidoreductases is evident in nitroheterocyclic-resistant parasites. Here, we define *G. duodenalis* derived from patients as 'isolates', and isolates established in continuous axenic laboratory culture as 'strains.' A strain that has been cloned or selected for drug resistance will be termed a 'line' (Nolan et al., 2011). Lines that exhibit resistance to a drug that they have not been previously exposed to, of equal or greater magnitude than that for the selected drug, are considered cross-resistant.

Metronidazole chemistry, cytotoxicity and metabolism

The prototypic 5-nitroimidazole, Mtz, is a pro-drug and is activated by intracellular reduction of the nitro group (Edwards, 1993a) (Figure 1.3). Univalent reduction yields a nitro radical anion, which can be re-oxidized by dO_2 in aerobic cells due to its very low redox potential (Table 1.2). Re-oxidation is termed 'futile redox cycling' (Figure 1.4c) and renders Mtz largely non-toxic to host cells during short course treatment. However, under the highly reduced conditions found in the cytoplasm of *G. duodenalis* and other microaerophiles, the nitro anion radical can be further reduced to reactive nitroso- and hydroxylamine intermediates. These unstable intermediates are thought to progressively acquire electrons by oxidizing biomolecules, finally forming the inert amine Mtz-NH_2 (Edwards, 1993a) (Figure 1.4a). Mtz is unequivocally mutagenic in *H. pylori* (Sisson et al., 2000), and damage to DNA via thymine dimerization is a widely accepted mechanism of cytotoxicity (Edwards, 1993a). Recent work correlating exposure to Mtz with histone 2A (H2A) phosphorylation (a marker of DNA damage) and arrest of cell cycle progression suggests that the drug may also damage DNA in *G. duodenalis* (Uzlikova and Nohýnková, 2014). However, the relatively short time to Mtz-induced cytotoxicity in microaerophiles (within 4-6 hrs) may be indicative of extensive oxidation of cytosolic biomolecules in addition to DNA, as DNA damage alone would be expected to result in delayed cell death (Edwards, 1993a; Leitsch et al., 2009). Furthermore, activated Mtz intermediates in the cytosol would be more likely to interact with proximal biomolecules or the nuclear membrane, rather than DNA itself (Leitsch et al., 2009). Indeed, differential two-dimensional electrophoretic analysis of proteins from Mtz-exposed trophozoites (strain 106), indicated the existence of covalent adducts between Mtz and proteins including pyrophosphate-dependent pyruvate kinase, alcohol dehydrogenase E (ADHE), structural proteins and a protein translation elongation factor EF-1γ (Leitsch et al., 2012b). Although the functional implications of these interactions are yet to be determined, permanent inactivation of proteins might also contribute to Mtz cytotoxicity in *G. duodenalis*.

At present, four enzymes are implicated in activating Mtz in G. duodenalis. Purified ferredoxin (reduced by PFOR) and recombinant NTR-1 have been shown to reduce Mtz in vitro (Leitsch et al., 2011; Townson et al., 1994b; 1996). Artificial suppression of PFOR expression in wild-type trophozoites increases Mtz tolerance (Dan et al., 2000). Similarly, recombinant TrxR reduces Mtz in vitro and its over-expression on a wild-type genetic background increases Mtz susceptibility (Leitsch et al., 2016). A fourth enzyme, NR-1, also increases Mtz susceptibility when over-expressed (Nillius et al., 2011). Conversely, NR-2 may completely detoxify the Mtz

pro-drug by multivalent reduction to an intert amine (Mtz-NH_2), as indicated by increased Mtz tolerance in lines over-expressing NR-2 (Müller et al., 2013) (Figure 1.4f).

Metronidazole resistance markers and cross-resistance

Mtz-resistant *G. duodenalis* lines have been selected using techniques including constant exposure to sub-lethal Mtz concentrations (lines 1062ID10 and WB-C5; Boreham et al., 1988; Müller et al., 2007a), and mutagenesis using ultra-violet radiation followed by exposure to moderate (WB-M1 and WB-M2; Tejman-Yarden et al., 2011), or high Mtz concentrations (WB-M3 and 713-M3; Townson et al., 1992) (Table 1. 3). The karyotypes of three of these lines have been investigated; 1062ID10, which was not mutagenized, exhibited partial deletion of chromosome 4 (Upcroft et al., 1992), and the mutagenized line WB-M3 exhibited duplication and partial deletion of chromosome 5 (Chen et al., 1994). Similar rearrangements are also claimed in the mutagenized line 713-M3, but not further described (Townson et al., 1994a). These reports suggest that Mtz exposure alone can produce genetic lesions. The translocation break-point in 1062ID10 is near a gene encoding a multidrug-resistance transporter homologue (Townson et al., 1994a), indicating that Mtz efflux may contribute to resistance. Further investigation of the abundance, structure and function of these membrane pumps in resistant *G. duodenalis* is therefore required.

In addition to genetic data, transcript abundance and/or enzyme activity data are available for six laboratory-derived Mtz-resistant lines. Comparisons of these lines with their respective Mtz-susceptible parents suggest that Mtz-resistance arises in part through decreases in PFOR, ferredoxin and NR-1 activity, in various combinations (Table 1. 3). (Ellis et al., 1993; Leitsch et al., 2011; Tejman-Yarden et al., 2011). Transcription of *pfor-2* is unchanged in the line WB-M2 (Tejman-Yarden et al., 2011), however *pfor-1* transcription has not been investigated in this line. Lower ferredoxin transcription/activity may be functionally equivalent to lower PFOR activity given that the two proteins work in concert to activate Mtz. The transcription of *ferredoxin-1* is lower in WB-M1 and WB-M2 (Tejman-Yarden et al., 2011), and ferredoxin activity is decreased in 713-M3 (Leitsch et al., 2011; Liu et al., 2000). Nitroreductase genes are also differentially transcribed in several resistant lines. NR-1 is transcriptionally suppressed in 713-M3, WB-M1 and WB-M2, and *nr-2* transcription is up-regulated in 713-M3 and 1062ID10 (Müller et al., 2013; Tejman-Yarden et al., 2011). A positive correlation between Mtz resistance and glutathione reductase activity (incorporating TrxR activity), and glutathione oxidase (incorporating peroxiredoxin) activity, was reported in 1062ID10 (Smith et al., 1988). Taken together, lower transcription/activity of the PFOR/ferredoxin couple is the most consistent

finding in lines selected for resistance to Mtz, and supports the finding that artificial suppression of *pfor-1* induces Mtz resistance (Dan et al., 2000). Additional mechanisms of resistance may include Mtz detoxification by NR-2, and neutralization of activated Mtz intermediates and damaged biomolecules through increased thioredoxin cycling (Smith et al., 1988). Furthermore, the recent identification of constitutive H2A phosphorylation in 713-M3 and 106-2ID10 (Uzlikova and Nohýnková, 2014) suggests that up-regulation of DNA repair pathways also contributes to resistance. Cross-resistance in lines selected for resistance to Mtz appears restricted to other 5-nitroimidazoles. 1062ID10 and WB-M2 are cross-resistant to tinidazole (TIN) and ornidazole (ORN) (Tejman-Yarden et al., 2011), suggesting that the mechanisms of action and resistance to these drugs overlap with Mtz. However, Mtz-specific resistance mechanisms must also exist, given that 713-M3 and WB-M1 show little cross-resistance to TIN, ORN or any other nitroheterocyclics (Tejman-Yarden et al., 2011) (Table 1. 3). The molecular basis of differential cross-resistance in these lines is presently unclear.

Mechanisms of action and resistance to other nitroheterocyclics

Relative to Mtz, mechanisms of resistance to other nitroheterocyclics in *G. duodenalis* are less well characterized. Two lines have been selected for resistance to a novel 5-nitroimidazole termed C17 (Crozet et al., 2009; Dunn et al., 2010). The line 106-C17 was selected for resistance to this compound from a nitroheterocyclic-susceptible parental line (106), whereas 713-M3-C17 was derived from the Mtz-resistant line 713-M3 (Dunn et al., 2010). The gene encoding NR-1 is transcriptionally down-regulated in both C17-resistant lines (Müller et al., 2013), and recombinant NR-1 appears able to reduce C17 (Müller et al., 2015). Interestingly, 106-C17 shows similar PFOR activity to its nitroheterocyclic-susceptible parent, but is cross-resistant to Mtz (Dunn et al., 2010; Leitsch et al., 2011). Similarly, both PFOR activity and Mtz resistance are higher in 713-M3-C17 than the already Mtz-resistant parent (Dunn et al., 2010; Leitsch et al., 2011). These data indicate that Mtz resistance is possible in the presence of active PFOR, and therefore lower *nr-1* transcription may contribute substantially to both C17- and Mtz resistance. Although there is broad agreement in the (albeit limited) available enzyme transcription/activity data for 106-C17 and 713-M3-C17, only 713-M3-C17 is also cross-resistant to TIN and ORN (Dunn et al., 2010; Tejman-Yarden et al., 2011).

Nitazoxanide (NTZ) may have a range of mechanisms of action within *G. duoenalis*. Recombinant NR-1 is reported to reduce NTZ (Müller et al., 2015), and overexpression of this enzyme in the WB background increases NTZ susceptibility (Nillius et al., 2011). Furthermore, the gene encoding NR-1 is down-regulated in the two NTZ-resistant laboratory lines reported

to date (WB-C4 and NTZII) (Müller et al., 2007a; 2008; 2013). Together, these data strongly suggest that NR-1 reduces NTZ to toxic intermediates within *G. duodenalis*, and that resistant lines avoid this by down-regulating *nr-1* transcription. Interestingly, NTZ may also act as a steric inhibitor of PDI and PFOR enzymes (Hoffman et al., 2007; Müller et al., 2007b). Transcription of *pdi-2*, *pdi-4* and *pfor-1* is increased in WB-C4 relative to the drug-susceptible parent (Müller et al., 2008), which may represent an attempt to compensate for chemical inhibition of the gene products. NTZ may also lead to protein mis-folding in *Giardia*, as microarray analysis of WB-C4 revealed the up-regulation of genes encoding the heat-shock proteins HSP70-B2 and HSP90, and other chaperones (Müller et al., 2008). Similar to C17-resistant lines, WB-C4 is cross-resistant to Mtz despite the marked up-regulation of *pfor-1* (Müller et al., 2008). If Mtz is activated in WB-C4, resistance may be partially due to the efficient management of protein oxidation by HSP chaperones.

Lastly, furazolidone (FUR)-resistant *G. duodenalis* lines have been developed *in vitro* (Townson et al., 1992; Upcroft et al., 1990), and resistant clinical isolates are reported (Ellis et al., 1993; Smith et al., 1988). As for Mtz, FUR-resistant lines have been created via a range of mutagenesis and exposure regimes (Townson et al., 1992). Similar to the Mtz-resistant line WB-M3, duplication and partial deletion of chromosome five is reported in the UV-mutagenized FUR-resistant line BAC2-F3 (Chen et al., 1994). The conservation of this mutation in lines resistant to both Mtz and FUR is puzzling, and could indicate either the existence of a gene(s) whose disruption protects against exposure to both drugs; or an effect of regional chromosomal sensitivity to nitroheterocyclic- or UV-induced stress that entails little fitness cost. Purified NADH oxidase is reported to activate FUR (Brown et al., 1996b), but clinical isolates from treatment-refractory patients exhibited little difference in NADPH oxidase or PFOR activity, relative to susceptible laboratory strains (Ellis et al., 1993). Similarly, no correlation between PFOR activity and FUR resistance was observed in isolates from diagnostic duodenal biopsies, but positive correlations were detected for both thiol-dependent peroxidase and reductase activity (representing TrxR and peroxiredoxin enzyme activity, respectively) (Smith et al., 1988). Together these data support a model of FUR resistance whereby the drug is activated by NADH oxidase and the ensuing oxidative damage is managed by elevated thioredoxin-based antioxidant activity. Cross-resistance has not been investigated in FUR-resistant *G. duodenalis* to date, but may be informed by a report of minimal cross-resistance to non-nitrofuran compounds in FUR-resistant *Clostridium difficile* (Kumar et al., 2014). Additionally, FUR is shown to be more effective than Mtz for inhibiting cyst viability (Hausen et al., 2006), perhaps due to greater penetration through the cyst wall (Paget et al., 1998).

In summary, results from laboratory-derived nitroheterocyclic-resistant lines suggest that loss of either of the PFOR/ferredoxin couple or NR-1 can lead to Mtz resistance, and that resistance may be further augmented by up-regulation of NR-2 and thioredoxin-cycling enzymes. Lower transcription of the gene encoding NR-1 is implicated in resistance to Mtz, NTZ and C17, however cross-resistance between these compounds is not universal, indicating that factors other than the aforementioned oxidoreductases must influence resistance. In contrast to resistance mediated through down-regulation of nitroheterocyclic drug-activating oxidoreductases, FUR resistance appears to be primarily mediated through the up-regulation of thioredoxin-based antioxidant enzymes.

Nitroheterocyclic resistance in other pathogens

Other protozoan and bacterial human pathogens that infect low-oxygen environments are also treated with nitroheterocyclic drugs and can develop resistance. As for *G. duodenalis*, treatment-refractory infections are reported, and complicate effective control. Comparisons of antioxidant systems and drug-resistance phenotypes across species are important for identifying universal features of resistance, and for inferring solutions to knowledge gaps in particular species.

Trichomonas vaginalis

Trichomonas vaginalis is the human pathogen most closely related to *G. duodenalis* (Leger et al., 2017), and infects the urogenital tract of ~280 million people. *T. vaginalis* causes urethritis/vaginitis, and increases susceptibility to HIV infection. Mtz resistance is widespread, attributed to both genetic and transcriptional changes (Bradic et al., 2016). *T. vaginalis* encodes a TrxR that is involved in activating Mtz and detoxifying H_2O_2 (Leitsch et al., 2009). Clinical Mtz resistance appears to rely on down-regulation of a dO_2 detoxification enzyme, flavin reductase, leading to futile redox cycling (Bradic et al., 2016). The *T. vaginalis* flavin reductase produces H_2O_2, which must be further detoxified by thioredoxin-dependent peroxiredoxin (Chapman et al., 1999; Coombs et al., 2004; Linstead and Bradley, 1988). The coupling of thioredoxin cycling to dO_2 detoxification in *T. vaginalis*, is proposed to account for the continued activity of TrxR in clinically Mtz-resistant isolates (Leitsch et al., 2012a). Resistance involving down-regulation of TrxR is possible under low dO_2 conditions in the laboratory, and may be contingent upon prior flavin reductase down-regulation (Kulda, 1999; Leitsch et al., 2012a). However this type of

resistance has not been observed in clinical isolates, likely due to the higher dO_2 conditions *in vivo* (Wagner and Levin, 1978). Conversely, clinical isolates of *G. duodenalis* exhibit a range of TrxR activities (Smith et al., 1988), and TrxR is not directly coupled to the major dO_2 detoxification system (i.e., NADH oxidase). Therefore TrxR down-regulation could theoretically precede, or occur independently of futile redox cycling in *G. duodenalis*, and may allow greater flexibility in resistance mechanisms *in vivo.*

Entamoeba histolytica

Entamoeba histolytica is a destructive parasite that can invade gut tissue (causing dysentery) and more oxygen-rich organs such as the liver (causing abscesses). Puzzlingly, although Mtz is the front-line treatment for ameobasis (Duchene, 2015; Löfmark et al., 2010), and resistance can be created in the laboratory, clinical Mtz resistance is hardly documented (Duchene, 2015). Two atypical NADPH-dependent oxidoreductases in *E. histolytica* exhibit ferredoxin:NAD reductase (FNR) activity, and also reduce ferric iron and activate Mtz (Carpenter et al., 2013; Jeelani et al., 2010). *E. hystolytica* also lacks the pentose phosphate pathway, relying instead on substrate-level conversion of NAD to NADP (Jeelani and Nozaki, 2014). Under oxidative stress, glycolytic intermediates are re-routed via glycerol in order to circumvent oxygen-sensitive PFORs (Husain et al., 2012). Such metabolic flexibility and atypical antioxidant enzymes await now investigation in *G. duodenalis.*

Helicobacter pylori

In similarity to *T.* vaginalis, Mtz resistance appears to develop through ordered genetic changes in the gastric ulcer-causing bacterium *Helicobacter pylori*. Mutations in a Mtz-activating nitroreductase (RdxA) typically occur early in the development of Mtz-resistance (Goodwin et al., 1998; Olekhnovich et al., 2009), and mutations in other genes subsequently confer greater levels of resistance (Albert et al., 2005). Secondary mutations in a FMN/FAD synthetase-coding gene are documented in a highly-resistant line (Albert et al., 2005), suggesting depletion of flavin co-factors that are essential to the function of numerous oxidoreductases, can lead to resistance. In addition to functional genetic mutations, transcriptional modulation is implicated in Mtz-resistant *H. pylori*. The *fur* gene that encodes an iron-dependent transcription factor, is mutated in resistant clinical isolates (Albert et al., 2005) and laboratory strains (Tsugawa et al., 2011), and likely results in differential transcription of oxidoreductases including superoxide dismutase (Carpenter et al., 2013).

Biotechnology and informatics for investigating drug response and resistance

Despite reports of genetic lesions in nitroheterocyclic-resistant *G. duodenalis*, several features of laboratory-derived resistant lines suggest that resistance may not be a stably encoded in the genome. 1062ID10 was observed to revert to Mtz sensitivity over several weeks of drug-free culture, during which time PFOR, TrxR and peroxiredoxin activity returned to levels similar to the susceptible parent (Smith et al., 1988). Gradual reversion to sensitivity was also observed in WB-M1 in the absence of Mtz (Tejman-Yarden et al., 2011). A striking demonstration of the reversibility of nitroheterocyclic resistance is found in the NTZ and Mtz-resistant line WB-C4, which reverted to sensitivity to both drugs during a single passage through the life cycle (encystation and excystation) (Müller et al., 2008). Concomitant with restored drug sensitivity, *nr-1* transcription in excysted trophozoites was restored to levels similar to the drug-sensitive parent, and *pdi-4*, *hsp40*, *hsp70* and *hsp90* transcription decreased significantly (Müller et al., 2008). Taken together with evidence of multiple perturbed gene products in resistant lines, these features suggest that dynamic transcriptional changes are fundamental in the development of resistance to nitroheterocyclic drugs.

Much work in oxidoreductase function and drug resistance in *G. duodenalis* was conducted prior to the publication of the *G. duodenalis* genome. The advent of affordable genome and RNA sequencing has since provided deep insights into the genetic architecture of different assemblages (Franzén et al., 2009; Jerlström-Hultqvist et al., 2010; Morrison et al., 2007), and snap-shots of steady-state transcription under standard culture conditions (Franzén et al., 2013). However as this thesis was commenced, only a single, microarray-based investigation of transcription in drug-resistant parasites was available (Müller et al., 2008). Further, the degree of transcriptional plasticity across the *G. duodenalis* genome had not been investigated with sufficient biological replication to detect statistically robust differentially transcribed genes. These technologies thus hold great promise for profiling the full complement of transcriptional changes in resistant lines, and identifying genetic lesions with high resolution.

RNA sequencing and differential transcription analysis

Illumina sequencing involves fragmentation of nucleic acid, and ligation of universal primers that hybridize to chip-bound oligonucleotides. Fragments are then amplified to yield a clonal cluster, and sequenced by successive rounds of addition of fluorophore-labelled ddNTPs, imaging, and fluorophore cleavage. Paired-end sequencing is performed by biotinylation of nucleotides at either end of a longer DNA/RNA molecule, which is then circularized and

fragmented for sequencing (Bentley et al., 2008). Reads from each end (the biotinylated sequence) are recorded, and are used *in silico* to orient shorter reads generated from unbiotinylated sequence which are otherwise difficult to confidently align. Strand-specific sequencing is useful for accurately assigning the origin of transcripts from over-lapping genes. This technology involves amplifying cDNA with nucleotides including uracil, which tags the second strand. After library preparation, strands incorporating uracil are digested by a uracil-specific excision reagent (USER), and thus only the complement of the original mRNA is sequenced (Levin et al., 2010). Differential gene transcription using Illumina data, involves entering raw RNA reads into software packages that filter out low-quality sequence (Lohse et al., 2012), and then assigning the high-quality reads to their corresponding genome sequence (usually a coding domain) using Burrows-Wheeler alignment algorithms (Li and Durbin, 2009; Mortazavi et al., 2008). Statistical software packages such as edgeR are then used to define genes that show significant differences in transcription between two or more conditions. edgeR incorporates sequencing depth normalization and correction for multiple comparisons, to confidently identify differentially transcribed genes (Robinson et al., 2009). Provided sufficient sequencing depth, single nucleotide polymorphisms (SNPs) can be identified in transcripts using bcftools (Li et al., 2009); and larger splice variants by comparing assembled transcripts with the reference genome (Roberts et al., 2012).

Experimental and computational investigation of gene function

Genome-wide analyses are only as useful as the functional information available for genes of interest, however. As many as 50% of the proteins predicted from the *G. duodenalis* WB genome currently lack functional annotation (release 31, GiardiaDB.org) (Morrison et al., 2007). The vast evolutionary distance between *Giardia* and other model eukaryotes renders many predicted protein-coding sequences beyond the reach of sequence-based homology searching algorithms such as BLAST (Altschul et al., 1997) and Hidden Markov Models (Karplus et al., 1998). Despite the obvious challenges of manipulating a tetraploid genome, the Cre/LoxP system has been adapted to *Giardia* and allows targeted gene deletion (Wampfler et al., 2014). The first complete gene knock-out was recently created through iterative replacement with an antibiotic resistance gene, selection, and excision of the resistance cassette using Cre/LoxP (Ebneter et al., 2016). An over-expression cassette is also available and can be used to study gene function and to purify natively produced proteins and complexes (Jerlstrom-Hultqvist et al., 2012). Such advances are laudable however not amenable to high-throughput reverse genetic screens, via which the functions of multiple genes may be inferred. In addition to a lack

of selection markers for simultaneous gene replacement, *G. duodenalis* remains stubbornly impervious to CRISPR/Cas9 genome editing. Therefore in lieu of high-throughput experimental technologies to infer gene function, *in silico* prediction of protein structure holds considerable promise for providing starting points for annotating the many hypothetical proteins predicted in this parasite. Protein structure informs function, and is robust to large variations in constituent amino acid sequence (Illergård et al., 2009). Although structure prediction remains computationally intensive, integration of template threading and molecular dynamics simulation approaches can predict protein structure with impressive accuracy (Huang et al., 2014; Tai et al., 2013). Functional information can then be inferred via structure-based alignment with solved crystal structures (Zhang and Skolnick, 2005).

Aims

Much important work has been undertaken on laboratory-derived Mtz-resistant *G. duodenalis* over the last 30 years. These organisms represent a genetically controlled system in which resistance-associated changes can be discerned from inter-strain variation. Given that multiple gene products are perturbed in drug-resistant lines, and substantial inconsistencies exist between lines resistant to the same drug (Table 1.3), description of resistance-associated transcriptional changes across the genome are required in order to understand common themes in the development of drug-resistance, and avenues for intervention. Furthermore, while it is clear that perturbations in the antioxidant system are cental to the parasite's response to Mtz, many elements of this system remain unresolved. Specifically, functional thioredoxins, rubredoxin-like and cytochrome-based electron transport chains are yet to be demonstrated in *G. duodenalis* (Leitsch et al., 2011; Mastronicola et al., 2014; Pazdzior et al., 2015; Pyrih et al., 2014; Testa et al., 2011b; Vicente et al., 2009). A widely inferred ferredoxin:NAD reductase, which would transport electrons from reduced ferredoxin to NAD(P)H (Ali and Nozaki, 2007; Brown et al., 1998; Ellis et al., 1993; Leitsch et al., 2011; Nixon et al., 2002; Upcroft and Upcroft, 2001), also remains undiscovered (Müller, 2003) (Figure 1.2). In addition to unannotated genes, many genes are currently under-annotated in the parasite genome. For example, the substrates of several gene products predicted interact with NAD(P)H are unknown. It is likely that yet undiscovered genes contribute to nitroheterocyclic metabolism and resistance. Experimental over-expression of putative NAD(P)H-dependent genes in wild-type parasites, can go some way to characterizing novel potential mediators of resistance.

Deep transcriptome sequencing combined with sensitive protein structural prediction technology, presents an exciting opportunity to explore transcriptional dynamics in *G. duodenalis* under conditions such as sub-lethal stress, and in drug-resistant states. Structure prediction can assist in the search for the genetic mediators of functions assumed to occur in the parasite but not evidenced to date.

Given the relative paucity of transcriptomic and genetic functional data available for *G. duodenalis*, this present work aimed to:

1. Apply an indirect functional annotation matching approach to identify high-confidence structural predictions for hypothetical proteins in *Giardia*;
2. Investigate changes in Mtz sensitivity in wild-type trophozoites upon overexpression of putative oxidoreductase enzymes;
3. Profile transcriptional changes in *Giardia duodenalis* trophozoites over time under standard axenic culture conditions;
4. Compare transcriptional responses to Mtz, oxidative and thermal stress in drug-susceptible trophozoites; and
5. Compare the transcriptional phenotypes and infer genetic lesions in three seminal laboratory-derived drug-resistant lines, relative to their drug-susceptible parents.

Table 1.1 Substrates, products and cofactors for antioxidant enzymes in *Giardia duodenalis*

Enzyme (abbreviation)	ORF no. (GL50803)	Catalytic cofactors	Electron donors	Substrates	Products	Notes	References
Pyruvate ferredoxin oxidoreductase 1 (PFOR1)	17063	Fe-S, thiamine pyrophosphate		Pyruvate, oxaloacetate, co-A, Fd (ox)	Acetyl co-A, Fd (red)	Named according to Müller et al. (2007a)	Townson et al. (1996), Leitsch et al. (2011)
Pyruvate ferredoxin oxidoreductase 2 (PFOR2)	114609	Fe-S, thiamine pyrophosphate		Pyruvate, oxaloacetate, α-ketobutyrate, co-A, Fd (ox)	Acetyl co-A, Fd (red)	Named according to Müller et al. (2007a)	Horner et al. (1999), Müller et al. (2007a), Townson et al. (1996)
Ferredoxin (Fd)	9662, 10329, 27266	Fe-S	PFOR (red)	MTZ-NO_2	MTZ-NO_2•$^-$		Townson et al. (1994), Liu et al. (2000), Leitsch et al. (2011), Tejman-Yarden et al. (2011)
Ferredoxin NAD(P) reductase (FNR)		FAD, FMN	Fd (red)	NAD, NADP	Fd (ox), NADH, NADPH	Existence inferred in but no genomic or enzymatic evidence to date	Nixon et al. (2002), Leitsch et al. (2011), Ellis et al. (1993), Upcroft et al. (2001), Brown et al. (1998), Müller et al. (2003)
Alcohol dehydrogenase E (ADHE)	93358		NADH	Acetyl-CoA, acetaldehyde	Ethanol	Regenerates NAD under anaerobic conditions	Sanchez et al. (1998)
Glutamate dehydrogenase (GDH)	21942		NADPH	Ammonia, α-ketogluterate	Glutamate	Reversible, more active in NADPH oxidation/glutamate formation; regenerates NADP under anaerobic conditions	Park et al. (1998)
NADH oxidase	33769	FAD	NADH, NADPH	O_2, FAD, FMN, FUR-NO_2	H_2O, $FADH_2$, $FMNH_2$, FUR-NO_2•$^-$	Published purified enzyme activity is likely derived from this gene product	Brown et al. (1996)
NADH oxidase	9719	FMN	NADH			Predicted FMN binding domain	Morrison et al. (2007)
NADH rubredoxin reductase			NADH	Rubredoxin (ox)	Rubredoxin (red)	*E. coli* homologue required for recombinant assays of flavodiiron protein and SOR	Testa et al. (2011b), Vicente et al. (2009), Mastronicola et al. (2011), DiMatteo et al. (2007)
Flavodiiron protein	10358	Fe, FMN	Rubredoxin (red)	O_2	H_2O	Recombinant *E. coli* NADH rubredoxin reductase and rubredoxin required for activity assays	Vicente et al. (2009), Mastronicola et al. (2011), DiMatteo et al. (2007)
Acetyl-coA synthetase	13608			ADP, acetyl-coA	ATP, acetate	Generates ATP under microaerobic conditions	Sanchez et al. (1999)
DT-diaphorase	15004	FAD	NADPH	O_2; menadione (ox)	H_2O_2 + O_2•$^-$; menadione (red)	Major contributor to ROS generation	Sanchez et al. (2001), Paget et al. (2004), Li & Wang (2006)
Superoxide reductase (SOR)	Ch1 NT 217012-216680	Fe	Rubredoxin (red)	O_2•$^-$	H_2O_2	Recombinant *E. coli* NADH rubredoxin reductase and rubredoxin required for activity assays	Testa et al. (2011b)
Thioredoxin reductase (TrxR)	9827	FAD	NADPH	Thioredoxin (ox); MTZ-NO_2	Thioredoxin (red); MTZ-NO_2•$^-$	May require reduced flavins ($FADH_2$) for activity	Brown et al. (1996), Leitsch et al. (2011)
Thioredoxin (Trx)	3910, 9355, 104250, 6289		TrxR	Oxidized protein	Reduced protein	Endogenous thioredoxin for TrxR yet to be identified	Leitsch et al. (2011), Ma'ayeh & Brook-Carter et al. (2012)
Peroxiredoxin 1a,b	16076, 14521, 15383		Thioredoxin (red)	H_2O_2; peroxynitrite; peroxidized lipids	H_2O; NO_2^-; neutralized lipids	Recombinant *E. coli* TrxR and thioredoxin required for activity assays	Mastronicola et al. (2014)
Nitroreductase 1 (NR1)	22677	Fe S, FMN	NADH	NO; MTZ-NO_2	NO_3^-; MTZ-NO_2•$^-$	Named according to Müller et al. (2007)	Müller et al. (2007a), Müller et al. (2008), Nillius et al. (2011)
Nitroreductase 2 (NR2)	6175	Fe S, FMN	NADH	NO; MTZ-NO_2	NO_3^-; MTZ-NH_2	Named according to Müller et al. (2013)	Müller et al. (2013)
Oxygen-insensitive nitroreductase 1 (NTR1)	15307	FMN	NADH, NADPH			Lacks a ferredoxin domain	Nixon et al. (2002), Pal et al. (2009), Olekhnovich et al. (2009), Martinez-Julvez et al. (2012)
Flavohaemoglobin	15009	Fe	NADH, NADPH	NO, O_2	NO_3^-		Rafferty et al. (2010), Mastronicola et al. (2010)

Enzymes without genetic or enzymatic evidence in *Giardia duodenalis*, and cofactors inferred through homology, are displayed in grey. Mutually exclusive substrates and products are separated by ";". For simplicity, the stoichiometry of half-reactions is omitted.

Table 1.2 Reduction potentials of antigiardial nitroheterocyclic drugs and biological redox pairs

Oxidized state	Reduced state	Standard Redox Potential E'_0 (V)	Reference
MTZ-NO_2	MTZ-$NO_2^{\bullet -}$	-0.486	ca Yarlett et al. (1986)
NTZ-NO_2	NTZ-$NO_2^{\bullet -}$	-0.360	Sisson et al. (2002)
Gd Ferredoxin (oxidized)	*Gd* Ferredoxin (reduced)	-0.360	Ellis et al. (1993)
NAD	NAD(P)H	-0.320	
NADP	NADPH	-0.320	
NF-NO_2	NF-$NO_2^{\bullet -}$	-0.250	
Hs Thioredoxin 1 (S-S)	*Hs* Thioredoxin 1 (S-H)	-0.230	
FAD	$FADH_2$	-0.220	
FMN	$FMNH_2$	-0.207	Mayhew (1999)
Acetldehyde	Ethanol	-0.200	
½ O_2	H_2O	+0.820	

The tendency to acquire electrons is lowest for MTZ and highest for O_2. Therefore MTZ can only be reductively activated in electon-rich (i.e., highly reduced) environments. For simplicity, free protons and electrons are omitted. The stated reduction potential of *Giardia duodenalis* ferredoxin is likely an average of multiple ferredoxin proteins in *G. duodenalis* see Ellis et al. (1993). MTZ: metronidazole, NTZ: nitazoxanide, NF: nitrofurans (e.g., furazolidone), *Gd: Giardia duodenalis*, *Hs*: *Homo sapiens*. Unless otherwise stated, reduction potentials for biological redox pairs are quoted from Berg et al. (2002).

Table 1.3 Differential activity/expression of redox-associated enzymes and infectivity of laboratory-derived Mtz-resistant *Giardia duodenalis*

Line	Selected resistance	Cross-resistance	Infectivity	MTZ activation					MTZ detoxification	NADPH metabolism		Protein chaperones & HDACs			References
				PFOR		Fd	TrxR	NR-1	NR-2	NADPH oxidase	GDH	PDI-2	PDI-4	Sir-2	
				PFOR-1 17063	PFOR-2 114609	Fd-1 9662	9827	22677	6175	†	21942	9413	103713	16569	
WB-M3	MTZ (UV)			a ↓											Townson et al. (1996)
713-M3	MTZ (UV)	•	0	a ↓		a ↓		t ↓*	t ↑*	a ↓					Leitsch et al. (2011), Müller et al. (2013), Liu et al. (2000), Townson et al. (1996)
WB-C5	MTZ			t ↓	t ↓			t -	t -		t ↓	t ↑	t -		Müller et al. (2007a), Müller et al. (2013)
1062ID$_{10}$	MTZ	TIN, ORN	10^5	a ↓		a -	a ↑	t -	t ↑*	a ↓					Leitsch et al. (2011), Smith et al. (1988), Müller et al. (2013), Townson et al. (1996)
WB-M1	MTZ (UV)	•	0		t ↓*	t ↓*	t -	t ↓*							Tejman-Yarden et al. (2011)
WB-M2	MTZ (UV)	TIN, ORN	10^6		t -	t ↓*	t -	t ↓*							Tejman-Yarden et al. (2011)
713-M3-C17	MTZ (UV), C17	TIN, ORN		a ↑		a -		t ↓*	t -	a ↓					Dunn et al. (2010), Leitsch et al. (2011), Müller et al. (2013)
106-C17	C17	MTZ	0	a -		a -		t ↓*	t -	a ↓					Dunn et al. (2010), Leitsch et al. (2011), Müller et al. (2013)
WB-C4	NTZ	MTZ		t ↑*	t -	t -	t -	t ↓*	t -	t -	t ↓	t ↑*	t ↑*	t ↓*	Müller et al. (2007a, 2008, 2013), Nillius et al. (2011)
NTZII	NTZ							t ↓*							Nillius et al. (2011)

The drug under which resistant lines were selected is underlined. Cross resistance is reported for compounds where an equal or greater increase in resistance is observed relative the compound used to select for resistance. Infectivity in suckling mice (no. trophozoites in small intestine 4 days post-infection) is stated according to Tejman-Yarden and colleagues (2011). The parent of 713-M3-C17 is 713-M3, which was selected for MTZ resistance prior to selection for C17 resistance (Dunn et al., 2010). ORF codes for strain WB (giardiadb.org) are displayed for relevant genes. Blank spaces indicate a lack of available data. † NADPH oxidase enzyme activity was tested in cell lysates and may result from multiple enzymes including NADH oxidase, DT-diaphorase, thioredoxin reductase and glutamate dehydrogenase (see text). • cross-resistance to other nitroheterocyclics tested but not evident at similar or greater levels than for the selected drug (see text); UV: trophozoites were mutagenized using ultra-violet radiation prior to selection on MTZ; a: enzyme activity; t: transcription; ↑ increase; ↓ decrease; - activity/transcription was tested but not found to be different from the drug-susceptible parent strain; * a test of significance was performed, and differential transcription was found to be significant. Tests of significance are not reported for tabulated enzyme activity assays. GDH: glutamate dehydrogenase, HDAC: histone deacetylase.

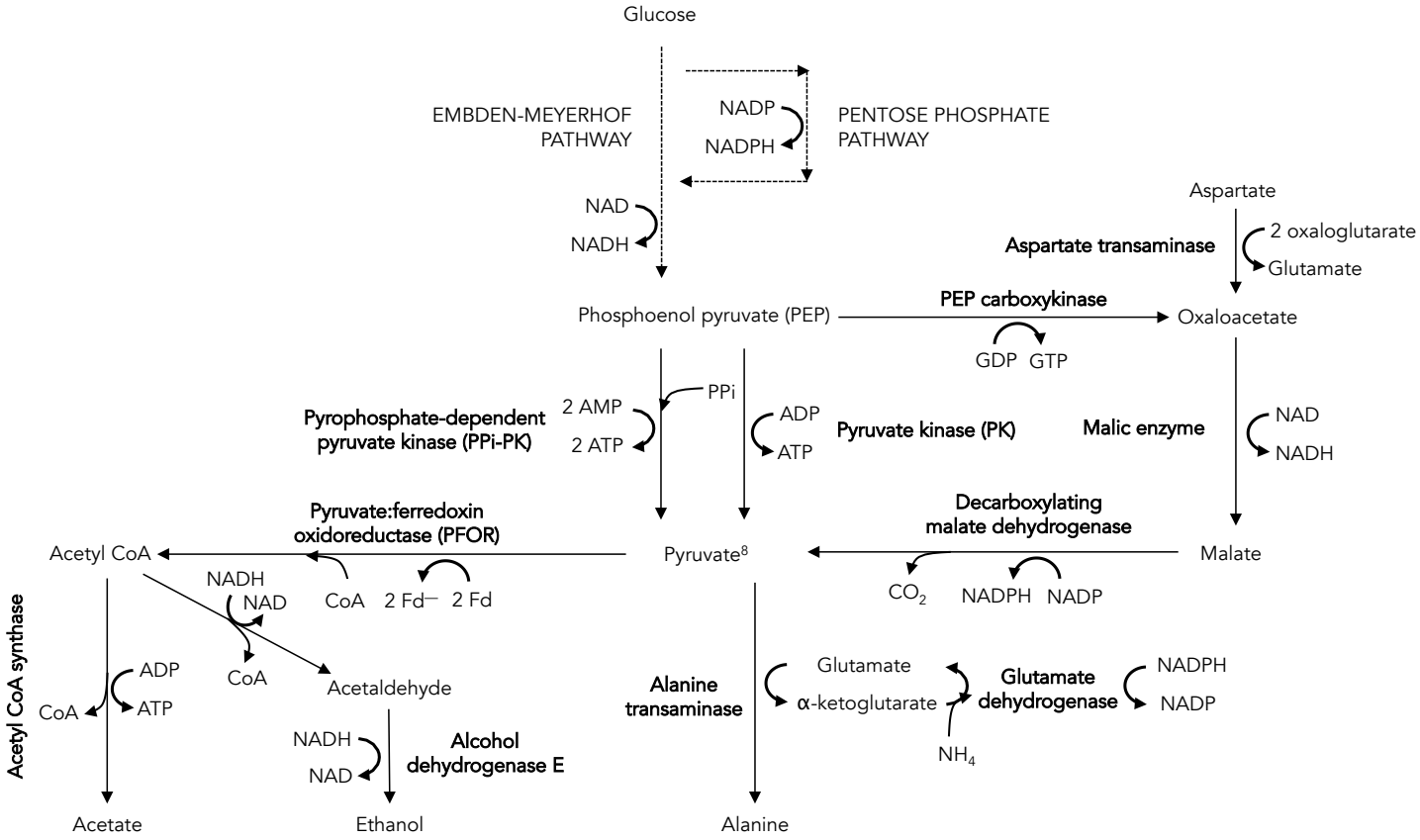


Figure 1.1. Glucose metabolism in *Giardia duodenalis*. Glucose, from endogenous and exogenous sources, and is converted to glucose-6-phosphate which may be diverted to the pentose phosphate pathway (PPP, aka hexose monophosphate shunt, HMS). The PPP yields two molecules of NADPH and can feed back into the classical Embden-Meyerhof pathway, where NADH is formed by glyceraldehyde-3-phosphate dehydrogenase. Under anaerobic conditions, NADP is regenerated from NADPH by the alanine shunt which converts pyruvate to alanine with the concomitant deamination of glutamate. NADPH donates electrons to regenerate glutamate from the resulting α-ketoglutarate, and ammonia. NADH is oxidized to NAD by alcohol dehydrogenase E (ADHE) in the process of reducing acetyl-coA to ethanol. Under microaerobic conditions (~5-80 μM dO_2), antioxidant enzymes regenerate NAD(P), and pyruvate is available for complete oxidation to acetyl-coA and acetate, yielding ATP. Abbreviated pathways are displayed with perforated lines.

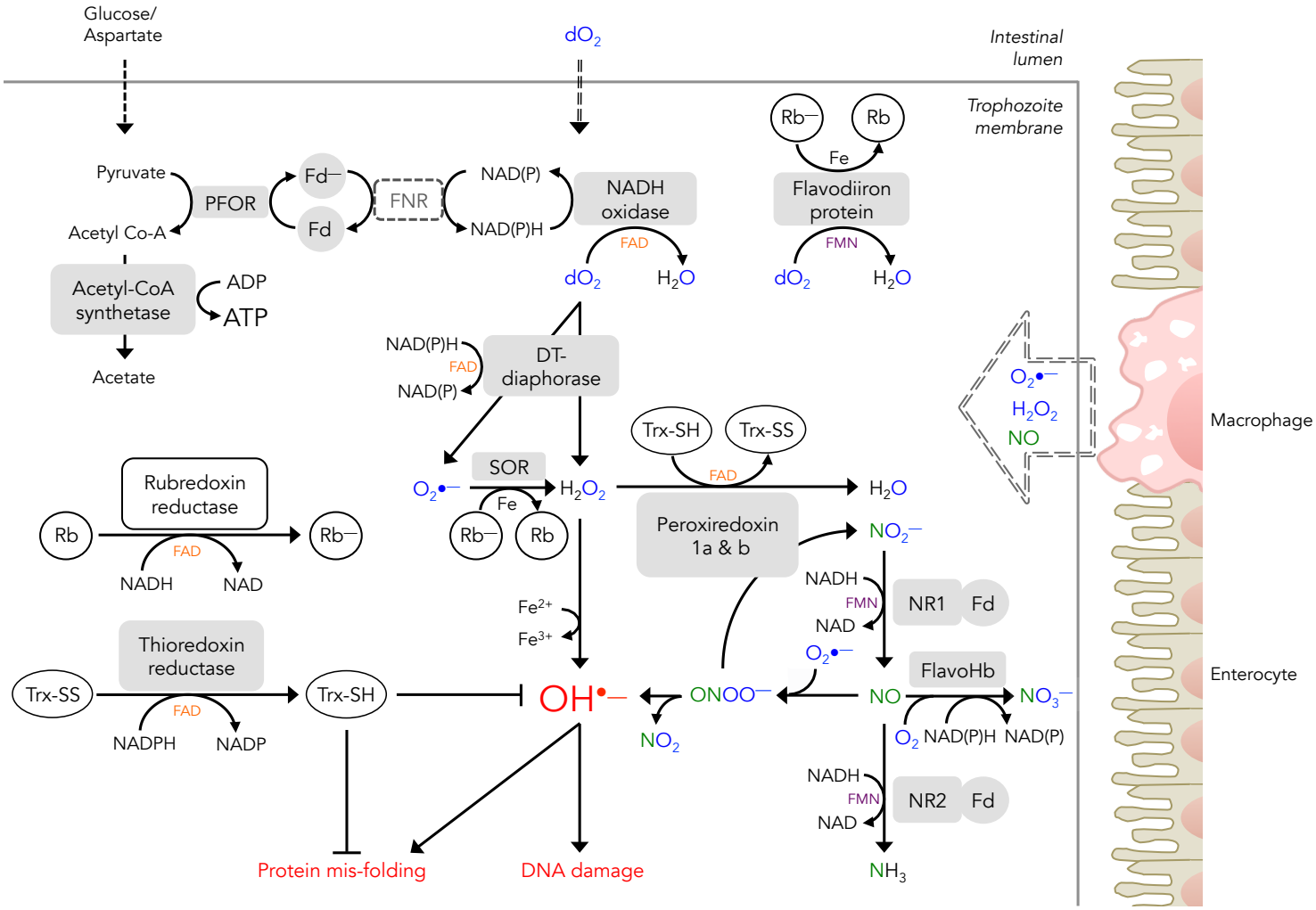


Figure 1.2. ATP production and the antioxidant system in *Giardia duodenalis* trophozoites in the context of a natural infection. Dissolved molecular oxygen (dO_2) and macrophage-generated hydrogen peroxide (H_2O_2), superoxide ($O_2•^-$) and nitric oxide (NO), diffuse into the parasite from the intestinal lumen. NADH and/or NADPH (collectively NAD(P)H) provide electrons to reduce dO_2, NO and associated reactive oxygen- and nitrogen species. Pyruvate and acetyl-coA are therefore available for further oxidation to acetate, yielding ATP. Functionally characterized enzymes are displayed with a solid outline. Enzymes shaded grey have not been characterized in *G. duodenalis* to date but functionally analogous enzymes are inferred to exist in the parasite based on experiments using *Escherichia coli* enzymes. Enzymes for which there is neither genomic nor functional evidence are displayed with perforated outline. PFOR: pyruvate ferredoxin oxidoreductase; Fd: ferredoxin; Fe^{2+}: ferrous iron; Fe^{3+}: ferric iron; NAD(P): oxidized nicotinamide adenine dinucleotide (phosphate); FAD: flavin adenine dinucleotide; FMN: flavin mononucleotide; FNR: ferredoxin NAD(P) reductase; Rb: rubredoxin; SOR: superoxide reductase; Trx-SH/SS: reduced/oxidized thioredoxin; NR: nitroreductase; FlavoHb: flavohaemoglobin; $ONOO^-$: peroxinitrite; $OH•^-$: hydroxyl radical.

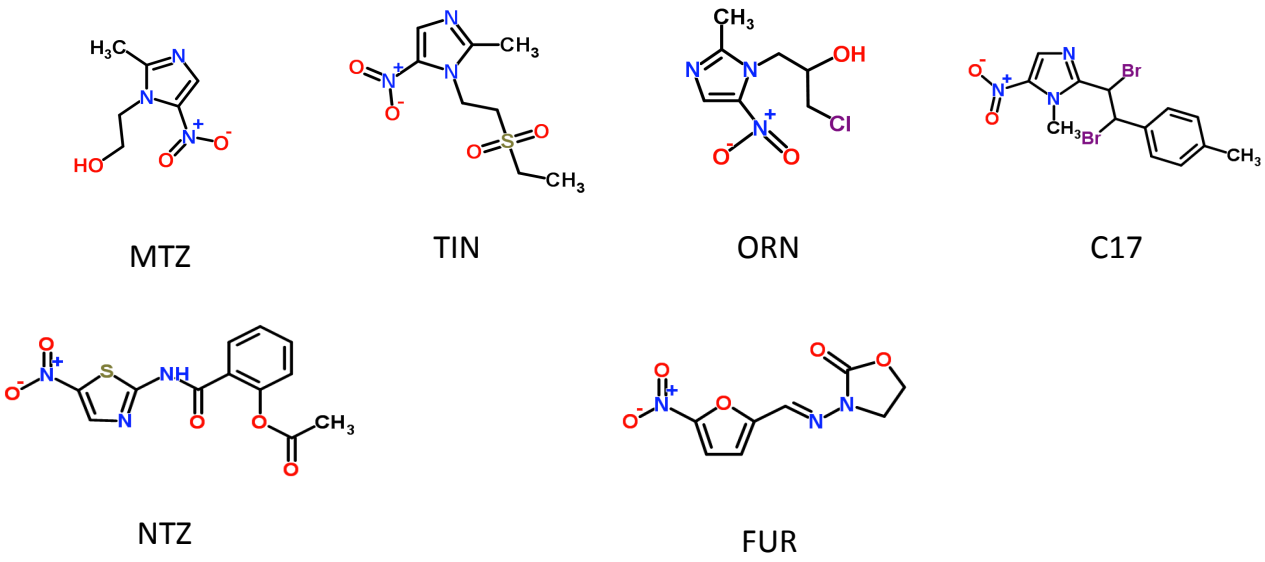


Figure 1.3. Structures of anti-giardial nitroheterocyclic compounds. 5-nitroimidazoles include metronidazole (MTZ), tinidazole (TIN), and ornidazole (ORN), and C17. Furazolidone (FUR) is a redox-active nitrofuran, Nitazoxanide (NTZ) is a nitrothiazole which may act as both a redox-active oxidant and a steric inhibitor of enzyme activity (see main text).

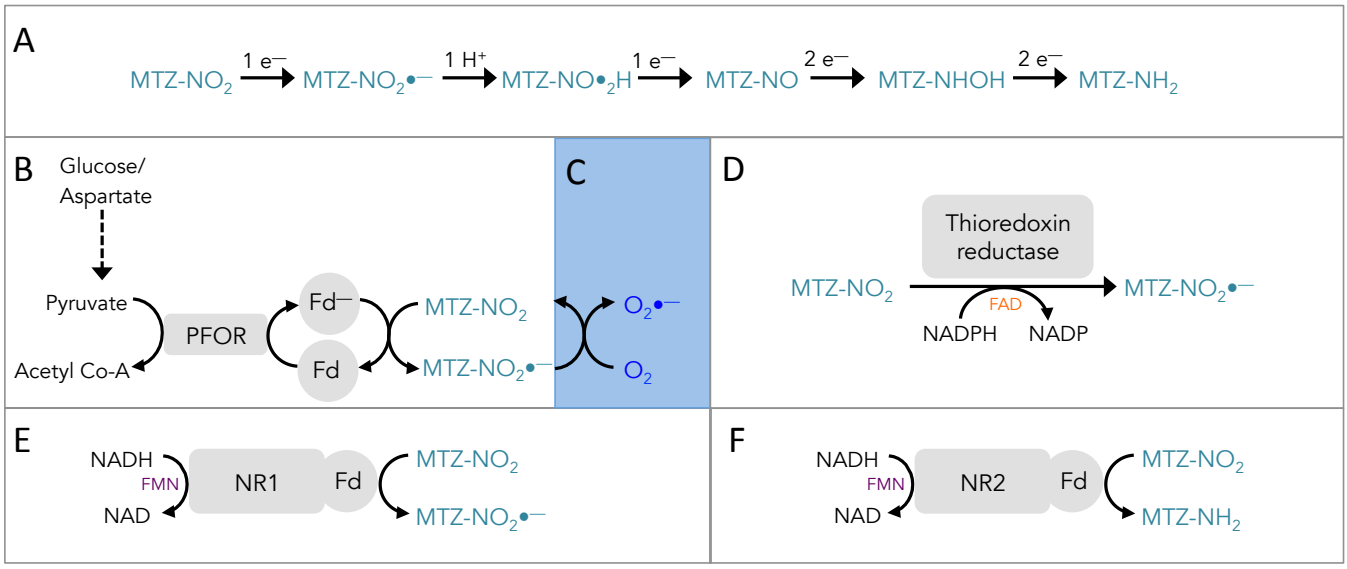


Figure 1.4. Mechanisms of metronidazole activation and detoxification in *Giardia duodenalis*. The metronidazole pro-drug (MTZ-NO_2) enters the cell via passive diffusion and requires univalent reduction by glycolytic or antioxidant enzymes to generate the nitro anion (MTZ-NO_2•$^-$). Further enzymatic reduction or oxidation of biomolecules provides five additional electrons to yield the inert amine (MTZ-NH_2; Panel A). MTZ can accept electrons from ferredoxin (Fd) via PFOR (Panel B), however oxygen can re-oxidize the nitro anion to the pro-drug with the concomitant production of superoxide (Panel C). Thioredoxin reductase can activate MTZ using NADPH as an electron donor (Panel D). Nitroreductase 1 is evidenced in activating MTZ to reactive intermediates (Panel E) whereas nitroreductase 2 may detoxify MTZ by completely reducing the pro-drug to an inert amine (Panel F). For simplicity, only the univalent reduction product is displayed in panels B,D,E & F, however these mechanisms may supply additional enzymes to activated intermediates. PFOR: pyruvate ferredoxin oxidoreductase; FNR: ferredoxin NAD reductase; NR: nitroreductase.

Chapter 2. Materials and Methods

Comprehensive materials and methods are provided within each research chapter.

Chapter 3. Annotation of the *Giardia* proteome through structure-based homology and machine learning

Abstract

BACKGROUND *Giardia duodenalis* is a genetically divergent eukaryote and a major intestinal parasite of humans, causing millions of cases of diarrheal disease annually. Research on this parasite is hampered by the vast number of divergent genes in its genome. The functions of these genes are not discoverable using conventional sequence-based annotation algorithms. Computationally powerful protein structure prediction tools, such as the I-TASSER suite, hold great promise for sensitive prediction of the function of divergent genes. However, methods to infer the quality of large sets of predicted structures are now required.

AIMS This study aimed to predict structures for the hypothetical *Giardia* proteome using I-TASSER, and then to informatically differentiate high- from low-quality predictions.

METHODS The peptide sequences of 4,626 hypothetical proteins were submitted to I-TASSER software, which produced a putative three-dimensional structure, and identified the closest experimentally-determined structural homologue of each hypothetical protein. Numerous metrics describing the alignment were also produced. Functional domains in the peptide sequences of each query and its closest structural homologue were identified using InterPro Scan. The extent of InterPro annotation agreement, and the structural alignment metrics were used as training factors and features respectively in a random forest classifier.

RESULTS Identical IPR annotations were found between 45% of BLAST-annotated query peptides and their closest structural homologues. For hypothetical proteins, this figure was 9%. A classifier trained on alignment metrics for annotated proteins only, classified the IPR match status of the training data with 91% accuracy, but performed poorly on a test set of hypothetical proteins. A training set expanded to include equal proportions of annotated and hypothetical protein alignment data performed with ~90% accuracy over the entire data set. The expanded classifier identified 375 'high-confidence-like' hypothetical protein structures (essentially false positive classifications). These structures included a cytochrome p450-like molecule and a ferredoxin:NAD(P)H reductase-like enzyme, which may complement the incomplete redox pathways reported in *Giardia* to date.

CONCLUSION Protein structure prediction software has great potential to illuminate the biology of genetically divergent organisms, including human pathogens. Using agreement in peptide sequence annotations as a proxy for structural alignment quality, can stratify predicted structures for further investigation. A classifier trained on this information identifies high-quality-like structures that are otherwise beyond the reach of informatic quality control.

Introduction

Giardia duodenalis is a microaerophilic, parasitic protist that causes diarrhoeal disease in 200-300 million people annually. *G. duodenalis* is also a deep-branching eukaryote, with little genetic similarity to model eukaryotes such as yeast. As such, at least one third of genes predicted in this parasite have not been functionally annotated (Morrison et al., 2007). The lack of functional information for these proteins precludes our ability to understand a range of essential biological functions in the parasite, including metabolism, signaling and stress response mechanisms. Similar problems beset research on many other pathogens, indluding the protists *Plasmodium vivax*, *Trichomonas vaginalis* and *Entamoeba histolytica*, and bacteria such as *Mycobacterium tuberculosis*. Because these pathogens encompass massive genetic diversity and are often incompatible with standard laboratory culture or reverse genetic technologies, insufficient functional gene annotation hampers basic research, and therapeutic development.

In the absence experimental functional characterization, the function of protein-coding domains is generally inferred by comparing the sequence of interest ('query') with functionally characterized genes of similar sequence ('homologous templates'). The predominant algorithms for sequence-based homology searching are Hidden Markov Modeling (HMM) (Karplus et al., 1998), and BLAST (heuristic local alignment) (Altschul et al., 1997). HMM can be more sensitive than BLAST, however the utility of both drops when amino acid (AA) sequence identity between the query and the template is less than 20% (Rost, 1999). The three-dimensional structure of a protein tends to tolerate large variations in the sequence of constituent amino acids, and is thus a robust predictor of function (Illergård et al., 2009). Comparison of three-dimensional structures can potentially provide a more sensitive method for inferring the function of highly divergent proteins, that is, those that lack sequence-based homologues. However, empirical determination of protein structure (for example using X-ray crystallography or nuclear magnetic resonance) remains laborious and expensive, and subject to chemical, purity and yield constraints. *In silico* prediction of protein structure provides an attractive alternative to empirical structure determination, which can be applied on a genome-wide scale to assist with functional gene annotation.

Numerous computational methods have been developed to predict protein structure from the constituent primary amino acid sequence (iTasser, modeller, rosetta). Since 2008, the I-TASSER software suite has consistently ranked among the best performing protein structure prediction programs, as tested in the biennial Critical Assessment of Structure Prediction (CASP)

competition (Roy et al., 2010). This software is capable of correctly predicting the structure of query peptides with < 20% AA identity to available templates (Wu et al., 2007). Named for Iterative Threading ASSEmbly and Refinement, I-TASSER uses peptide sequence homology combined with secondary structure prediction, to support iterative refinement of predicted tertiary structures which are modeled on homologous regions of empirically-determined protein structures available in the RSCB Protein DataBank (PDB). The structure of any non-homologous region in the query is predicted *ab initio*, and molecular dynamics simulation is then used to minimize the free energy of up to five independently predicted models— each representing the entirety of the query peptide in three-dimensional space. The TM-align module compares the best model, (defined as that with the highest confidence score, described below) is compared to empirically determined protein structures in the PDB, and the functional information for the closest structural homologue (or 'best hit'), can be inferred for the model (Roy et al., 2010). The I-TASSER web-server allows the prediction of protein structure and assignment of structural homologues for individual proteins up to 1,500 AA within three to five days. A stand-alone version permits parallelization of these predictions. Although a substantial undertaking, with a sufficiently high-throughput computing cluster, it is possible to predict the structures and respective best hits for an entire proteome.

A number of metrics are generated by I-TASSER to describe the alignment between the query and the best hit. Firstly, the extent of structural homology between the predicted model and the best hit is expressed in the TM score; a product of the root mean squared deviation (RMSD, Å) of α carbon atoms in each structure, the proportion of the query aligned against the best hit ('coverage') and the AA identity in the aligned region. A simple ratio of the total query AA length to the total hit AA length ('Len Ratio') is easily calculated. Inherent properties of the predicted structures may also be informative. The likelihood of each AA in a peptide to form an α helix, β strand or coil region is conveyed in the secondary structure (SS) prediction. Assuming that a structure with equal proportions of these three secondary structures is of greatest complexity, a crude estimate of complexity can be calculated as 0.3 ÷ the highest proportional SS. A confidence score (C-score) conveys the quality of the model based on the degree of convergence from multiple threading iterations. A predicted TM score and RMSD are calculated as a function of the C-score for the model, based on previous benchmarking of these measurements using 500 non-homologous proteins (Zhang 2008), and are hereafter termed 'TM-model' and 'RMSD-model'. Predicted error for these measurements is also provided ('TM-sd-model' and 'RMSD-sd-model'). These measures differ from the TM and RMSD calculated between the model and the best hit in the PDB.

Unlike output from BLAST or HMM searches, which can be independently validated by inspecting query:template sequence alignments, predicted structures are difficult to assess independent of the quality metrics that accompany the software output (detailed above). Furtherm, as manual inspection of the alignment between each model and its best hit is impractical on a genome-wide scale, informatic approaches are now required to expedite a more independent assessment of the quality of predicted structures. One approach is to use test for agreement between sequence-based annotations for the query peptide, and the closest empirically-determined structural homologue (i.e., the 'best hit'). Those predicted structures for which query annotations match with annotations for the best hit, can be considered 'high confidence' structures. Metrics describing the alignment between the query and the best hit in three-dimensional space (detailed above), can be used to train a classifier to identify the salient properties of high-confidence structures, and thus to identify 'high-confidence-like' structures for which sequence-based annotations cannot be generated, or do not agree with the best hit. The InterPro (IPR) database integrates the functional predictions from multiple HMM (sequence-based) search algorithms, into a unified nomenclature with associated IPR codes. These codes can be assigned relatively quickly to any proteome using InterProScan software (Jones et al., 2014), and comprise a hierarchy of protein families, domains and conserved sites. For example, the 'protein phosphatase 2A family' (IPR000009) is the 'parent' of a repeat domain 'WD40 repeat' (IPR001680) and two conserved sites: 'PP2A PR55 CS' (IPR018067) and 'WD40 repeat CS' (IPR019775). IPR codes are available for many protein structures in the PDB. Thus it is possible to compare IPR codes assigned to a query peptide, with those available for its closest predicted structural homologue (see schematic Figure 3.1). In this work, predicted structures for which at least one sequence-derived IPR code matches with a structure-derived IPR code, are considered 'high-confidence' structures (see schematic Figure 3.1).

Here, we use high-powered computing to predict the structures of ~3,700 hypothetical proteins encoded in the *Giardia duodenalis* genome (strain WB-C6), and create a random forest classifier to assist with prioritizing structures for further investigation. The classifier learns the salient features of high-confidence structures, and thereby identifies 'high-confidence-like' structures that would otherwise lie beyond the reach of informatic validation. To our knowledge, this represents the most sensitive and ambitious application of structural genomics to a pathogenic protist yet reported.

Materials and Methods

Peptides identified in the *Giardia duodenalis* WB-C6 genome strain (assemblage A) as 'hypothetical protein' were downloaded from GiardiaDB.org (release 25) and peptides of at least 30 and not greater than 1,500 amino acids in length were selected. A control set of 234 *G. duodenalis* proteins with a functional annotation available via BLAST were also selected. Primary amino acid sequences were submitted to InterProScan (v5-44.0) for IPR code annotation. Paralogous protein groups were identified using inParanoid as implemented in orthomclPairs (v2.0) (Li et al., 2003). The stand-alone implementation of I-TASSER (v3.0) was run in serial on x86 cores with the following parameters: runI-TASSER.pl -light true -LBS true -GO true -nmodel 1, stipulating a light implementation with ligand binding sites and GO terms predicted for a single model. TM-align was used to search among predicted *Giardia* protein structures for crystal structure homologues.

For each hypothetical or control protein sequence ('query'), the primary AA length was extracted from GiardiaDB.org. Metrics for the predicted structure (model) including C-score, TM-model, TM-sd-model, RMSD-model and RMSD-sd-model were extracted from the 'C-score' output file. The SS complexity was expressed as (0.3 ÷ highest proportional SS), using the 'seq.ss' output. The PDB code and chain identifier for the closest structural homologue in the PDB, and associated TM score, RMSD, coverage and percent AA identity metrics, were extracted from the 'similarpdb_model1.lst' file output. Species and molecule descriptions, and primary AA length for the closest structural homologue ('best hit') were extracted via rcsb.org/pdb/ using curl (Unix). Similarly, IPR codes associated with each best hit were extracted via https://www.ebi.ac.uk/pdbe/api/mappings/interpro/. Obsolete PDB codes were updated based on ftp://ftp.wwpdb.org/pub/pdb/data/status/obsolete.dat. The primary AA length of the query was transformed as a ratio of the length of the best hit.

The hierarchy for IPR codes was extracted from ftp://ftp.ebi.ac.uk/pub/databases/interpro/interpro.xml.gz. Query sequences were divided into two groups based on the extent of agreement between IPR codes assigned via InterProScan, and those assigned to the best hit. Sequences for which at least one sequence-derived IPR code was identical to a structure-derived code were termed 'IPR-exact' matches. Those for which no agreement was found were termed 'noMatch.' Pairwise correlations for each continuous metric were visualized using the R packages 'ggplot2' and 'GGally'. The 'caret' package was used to train a random forest classifier, with all of the above variables supplied

and the 'IPR-exact' category as the factor of interest. Five-fold cross-validation was used to refine the classifier. The relative contribution of each variable was calculated as the mean decrease in Gini co-efficient. Three dimensional scatter plots and transcriptional clustering heat maps were generated with the R packages 'scatterplot3d' and 'gplots' respectively. Protein structures were visualized using USCF Chimera (Pettersen et al., 2004). For brevity *G. duodenalis* gene identifier prefices are abbreviated from GL50803 to 'GL'. Online supplementary material is available at DOI: 10.13140/RG.2.2.26965.73440

Results

Structures were predicted for 234 randomly selected BLAST-annotated proteins and 4,626 hypothetical proteins, of which 117 (50% of total) and 893 (19.3%) respectively were annotated with InterPro (IPR) codes via InterProScan. These sequence-derived IPR codes were compared with codes assigned to the best structural hit in the PDB inferred by I-TASSER. Statistics for IPR code matches are presented in Table 1. For preliminary analysis, structures were grouped according to their IPR match status ('IPR-exact,' or 'noMatch'). Those structures for which at least one sequence-derived IPR code matched exactly with a structure-derived code, are considered 'high-confidence' structures (Figure 3.1). Those structures for which sequence- and structure-derived IPR codes do not match, are designated 'lower-confidence.' Density distributions for query:match alignment variables, and pairwise scatter plots and Pearson product-moment correlation coefficients (*r*), are presented in Figure 3.2 (BLAST-annotated proteins) and Supplementary Figure 3.1 (BLAST annotated and hypothetical proteins). Examples of query:hit alignments for high-confidence annotated and hypothetical proteins are displayed in Figure 3.3a and 3b. Descriptions of the continuous variables and all data used for this work are available in Supplementary Table 3.1 (available on request).

To determine the inherent structural features and query:hit alignment features that best predict the high-confidence (i.e., 'IPR-exact') category, a random forest model was trained on 234 BLAST-annotated control proteins. This model accurately classified 95% and 87% of high- and lower confidence structures in the training set, respectively. On the test data set of 4,626 hypothetical protein structures (omitting five structures with C-scores < -5), the model classified 97% of lower confidence structures correctly, but only 50% of high-confidence

structures. The sub-optimal performance of the classifier on the latter category may be due to the conservative and relatively small training set, which contains only proteins with relatively high amino acid identity to proteins in other species. We therefore incorporated into the training set data from a further 100 high-, and 100 lower-confidence structures, which lack a BLAST annotation (i.e., hypothetical proteins). The expanded model classified structures in the original training set with 100% accuracy, and classified high- and lower confidence structures in the test set with 87% and 91% accuracy, respectively (Table 2). Amino acid identity was the most informative predictor of high-confidence structures, accounting for at least 50% of classification accuracy in both the original and expanded models. The C-score and TM score for the predicted structure (TM_model) independently accounted for at least 10% of the classification accuracy in both models, however the ratio of the query-to-hit peptide length (Len Ratio) was vastly more predictive in the expanded model. All other variables accounted for < 10% of classification accuracy in both models (Figure 3.4a). From this we conclude that high-confidence structures tend to have ≥ 8% AA identity with the best structural hit, C-scores ≥ -4.4 and query:hit AA length ratios ≥ 0.21. Indeed, IPR-matched and unmatched structures can be reasonably well separated on these three variables (Figure 3.4b), although these parameters still permit approximately 1,800 lower-confidence structures, indicating limited sensitivity. When IPR codes were aggregated for high-confidence and HCL proteins, on average 2 unique sequence-derived codes were available for each high-confidence protein, whereas on average 6.4 unique IPR codes could be inferred through structural homology searching. For HCL proteins, on average 0.4 sequence-derived terms were available per peptide, which increased to 4.38 when structure-derived terms were added. Combining unique IPR codes from both sources thus increases the functional information available for high-confidence and HCL proteins by factors of 3 and 4 respectively (Figure 3.4c).

Importantly, this classification approach is able to detect structures without matching IPR codes (i.e., lower-confidence category) that have similar qualities to high-confidence structures. Some 93 lower-confidence structures were classified as high-confidence by the original model. The expanded model detected 375 such structures, including 72 of the 93 structures identified by the original model. These structures are hereafter referred to as 'high-confidence-like' (HCL) (Table 3). Twenty-three HCL structures were associated with sequence- and structure-derived IPR codes within the same IPR hierarchy. Further, 57 HCL structures assorted with at least one other HCL structure into 23 paralogous groups, as defined by inParanoid (sequence-based clustering). Examples of HCL query-hit alignments are displayed in Figure 3.3c, and all alignments are available in supplementary materials.

Further investigation of the high-confidence (BLAST annotated and un-annotated; n = 456) and HCL (un-annotated; n = 375) structures, revealed a number of interesting putative biological functions. For example, GL_15897 is a high-confidence hypothetical protein with predicted structural similarity to a human nitric oxide synthase/cytochrome P450 reductase (CYPOR) family enzyme (PDB code 1TLL). The *Giardia* enzyme shares 21% AA sequence identity with an annotated NO synthase, GL_91252, and FMN, FAD and NADP binding domains have been annotated in both peptide sequences (Jedelský et al., 2011). Although the pair are not classified as paralogues by inParanoid or orthoMCL, their predicted structures are highly similar (RMSD = 0.81 Å over 376 AA)(Figure 3.5). The presence of putative CYPORs in *Giardia* is puzzling because the substrate, cytochrome P450, has not been identified to date (Pazdzior et al., 2015). It is therefore interesting to note a putative cytochrome P450 (GL_9900) among the HCL hypothetical proteins in our data, in which both heme and non-peptide substrate binding sites are predicted. GL_9900 and GL_91252 diverge from GL_15897 and cytochromes b5 in transcriptional clustering analysis (Figure 3.5).

Another intriguing HCL hypothetical protein, GL_87577, shows predicted structural homology with a bacterial glutamate synthase family enzyme (PDB code 2VDC). GL_87577 appears truncated at the N-terminal relative to the annotated *Giardia* glutamate synthase (GL_7195), itself a putative product of horizontal gene transfer (Andersson and Roger, 2002). The glutamate synthase β sub-unit fold also resembles that of the ferredoxin:NADP reductase (FNR) β sub-unit (Demmer et al., 2015). FNR activity is assumed to occur in *Giardia*, which relies heavily on ferredoxin-based electron transport for glycolysis and antioxidant activity, but has not been identified to date (reviewed in Chapter 1). In addition, two enzymes formerly annotated as glutamate synthase β-subunits in *Entamoeba histolytica* are reported to lack glutamate synthase activity and instead to function as FNRs (Jeelani et al., 2010). These enzymes reductively activate the anti-amoebic drug metronidazole, which is also a major anti-giardial treatment, and form hydrogen peroxide under aerobic conditions. The predicted structures of both *E. histolytica* enzymes resemble that of GL_87577 and GL_7195 (Figure 3.6). In many bacteria, FNRs function as a heterodimer (Demmer et al., 2015), however the *E. histolytica* FNR functions without an α sub-unit. Similarly, structural homology searching of predicted *Giardia* hypothetical protein structures using the *T. maratima* FNR α-subunit (Demmer et al., 2015) were unsuccessful. GL_7195 is significantly up-regulated in the metronidazole-resistant line 713-r, and GL_87577 is up-regulated in 713-r and 106-r (Chapter 7). Both genes are down-regulated after exposure to sub-lethal metronidazole and thermal

stress, however, and GL_87577 is up-regulated after exposure to hydrogen peroxide (Chapter 6).

Discussion

Protein structure prediction is a relatively inexpensive and potentially highly valuable tool for gaining insight into the biology of genetically divergent organisms. Decreasing computing costs coupled with increasing power will likely support the wide-spread use of structural genomics in functional genome annotation in the near future. However, metrics supplied by structure prediction programs tend to be highly correlated, and 'rules of thumb' suggested by software authors for judging the quality of computed structures can be difficult to interpret. Informatic approaches that rapidly assess the quality of structure-based functional predictions on a proteome-wide scale, are now needed. To this end, we used agreement between sequence-derived InterPro (IPR) codes for query peptides and their best structural hits, as an 'independent' proxy for protein structural alignment quality. Thus permitted, we infer higher confidence in the structural and functional information predicted for query peptides when at least one IPR code match exists. We created a random forest classifier to predict membership of the high-confidence category, using structural alignment metrics generated by I-TASSER, and additional coefficients calculated therefrom, in order to define the relative contribution of each metric to classification accuracy. This further enabled the identification of high-confidence-like (HCL) structures, which may be highly genetically divergent but maintain a conserved fold. It is not surprising that the AA identity between the query and best structural hit is the most informative predictor of high-confidence structures. Sequence similarity is the standard measure of structural and functional similarity, and I-TASSER incorporates this metric where applicable, to identify potential structural templates (Roy et al 2010). The coverage metric calculated by the software had less predictive power than the simpler query:hit length ratio derived especially for this analysis. This may be because coverage is insensitive to cases where the query is vastly shorter than the best hit, which occur frequently in our data. Although it is tempting to define simple thresholds for the most predictive values that might separate high-confidence structures, this will generally be a poor substitute for the high sensitivity of a trained classifier.

The high-confidence and HCL categories could be used to stratify predicted protein structures, whereby high-confidence structures are prioritized for further experimental investigation, or their annotations incorporated into functional informatic analyses, followed by HCL structures. We suggest that sequence-derived IPR codes should be retained when available, and

augmented with structure-derived codes for high-confidence and HCL proteins. Structure-derived IPR codes for lower-confidence structures should be treated with caution. Extension of the approach presented here could try to improve the resolution of information associated with high-confidence structures by incorporating hierarchical IPR information into the random forest model; weighting alignment metrics according to the number of matched IPR codes; and differentiating matches according to the code sub-type (family, active site, binding site, or domain). It would also be valuable to create independent classifiers using expertly curated high-confidence structural alignments, and to compare their performance to our unsupervised IPR code-matching approach. An important question remains as to whether a classifier trained on one organism is useful for other genetically distant organisms. Predicting structural proteomes for a diversity of phyla and applying this classification approach, can shed light on the potential for developing a broad-specificity classifier for prioritizing predicted protein structures, or whether bespoke classifiers are best. On this point, we expect that the classifier developed in this work should be relatively conservative, given the vast evolutionary distance between *Giardia* and the model organisms from which the majority of experimental structures are derived.

Technical considerations aside, this work demonstrates the exceptional value of structural genomics for illuminating understudied and genetically divergent biological systems, such as *Giardia*. The electron transport systems in *Giardia* are of particular interest given the sensitivity of this parasite to nitroheterocyclic drugs, namely metronidazole, which must be enzymatically reduced to become activated (Edwards, 1993a). Many electron transport enzymes in the parasite incorporate ferredoxin domains, which bind iron-sulfur clusters that support the flow of electrons. Metronidazole activation has been mostly attributed to ferredoxin family enzymes to date, however because electron transport chains remain incompletely described, other components are likely to be involved. In higher eukaryotes, cytochromes P450 couple with P450 reductases (CYPORs) to form broad-specificity drug detoxification systems (Zanger and Schwab, 2013). CYPORs are oxidoreductases that accept electrons from NADPH, and shuttle them via bound FMN and FAD cofactors to reduce heme bound in cytochrome P450 (Hamdane et al., 2009; Hubbard et al., 2001). The heme group is then oxidized by molecular oxygen, and detoxification of a proximally bound substrate occurs through monoxygenation (Schenkman and Jansson, 2003). Although cytochrome P450 orthologues have not been described in *Giardia* to date, cytochromes b5 are well documented (Pazdzior et al., 2015; Pyrih et al., 2014; Yang et al., 2016), and are reduced by GiOR-1 (GL_91252) *in vitro* (Pyrih et al., 2014). Cytochromes b5 are thought to increase the efficiency of the reduction of cytochromes P450 by CYPORs

(Schenkman and Jansson, 2003). The putative cytochrome P450 identified among HCL structures in this work (GL_9900), is exciting given that no functional information has previously been generated for this peptide. Transcriptional profiles are available, however, and reveal that GL_9900 is transcribed in a similar manner to GiOR-1, while the putative CYPOR GiOR-2 (GL_15897) and cytochromes b5 exhibit more diverse transcriptional profiles. A possible physiological interaction between GiOR-1 and GL_9900 would be further supported by localization of the latter to the mitosomes (vestigial mitochondria), as is demonstrated for GiOR-1 (Jedelský et al., 2011). Further, clinical studies and experimental perturbation of human hepatocytes indicate that cytochromes P450 may be inhibited by metronidazole (Kazmier, 1976; Kudo et al., 2014), raising the prospect that GL_9900 interacts with metronidazole in *Giardia*. Work is now required to determine whether GL_9900 constitutes an electron acceptor in a cytochrome redox system in *Giardia*, and whether any interactions with metronidazole produce reduction products suggestive of a novel drug activation mechanism.

The bacterial glutamate-synthase-like structures identified in this work provide further insight into electron transport systems in *Giardia*. As mentioned previously, ferredoxin-based electron transport chains predominate in this parasite, being essential for energy generation and antioxidant activity. Pyruvate decarboxylation is linked to reduction of soluble ferredoxins, and oxygen is assumed to act as a terminal electron acceptor when available (reviewed in Chapter 1). Ferredoxin:NAD(P)H reductase (FNR) activity is likely required to link glycolysis with reduction of oxygen, and has been theoretically attributed to ferredoxin-nitroreductases (Ali and Nozaki, 2007 Chapter 7), however such activity is yet to be demonstrated. Here we identify GL_87577 as a glutamate synthase-like structure in the HCL category. The only functional information previously available for this peptide is a 'nucleotide binding domain' annotation (GiardiaDB.org). Output from I-TASSER predicts that this nucleotide is FAD (flavin adenine dinucleotide). The structural similarity between GL_87577, the C-terminal domain of the annotated glutatmate synthase (GL_7195), and FNRs in *E. hystolytica* and *T. maratima* (Figure 3.6) strongly support the possibility that GL_87577 and/or GL_7195 function as FNRs in *Giardia*. The large ferredoxin domain in the N-terminal of GL_7195 renders this the most parsimonious FNR candidate. However, because the relatively truncated N-terminal domain in the *E. histolytica* orthologue is sufficient to support FNR activity, the potential for this activity in GL_87577 also warrants testing. For example, it is conceivable that the numerous soluble ferredoxins in *Giardia* may associate with the N-terminal of GL_87577 to facilitate the FNR reaction. Lastly, that the genes encoding both GL_87577 and GL_7195 are transcriptionally up-regulated in *Giardia* trophozoite lines that are resistant to metronidazole, further supports a

potential role in electron transport, as modulation of ferredoxin-based electron transport chains is a common feature of metronidazole resistance (Chapter 7).

This work presents a novel approach for classifying computationally predicted protein structures *en masse*. We used the I-TASSER suite to predict the structure of 4,860 *Giardia duodenalis* proteins, including around 3,700 hypothetical proteins for which no functional information was available previously. We devised a triangulation approach wherein agreement between InterPro annotations for a query peptide and its closes structural hit serves as a proxy for structural alignment. The random forest model trained on this data correctly classified the vast majority of high- and lower-confidence structures, but also revealed hundreds of high-confidence-like (HCL) structures which lie beyond the reach of IPR code triangulation. This approach therefore vastly increases the functional information available for hypothetical proteins. It is important to note that lower-confidence structures, for which IPR codes are not available, or for which sequence- and structure-derived IPR codes do not match, are not necessarily poor predictions. Rather, we cannot infer the quality of those predictions using the present approach. Functional information for the highly divergent peptides that predominate among lower-confidence structures may yet be inferred through the development of a more refined classifier, possibly in conjunction with expression clustering, or high-throughput sub-cellular localization analysis (Dawson and House, 2010; Hagen et al., 2011), for example.

Structural genomics is likely to prove particularly important for further understanding pathogens and archaea that are intractable in the laboratory, or lack sufficient research funding. We have focused on the human intestinal pathogen *Giardia* to demonstrate the utility of computational structural approaches for illuminating long-standing biochemical questions which are relevant for understanding mechanisms of anti-giardial drug action. The high-confidence and HCL structures we identify provide a starting template for experimental crystallographic structure prediction, drug docking experiments, and mutational analysis. Importantly, this approach has the potential to provide valuable additional functional information for any organism with a sequenced genome of reasonable quality, and should be amenable to output from other structure prediction software (e.g. MODELLER (Eswar et al., 2006), Rosetta (Kim et al., 2004)). We look forward to further refinement and implementation of this approach, and its potential both for probing divergent biological systems, and fighting disease.

Table 3.1. Sequence- and structure-derived InterPro code summary for annotated and hypothetical *Giardia* proteins.

		IPR code available via		IPR match (% of total)
BLAST annotation	Total	InterProScan	PDB structure	Exact
Present	234	117	198	107
Absent	4626	893	3071	401

Table 3.2. Random forest classification accuracy.

			Accuracy			Accuracy		
	Test set	Train 1	Train 1	Test	Train 2	Train 1	Train 2	Test
IPR match	401	107	0.95	0.50	207	1	0.92	0.87
IPR no match	4225	127	0.87	0.98	227	1	0.90	0.91
BLAST annotation	0	234			234			
Total	4626	234			434			

Test set: test data set; Train 1: training set of BLAST-annotated peptides; Train 2: training set of BLAST-annotated and additional un-annotated peptides.

Table 3.3. Classification of un-annotated (hypothetical) proteins by random forest models.

			Train 1		Train 2	
TRUE	PREDICTED	Category	N. structures	% of total	N. structures	% of total
IPR exact	IPR exact	High-confidence	201	4.3	349	7.5
IPR exact	No match	Lower-confidence-like	200	4.3	52	1.1
No match	IPR exact	High-confidence-like	93	2.0	375	8.1
No match	No match	Lower confidence	4132	89.3	3850	83.2

Train 1: Random forest model trained on BLAST-annotated peptides; Train 2: Model trained on combination of BLAST-annotated and un-annotated peptides (see Table 3.2).

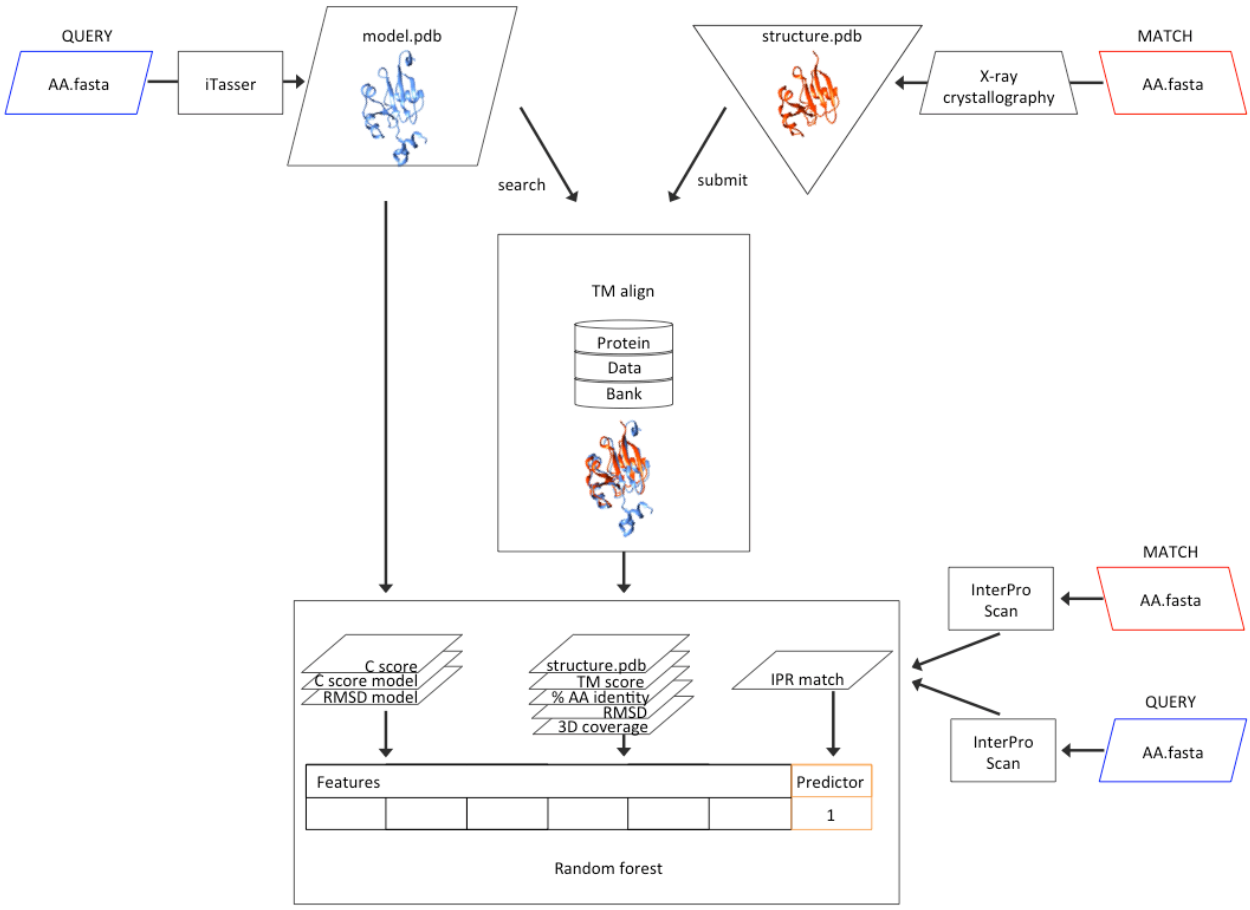


Figure 3.1. InterPro code agreement as a proxy for quality of alignment between computationally predicted and experimentally solved protein structures. Three dimensional protein structure is predicted from the *Giardia* query protein sequence using I-TASSER software, and searched against the protein databank of experimentally solved protein structures, using TM-align. InterPro codes are predicted from primary amino acid (AA) sequences using InterPro Scan software. InterPro codes assigned to the query and the best structural homologue ('match') are compared, and structural alignments associated with an exact code match (such as in this example, denoted '1'), are considered 'high-confidence'. Metrics describing the structural alignment between the query and the best hit for high-confidence alignments, are used as features to train a random forest classifier, which can then identify 'high-confidence-like' alignments. As per audit flow-chart conventions, rhombi denote input/output files; rectangles denote computational processes; trapezoids and triangles denote manual processes, and manually created files respectively. The cylinder denotes a database.

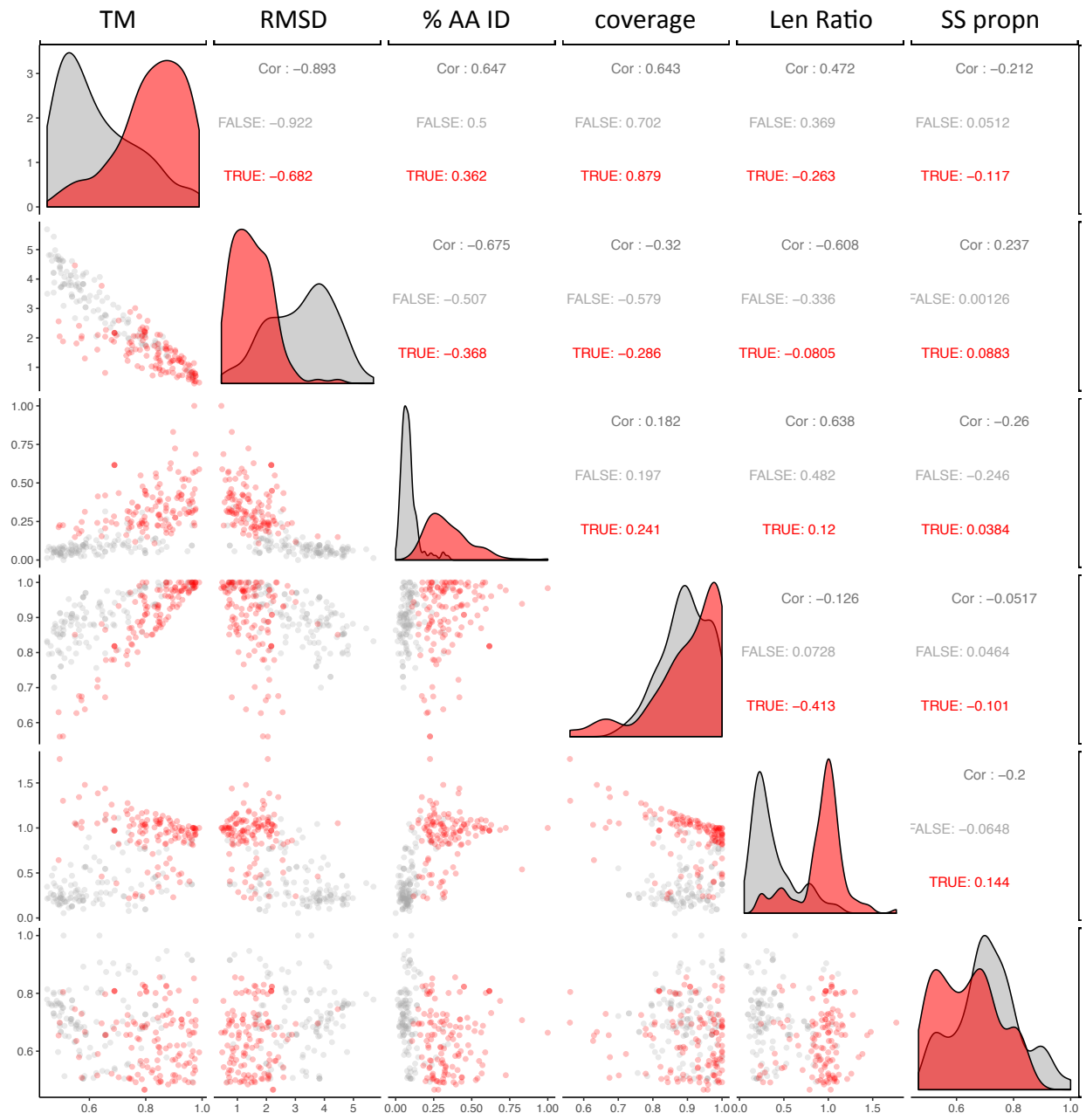
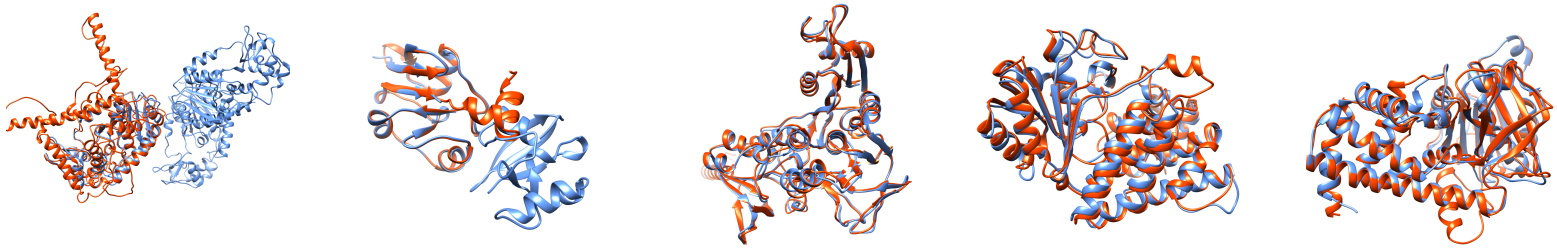
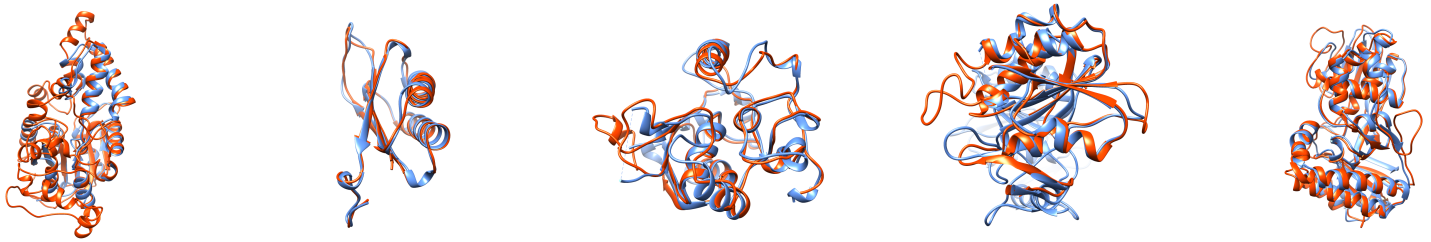


Figure 3.2. Distribution and pair-wise correlation for structural alignment metrics for control structures. Density distributions for query: hit alignment variables (described in text), and pairwise scatter plots and Pearson product-moment correlation coefficients (*r*), for high-confidence (red) and lower-confidence (grey) alignments for BLAST-annotated proteins.

A. Annotated high-confidence



B. Non-annotated high-confidence



C. Non-annotated high-confidence-like

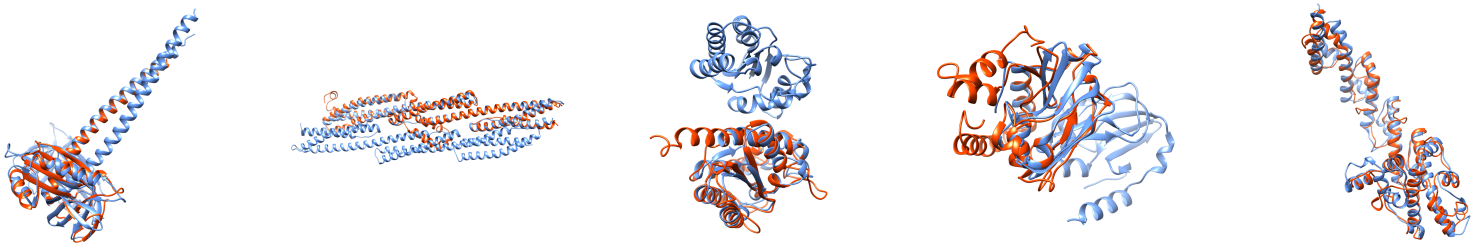
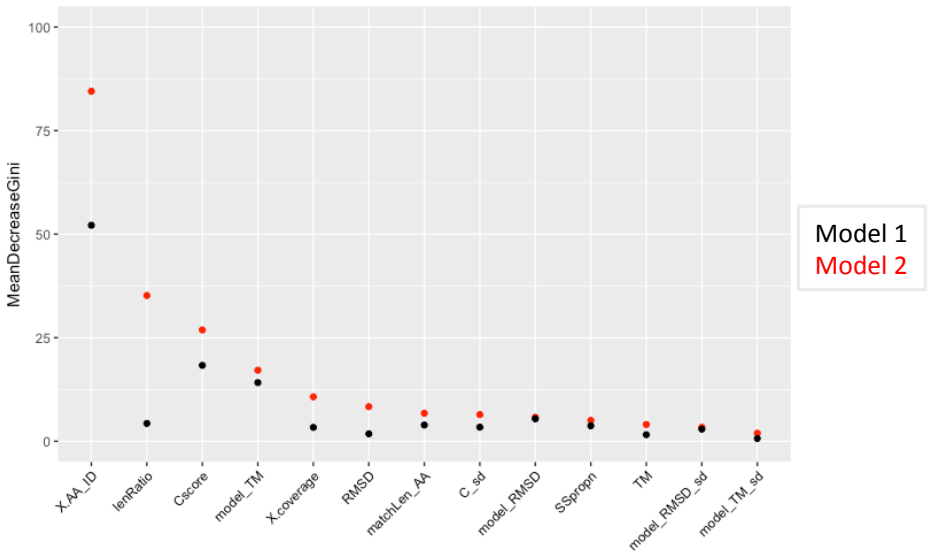
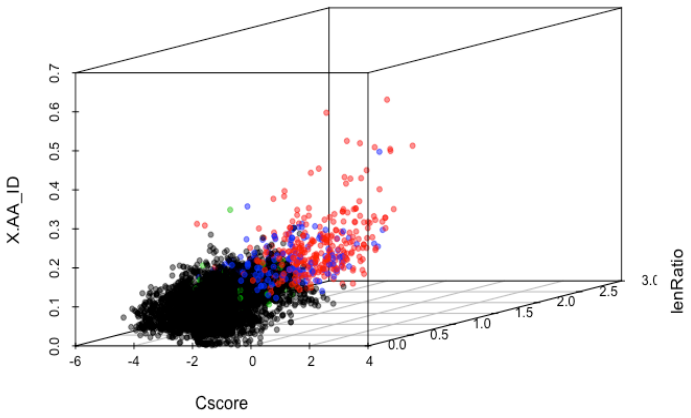


Figure 3.3. Examples of high-confidence and high-confidence-like structural alignments. A) Computationally predicted structures for high-confidence proteins associated with a BLAST annotation (positive controls, displayed in red), and the closest structural homologue within the protein databank of experimentally solved structures (displayed in blue). B) Predicted structures for high-confidence proteins lacking a BLAST annotation ('hypothetical proteins'). C) Predicted structures for proteins lacking a BLAST annotation and lacking an InterPro code match between the query and the best hit, but which are classified as 'high-confidence' by the expanded random forest classifier. These alignments are 'high-confidence-like'.

A



B



True	Predicted
High Conf.	High Conf.
Lower Conf.	High Conf.
High Conf.	Lower Conf.
Lower Conf.	Lower Conf.

C

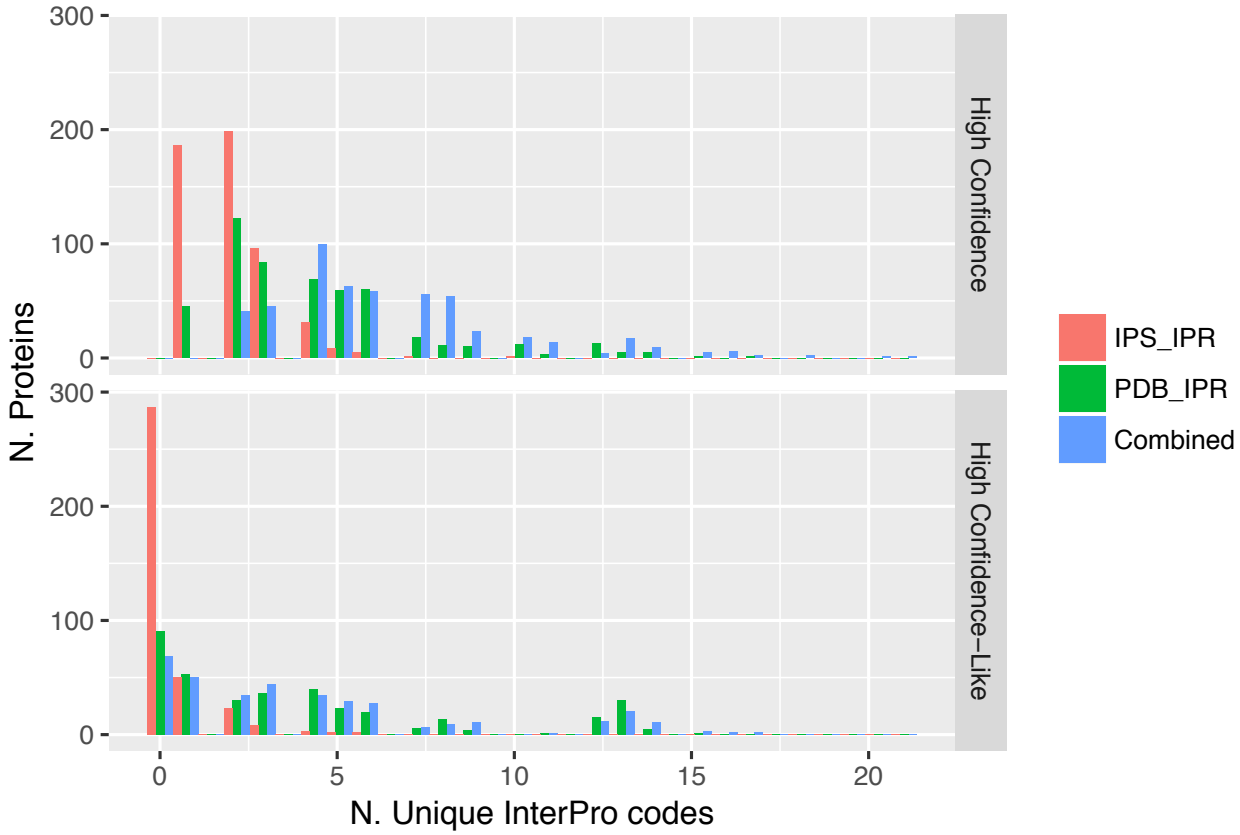


Figure 3.4. Predictive value of structural alignment metrics and InterPro annotation enhancement. A) Contribution of each structural alignment metric to accuracy of the original random forest classifier (black points) and the expanded classifier (red points), measured as mean decrease in Gini co-efficient. Alignment metrics are described in text. B) Separation of high-confidence (red), lower-confidence (black), high-confidence-like (blue) and lower-confidence-like (green) alignments by the three most informative alignment metrics: C-score (x axis), percent primary amino acid identity (y axis) and query:match primary peptide length ratio (Len Ratio; z axis). C) Top panel: Histogram summarizing high-confidence proteins by the number of unique InterPro codes available via sequence searching (InterPro Scan; 'Sequence') and structural homology searching (via TM-align and InterPro code matching; 'Structure'). Bottom panel: Summary of InterPro codes available for high-confidence-like proteins if sequence- and structure-derived codes are combined.

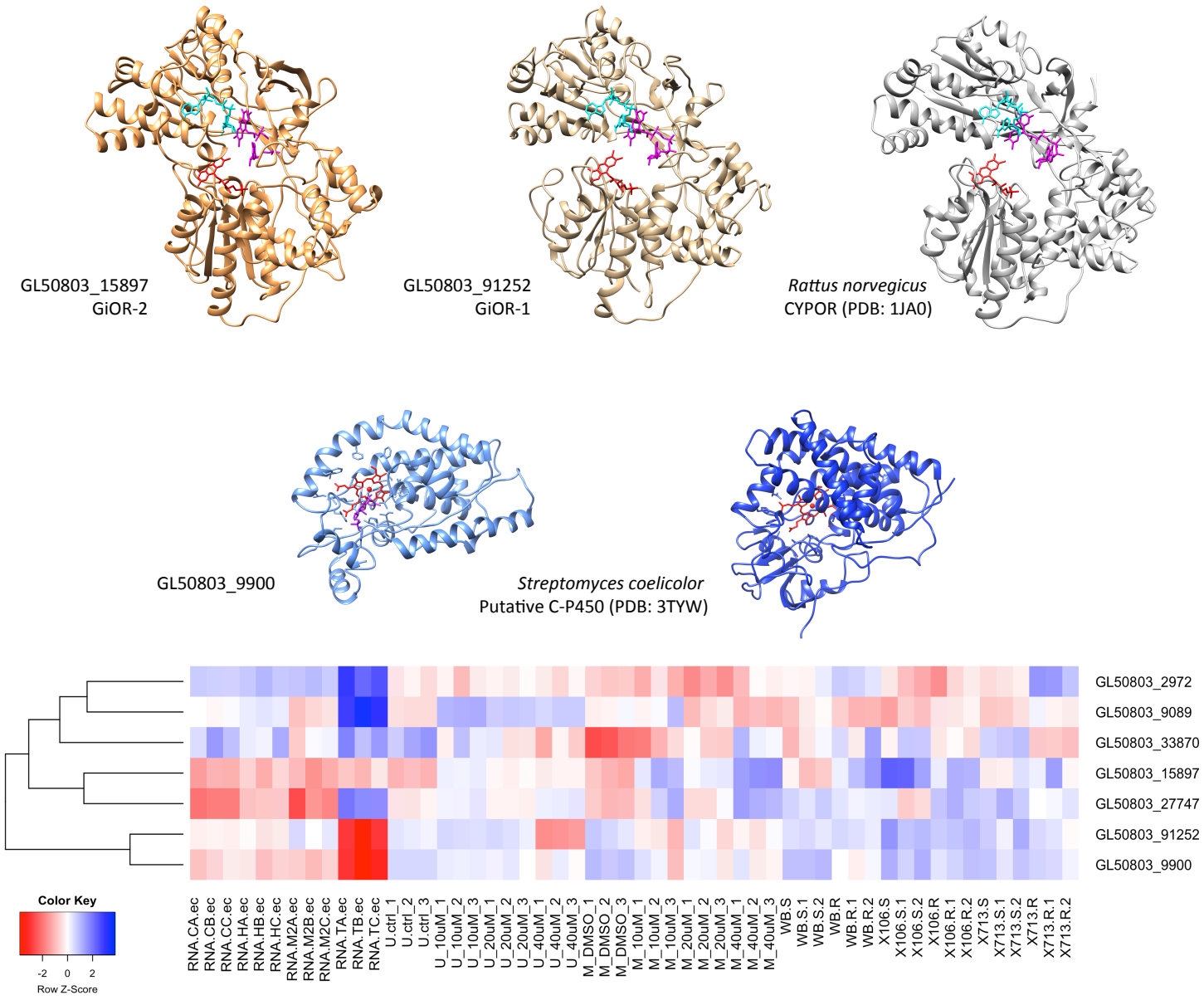


Figure 3.5. Computationally predicted structures and transcriptional clustering for putative *Giardia* cytochrome P450 reductases and cytochrome P450. Top panel: Predicted structures for the high-confidence hypothetical protein GL_15897 (orange) is extremely similar to that for GL_91252 (annotated cytochrome P450 reductase-like enzyme, high-confidence category; tan), despite lacking sufficient sequence identity to classify as paralogues. The most structurally similar solved crystal structure for both predicted structures is displayed in grey. Approximate binding positions for NADH (teal), FMN (magenta) and FAD (red) are inferred in *Giardia* structures based on the crystal structure. Middle panel: The putative *Giardia* cytochrome P450 (light blue) is a high-confidence-like structure predicted to bind haeme (red). A representative non-peptide substrate binding-site (vitamin D; teal) is also predicted. The closest crystal structure homologue is displayed in blue. Bottom panel: Unsupervised clustering of transcriptional profiles for putative cytochrome P450 reductases, putative cytochrome P450, and cytochromes b. Transcriptional data derived from WB-M1 trophozoites exposed to metronidazole, hydrogen peroxide and thermal stress at sub-lethal levels (Chapter 6), and metronidazole-resistant and –susceptible assemblage A trophozoite lines (Chapter 7, and un-published).

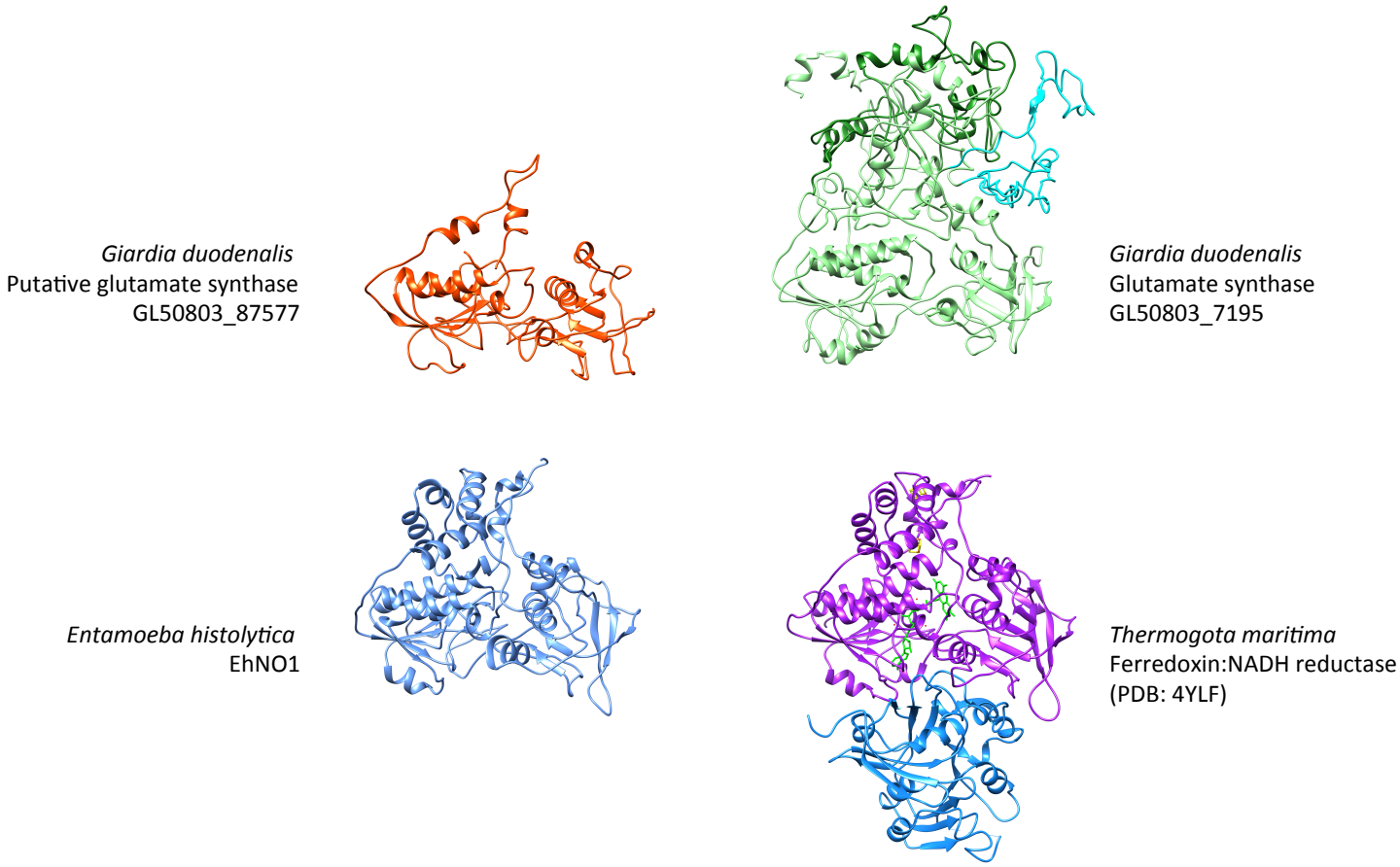


Figure 3.6. Computationally predicted structures for putative ferredoxin:NAD(P)H reductases (FNRs). The high-confidence-like structure predicted for GL_87577 is similar to the C-terminal of the structure predicted for the annotated *Giardia* glutamate synthase (high-confidence category). The ferredoxin N-terminal domain is displayed in dark green, and an additional uncharacterized domain in teal. An *Entamoeba histolytica* protein previously annotated as a glutamate synthase (EhNO1) exhibits FNR activity and does not require an alpha sub-unit, as is the case for bacterial enzymes such as the *Thermogota maritime* FNR (beta sub-unit: purple; alpha sub-unit: azure; FMN co-factor: green).

Supplementary Figure 3.1 (available at DOI: 10.13140/RG.2.2.26965.73440)

Supplementary Figure 3.1. Distribution and pair-wise correlation for structural alignment metrics for annotated, and hypothetical protein alignments. Density distributions for alignment metrics and inherent features of predicted protein structures (described in text), pairwise scatter plots and Pearson product-moment correlation coefficients (*r*), for high-confidence (red), high-confidence-like (green), lower-confidence (grey) and lower-confidence-like (blue) alignments.

Ch 4. Characterization of two oxygen-insensitive nitroreductases from *Giardia duodenalis*

Abstract

BACKGROUND *Giardia duodenalis* is a gastrointestinal parasite of humans that causes millions of cases of diarrheal disease each year. Metronidazole is a front-line anti-giardial treatment, however treatment failure is relatively common, and attributed in part to metronidazole resistance. This drug is reductively activated by oxidoreductases in *Giardia*. Perturbation of the transcription and activity of oxidoreductases, including ferredoxin-dependent nitroreductase enzymes, appears important for conferring metronidazole resistance. However, iron-independent enzymes such as thioredoxin reductase are also involved in activating metronidazole, and implicated in resistance. Other yet-uncharacterized enzymes are also likely to contribute to this phenomenon.

METHODS Hypothetical proteins in the *Giardia* genome were interrogated to identify those with putative nitroreductase activity. The three dimensional structure of putative nitroreductases was predicted, and functionally important features were inferred via structural homology searching. Enzymes were over-expressed in trophozoites using an episomal over-expression vector. The metronidazole sensitivity and intracellular NAD(P)H concentrations of the transfectants were tested to assay the contribution of each enzyme to metronidazole activation.

RESULTS The oxygen-insensitive nitroreductase 1 (NTR1) is predicted to be most structurally similar to a bacterial homo-dimeric nitroreductase. Overexpression of this gene increases Mtz tolerance, indicating a possible role in drug detoxification. The hypothetical nitroreductase-like enzyme hNR is present in all available *Giardia* sub-species genomes but appears relatively unique to this parasite. A single solvent-exposed active site is predicted in hNR, which likely requires an interacting partner to function. Over-expression of the enzyme caused a marginal decrease in metronidazole tolerance. Intracellular NAD(P)H concentrations were highly variable and not significantly changed in either of the test lines.

CONCLUSION Over-expression of nitroreductase-like *Giardia* enzymes modulates metronidazole sensitivity. The oxygen-insensitive nitroreductase may be involved in drug detoxification whereas the hypothetical nitroreductase may contribute slightly to drug activation. Further biochemical investigation is now required.

Introduction

Giardia duodenalis is a parasitic protist that infects the gastrointestinal tract of humans, and causes more than 200 million episodes of diarrheal disease each year (Lane and Lloyd, 2002). Metronidazole (Mtz), a nitroheterocyclic drug, is a major anti-giardial treatment. This drug is thought to enter *Giardia* trophozoites as an inactive pro-drug, where it is enzymatically reduced to cytotoxic intermediates that oxidize proteins, lipids and nucleic acids, leading to parasite death. Resistance to Mtz is evidenced in isolates from treatment-refractory patients (Adagu et al., 2001; Lemée et al., 2000). Resistant lines are also readily generated in the laboratory through chronic sub-lethal exposure (Müller et al., 2008; Smith et al., 1988; Townson et al., 1992). However, mechanisms of Mtz resistance in *G. duodenalis* remain relatively poorly understood.

At present, three oxidoreductase enzymes are implicated in activating Mtz in *Giardia*. The first involves electron transport between a pair of proteins: pyruvate:ferredoxin oxidoreductase (PFOR), and soluble ferredoxin. In the course of oxidative de-carboxylation of pyruvate, PFOR shuttles liberated electrons via a series of bound iron-sulfur clusters, which reduce similar clusters in ferredoxin. Purified ferredoxin, reduced by PFOR, has been shown to activate Mtz *in vitro* (Leitsch et al., 2011). Further, assays of gene transcription and enzyme activity indicate that this electron transport system is suppressed in Mtz-resistant lines (reviewed Chapter 1). Secondly, a thiol-cycling enzyme, thioredoxin reductase, has been shown to reduce Mtz *in vitro*, and to increase trophozoite sensitivity to Mtz when over-expressed on a wild-type genetic background (Leitsch et al., 2011; 2016). TrxR activity appears lower in resistant lines, although its expression is unchanged. A third Mtz-activating enzyme in *Giardia*, is a ferredoxin-nitroreductase fusion protein, NR1, which is predicted to bind both iron-sulfur and flavin mononucleotide (FMN) cofactors. Purified recombinant NR1 exhibits NADH-dependent reduction of Mtz *in vitro*, and is transcriptionally down-regulated in a number of resistant lines (Chapter 1). Further, experimental over-expression of NR1 in both *Giardia* and *E. coli*, increases Mtz sensitivity (Müller et al., 2008; 2013; 2015; Nillius et al., 2011). In contrast to partial reduction of Mtz to toxic intermediates, a second ferredoxin-nitroreductase, NR2, is suggested to completely reduce the pro-drug to an inert amine. Recombinant NR2 reduces Mtz *in vitro* (Müller et al., 2015), and its transcription is increased in certain resistant lines (Müller et al., 2013), suggesting this enzyme may act to detoxify Mtz.

In addition to thioredoxins and ferredoxin family enzymes, *Giardia* encodes an oxygen-insensitive nitroreductase, NTR1, so-called because it lacks a ferredoxin domain and is thus insensitive to oxidative inactivation. Recombinant NTR1 has been shown to reduce Mtz *in vitro*

(Pal et al., 2009), but its role *in vivo* is yet to be elucidated. Whereas ferredoxin-nitroreductase fusion proteins appear evolutionarily confined to microaerobic parasites and archaea (Nixon et al., 2002; Pal et al., 2009), oxygen-insensitive nitroreductases are ubiquitous in protists and bacteria, including in the ulcerative gastric pathogen *Helicobacter pylori*. RdxA from *H. pylori* is capable of activating Mtz, and mutations in the encoding gene are associated with Mtz resistance. Specifically, cysteine 159 (Cys159) is implicated in lowering the reduction potential of the bound FMN cofactor, which makes reduction of Mtz energetically favourable (Martínez-Júlvez et al., 2012).

Giardia lines selected for Mtz resistance in different laboratories, exhibit different magnitudes of Mtz tolerance (measured as half-maximal inhibitory concentration (IC_{50}), or minimal total inhibitory concentration (MIC)), the basis for which is unclear. For example, the resistant lines WB-C4 and 106-C17A tolerate seven- and 17-fold greater Mtz concentrations than their respective drug-susceptible parents. Despite this difference, the changes in PFOR, ferredoxin and nitroreductase transcription/activity reported for these lines are very similar (Dunn et al., 2010; Müller et al., 2007a; Tejman-Yarden et al., 2013). Such inconsistencies lead us to posit that changes in other, yet undocumented gene products, may play important roles in Mtz resistance. To investigate this hypothesis, we searched the *G. duodenalis* assemblage A genome for additional nitroreductases, predicted their 3D protein structure, and used over-expression vectors to infer their contribution to Mtz metabolism.

Methods

Protein domain searching, structure prediction and comparison

To identify proteins in *Giardia* with nitroreductase-like folds, the assemblage A genome (strain WB clone C6; ATCC 50803; Morrison et al., 2007) was interrogated for proteins annotated with the InterPro domain 'Nitroreductase-like' (IPR000415) using GiardiaDB (www.giardiadb.org). Sequence-based homologs in the NCBI non-redundant sequence database were identified by BLAST (Altschul et al., 1997). Three-dimensional structures were predicted for proteins of interest using a local implementation of the I-TASSER software (Roy et al., 2010). This software integrates sequence homology, secondary structure prediction and molecular dynamics simulation to predict protein structure. Binding sites for interacting ligands were also predicted, and close structural homologues in the RCSB Protein DataBase were identified. UCSF Chimera

software (Pettersen et al., 2004) was used to visualize protein structures. The MatchMaker module was used to align experimentally determined and predicted protein structures, and to compute structure-based multiple sequence alignments.

Cloning and transfection of over-expression vectors

Genes of interest were amplified by PCR from *G. duodenalis* genomic DNA (WB C6), using the primers listed in Table 6.1 and the following reagents: 0.5 µL of Phusion DNA polymerase (Thermo Fisher, #F-530L), 10 µL of 5x Phusion HF buffer, 500 nmol forward and reverse primers, 10 ng genomic DNA, 500 µmol of dNTPs, and deionized sterile H_2O to a total volume of 50 µL. Amplicons were generated by incubating the mixture in a thermocycler (Arktic, Thermo Scientific) under the following conditions: initiation: 98 °C, 30 sec; denaturation: 98 °C, 10 sec; annealing: 58 °C, 20 sec; extension: 72 °C, 60 sec, for 30 cycles, followed by 3 min final extension at 72 °C. After incubation, the reaction mixtures were electrophoresed on a 1% TAE agarose gel (100 V) and PCR products were excised from the gel using a Safe Imager Transilluminator (ThermoFisher) and extracted using the QIAquick Gel extraction kit (Qiagen, #28704) according to the manufactuer's instructions .

For episomal expression of genes of interest under their native promoters, amplicons were cloned into the pPAC vector, which encodes a 3x haemaglutinin (HA) tag and a puromycin acetyltransferase (pac) gene to confer resistance against puromycin for the selection of tranfectants (Jerlstrom-Hultqvist et al., 2012). For episomal over-expression of selected genes, amplicons were cloned into the OCT-pPAC vector, which includes 200 bp of the ornithine carbamoyl transferase (OCT) promoter upstream of the 5' restriction site. The vector and amplicon were independently incubated for 1 hour at 37 °C with 1 µL of required restriction enzymes (Table 6.1), in 3 µL of 10x FastDigest buffer (Thermo Scientific) with deionized sterile H_2O to a final volume of 30 µL. Digested amplicons were ligated into 50 ng of purified, digested OCT-pPAC vector at a 3:1 ratio (insert:vector) using Ready-To-Go T4 DNA Ligase (Amersham Biosciences); or 0.5 µL of T4 DNA ligase (2U/µL), 2 µL of 10x T4 Ligase buffer (Thermo Scientific, #EL0016), and sterile deionized H_2O to a total volume of 20 µL, at 16 °C for 16 h.

30 µL of the ligation reaction was added to a newly thawed 100 µL pellet of One Shot TOP10 competent *Escherichia coli* cells (ThermoFisher, #C404010), incubated on ice for 20 min, then heat-shocked at 42 °C for 35 sec before incubation on ice for a further 2 min. The mixture was added to 250 µL of LB broth and spread on pre-warmed LB agar plates containing 50 µg/mL

ampicillin. Plates were incubated for 16 h at 37 °C. Single colonies were picked using a 20 µL pipette tip, and re-suspended in 40 µL of sterile H_2O. Ten µL of re-suspended cells was added to 12.5 µL of 2x PCR Mastermix (ThermoFisher, #K0171) with 0.5 µL of 10 µM forward and reverse primers specific to the cloned insert, QS with H_2O to 25 µL total volume. The presence of inserts was confirmed by incubation in a thermocycler (Arktic, ThermoScientific) under the following conditions: initiation: 95 °C, 2 min; denaturation: 95 °C, 30 sec; annealing: 55 °C, 30 sec; extension: 72 °C, 60 sec, for 30 cycles, followed by 2 min final extension at 72 °C; after which 2 µL of 6x loading dye was added to 10 µL of PCR mixture and electrophoresed through 1% agarose gel in TAE buffer at 100 V.

The remaining 30 µL cell suspension was added to 50 mL of LB with 50 µg/mL ampicillin and incubated at 37 °C for 16 h. The complete vector was purified on multiple columns using the QIAprep Spin MiniPrep Kit (Qiagen, #27104) according to the manufacturer's protocol, and concentrated by repeated elution in 100 µL sterile H_2O, pre-heated to 70 °C. Approximately 1 µg of the purified complete plasmid was digested as described above to confirm the presence of a single insert, and the presence and correct orientation of the native gene sequence was confirmed by Sanger sequencing (Uppsala Genome Center).

For each transfection, 5 mL of chilled suspended trophozoites from a sub-confluent 10 mL tube were concentrated by centrifugation (680x *g*, 5 min, 4 °C), re-suspended in 300 µL of TYDK medium, transferred to pre-chilled 0.4 cm cuvettes (Bio-Rad Gene Pulser, #165-2088) and stored on ice. Approximately 40 µg of purified plasmid DNA was added, and the cells were electroporated (capacitance extender set at 350 V; 960 µF; 800 Ω) in a Gene Pulser (Bio-Rad), incubated on ice for 15 min and transferred to 10 mL tubes containing fresh pre-warmed TYDK. After 20 h incubation at 37 °C, 10 µL of 50 mg/mL puromycin was added and flasks were monitored for cell death for four days. Dead cells were discarded and fresh TYDK medium with pyromycin, was added as necessary. Transfectants were maintained by sub-culturing at confluence with the constant presence of puromycin.

Immunolocalization of recombinant gene products

A 4 mL aliquot of sub-confluent transfectant culture was chilled, and suspended cells were concentrated (680x *g*, 5 min, 4 °C), washed in 10 mL ice-cold PBS and then re-suspended in 100 µL PBS. 20 µL of the concentrated suspension was transferred to poly-L-lysine coated slides (Thermo Scientific, #ER-208B-CE24) in duplicate, and incubated at 37 °C in a humid chamber

for 10 min to allow attachment. Cells were fixed by addition of 20 µL of 4% paraformaldehyde in PBS and incubated at 37 °C for a further 20 min. Fixative was removed via low-pressure vacuum and cells were washed twice with 40 µL of PBS before addition of 20 µL 0.1 M glycine in PBS and incubation at RT for 10 min. The quencher was removed and cells were washed twice with PBS. 20 µL of 0.2% TritonX-100 in PBS was added and slides were incubated for 30 min at RT to permeablize cells. The supernatant was removed and slides were blocked with 20 µL of antibody block solution (2% BSA + 0.05% TritonX-100 in PBS) overnight at 4 °C in a humid chamber. Blocking solution was removed and 20 µL of HA.11 Clone 16B12 Monoclonal Antibody, Alexa Fluor 488 Labeled (Covance, #A488-101 L; diluted 1:1000 in antibody block solution), was added. Slides were incubated at RT in a humid chamber for 1 h and then washed 6x with 40 µL of PBS + 0.1% TritonX-100. The wash solution was removed and cells were mounted under a cover slip in 3 µL of Vectashield containing DAPI (Vector Laboratories, #H1-100). Cells were viewed using an Axioplan2 fluorescence microscope (Carl Zeiss GmbH), and images were processed using AxioVision (LE release 4.8.2.0) or Zen software (v7.0.0.285) (Carl Zeiss GmbH).

Metronidazole susceptibility and intracellular NAD(P)H assays

Confluent tubes were chilled on ice, pelleted (680x *g*, 5 min, 4 °C) and re-suspended in fresh TYDK containing puromycin. Cells were enumerated in a haemocytometer (Neubauer) and diluted to seed concentrations according to growth rate. Lines transfected with the empty vector, VSP and GL_15307 over-expression vectors, were diluted to 10^4 cells/mL in complete TYDK. The GL_8377 and Cas9 transfectants were diluted to $3x10^4$ and $4x10^4$ cells/mL respectively. 40 µL of suspended cells was added per well of a white-walled, clear-bottom 96-well plate (Corning, #3610), and the peripheral wells were filled with 200 µL sterile H_2O to limit evaporation. Plates were inserted into a GasPak EZ anaerobe pouch (BD, #260863) with an anaerobic sachet, which was sealed and incubated at 37 °C for 2 h to allow cells to attach and equilibrate, and media to sparge. Metronidazole (Mtz; Sigma Aldrich, #M3761; 200 mM in DMSO) was serially diluted in complete TYDK containing puromycin and added to wells in duplicate to achieve final concentrations from 0.25 to 250 µM. The highest DMSO concentration was 0.25% (v/v). Plates were re-introduced to pouches with a new anaerobic sachet and incubated at 37 °C for 48 h. Reconstituted CellTiter-Glo luminescent cell viability reagent (Promega, #G7570) was stored at -20 °C and thawed to RT 30 min prior to use. 50 µL of reagent was added to wells containing trophozoites and plates were incubated by shaking for 15 min at RT. Luminescence (corresponding to live cells/well) was measured using an Infinite 200 microplate reader (Tecan) and cell viability as a proportion of negative controls was calculated using Excel (Microsoft).

Luminescence values from negative controls were used to infer growth between lines. IC_{50} values were calculated by fitting ATP luminescence values with the 'log(inhibitor) vs. normalized response -- variable slope' module in Prism (GraphPad). Results were visualized in R (ggplot2 package).

To assay intracellular NADH, cells were prepared and incubated as for Mtz response testing in a total volume of 50 µL, without drug. NAD(P)H-Glo reagent (Promega, #G9061) components were stored at -20 °C and thawed and prepared prior to use according to the manufacturer's instructions. At 48 h, 50 µL of reagent was added to wells and plates were incubated with shaking for 3 min, RT, then allowed to stand for 40 min prior to luminescence measurement. NAD(P)H-based luminescence was divided by ATP-based (i.e., CellTitre-Glo reagent) luminescence to normalize for cell number.

Statistical analyses

Metronidazole tolerance and intracellular NAD(P)H concentrations were compared between lines transfected with nitroreductase over-expression vectors, and controls. A line transfected with the empty vector was used to control for the effect of the puromycin resistance gene, and lines transfected with over-expression vectors harbouring a heterologous Cas9 enzyme, and the *G. duodenalis* VSP TSA417, which are not expected to metabolize metronidazole, were included to control for the effect of protein over-expression. Fisher permutation tests (10,000 iterations, two-sided) were performed to identify significant differences in Mtz IC_{50} values and intracellular NAD(P)H concentration between lines over-expressing (oe) putative nitroreductases, and controls (empty vector, oe-Cas9 and oe-VSP, pooled), using the R coin package.

Results

Sequence identification and predicted structure analysis

The *G. duodenalis* assemblage A encodes four proteins with predicted nitroreductase-like activity. These include the previously characterized ferredoxin-nitroreductase fusion proteins NR1 and NR2 (Müller et al., 2007b; 2015; Nillius et al., 2011), the oxygen insensitive nitroreductase (GL50803_15307) (NTR1; Nixon et al., 2002; Pal et al., 2009), and a yet-uncharacterized hypothetical protein (hereafter 'hNR'; GL50803_8377). Each gene is also present as a single copy orthologue in the *Giardia duodenalis* assemblage B and E genomes (Franzén et al., 2009; Jerlström-Hultqvist et al., 2010).

To improve the functional annotation of NTR1 and hNR, and to explore potential roles in Mtz metabolism, we predicted the three-dimensional structure of each protein and identified the nearest structural homologs in the Protein DataBank (PDB) of solved structures. The predicted structure of NTR1 was most similar to the crystal structure for a putative NADH dehydrogenase/NAD(P)H nitroreductase from *Parabacteroides distasonis* (3M5K; unpublished). The closest published structural homolog was the flavin-containing oxidoreductase YcnD from *Bacillus subtilis* (PDB code 1ZCH; Morokutti et al., 2005)(Table 6.2). All structural homologues of NTR1 are homodimers that bind FMN cofactors at the dimer interface. We used this information to model NTR1 as a homodimer, with FMN positions imputed from the 3M5K crystal structure (Figure 6.1a). Given the conservation of oxygen-insensitive nitroreductases in bacteria, we performed a structure-based multiple sequence alignment between *Giardia* nitroreductases, 3M5K, and RdxA from *H. pylori* (Figure 6.2). Cysteine159, a residue essential for Mtz reduction by RdxA, is poorly conserved between 3M5K and RdxA, however NR1, NR2 and NTR1 exhibited cysteine residues within two amino acids from Cys159. Most interestingly, NTR1 exhibits Ser114 in the equivalent position to RdxA Cys159, and cysteine in the adjascent position (Cys113) (Figure 6.1b).

The predicted structure of hNR matched most closely to a putative nitroreductase (ava_2154) from *Anabaena variabilis* (3EO7; unpublished). The closest published structural homolog for hNR was also the *B. subtilis* YcnD. hNR exhibited a nitroreductase domain and FMN binding site in the N-terminus (Figure 6.3a, b), whereas the C terminus comprised two α helices that showed little structural agreement with the closest structural homologues (Figure 6.3a). The FMN

binding site appeared solvent-exposed, which together with the single nitroreductase domain in this peptide, suggests it may form a part of a multimer. Attempts to model hNR as a homodimer based on the 1ZCH template were unsuccessful, however sequence homology (NCBI BLAST) searches returned bacterial and diplomonad oxygen-insensitive nitroreductases as distant homologues (Figure 6.3c), suggesting that the hNR may be a highly divergent member of this enzyme class.

Expression and localization of putative nitroreductases

In order to determine the cellular localization of NTR1 and hNR, each protein was HA-tagged and over-expressed (oe) in WB-C6 trophozoites and localized by immunofluorescence. oe-NTR1 was associated with the edge of the ventral disc and the cytosol (Figure 6.4a). Although oe-hNR is the only nitroreductase with a putative signal sequence, it was expressed throughout the trophozoite cytosol, with a punctate pattern in some cells (Figure 6.4b).

Effect of hNR, NTR1 and VSP over-expression on Mtz susceptibility

Over-expression of the nitroreductases NR1 and NR2 affect metronidazole sensitivity (Müller et al., 2013; 2015; Nillius et al., 2011). We therefore tested the contribution of NTR1 and hNR to metronidazole sensitivity. Trophozoites over-expressing NTR1 showed an approximate 50% increase in Mtz tolerance relative to the pooled EV, oe-Cas9 and oe-VSP control ($p < 0.001$). The mean IC_{50} concentration for oe-hNR was marginally lower than for controls, indicating decreased Mtz tolerance ($p = 0.006$)(Figure 6.5a).

Effect of hNR, NTR1 and VSP over-expression on intracellular NAD(P)H concentrations

Assays of intracellular NAD(P)H concentration were performed for each transfectant line and adjusted for final cell concentration. Neither oe-NTR-1 nor oe-hNR exhibited significant changes in NAD(P)H relative to the pooled control, however there was considerable variation in the control. Specifically, intracellular NAD(P)H was significantly lower in the oe-VSP line relative to the other controls ($p = 0.005$). When oe-VSP was omitted from the pooled control, NAD(P)H concentrations in oe-NTR1 were significantly decreased ($p = 0.03$) (Figure 6.5b).

Discussion

The molecular phenotypes of Mtz-resistant *Giardia* lines reported to date, although incomplete, strongly suggest that resistance is polygenic, that is, likely to involve changed expression and/or activity of multiple gene products. To fully understand Mtz resistance, comprehensive characterization of gene expression in resistant lines is required, together with reverse genetic approaches to determine the contribution of individual gene products to resistance. In the present study, we identified under-studied nitroreductases encoded in *Giardia*, and found that over-expression of NTR1 *in vivo* increased Mtz tolerance, whereas over-expression of hNR led to a marginal increase in susceptibility. Building on the initial characterization of NTR1 as an enzyme capable of using NADH to reduce Mtz *in vitro* (Pal et al., 2009), our structural modeling results suggest that NTR1 may act as a homodimer. Further to this, the increase in Mtz tolerance observed in trophozoites over-expressing NTR1 indicates that this enzyme may detoxify Mtz.

Because the reduction potential of Mtz is very low (-460 mV), it is only active against cells such as *Giardia* that feature highly reduced (i.e., electron-rich/oxygen-poor) intracellular environments, and which express enzymes with sufficiently low redox potentials to reduce the pro-drug (reviewed in Chapter 1). In aerobic cells, any reduced Mtz is spontaneously re-oxidized to the pro-drug form, with the concomitant production of superoxide. Subtle biochemical differences in enzymes that interact with Mtz may result in partial, or complete reduction of the pro-drug, with opposing effects on cell survival (Müller et al., 2015). Free FMN has a much higher reduction potential than Mtz, at around 190 mV (Martínez-Júlvez et al., 2012). In order for Mtz reduction to occur, therefore, the reduction potential of bound FMN cofactors in nitroreductase enzymes must be lowered substantially. A catalytic cysteine in the FMN binding pocket of *H. pylori* nitroreductase RdxA, is demonstrated to affect the ability of that enzyme to reduce Mtz, possibly by altering the local redox environment to favour electron transport to the pro-drug (Martinez-Julvez et al., 2012). It is most interesting, therefore, that the two ferredoxin-nitroreuctases in *Giardia*, and NTR1, encode a cysteine residue within two amino acid positions relative to RdxA Cys159. The stoichiometry of Mtz reduction by NTR1, and the importance of residues such as Cys113 in the FMN binding pocket, now warrant further investigation.

An alternative explanation for the increase in Mtz tolerance observed in oe-NTR1 transgenic parasites, is that NTR1 may consume NAD(P)H but preferentially reduce an endogenous substrate other than Mtz. In this case, NTR1 over-expression might deplete intracellular NAD(P)H concentrations and thus limit the function of NAD(P)H-dependent enzymes such as

NR1 that activate the drug. Indeed, assays performed here suggested decreased NAD(P)H concentrations within the oe-NTR1 line, although the high variability in NAD(P)H measured in controls necessitates further experimentation. The endogenous substrates of nitroreductases are a subject of ongoing research (Müller et al., 2015), as is the complete elucidation of electron transport chains more broadly (Chapter 1; Chapter 5; Chapter 7; Alam et al., 2012; Pazdzior et al., 2015; Pyrih et al., 2014). Further investigation of NTR1 regulation in lines selected for Mtz resistance, is also warranted.

Overexpression of hNR in *G. duodenalis* produced a moderate increase in Mtz susceptibility, which does not support a prominent role for hNR in Mtz metabolism. The predicted structure for hNR is unusual, and the amino acid sequence diverges substantially from other oxygen-insensitive nitroreductases. Given that there is only a single predicted nitroreductase domain in hNR, and that the FMN binding site is relatively exposed, we expect this enzyme to participate in a multimer, most likely a homodimer, as suggested for other *Giardia* nitroreductases (Müller et al., 2015). hNR is conserved in all *Giardia* assemblages, which together with its apparent evolutionary divergence, may present an attractive target for chemotherapy. Further elucidation of the interacting partners, endogenous substrates, and physiological role of this enzyme are now required.

Conclusion

We over-expressed and predicted the structure of two under-studied nitroreductases in *G. duodenalis*. Over-expression of an oxygen-insensitive nitroreductase (NTR1) increased metronidazole (Mtz) tolerance and might decrease intracellular NAD(P)H concentrations. *In silico* structural investigations suggest NTR1 may function as a homo-dimer, and that metabolism of Mtz may involve a redox-sensitive cysteine in the FMN binding site. Conversely, over-expression of a hypothetical and structurally divergent oxygen-insensitive nitroreductase-like enzyme, hNR, had a modest effect on Mtz tolerance, suggesting minimal interaction with the drug. These results expand the complement of putative Mtz detoxification enzymes in *Giardia*, and further inform the polygenic phenomenon of Mtz resistance in this important pathogen.

Table 6.1. Primers for amplification of genes of interest

Target gene & description		Forward primer	Reverse primer	5'/3' restriction enzymes	Vector	Reference
GL_15307 Oxygen-insensitive nitroreductase 1 (NTR1)		CCGATCGGATCCATGCCTCCCATTTGTGAC GCTATC	CCGATCGCGGCCGCAGCTCTATCATATAAATT CGTCCG	BamHI/NotI	OCT-pPAC	Jerlström-Hultqvist et al. (2012)
GL_8377 Hypothetical nitroreductase (hNR)		CCGATCGGATCCATGATACTAACTATTTTA GCTGTT	CCGATCGCGGCCGCAGATTATGTGCTTGTAG CCTCAAG	BamHI/NotI	OCT-pPAC	
GL_113797 Variant-specific surface protein (VSP), TSA417	OCT promoter	TTAATTAACGCAACGAAAAACAACGCCGAA TGAACCTG		PacI	pPAC	
	OCT-GL_113797 fusion (GL_113797 start codon underlined)		GACGATCGCGAGCAAAAATCTGCCGAACATT TTAATTTTCAGCCTCTACTGTAGAGCGTTTAG			
	GL_113797-HA fusion (HA tag underlined)	CGCGTAGTCTGGGACATCGTATGGGTAAG CTTCTTGGGTGCAGGCTGTCCGTGCCAG	TACCCATACGATGTCCCAGACTACGCGGACG ATGGAAAGTGTAAAACGTGTGGCGTCACC			
	GL_113797 (HA tag underlined)		GAGCTCTGGCTGAGACCCTGCTGTCTGTGCT AGCAG	SacI		
NP_269215.1 *Streptococcus pyogenes* Cas9		TATGGATCCATGGAGTCCCAGCAGCCGAC	TATGCGGCCGCCAGTCGCCTCCCAGCTGAG	BamHI/NotI	OCT-pPAC	Ferretti et al. (2001)

Table 6.2. Top three crystal structure homologues for putative *Giardia duodenalis* nitroreductases

	Crystal structure homologues							
Giardia duodenalis **Accession no.**	**PDB code**	**Chain**	**Species**	**Description**	**TM score**	**RMSD (Å)**	**%AA identity**	**%3D coverage**
GL50803_15307 (NTR1)	3m5k	A	*Parabacteroides distasonis* ATCC 8503	Putative NADH dehydrogenase/NAD(P)H nitroreductase (BDI_1728)	0.884	1.2	0.261	0.92
	3kwk	A	*Bacteroides thetaiotaomicron*	Putative NADH dehydrogenase/NAD(P)H nitroreductase (NP_809094.1)	0.8743	1.22	0.256	0.9143
	1zch	A	*Bacillus subtilis*	Flavin-containing oxidoreductase (YcnD)	0.8447	1.94	0.182	0.9429
GL50803_8377 (hNR)	3eo7	A	*Anabaena variabilis* ATCC 29413	Putative nitroreductase	0.6407	4.1	0.113	0.8182
	1vkw	A	*Thermotoga maritima*	Putative nitroreductase (tm1586)	0.6141	2.8	0.197	0.7003
	1zch	A	*Bacillus subtilis*	Flavin-containing oxidoreductase (YcnD)	0.4974	3.48	0.121	0.5926

TM score is a global goodness-of-fit measure (Roy et al., 2010); RMSD: root-mean squared deviation of α carbon atoms; AA: amino acid.

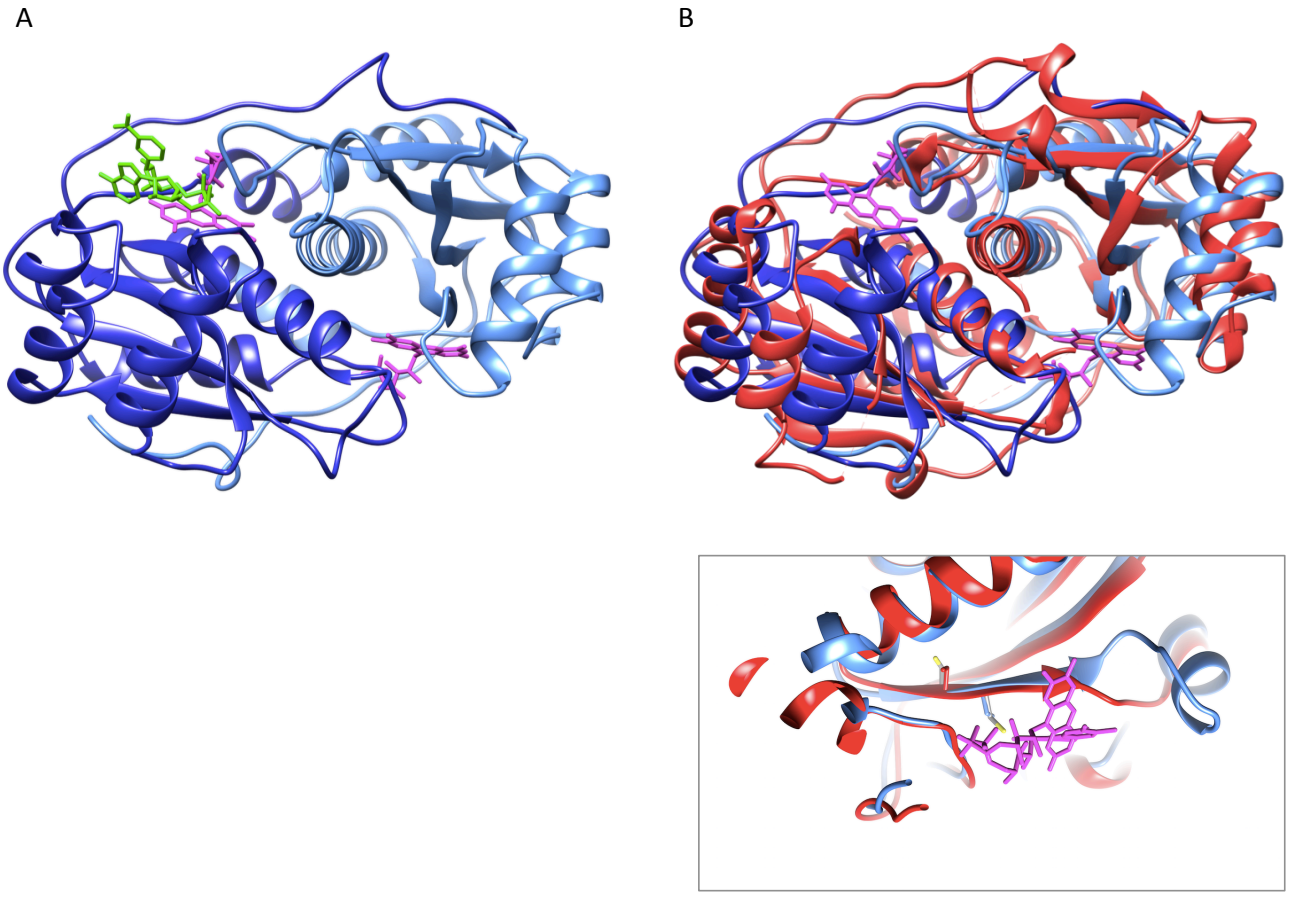


Figure 6.1. Predicted structure of NTR1. A: NTR1 is modelled as a homodimer with the predicted binding positions of the FMN co-factors (two sites, magenta) and NADH electron donor (one of two inferred sites, green). B: NTR1 homodimer (blues) overlaid with the crystal structure of *Helicobacter pylori* RdxA (red; RSCB PDB code: 3QDL). Inset: Two possible orientations of the FMN cofactor (magenta) subtending a β-sheet with catalytic cysteine (RdxA Cys159; red, sulphur atoms coloured yellow) and serine residues displayed. Structural comparison between NTR1 and 3QDL, revealed a mean 1.74 Å RMSD across 94 α-carbon atoms, for each aligned monomer.

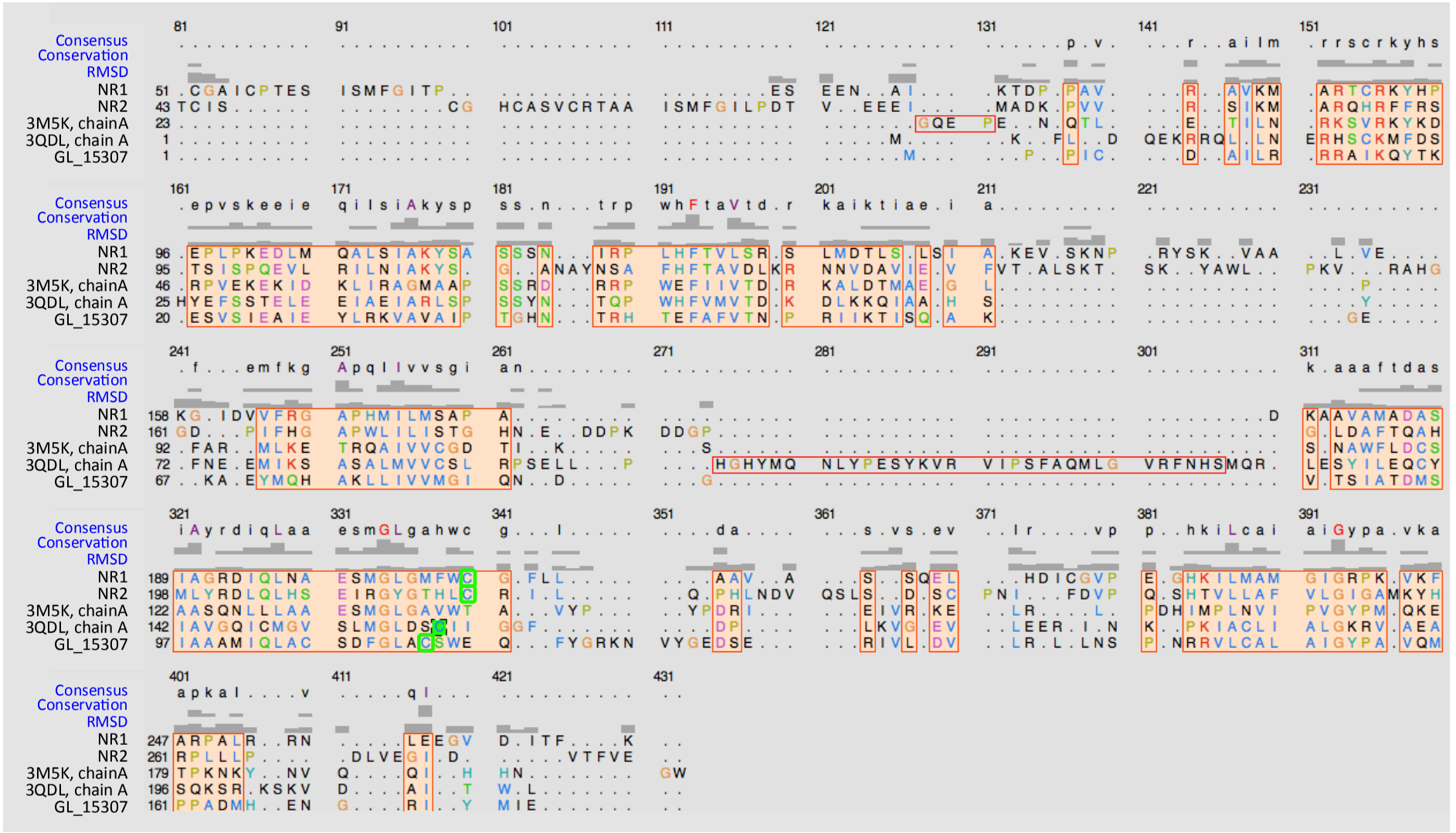

Consensus
Conservation
RMSD
NR1
NR2
3M5K, chainA
3QDL, chain A
GL_15307

Figure 6.2. Structure-based alignment *Giardia* nitroreductases with crystal structure homologues. Cysteine 159 implicated in metronidazole reduction by RdxA (Martínez-Júlvez et al., 2012) is highlighted in green. Cysteine residues within predicted structures for *G. duodenalis* enzymes that may be analogous to C159, are outlined in green. NR1: GL50803_22677; NR2: GL50803_6175; NTR1: GL50803_15307; 3M5K: *Parabacteroides distasonis* Putative nitroreductase; 3QDL: *Helicobacter pylori* RdxA.

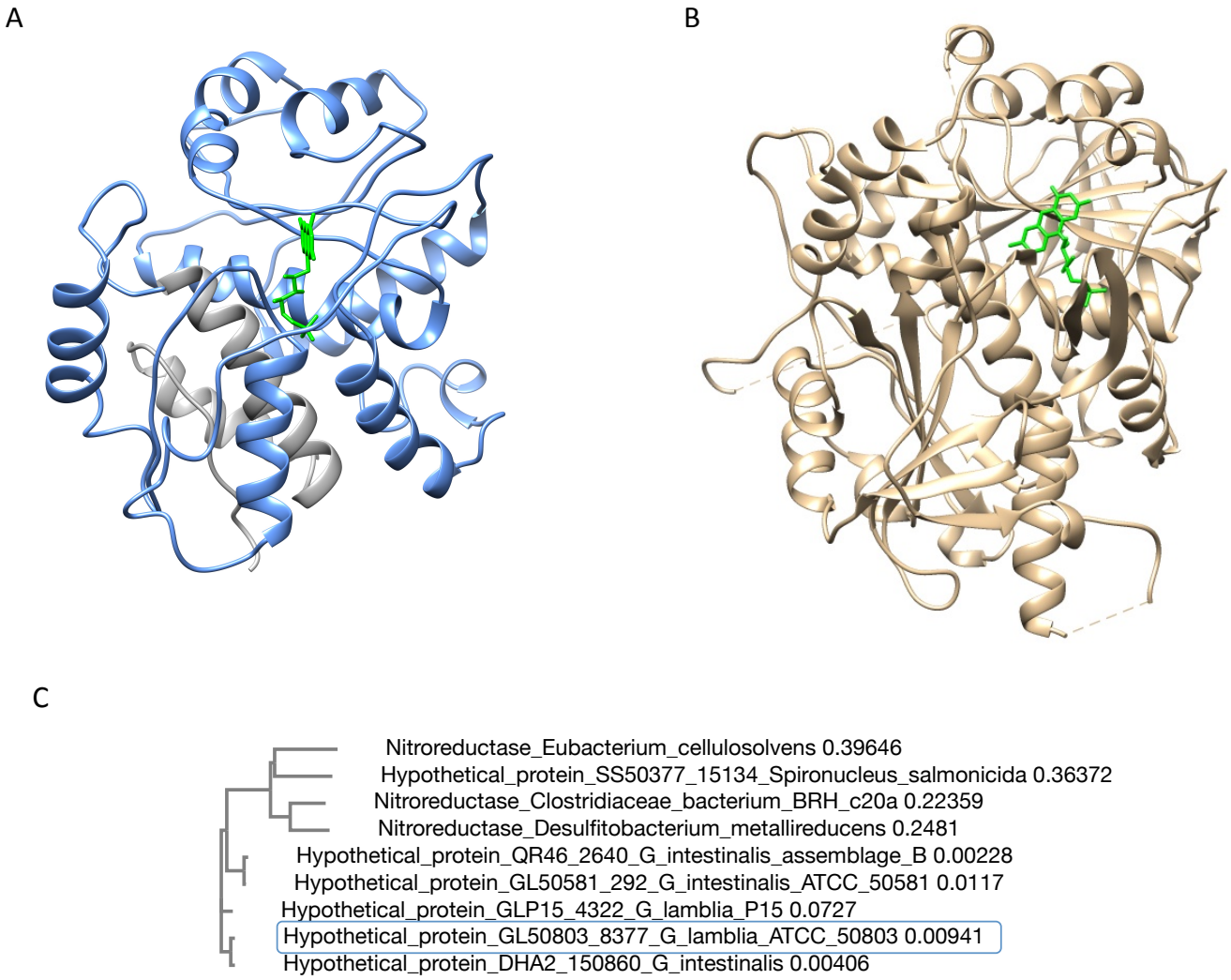
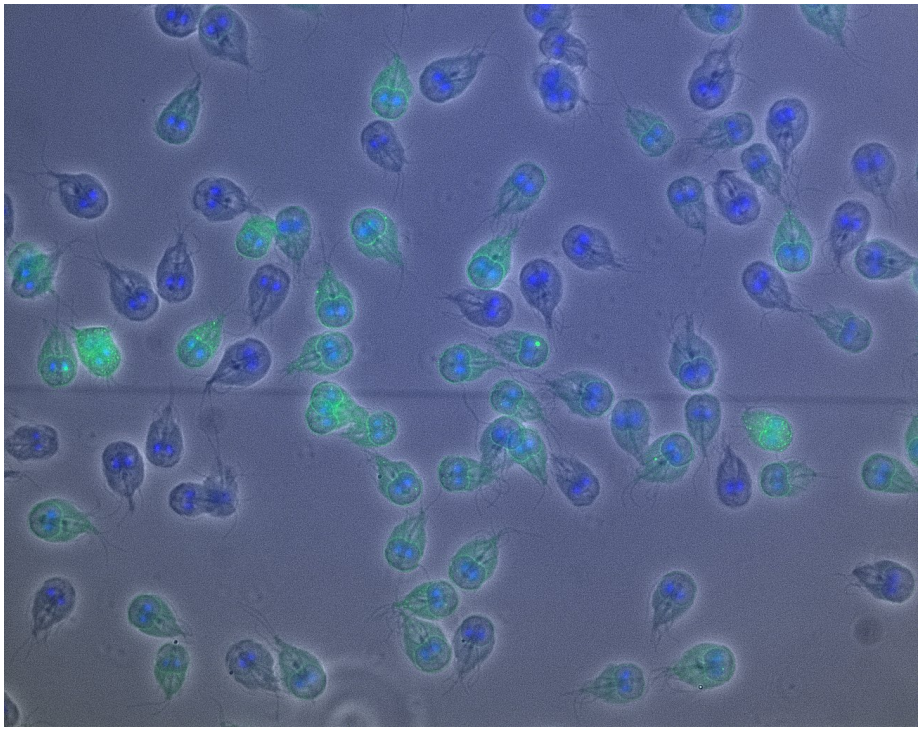


Figure 6.3. Predicted structure of hNR. A: Predicted nitroreductase domain (blue) with bound FMN (green) and C-terminal helices (grey). B: Crystal structure of *Parabacteroides distasonis* Putative nitroreductase (3M5K), a di-nitroreductase monomer, with bound FMN (green). C: Neighbour-joining phylogram of the eight closest sequence-based homologues of hNR (outlined in blue), with Jukes-Cantor distances printed at right.

A



B

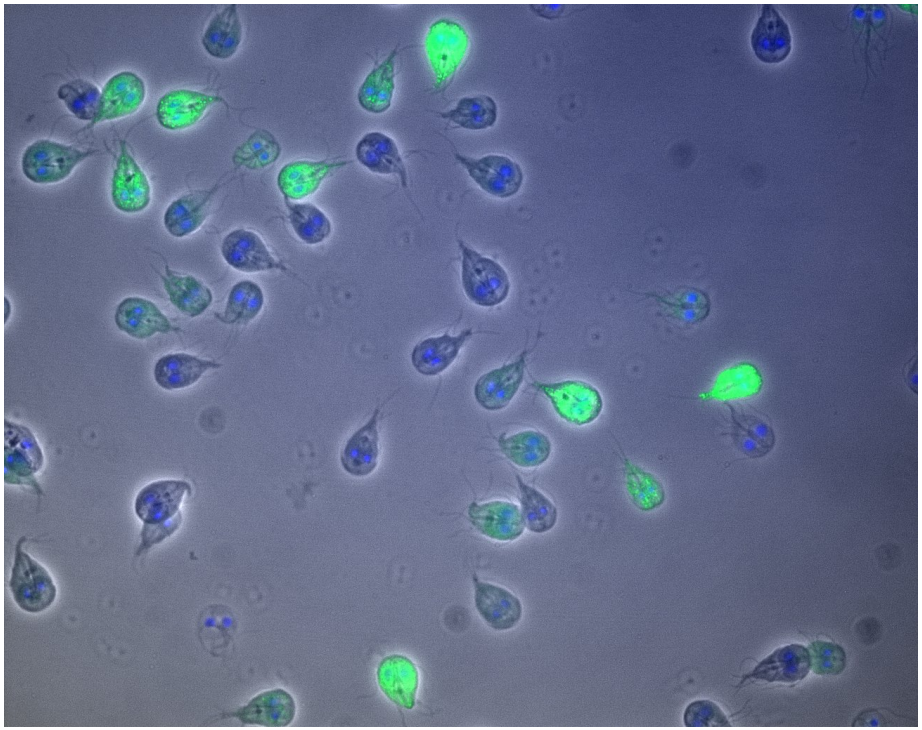


Figure 6.4. Localization of hNR and NTR1. oe-NTR1 localizes in the cytosol and at the periphery of the ventral disk (A). oe-hNR is expressed throughout the cytosol and exhibits a punctate pattern in some cells (B). Nuclei are stained blue.

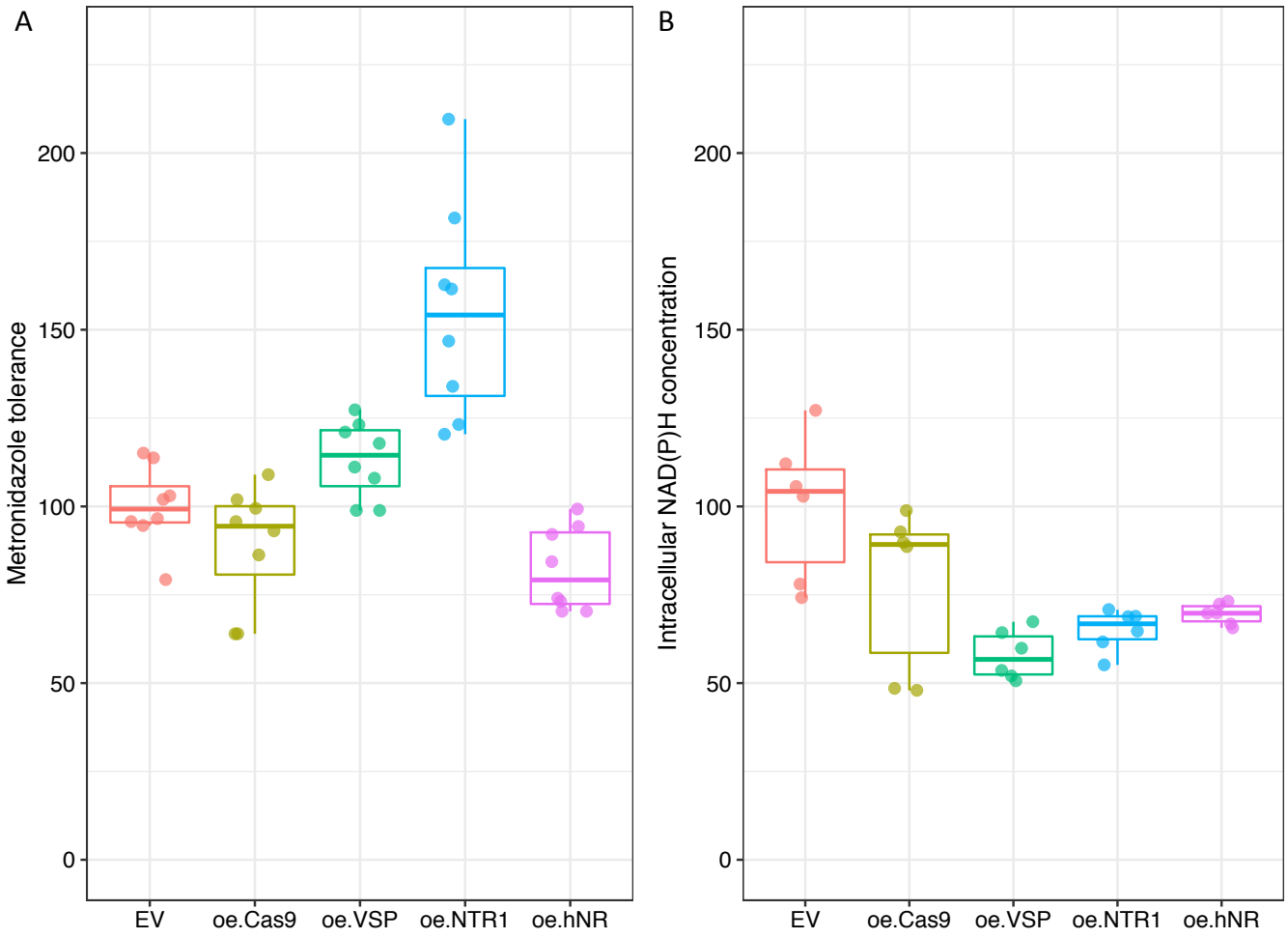


Figure 6.5. Metronidazole susceptibility and intracellular NAD(P)H concentrations in transgenic lines. Metronidazole tolerance of transgenic lines is displayed as a percentage of the mean IC_{50} of the empty vector (EV) control (A). Intracellular NAD(P)H as a percentage of the mean value recorded for the empty vector control (B). NAD(P)H-based luminescence values are adjusted for cell concentration. Data from at least three biological replicates are shown.

Chapter 5. Time-dependent transcriptional changes in axenic *Giardia duodenalis* trophozoites

Brendan R E Ansell, Malcolm J McConville, Louise Baker, Pasi K Korhonen, Neil D Young, Ross S Hall, Cristian A A Rojas, Staffan G Svärd, Robin B Gasser, Aaron R Jex. *PLoS Neglected Tropical Diseases* 12/2015; 9(12). DOI: 10.1371/journal.pntd.0004261

PLOS | NEGLECTED TROPICAL DISEASES

RESEARCH ARTICLE

Time-Dependent Transcriptional Changes in Axenic *Giardia duodenalis* Trophozoites

Brendan R. E. Ansell[1]*, Malcolm J. McConville[2], Louise Baker[1], Pasi K. Korhonen[1], Neil D. Young[1], Ross S. Hall[1], Cristian A. A. Rojas[1], Staffan G. Svärd[3], Robin B. Gasser[1], Aaron R. Jex[1]

1 Faculty of Veterinary and Agricultural Sciences, University of Melbourne, Parkville, Victoria, Australia, **2** Bio21 Molecular Science and Biotechnology Institute, University of Melbourne, Parkville, Victoria, Australia, **3** Department of Cell & Molecular Biology, Biomedical Center, Uppsala University, Uppsala, Sweden

* bransell@unimelb.edu.au

CrossMark
click for updates

OPEN ACCESS

Citation: Ansell BRE, McConville MJ, Baker L, Korhonen PK, Young ND, Hall RS, et al. (2015) Time-Dependent Transcriptional Changes in Axenic *Giardia duodenalis* Trophozoites. PLoS Negl Trop Dis 9(12): e0004261. doi:10.1371/journal.pntd.0004261

Editor: Adrian B. Hehl, University of Zurich, SWITZERLAND

Received: July 31, 2015

Accepted: November 3, 2015

Published: December 4, 2015

Copyright: © 2015 Ansell et al. This is an open access article distributed under the terms of the Creative Commons Attribution License, which permits unrestricted use, distribution, and reproduction in any medium, provided the original author and source are credited.

Data Availability Statement: Relevant data are within the paper and its supporting information files except for the Raw RNA seq reads which are available through the NCBI Sequence Read Archive (http://www.ncbi.nlm.nih.gov/sra/SRP064772) with the accession number SRP064772.

Funding: BREA is supported by an Australian Post-graduate Award (Australian Government) and the Victorian Life Sciences Computation Initiative (Victoria, Australia). MJM and ARJ are partially supported by an Australian Research Council Linkage Grant (number LP120200122). RNA sequencing was partially funded by YourGene

Abstract

Giardia duodenalis is the most common gastrointestinal protozoan parasite of humans and a significant contributor to the global burden of both diarrheal disease and post-infectious chronic disorders. Although *G. duodenalis* can be cultured axenically, significant gaps exist in our understanding of the molecular biology and metabolism of this pathogen. The present study employed RNA sequencing to characterize the mRNA transcriptome of *G. duodenalis* trophozoites in axenic culture, at log (48 h of growth), stationary (60 h), and declining (96 h) growth phases. Using ~400-times coverage of the transcriptome, we identified 754 differentially transcribed genes (DTGs), mainly representing two large DTG groups: 438 that were down-regulated in the declining phase relative to log and stationary phases, and 281 that were up-regulated. Differential transcription of prominent antioxidant and glycolytic enzymes implicated oxygen tension as a key factor influencing the transcriptional program of axenic trophozoites. Systematic bioinformatic characterization of numerous DTGs encoding hypothetical proteins of unknown function was achieved using structural homology searching. This powerful approach greatly informed the differential transcription analysis and revealed putative novel antioxidant-coding genes, and the presence of a near-complete two-component-like signaling system that may link cytosolic redox or metabolite sensing to the observed transcriptional changes. Motif searching applied to promoter regions of the two large DTG groups identified different putative transcription factor-binding motifs that may underpin global transcriptional regulation. This study provides new insights into the drivers and potential mediators of transcriptional variation in axenic *G. duodenalis* and provides context for static transcriptional studies.

Author Summary

Giardia is the most common gastrointestinal protozoan parasite of humans. This parasite causes diarrheal disease and is correlated with post-infectious conditions such as irritable

Biosciences (Taiwan). The funders had no role in study design, data collection and analysis, decision to publish, or preparation of the manuscript.

Competing Interests: The authors have declared that no competing interests exist.

bowel syndrome. In the absence of a vaccine, treatment is limited to drugs such as metronidazole, against which clinical resistance is reported. Effective control of *Giardia* requires a detailed understanding of its biology, and in turn, complete characterization of the standard *in vitro* culture system. Using RNA sequencing assisted by informatics to functionally annotate hypothetical proteins, we investigated transcriptional changes in axenic *Giardia* trophozoites at three growth phases over 96 hours. We found two large groups of differentially transcribed genes that indicate changes in the antioxidant system and central carbon metabolism over time. A putative novel signaling pathway may act together with putative transcription factor-binding motifs to regulate these transcriptional changes. Our results suggest that dissolved oxygen in *Giardia* culture medium may cause oxidative stress early during *in vitro* growth and that oxygen depletion may limit the efficiency of glycolysis in the declining phase. This work enhances our understanding of the transcriptional flexibility and metabolism of *Giardia in vitro*.

Introduction

Giardia duodenalis (syn. *G. lamblia* or *G. intestinalis*) is a gastrointestinal protozoan parasite, and a major cause of chronic infectious diarrhoea in the developed and developing world. *G. duodenalis* infects approximately one billion people world-wide, causing 200–300 million reported clinical cases each year [1]. *G. duodenalis* is proposed to account for ~15% of cases of childhood diarrhoea in developing countries [2]. High rates of chronic diarrhoea in the first two years of life is significantly associated with physical and cognitive 'stunting,' and predisposes sufferers to a variety of adult-onset metabolic disorders [3]. In particular, infection with *G. duodenalis* is associated with post-infectious gastrointestinal disorders such as irritable bowel syndrome, chronic fatigue, and obesity [4,5]. Control of giardiasis depends primarily on chemotherapeutic treatment with one of two major drug classes: nitroheterocyclics (e.g., metronidazole) and benzamidazoles (e.g., mebendazole) [6,7]. Treatment failure rates as high as 30% are reported for these compounds [8,9], and *in vitro* resistance to widely used chemotypes is documented in isolates from treatment-refractory patients (reviewed in [8,10]). The recently reported increasing incidence of metronidazole treatment-failure in travellers returning to the United Kingdom [11], and toxicity associated with most nitroheterocyclics [6], highlight the need for continued development of anti-giardial drugs. This in turn requires a thorough understanding of the molecular biology of the parasite. Aside from its medical importance, *G. duodenalis* is thought to belong to one of the earliest eukaryotic lineages, and therefore serves as a useful model for studies of eukaryotic features such as secretory and organellar protein trafficking [12], cellular differentiation [13,14] and RNA interference [15–17].

G. duodenalis can be cultured in complex, host cell-free media, which is a rarity among parasitic protists and of great advantage for conducting molecular research. Axenic culture provides an excellent system in which to explore the biology of *G. duodenalis* over time and in response to external stimuli, drug perturbation [18–21] and other stressors [22,23]. System-level transcriptomic investigations based on microarray or serial analysis of gene expression, have established that *G. duodenalis* trophozoites exhibit clear transcriptional responses to encystation medium [13], protein folding stress [23] and the presence of intestinal epithelial cells [24,25]. More recently, RNA sequencing (RNA-seq) has been used to identify transcriptional start-sites [26], 3' un-translated regions and polyadenylation variants in mRNA [27], and to compare transcription between different *G. duodenalis* assemblages [27]. RNA-seq has also recently been applied to investigate the transcriptional response to oxidative stress in

trophozoites [28], and to ultraviolet irradiation in trophozoites and cysts [29]. However, considering the complex nature of the standard culture medium (TYI-S33) for *G. duodenalis* trophozoites, and variation between laboratories in how this medium is prepared, comparing studies is challenging, particularly given that each study represents a static time-point observation. Understanding how transcription varies over time in TYI-S33 medium is important to provide context to single time-point studies. In terms of the axenic growth of the parasite, such research can also provide insight into the changes in the metabolic behaviour and demands of *G. duodenalis* during different growth phases.

A major challenge for genomic investigations of divergent organisms such as *G. duodenalis* relates to the vast numbers of functionally un-annotated gene products. Indeed, around 50% of the proteins predicted in this protist lack functional information. In lieu of *in vitro* characterization, computational protein structure-prediction approaches can provide substantial insight into the putative function of hypothetical proteins [30]. Here, we used RNA-seq coupled with structural homology-based protein annotation, to investigate the longitudinal transcriptional behavior of *G. duodenalis* assemblage A (WB isolate) trophozoites under standard laboratory conditions in TYI-S33 medium. This represents the first high-resolution, longitudinal transcriptional data set for this protist. We hypothesize that differential transcription will be evident between log, stationary, and declining growth phases, and that these changes will reflect the metabolic preferences of *G. duodenalis* and the pressures of resource exhaustion.

Materials and Methods

Trophozoite culture and growth time-point sampling

Giardia duodenalis trophozoites (assemblage A, strain WB-1B; [31]) were generously provided by Drs Jaqueline Upcroft and Peter Upcroft and maintained in axenic culture in filtered, complete modified TYI-S33 medium in close-capped t25 flasks (Falcon) according to standard protocols [32]. The growth kinetics of attached trophozoites was charted over 96 hours (h; S1 Fig), from which the following growth phases were estimated: lag (0–24 h), log (24–60 h), stationary (60–72 h) and declining (72–96 h). As attached and suspended populations exhibited generally similar growth dynamics, we focused on the attached population in order to enrich samples for viable trophozoites and minimize the risk of contamination with degraded mRNA from dead cells. In our hands the generation time of WB1B was 5.4 ±1.2 h during log phase. Samples for sequencing were generated on four different weeks as follows. Nine t25 flasks (64 mL total capacity) were filled with 56 mL of medium, inoculated with 10^5 trophozoites from confluent t25 flasks, and incubated at 37°C. At 48, 60 and 96 h after inoculation, three flasks were selected at random, and supernatant and suspended cells were discarded and replaced with ice-cold phosphate-buffered saline (PBS). Flasks were incubated on ice for no more than 5 minutes to ensure detachment of trophozoites, and the suspensions were transferred to 50 mL falcon tubes and pelleted at 680 x *g* for 5 min at 4°C. Supernatants were discarded, and pellets were combined through re-suspension in 1 mL of PBS before transfer to a 1.5 mL Eppendorf tube. The suspension was pelleted (770 x *g*, 2 min, 22–24°C), re-suspended in 1 mL of TriPure reagent (Roche), and stored at -80°C.

RNA extraction, library preparation and sequencing

RNA was extracted from TriPure reagent according to the manufacturer's instructions within four weeks of sample preparation. The dried RNA pellet was re-suspended in reverse-osmosis deionized water (H_2O) and treated with Turbo DNAse (Ambion) according to the manufacturer's instructions. The DNAse-treated RNA was electrophoresed, and large and small subunits of nuclear rRNA bands were examined as a proxy for RNA integrity. RNA concentration was

estimated by fluorometry (Qubit) and further quality control was performed using a BioAnalyzer (Agilent). Polyadenylated RNA was purified from 10 μg of total RNA using Sera-mag oligo (dT) beads, fragmented to a length of 100–500 bases, reverse transcribed using random hexamers, end-repaired, and adaptor-ligated, according to the manufacturer's instructions (Illumina). Ligated products (~300 bp) were excised from agarose and PCR-amplified. Products were purified over a MinElute column (Qiagen) and paired-end sequenced (100 bp; non-normalised cDNA) using the Ilumina HiSeq 2000 (Yourgene Biosciences, Taiwan).

Bioinformatic processing

Adapters were trimmed from raw reads using Trimmomatic [33] (sliding window: 4 bp, minimum average PHRED quality: 20; leading and trailing: 3 bp; minimum read length: 40 bp), and overlapping read pairs were merged using SeqPrep (downloaded 2 June 2014 https://github.com/jstjohn/SeqPrep) with default parameters. The merged reads were combined with unpaired and non-overlapping paired reads from Trimmomatic output, and all were mapped as single-ended reads to the accepted *G. duodenalis* gene models (assemblage A genome, WB strain, release 3.1; GiardiaDB.org; [27][34]), using RSEM [35]. Transcripts-per-million (TPM) for each gene were averaged across replicates from each growth phase, and used to rank genes according to relative transcriptional abundance. Expected counts for each gene were submitted to EBSeq [36], incorporating median normalization, and DTGs were identified using a false discovery rate (FDR) of <0.05. Fold-change in transcription between growth phases was calculated using the normalized mean expected counts output from EBSeq. As a further filter, only those genes with at least 10 mean expected counts in at least one growth phase were included in further analysis.

Data analysis

Feature detection was calculated as a function of mapped read depth, using the counts module in QualiMap (v1.0) with the–k 10 flag (denoting a minimum mapped read threshold of 10) [37]. Saturation plots were displayed in Excel (Microsoft). Heat maps were generated in R (v3.0.2) using the heatmap module. KEGG BRITE terms associated with peptides in the Kyoto Encyclopedia of Genes and Genomes (KEGG) database (release 69.0), were transferred to the closest homolog in *G. duodenalis* using BLASTp (lower expect threshold of 10^{-5}; [38]). Gene ontology (GO) terms for the predicted *G. duodenalis* proteome were retrieved from GiardiaDB.org; and sensitive structure-based homology searches were performed for DTGs annotated as 'hypothetical' or 'deprecated,' and for peptides encoded by highly transcribed (top 100) genes, using I-TASSER software (v3.0; [30,39]). Briefly, I-TASSER generates putative three-dimensional structural models from amino acid sequences, incorporating predicted secondary structure and the consensus model from multiple threading programs, followed by iterative molecular dynamics simulation to minimize free energy [30]. The closest structural homolog available in the Research Collaboratory for Structural Bioinformatics Protein Data Bank (RCSB PDB; rcsb.org), and consensus GO terms associated with the ten best structural matches, are then inferred for the putative model. Bar charts and box plots describing transcriptional abundance were generated using Excel (Microsoft) and Prism software (GraphPad). For bar charts, mean normalized expected counts are plotted with standard error derived from pre-normalised expected counts for biological quadruplicates. Putative transcription factor (TF)-binding motifs in the promoter regions of DTGs were identified within 400 bp upstream of the start codon in non-overlapping (i.e., non-coding) regions using DREME [40]; cf [41]. Promoters from a DTG group of interest were interrogated using promoters from another DTG group as the background. Interacting TFs for homologous motifs in yeast (all available

databases) were predicted using TOMTOM [42]. For each motif, the density of the 5' nucleotide position (both forward, and reverse complement) was calculated as a function of promoter length, and displayed together with a histogram of the corresponding promoter lengths using R.

Statistical analysis

The coefficient of variation (SD ÷ average; denoting variation in transcript abundance between biological replicates) was calculated for all transcribed genes encoding variant-specific surface proteins (VSPs). Pearson correlation was used to compare transcriptional abundance (FPKM and RPKM) values from independently generated transcriptomic data sets. Fisher exact tests were used to determine significantly over-represented (i.e., enriched) KEGG BRITE terms within DTG groups. GO enrichment analysis was performed using the BinGO module in Cytoscape [43,44] by firstly providing a background of GO terms specific to *G. duodenalis*, incorporating all GO terms from GiardiaDB.org and those terms from I-TASSER with confidence scores $\geq$0.3. The enriched Biological Process GO terms within DTG groups were then identified using Fisher exact testing (FDR $<$ 0.05). To further minimize false positives in this analysis, resultant GO terms with fewer than ten associated genes in the background, were discarded. Fisher permutation tests were also used to compare the average transcription level of genes of interest between growth phases.

Accession numbers

Open reading frames for genes in this article, quoted according to GiardiaDB.org: GL50803_87577; GL50803_7195; GL50803_10403; GL50803_33769; GL50803_27266; GL50803_23756; GL50803_16568; GL50803_27266.

Results

We compared the transcriptomes of the attached population of *G. duodenalis* trophozoites harvested at 48, 60 and 96 h during axenic culture. These time points corresponded to log phase (~ 28 x 10^4 attached cells/cm^2), stationary (confluent monolayer on the flask wall; 72 x 10^4 cells/cm^2), and declining phases (detaching; 42 x 10^4 cells/cm^2) respectively (Figs 1A and S1). In total, 473.76 million RNA-seq reads were produced. For each of 12 samples, an average of 25.25 million high-quality reads (i.e. 92% of all filtered reads) were mapped to the *G. duodenalis* gene models (WB strain [27,34]). The average coverage depth was 405-times (S1 Table), and novel transcript detection as a function of the number of mapped reads was saturated for all samples (S2 Fig). After filtering, transcripts were detected from 7,637 ORFs (78.9% of all predicted ORFs), of which 2,347 had functional annotations (98.8% of all annotated), 3,208 were hypothetical (90.5% of all hypothetical), and 2,082 were deprecated (55.3% of all deprecated). When the relative transcriptional abundance (TPM) for genes at each growth phase was compared, values ranged across four orders of magnitude (S3 Fig). The five most highly transcribed genes across the three phases were a translation elongation factor (EF1-beta), ornithine carbamoyltransferase, glyceraldehyde-3-phosphate dehydrogenase, and two ribosomal proteins (S15A and P2C). Among the top 100 most highly transcribed genes in each phase were arginine deiminase, carbamate kinase, enolase, variant-specific surface proteins (VSPs), peroxiredoxin-1ai, two putative thioredoxins and two protein disulfide isomerases (S2 Table). The normalized mean expected counts for genes at each growth phase were displayed in a heat map, and a progressive trend of up- or down-regulation was identified for the majority of the detected genes (Fig 1B). During the axenic growth and decline of *G. duodenalis* trophozoites over 96 hours, 754 genes were differentially transcribed at statistical significance (S3 Table); including 438

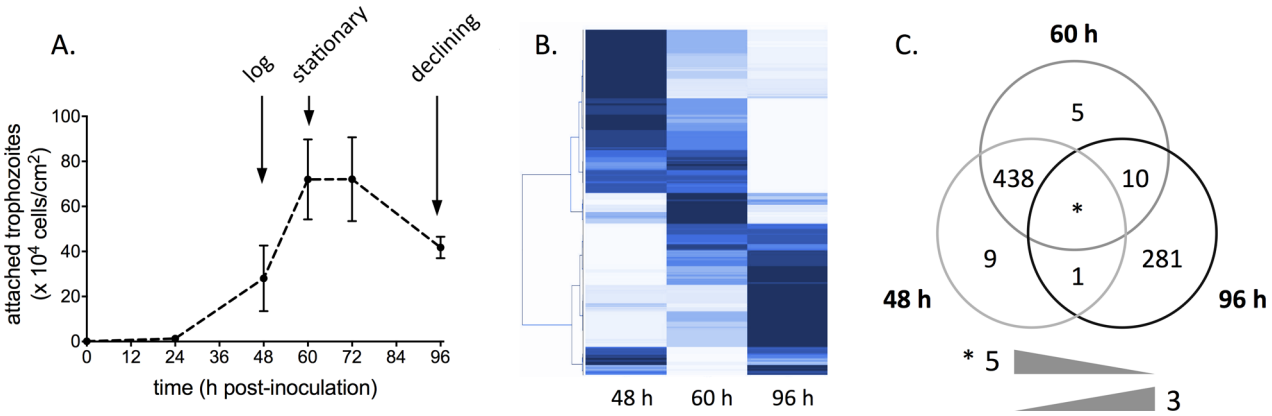


Fig 1. Trophozoite growth profile and differential gene transcription. A: Average density of attached *Giardia duodenalis* trophozoites during *in vitro* growth. Error bars represent ± 1 SEM. B: Heat map displaying transcriptional abundance of all transcribed genes at successive growth phases. Light and dark blue indicate high and low transcriptional abundance respectively. C: Differentially transcribed genes at log, stationary, and declining phases of *in vitro* growth. Numbers represent up-regulated genes relative to other phase(s). *Five and three genes were significantly up- and down-regulated respectively at successive phases.

doi:10.1371/journal.pntd.0004261.g001

genes (47% hypothetical; 6% deprecated) down-regulated at the declining phase relative to the log and stationary phases; and 281 genes (49% hypothetical; 19% deprecated) up-regulated at the declining phase relative to both of the earlier phases. On average, fewer than ten genes were differentially transcribed in other comparisons (Fig 1C), and thus statistical analyses were restricted to the two large DTG groups, hereafter termed 'down-regulated' and 'up-regulated' in the declining phase.

The median fold change for differentially transcribed down- and up-regulated gene groups was 1.85 (IQR = 0.77) and 2.12 (IQR = 0.8) respectively. Using I-TASSER [30], putative structures could be generated for 224 of 234 (95.2%) hypothetical and deprecated proteins within the down-regulated group, and 141 of 190 (74.2%) such proteins in the up-regulated group. The lower availability of structural models for the up-regulated group is due to the presence of 31 genes (16.3%) encoding peptides of >1500 amino acids, which are too large for analysis in the I-TASSER software [30].

Gene functions down-regulated during axenic growth

GO enrichment analysis revealed significant over-representation of 113 'Biological Process' terms in the down-regulated gene group, of which 49 were unique to this group, including 'energy derivation by oxidation of organic compounds,' 'signaling,' and 'locomotion' (S3 Table). Enriched KEGG BRITE annotations included the NEK kinase family, threonine peptidases, ubiquitin conjugating enzymes (E2) and the T1 proteasome family (S4 Table). The down-regulated genes annotated with oxidoreductase activity (GO:0055114 and/or GO:0016491) included glutamate synthase, 6-phosphogluconate dehydrogenase, alcohol dehydrogenase and nitroreductase-1 as well as a number of hypothetical proteins with predicted structural similarity to glutamate synthase, hydroxylamine oxidoreductase, thiol-cycling enzymes (protein disulfide isomerase and thiol:disulfide protein dsbA), a ferretin-like Dps-like peroxide resistance protein and a nickel-binding superoxide dismutase (Table 1). Further investigation of down-regulated genes associated with ubiquitin-conjugating and protease activity, revealed four ubiquitinylating enzymes (two paralogs of a 28.4 kDa E2, a 17 kDa E2 and the ubiquitin ligase UBC3), and four beta-subunits of the 20S proteasome (S4 Fig).

Table 1. Down-regulated genes with predicted oxidoreductase activity (GO:0055114 'oxidation reduction' and/or GO:0016491 'oxidoreductase activity').

		Closest structural homolog in the Protein Data Bank						
Accession no. (GL50803)	**Genome annotation**	**Species**	**Protein name**	**PDB code**	**TM score**	**RMSD (Å)**	**% AA identity**	**% Coverage**
14759	6-phosphogluconate dehydrogenase, decarboxylating							
13350	Alcohol dehydrogenase lateral transfer candidate							
7260	Aldose reductase							
15460	Dynein-like protein							
7195	Glutamate synthase*	*Methylophilus methylotrophus*	Trimethylamine dehydrogenase	1DJQ	0.7084	1.41	10.0	71.86
6175	Nitroreductase 1**							
88581	Synaptic glycoprotein SC2							
9068	Hypothetical protein	*Thermus thermophilus*	Cytochrome c oxidase polypeptide i+iii	2YEV	0.7059	2.72	12.1	90.91
15154	Hypothetical protein	*Streptococcus pyogenes*	Dps-like peroxide resistance protein	2WLA	0.6592	2.42	11.4	75.12
4690	Hypothetical protein	*Legionella pneumophila*	Effector protein B	4JW1	0.8506	1.61	7.5	91.62
87577	Hypothetical protein	*Azospirillum brasilense*	Glutamate synthase [NADPH] small chain	2VDC	0.9178	2.07	14.1	98.68
15445	Hypothetical protein	*Megathura crenulata*	Hemocyanin KLH1	4BED	0.8475	2.43	12.8	95.45
17278	Hypothetical protein	*Megathura crenulata*	Hemocyanin KLH1	4BED	0.7172	3.43	5.6	87.54
29796	Hypothetical protein	*Megathura crenulata*	Hemocyanin KLH1	4BED	0.7377	3.19	8.7	82.69
4692	Hypothetical protein	*Megathura crenulata*	Hemocyanin KLH1	4BED	0.8456	2.56	10.6	98.74
14921	Hypothetical protein	*Candidatus kuenenia stuttgartiensis*	Hydroxylamine oxidoreductase	4N4J	0.8553	2.94	10.3	93.57
27887	Hypothetical protein	*Bacillus subtilis*	Methylthioribose-1-phosphate isomerase	2YVK	0.6671	2.73	9	92.86
15599	Hypothetical protein	*Homo sapiens*	Neuronal acetylcholine receptor subunit α7	2MAW	0.6878	1.68	8.1	75.00
88556	Hypothetical protein	*Homo sapiens*	Otu domain-containing protein 5	3TMP	0.4592	2.11	14.3	49.09
17400	Hypothetical protein	*Saccharomyces cerevisiae*	Pho85 cyclin Pho80	2PK9	0.6544	1.89	13.3	69.11
17375	Hypothetical protein	*Vitis vinifera*	Polyphenol oxidase, chloroplast	2P3X	0.7217	3.04	13.4	82.60
3951	Hypothetical protein	*Saccharomyces cerevisiae*	Protein disulfide-isomerase	3BOA	0.8572	1.98	12.5	92.36
103988	Hypothetical protein	*Neisseria meningitidis*	Putative uncharacterized protein	3VJZ	0.5651	3.83	12.3	82.26
11341	Hypothetical protein	*Vibrio parahaemolyticus*	Sensor protein	3I9Y	0.7838	1.9	7.9	96.20
8048	Hypothetical protein	*Escherichia coli*, *homo sapiens*	Soluble cytochrome b562 and glucagon receptor	4L6R	0.816	2.73	7.7	90.02
3581	Hypothetical protein	*Streptomyces coelicolor*	Superoxide dismutase [Ni]	3G4X	0.7515	1.94	8.8	85.07
5810	Hypothetical protein	*Psychrobacter arcticus*	Uncharacterized protein	2RE7	0.8112	1.92	16.1	94.66

(*Continued*)

Table 1. (*Continued*)

Accession no. (GL50803)	Genome annotation	Closest structural homolog in the Protein Data Bank		PDB code	TM score	RMSD (Å)	% AA identity	% Coverage
		Species	Protein name					
11129	Hypothetical protein	*Homo sapiens*	Uncharacterized protein Kiaa0174	3FRR	0.5589	1.51	12.6	57.78
10244	Deprecated	*Helicobacter pylori*	Cag pathogenicity island protein (Cag18)	3ZCI	0.6398	2.86	4.2	84.43
14932	Deprecated	*Zea mays*	Histidine-containing phosphotransfer protein	1WN0	0.7383	2.39	16.4	87.01
35700	Deprecated	*Listeria monocytogenes*	Lmo 0438 protein	2XL4	0.7886	1.74	6.1	98.00
37288	Deprecated	*Vibrio cholerae*	Thiol:disulfide interchange protein DsbA	2IJY	0.5567	2.92	3.5	82.26

Structural homology information not determined for annotated ORFs.

* Annotated glutamate synthase disambiguated from GL50803_87577 by structural homology searching

** Referred to as NR-2 by Müller et al [86].

doi:10.1371/journal.pntd.0004261.t001

A putative two-component redox-response system in *Giardia duodenalis*

We identified an annotated and a hypothetical glutamate synthase in the down-regulated gene group. Interrogation of putative structures for each protein revealed that the hypothetical glutamate synthase (GL50803_87577) was most structurally similar to a bacterial glutamate synthase beta sub-unit (PDB code: 2VDC), whereas surprisingly, the annotated glutamate synthase (GL50803_7195) was most similar in structure to trimethylamine (TMA) dehydrogenase from *Methylophilus methylotrophus* (PDB code: 1DJQ). Putative homologs of a TMA sensor protein, a Rap modulator protein (C-terminal domain only), and a phosphotransfer protein were also present in the down-regulated gene group. The former two are present as single-copy orthologs in other *G. duodenalis* assemblages (B and E; GiardiaDB.org). These findings suggest the presence of a two-component-like signaling system in *G. duodenalis*. Histidine kinases are integral to two-component systems, and further interrogation of putative structures for hypothetical proteins revealed putative histidine kinase activity for GL50803_10403 (Fig 2).

Gene functions up-regulated in the declining phase

The up-regulated gene group was enriched for 107 'Biological Process' GO terms (43 unique), including 'gene silencing,' 'mitosis,' and 'microtubule-based process' (S3 Table). Enriched KEGG BRITE annotations in this group related to carbon fixation, oxidoreductases and the cytoskeleton (S4 Table). Further investigation of oxidoreductase-related genes in the up-regulated group revealed two pyruvate:ferredoxin oxidoreductase (PFOR) paralogs, and a hypothetical protein with structural homology to a GntR transcription factor (S2 Table).

Changes in antioxidant and glycolytic enzyme transcription

To contextualize the oxidoreductase-related genes that were differentially transcribed between growth phases, we investigated the transcription of other genes involved in the antioxidant system and glycolysis. Progressive but non-significant decreases in transcriptional abundance were identified for thioredoxin reductase, three putative thioredoxins, three peroxidredoxins

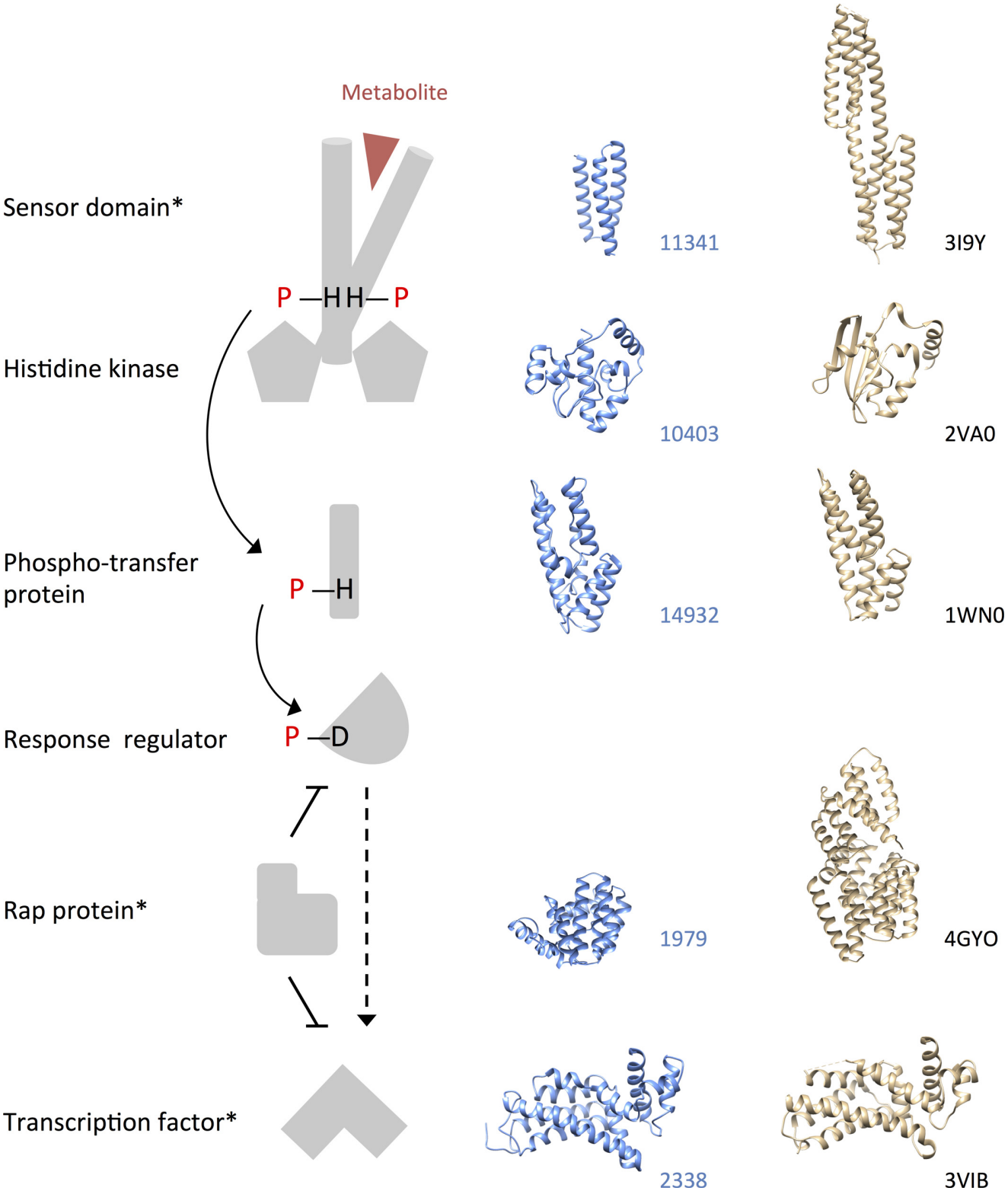


Fig 2. A putative two-component-like signaling pathway in *Giardia duodenalis*. A generalized complete two-component signaling pathway cartoon is displayed in grey. Putative structures for hypothetical *G. duodenalis* proteins are displayed in blue, with accession numbers (GL50803) at right. The genes encoding these hypothetical proteins are down-regulated at the declining phase relative to log and stationary phases, with the exception of the histidine

kinase. For each putative *G. duodenalis* structure, the closest structural match available in the Research Collaboratory for Structural Bioinformatics Protein Data Bank is shown in gold, with the PDB code at right. *single-copy ortholog identified in *G. duodenalis* assemblages B and E (GiardiaDB.org).

doi:10.1371/journal.pntd.0004261.g002

and five thioredoxin domain-containing protein disulfide isomerases. Similar patterns were observed for transcripts encoding the oxygen-consuming enzymes NADH oxidase (GL50803_33769; [45]) and flavodiiron protein [46,47] (Fig 3A). The collective transcription of annotated antioxidant enzymes was significantly lower in the declining phase compared to earlier phases (Fisher permutation test, 1000 iterations, $p = 0.037$; Fig 3A).

The presence of genes encoding glycolytic oxidoreductases in both down- and up-regulated gene groups suggested changes in central carbon metabolism during *in vitro* growth. A hexose transporter, and the non-oxidative glycolytic enzyme glucose-6-phosphate isomerase, were also down-regulated over time. Indeed, transcription of the majority of genes representing glycolytic enzymes in both the pentose phosphate and Embden-Meyerhoff pathways, was lowest in the declining phase (Fig 4). Conversely, transcription of a number of glycolytic enzymes downstream of pyruvate increased over time. In addition to significant up-regulation of PFOR-coding genes in the declining phase, genes encoding one of three ferredoxins (GL50803_27266) and a glutamate dehydrogenase also showed greatest transcriptional abundance in this phase (Fig 4).

Comparison with an/aerobic transcriptomes

Given the robust transcriptional changes in the antioxidant system, we compared the transcriptome for each growth phase with independently generated transcriptomes for WB strain trophozoites cultured under aerobic and anaerobic conditions, as reported by Ma'ayeh et al [28]. When all transcribed genes were considered, our data correlated most closely with the anaerobic transcriptional profile. The transcriptional abundance of annotated antioxidant genes at log and stationary phase, however, correlated best with the aerobic transcriptome, and in the declining phase we observed a shift to stronger correlation with the anaerobic transcriptome (S5 Fig, panels A & B). When glycolytic genes were investigated, there was a trend of increasing correlation with the anaerobic profile over time, and the correlation with the aerobic profile declined after stationary phase. Further dissection of this result revealed separate underlying trends, wherein the genes upstream of pyruvate diverged markedly from the aerobic profile after stationary phase, but little change was seen in genes downstream of pyruvate (S5 Fig, panels C-E).

Membrane protein transcription during axenic growth

Eleven genes encoding VSPs were identified in the up-regulated group as opposed to only two such genes in the down-regulated group. Further investigation of the transcription levels of 193 transcribed VSPs in our data revealed seven prominently transcribed genes, whereas the rest of the population was relatively lowly transcribed (S6 Fig). Aggregate VSP transcription increased over time, driven by increases in the seven most highly transcribed genes (Fig 3B and 3C), which were consistently highly transcribed in all replicates (S7 Fig). Interestingly, a marked decrease in inter-experimental variation was evident for highly transcribed VSPs in the declining phase relative to earlier phases (S8 Fig). These results prompted investigation of the other major class of membrane proteins in *G. duodenalis*, the 60 high-cysteine membrane proteins (HCMPs), whose aggregate transcription in contrast to the VSPs, decreased progressively over time, driven by declining abundance of the most highly transcribed gene quartile (Fig 3B).

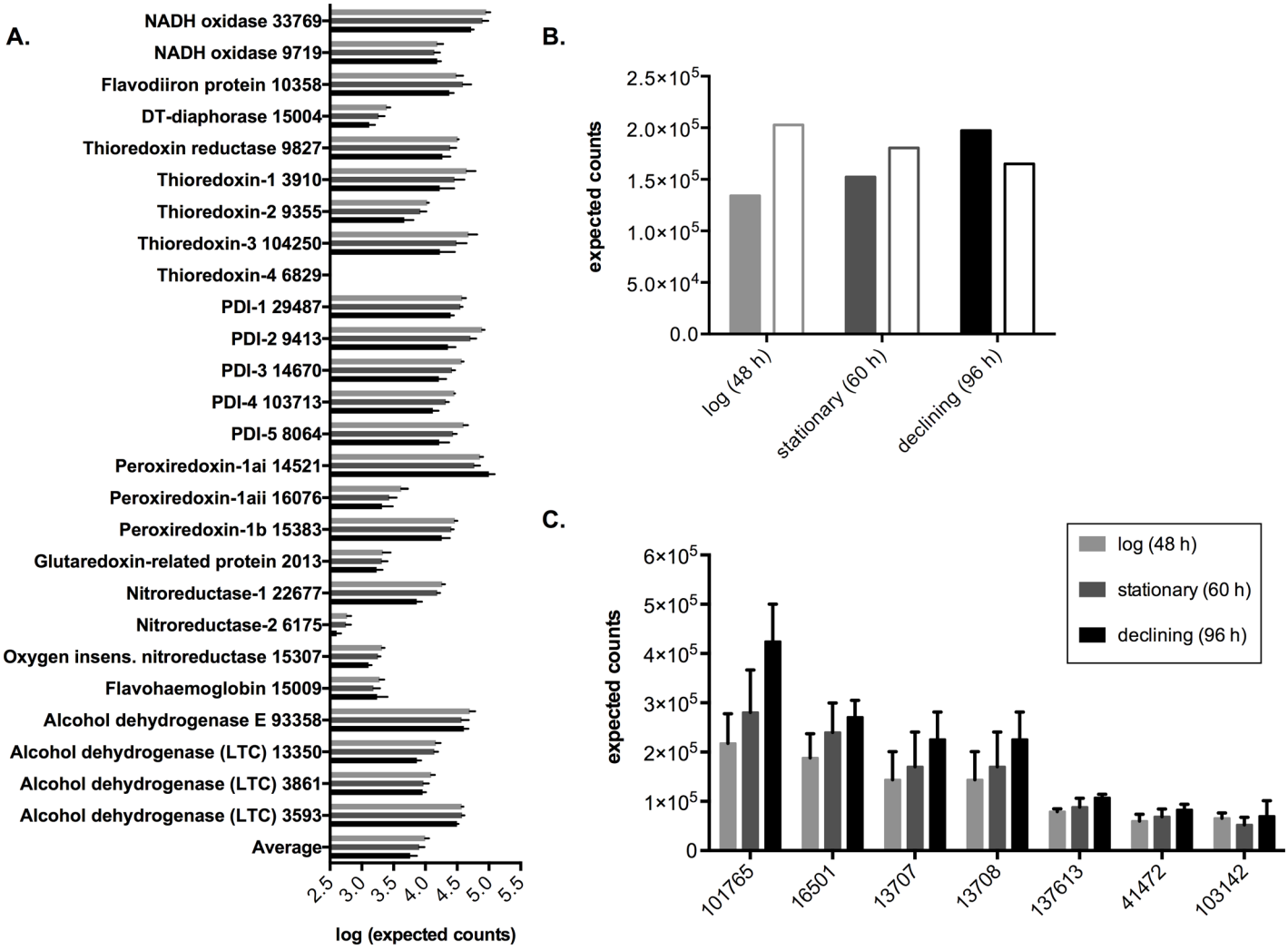


Fig 3. Transcriptional profiles for the antioxidant system and surface proteins during *in vitro* growth. A: Transcriptional abundance for currently annotated antioxidant genes, and average (note the log scale). Gene accession numbers (GL50803) are displayed after the gene description. B: Aggregate transcription for variant-specific surface protein (VSP)-coding genes (filled; expected counts ÷ 10 for display purposes) and high-cysteine membrane protein (HCMP)-coding genes (outline). C: Transcriptional profiles for the seven most highly transcribed VSPs. Mean normalized transcriptional abundance is presented for panels A and C. Error bars represent ±1 SEM, calculated from pre-normalized expected counts for biological quadruplicates. PDI: protein disulfide isomerase; LTC: lateral transfer candidate; insens.: insensitive.

doi:10.1371/journal.pntd.0004261.g003

Putative promoter-based transcriptional regulation

We hypothesize that DNA-binding transcription factors (TFs) may mediate the dynamic variation in gene transcription evident in *G. duodenalis* during axenic growth. The down-regulated gene group did not contain annotated TFs, but did include a putative homolog of the *Neisseria gonorrhoeae* MtrR repressor among three hypothetical protein-coding genes with GO annotations relating to transcriptional regulation (GO:0001071; Fig 2 and S2 Table). The up-regulated group contained an E2F-like TF (GL50803_23756; [48]), a putative TF (GL50803_16568) and four hypothetical proteins annotated with GO:0001071 including the aforementioned GntR homolog (S2 Table). In order to identify putative TF-binding motifs within the promoter regions of genes in the two large DTG groups, we used a similar method to Xu et al. [41] for

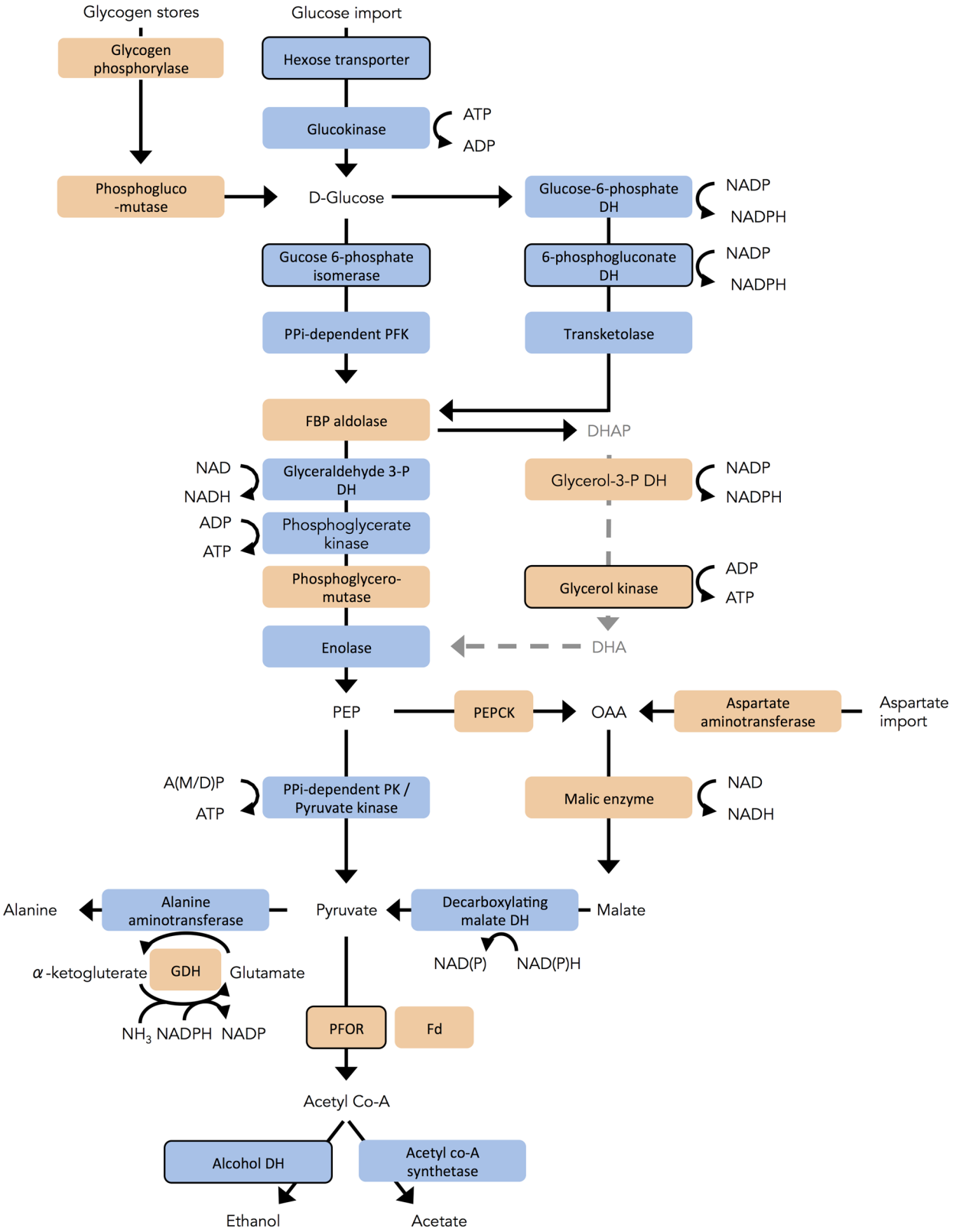


Fig 4. Transcriptional trends for genes encoding glycolytic enzymes. Orange indicates higher transcriptional abundance at the declining phase relative to log phase; and blue indicates the opposite trend. Significant differential transcription is indicated by a dark outline. Only one of three ferredoxin-coding genes (GL50803_27266) exhibits increased transcription in the declining phase. Readers are referred to S5 Table for further information on transcription

levels. DH: dehydrogenase; OAA: oxaloacetate; PK: pyruvate kinase; PEP(CK): phosphoenolpyruvate (carboxykinase); DHA(P): dihydroxyacetone (phosphate); A(M/D)P: AMP or ADP; GDH: glutamate dehydrogenase; Fd: ferredoxin.

doi:10.1371/journal.pntd.0004261.g004

analysis of the related diplomonad *Spironucleus salmonicida*. Totals of 283 and 178 non-overlapping promoter regions of 8 bp to 400 bp were available for the down- and up-regulated gene groups, respectively. The motif AWTTW was significantly over-represented in the promoters of down-regulated genes relative to promoters of up-regulated genes, and the motif GRGGTM was over-represented in the up-regulated gene promoters in the same way (Table 2). After correction for multiple comparisons, no significant matches to known TF-binding motifs in yeast were found for either motif using TOMTOM. An analysis of the position of each motif within promoter regions revealed robust positional conservation for the AWTTW motif within 100 bp of the start codon, but not for GRGGTM. There was no evidence to suggest that these results are biased by the proportion of non-overlapping genes available for analysis in each group (76% and 72%, respectively); moreover, the motif positional densities remain when only the (artificially truncated) 400 bp promoter regions are considered, indicating little effect of promoter length on motif location (Fig 5).

Discussion

We studied the transcriptional dynamics of axenic *G. duodenalis* trophozoites over the log, stationary, and declining phases (48, 60 and 96 h) of *in vitro* growth. We also generated putative structures for the majority of hypothetical and deprecated proteins encoded by DTGs, gaining insights into the function of divergent gene products that lie beyond reach of conventional sequence-based annotation tools. The majority of genes were transcribed in at least one of the three growth phases investigated, and clear transcriptional variation was evident, implicating effective and directed mechanisms of transcriptional regulation. Strikingly, and contrary to our original hypothesis, trophozoites in non-sparged axenic culture exhibited little difference in transcription between log and stationary phases. Indeed, at both phases, we observed high transcription of a number of genes involved in managing oxidative stress. It should be noted that in order to limit the influence of dead or dying cells on our transcriptomic data, we confined our analyses to adherent cells, and discarded suspended cells prior to sequencing. The suspended

Table 2. Putative transcription factor-binding motifs over-represented in promoters of the down- and up-regulated gene groups.

	Forward	Reverse complement	*p* value	E value
Down-regulated group				
Combined motif	**AWTTTW**	**WAAAWT**	**4.20E-10**	**3.80E-04**
Constituents	AATTTT	AAAATT	6.80E-08	6.30E-02
	ATTTTA	TAAAAT	8.80E-07	8.00E-01
	ATTTTT	AAAAAT	6.90E-04	6.40E+02
	AATTTA	TAAATT	3.60E-03	3.30E+03
Up-regulated group				
Combined motif	**GRGGTM**	**KACCYC**	**3.00E-12**	**2.20E-06**
Constituents	GAGGTC	GACCTC	3.60E-06	2.60E+00
	GAGGTA	TACCTC	3.20E-04	2.40E+02
	GGGGTC	GACCCC	3.90E-03	2.90E+03
	GGGGTA	TACCCC	7.40E-03	5.40E+03

Nucleotide ambiguity codes. W: A or T; R: A or G; M: A or C; K: G or T; Y: C or T.

doi:10.1371/journal.pntd.0004261.t002

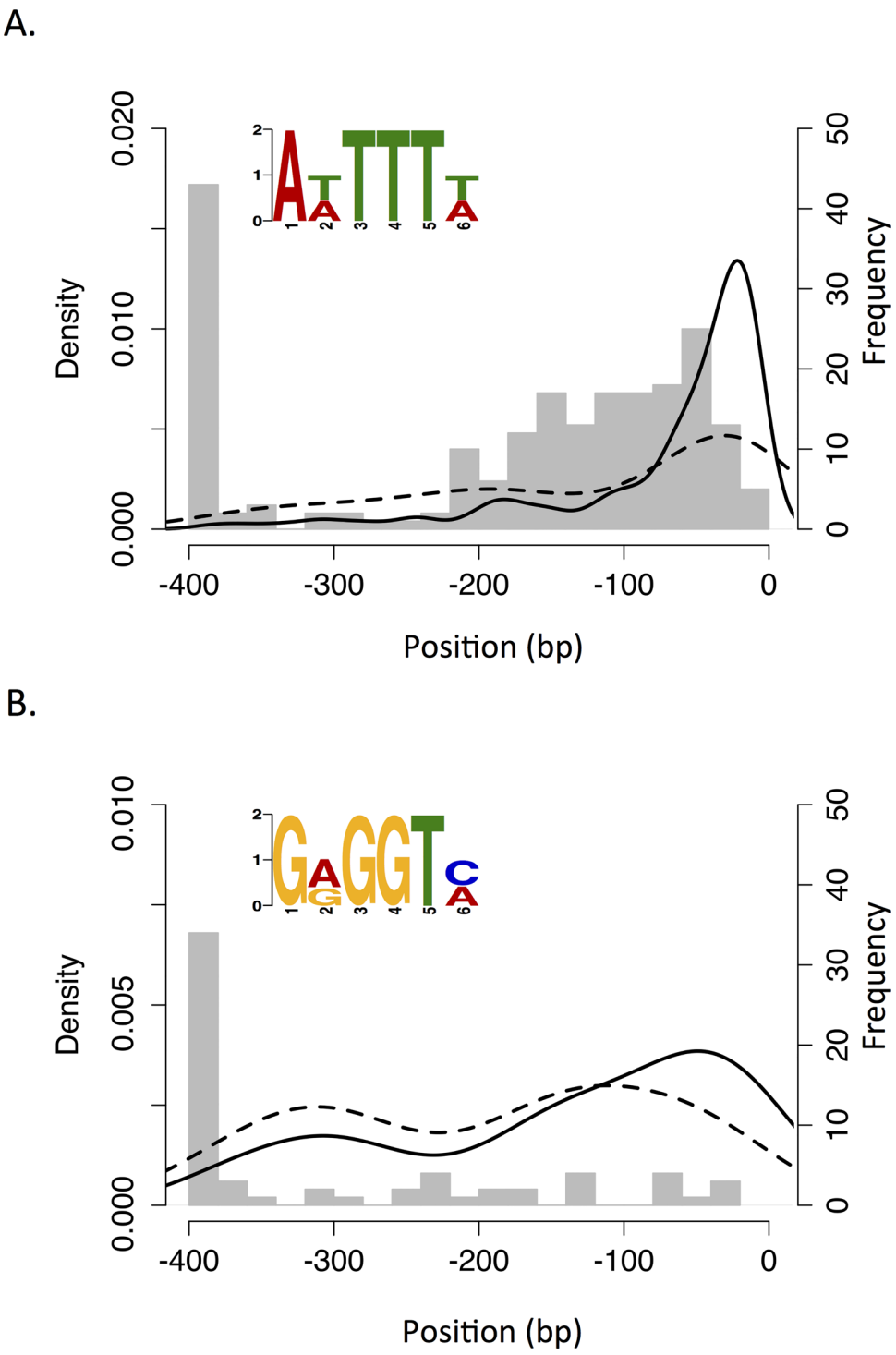


Fig 5. Putative transcription factor-binding promoter motifs in down- and up-regulated differentially transcribed gene groups. A: The AWTTW motif (logo inset) identified in the down-regulated gene group. B: The GRGGTM motif in the up-regulated group. The density of constituent motifs within 400 bp upstream of genes in the DTG group (unbroken line) and in artificially truncated 400 bp promoters (perforated line) is displayed together with a histogram of promoter lengths (grey bars). See Table 2 for motif constituents and statistics.

doi:10.1371/journal.pntd.0004261.g005

population would likely be enriched for both dividing cells and non-viable/dying cells, and it would be of interest to analyze the transcriptomes of these different populations if they could be fractionated. As trophozoites consume oxygen [49,50] and are cultured in a closed system, the pronounced shift in oxidoreductase transcription between log and stationary phases, and the declining phase of axenic growth, is consistent with declining oxygen tension in TYI-S33 medium, and might be associated with a concomitant decline in glucose catabolism and/or entry into a metabolically quiescent state. The present work also found informatic evidence for a two-component–like signaling system that might mediate cytosolic redox or metabolite sensing, and identified different promoter motifs within DTG groups which, together, could contribute to transcriptional regulation.

Indicators of oxidative stress early during *in vitro* culture

G. duodenalis features an elaborate antioxidant system that utilizes NAD(P)H to reduce intracellular oxygen and associated reactive oxygen species (ROS). This system both protects iron-containing enzymes, such as PFORs, from oxidative inactivation [51,52] and allows maximal ATP production from glycolysis [53]. As a 'microaerophile', *G. duodenalis* thrives under dissolved oxygen (dO_2) concentrations between 5–25 μM, above which dO_2 becomes cytotoxic [54]. In accordance with the standard trophozoite maintenance protocol [32], we did not sparge dO_2 from the TYI-S33 medium for this experiment, and medium is expected to contain dO_2, particularly during the log phase of trophozoite growth. The abundant transcription of genes encoding peroxiredoxin, oxygen-consuming NADH oxidases, thioredoxins and other protein disulfide isomerases is consistent with previous reports [27–29,55]. However, the dynamics of antioxidant transcription in *G. duodenalis* under standard culture conditions has not been studied previously. It is likely that the antioxidant system is constitutively highly transcribed to manage transient increases in gut dO_2 [28,56]. Nevertheless, against this background, we observed down-regulation of the vast majority of antioxidant-coding genes over time, suggesting global regulation of antioxidant transcription.

A number of our results indicate that *G. duodenalis* trophozoites may be under oxidative stress at early stages of *in vitro* culture. Firstly, although it was not possible to directly measure dO_2 without perturbing the standard culture system, correlations with independently generated transcriptional profiles for trophozoites under aerobic and anaerobic conditions [28] can be considered as a proxy measure of dO_2 tension. At successive growth phases, antioxidant and glycolytic gene transcription shifted from resembling the aerobic transcriptional profile, to the anaerobic profile. The correlation was influenced more strongly by antioxidant transcription than glycolytic enzyme transcription, however glycolytic genes upstream of pyruvate appeared most sensitive to changes in oxygen tension. This strongly suggests that oxygen tension decreases progressively in axenic culture. Furthermore, genes that were down-regulated in our data at the declining phase, encode putative antioxidant proteins, such as an iron-independent superoxide dismutase, and a ferritin-like (iron-sequestering) protein. TYI-S33 medium is supplemented with ammonium ferric citrate, as iron is essential for the activity of enzymes such as PFOR. However iron can also react with dO_2 to generate ROS. Thus the greater transcriptional abundance of putative iron-sequestering and iron-independent antioxidant proteins at early growth phases, may represent a response to iron- and oxygen-induced oxidative stress. In addition, PFOR enzymes are sensitive to oxidative inactivation [51,52,57], and both PFOR paralogs showed a significant increase in transcription in the declining phase, which is consistent with lower oxygen tension. Lastly, the greater abundance of transcripts encoding elements of the ubiquitin system and proteasomal components at earlier phases, may reflect heightened

turn-over of oxidized proteins [58]. However as the proteasome is also important for the demands of protein folding in actively dividing cells, this result requires further investigation.

In the context of global changes in antioxidant transcription, and a suggested decline in dO_2, we observed inverse transcriptional patterns for the high-cysteine membrane proteins (HCMPs), and variant-specific surface proteins (VSPs), which may indicate differential sensitivity to dO_2. HCMPs contain disulfide motifs that are common in antioxidant proteins and can both oxidize and reduce substrates such as misfolded proteins, and reduce ROS [59]. HCMPs localize to the nuclear envelope, endoplasmic reticulum, and possibly to the trophozoite plasma membrane [24,59]. The greater aggregate transcription of HCMPs early during *in vitro* growth might relate to protecting membranes from peroxidation [59]. Conversely, aggregate VSP transcription increased over time, which was largely due to progressively greater transcription of seven highly abundant VSP-coding genes, rather than induction of new genes. *G. duodenalis* trophozoites transcribe multiple VSP-coding genes, all but one of which are degraded by RNA-interference [17], and thus only a single VSP gene product is displayed on the trophozoite membrane at any time. Our results support previous reports that WB trophozoite populations express relatively few VSPs [60], which may be due to slower VSP turnover in this strain [61]. Specific VSPs are proposed to modulate trophozoite sensitivity to host defenses such as intestinal proteases [62], and VSP suppression is associated with nitroimidazole resistance [19]. Given that the variation in VSP transcription between replicates is particularly low for highly transcribed VSPs in the declining phase, it would be interesting to test whether VSPs are under selection in TYI-S33 medium, or whether the transcriptional increase merely reflects, for example, lower competition from HCMPs for membrane occupancy.

Glycolysis, oxygen availability & alternative energy sources

The functionally reduced mitochondria, or mitosomes, of *G. duodenalis* do not contain enzymes for the tricarboxylic acid cycle or oxidative phosphorylation [34], and this protist is dependent on glycolysis and fermentative metabolism to generate energy from glucose. ATP is generated by direct phosphorylation of AMP and ADP [63]. Electrons liberated during glycolysis are accepted by NAD and NADP, forming NAD(P)H, which must be re-oxidized. Under anaerobic conditions, pyruvate is diverted to ethanol to regenerate NAD, whereas NADP is regenerated through a 'shunt' incorporating glutamate dehydrogenase and alanine aminotransferase. Conversely, in the presence of dO_2, oxidoreductases in the antioxidant system consume NAD(P)H to neutralize dO_2, ROS, and oxidized biomolecules. Under these conditions, pyruvate is not required for NAD(P) regeneration, and can be further oxidized to acetate. This 'micro-aerobic' metabolism maximizes the ATP that is generated from glycolysis.

Here, we observed a trend of decreasing transcriptional abundance for the majority of genes encoding enzymes in the Embden-Meyerhoff and pentose phosphate glycolytic pathways, that convert glucose to pyruvate (Fig 4). TYI-S33 medium contains very high glucose concentrations (55 mM) [32], and thus it is highly unlikely that glucose is exhausted at the declining phase. Instead, the apparent down-regulation of glycolytic pathways may be due to declining dO_2 availability, which could limit the efficiency of glycolysis. If glycolysis is progressively down-regulated as dO_2 declines, *G. duodenalis* may rely on alternative energy sources. This protist is capable of converting arginine, aspartate and alanine to pyruvate [64,65]. The arginine dihydrolase pathway provides a ready source of ATP in *G. duodenalis* and is highly transcribed and stable across all time points studied here. In contrast to glycolysis, which must be coupled to NAD(P)+ regeneration mechanisms, the catabolism of aspartate to pyruvate is effectively redox-neutral in that it does not generate excess NAD(P)H [65]. We observed progressive, but non-significant increases in transcription of two genes involved in aspartate

catabolism (Fig 4), which may reflect greater reliance on aspartate for energy as dO_2 declines. Significant up-regulation of PFORs at the declining phase, and the concomitant down-regulation of alcohol dehydrogenase-coding genes, suggests that a substantial amount of pyruvate is converted to acetate for ATP production even under limited dO_2 availability (Fig 4). This is supported by reports of acetate production under complete anaerobiasis in *G. duodenalis* [64], indicating that pyruvate flux through acetyl-CoA synthase is a resilient mechanism of ATP generation.

The identification of a putative trimethylamine (TMA) dehydrogenase and elements of a putative TMA-NO sensing system (discussed below) in the down-regulated genes, raise the possibility that *G. duodenalis* can utilize TMA-NO as a terminal electron acceptor. TMA-NO metabolism has been demonstrated for a variety of gut commensals [66], and the acquisition of key metabolic genes in *G. duodenalis* via horizontal gene transfer is well documented [34, 67, 68]. Lastly, the significant up-regulation of glycerol kinase at the stationary and declining phases relative to log phase, could indicate a glycerol-dependent ATP generation pathway in *G. duodenalis*. The metabolically similar protist *Entamoeba histolytica* has been shown to divert glycolytic intermediates to glycerol when central glycolytic enzymes are experimentally inactivated, and glycerol kinase is suggested to function in ATP generation [69]. Thus, it would be interesting to investigate the potential of this 'glycerol shunt' as an alternative source of ATP in *G. duodenalis*.

Transcriptional regulation

The major shift in transcription between the log and stationary, and the declining growth phases, is likely to involve signaling between cytosolic proteins and nuclear transcription factors. Intriguingly, the observed transcriptional down-regulation of genes related to glycolysis might be mediated by redox-dependent TFs. A putative GntR homolog is up-regulated at the declining phase. In *Corynebacterium glutamicum*, GntR is reported to repress transcription of the gene encoding 6-phosphogluconate dehydrogenase, which is associated with the production of NADPH in the pentose-phosphate pathway. Notably, the gene encoding 6-phosphogluconate dehydrogenase is transcriptionally down-regulated at the declining phase in our dataset, and as mentioned above, transcription of glycolytic genes upstream of pyruvate, such as 6-PGDH, seem to vary more greatly in response to changes in dO_2 tension (S5 Fig, panel D). Taken together, these findings suggest that declining dO_2 may inhibit glycolysis and lead to the accumulation of intracellular NAD(P)H. The apparent metabolic shift away from glycolysis may be mediated, at least in part, by redox-sensitive TFs such as the GntR homolog.

Conserved kinases have been classified in *G. duodenalis*, many of which localize to the cytoskeleton and might participate in regulation of cell structure or motility. Other kinases, particularly within the massively expanded NEK kinase family, are predicted to lack catalytic activity [70]. Although complete signaling pathways have not been resolved in *G. duodenalis*, here we have identified several differentially transcribed structural homologs of proteins that participate in two-component signal transduction. Two-component systems feature histidine kinases and associated sensor domains that detect changes in cytoplasmic or extracellular environmental conditions. Conformational changes in the sensor domain induce histidine autophosphorylation proximal to the kinase domain, and the charged phosphate is subsequently transferred to an effector protein either directly, or via phosphotransferase intermediates. In many cases, the effector translocates to the nucleus to elicit a transcriptional response [71]. Two-component systems are prevalent in bacteria, fungi, plants and free-living protozoa [72], but are little documented in parasitic protozoa and reportedly absent from *Plasmodium falciparum* [73–75]. The putative sensor protein in our data is structurally similar to a transmembrane protein

that detects trimethylamine (TMA) in the bacterial periplasm. The predicted *G. duodenalis* structure is truncated however, which may indicate a role in intra-membrane or cytosolic chemotaxis. We also identified a histidine kinase homolog, which could represent a kinase class that was previously thought to be absent in *G. duodenalis* [70]. Furthermore, the down-regulated gene group included a gene encoding a hypothetical protein with putative structural homology to the MtrR repressor, a TF that is regulated by two-component signaling in *Neisseria gonorrheae* [76] (Fig 2).

Although we did not identify a dimerization domain in the putative histidine kinase or a candidate for the response regulator, the sensor domain, Rap modulator and MtrR homologs are conserved between assemblages B and E of *G. duodenalis*, emphasizing the functional importance of these gene products among members of the species complex (Fig 4). Given the absence of two-component systems from metazoans [74], this putative pathway warrants detailed investigation as a possible target for chemotherapeutic intervention.

In further support of coordinated transcriptional regulation, we performed the most comprehensive and sensitive promoter motif search on this species to date, and identified motifs that are enriched in the promoter regions of down- and up-regulated DTG groups. The motif enriched in the down-regulated group (AWTTTW), occurs close to the translation start codon and is likely to be related to the AT-rich transcription initiator motifs reported in previous studies [26,77,78]. At present, little is known about TFs in *G. duodenalis* other than those involved in inducing encystation [48,79–82]. It is conceivable that, in the presence of abundant nutrients, transcription is relatively tightly regulated via TF binding to initiator regions. Subsequently, in the declining phase when trophozoites appear to be metabolically stressed, and display physiological changes such as a loss of cytoadherence, less energy might be expended on transcriptional regulation. The GRGGTM motif, which is enriched in the promoters of up-regulated genes, exhibits little positional conservation, perhaps due to the relatively low number of positive promoter sequences (64 *vs* 209 for the AWTTTW motif). Although neither the of the motifs identified in down- and up-regulated genes matched to known TF-binding motifs in yeast, the MtrR and GntR putative TFs identified in these groups are worthy candidates for further investigation, which could link redox/metabolite sensing and transcriptional regulation.

Conclusions and implications for future studies

By characterizing the dynamics of the mRNA transcriptome of axenically cultured *G. duodenalis* trophozoites across growth phases, we identified major changes in gene transcription that relate to central carbon metabolism and the antioxidant system. We also identified a putative signaling pathway and promoter motifs upstream of DTGs that might contribute to transcriptional regulation. We show that transcriptional behaviour of *G. duodenalis* trophozoites differs markedly over time in axenic culture, likely reflecting the exploitation and depletion of essential nutrients in a closed culture system. Importantly, the present data indicate that culturing *G. duodenalis* under micro-aerobic or entirely anaerobic conditions (through sparging medium) is likely to have a significant impact on transcriptional behaviour, particularly in relation to the oxidative stress response. Therefore, we suggest that the modularity of antioxidant transcription in this protist be further tested under precisely defined atmospheres, together with metabolomic profiling. The consistently high transcription of these pathways during log and stationary phases—when trophozoites are typically harvested for experimentation—is also relevant for contextualizing single time-point studies in these parasites.

Consistent with previous findings that *G. duodenalis* exhibits specific stress responses and considerable transcriptional flexibility, the present study indicates that major shifts in transcription in *G. duodenalis* might be regulated at least in part through key transcription factors

(i.e., MtrR, GntR), and a number of distinct motifs consistent with TF-binding sites, that are enriched in the promoter regions of down- and up-regulated DTGs respectively. The possible role of a two-component-like signal transduction system is particularly interesting and could link cytosolic redox or metabolite sensing and transcriptional changes. This work has been greatly enhanced by the large-scale prediction of putative structures and structural homologs for hypothetical and deprecated proteins, among which were novel antioxidant and signaling proteins among many others. This approach has great potential for illuminating the functions of vast numbers of under-annotated and un-annotated gene products in other important pathogens. The present study also provides a starting point for re-examination of the constituents of the standard trophozoite culture medium, and a reference against which future studies of targeted alterations could be compared. For example, the reaction of dissolved oxygen (dO_2) with iron may be a source of oxidative stress at early phases during *in vitro* culture of *G. duodenalis* trophozoites, and thus concentrations of ammonium ferric citrate and ascorbic acid might need to be reconsidered, particularly as work in other systems has linked ascorbic acid with intracellular iron concentrations [83]. A major finding is that glucose is likely to be in excess in the standard culture media, but its utilization as a carbon source might be limited by the availability of dO_2, inducing trophozoites to rely on less efficient energy generation pathways in the declining phase. In the future these findings and the detailed longitudinal transcriptomic information presented here, should be used in conjunction with targeted metabolomic investigations in *G. duodenalis*, with the aim of creating a completely defined medium. Whereas the present study has used the *G. duodenalis* assemblage A genome strain (WB), single time-point profiling of assemblages B [84] and E [85] indicate different transcriptional patterns, which could result from different genomic organization [27,60]. Therefore, similar longitudinal transcriptional investigations of other assemblages are required to better characterize the degree of transcriptional flexibility and the drivers and mediators of transcriptional responses across the species. This work should facilitate a better understanding of the transcriptional flexibility and metabolic preferences of *G. duodenalis* under standard culture conditions, and contribute to the development of a completely defined medium for more refined investigations into the biology of this important model eukaryote and pathogen.

Supporting Information

S1 Table. RNA-seq read processing and mapping statistics.
(XLSX)

S2 Table. Average transcriptional abundance, ranking and fold change for all genes. Differential transcription statistics (FDR <0.05) and putative structural homologs for selected gene products.
(XLSX)

S3 Table. Gene Ontology terms in the Biological Process category that are enriched within large differentially transcribed gene groups.
(XLSX)

S4 Table. KEGG BRITE terms that are enriched within large differentially transcribed gene groups.
(XLSX)

S5 Table. Average transcriptional abundance for glycolytic enzymes in Fig 4.
(XLSX)

S1 Fig. Attached, suspended and total *Giardia duodenalis* trophozoite numbers over 96 hours of axenic culture. Flasks were seeded with 10^5 trophozoites. The decline in total cell number is due to the omission of the pellet of dead and dying cells from the cell count. Error bars represent ± 1 SD, n = 3.
(TIFF)

S2 Fig. Total and novel transcript detection as a function of mapped reads for replicate filtered RNA-seq read libraries representing the log, stationary, and declining phases of axenic *Giardia duodenalis* trophozoites.
(TIFF)

S3 Fig. Distribution of median-normalized transcriptional abundance for all genes at three growth phases.
(TIFF)

S4 Fig. Transcriptional profiles for ubiquitinylation and proteasomal enzymes. Transcriptional profiles for down-regulated ubiquitinylation enzymes (A); ubiquitinylation enzymes that were not significantly differentially transcribed (B); and proteasome component proteins (C). *significantly differentially transcribed genes encoding proteasome components. Error bars represent ± 1 SEM. UCE: ubiquitin-conjugating enzyme.
(TIFF)

S5 Fig. Pearson correlations for transcriptional abundance in the log, stationary and declining growth phases (corresponding to 48, 60 and 96 h; x axis), and transcriptional profiles for WB trophozoites cultured under aerobic (perforated line) and anaerobic conditions (unbroken line) as reported by Ma'ayeh et al. [28]. Correlation between all transcribed genes (A); annotated antioxidant genes (B); annotated glycolytic genes (C); and glycolytic genes encoding proteins involved in glycolysis upstream- (D) and downstream (E) of pyruvate (see Fig 4).
(TIFF)

S6 Fig. Transcriptional abundance for variant-specific surface proteins (VSPs) at three growth phases. Gene accession numbers (GL50803) are displayed above the seven most abundant genes.
(TIFF)

S7 Fig. Top 20 variant-specific surface proteins (VSPs), ranked by transcriptional abundance for each replicate.
(TIFF)

S8 Fig. Transcriptional variation relative to mean transcriptional abundance for variant-specific surface proteins (VSPs) at three growth phases. Transcriptional variation between replicates for the same growth phase is expressed as the coefficient of variation (CV; standard deviation ÷ average; y axis). Note the x axis (mean transcriptional abundance) is log. Linear regression lines are displayed.
(TIFF)

Author Contributions

Conceived and designed the experiments: BREA LB ARJ. Performed the experiments: BREA. Analyzed the data: BREA PKK NDY RSH SGS MJM CAAR ARJ. Contributed reagents/materials/analysis tools: LB CAAR MJM RBG. Wrote the paper: BREA MJM SGS RBG ARJ.

References

1. Lane S, Lloyd D (2002) Current trends in research into the waterborne parasite *Giardia*. Crit Rev Microbiol 28: 123–147. PMID: 12109771
2. McCormick BJ (2014) Frequent symptomatic or asymptomatic infections may have long-term consequences on growth and cognitive development. In: Heitdt PJ, Lang D, Riddle MS, Walker RI, Rusch V, editors Old Herborn University Seminar Monographs 23–39.
3. Guerrant RL, DeBoer MD, Moore SR, Scharf RJ, Lima AAM (2012) The impoverished gut—a triple burden of diarrhoea, stunting and chronic disease. Nat Rev Gastroentero 10: 220–229.
4. Halliez MC (2013) Extra-intestinal and long term consequences of *Giardia duodenalis* infections. World J Gastroenterol 19: 8974. doi: 10.3748/wjg.v19.i47.8974 PMID: 24379622
5. Verdu EF, Riddle MS (2012) Chronic gastrointestinal consequences of acute infectious diarrhea evolving concepts in epidemiology and pathogenesis. Am J Gastroenterol 107: 981–989. doi: 10.1038/ajg.2012.65 PMID: 22508147
6. Escobedo AA, Cimerman S (2007) *Giardia*sis a pharmacotherapy review. Expert Opin Pharmacother 8: 1885–1902. PMID: 17696791
7. Watkins RR, Eckmann L (2014) Treatment of *Giardia*sis Current Status and Future Directions. Curr Infect Dis Rep 16: 396. doi: 10.1007/s11908-014-0396-y PMID: 24493628
8. Wright JM, Dunn LA, Upcroft P (2003) Efficacy of anti*Giardia*l drugs. Expert Opin Drug Saf 2: 529–541. PMID: 14585063
9. Solaymani-Mohammadi S, Genkinger JM, Loffredo CA, Singer SM (2010) A meta-analysis of the effectiveness of albendazole compared with metronidazole as treatments for infections with *Giardia duodenalis*. PLoS Negl Trop Dis 4: e682. doi: 10.1371/journal.pntd.0000682 PMID: 20485492
10. Lalle M (2010) *Giardia*sis in the post genomic era treatment, drug resistance and novel therapeutic perspectives. Infect Disord Drug Targets 10: 283–294. PMID: 20429863
11. Nabarro LEB, Lever RA, Armstrong M, Chiodini PL (2015) Increased incidence of nitroimidazole-refractory *Giardia*sis at the Hospital for Tropical Diseases, London 2008–2013. Clinical Microbiology and Infection 21: 791–796. doi: 10.1016/j.cmi.2015.04.019 PMID: 25975511
12. Hehl AB, Marti M (2004) Secretory protein trafficking in *Giardia intestinalis*. Mol Microbiol 53: 19–28. PMID: 15225300
13. Morf L, Spycher C, Rehrauer H, Fournier CA, Morrison HG, Hehl AB (2010) The transcriptional response to encystation stimuli in *Giardia lamblia* is restricted to a small set of genes. Eukaryot Cell 9: 1566–1576. doi: 10.1128/EC.00100-10 PMID: 20693303
14. Sonda S, Morf L, Bottova I, Baetschmann H, Rehrauer H, Caflisch H, et al. (2010) Epigenetic mechanisms regulate stage differentiation in the minimized protozoan *Giardia lamblia*. Mol Microbiol 76: 48–67. doi: 10.1111/j.1365-2958.2010.07062.x PMID: 20132448
15. Macrae IJ, Zhou K, Li F, Repic A, Brooks AN, Cande WZ, et al. (2006) Structural basis for double-stranded RNA processing by Dicer. Science 311: 195–198. PMID: 16410517
16. Shabalina S, Koonin E (2008) Origins and evolution of eukaryotic RNA interference. Trends in Ecology & Evolution 23: 578–587. doi: 10.1016/j.tree.2008.06.005 PMID: 18715673
17. Prucca CG, Slavin I, Quiroga R, Elías EV, Rivero FD, Saura A, et al. (2008) Antigenic variation in *Giardia lamblia* is regulated by RNA interference. Nature 456: 750–754. doi: 10.1038/nature07585 PMID: 19079052
18. Müller J, Sterk M, Hemphill A, Müller N (2007) Characterization of *Giardia lamblia* WB C6 clones resistant to nitazoxanide and to metronidazole. J Antimicrob Chemother 60: 280–287. PMID: 17561498
19. Müller J, Ley S, Felger I, Hemphill A, Müller N (2008) Identification of differentially expressed genes in a *Giardia lamblia* WB C6 clone resistant to nitazoxanide and metronidazole. J Antimicrob Chemother 62: 72–82. doi: 10.1093/jac/dkn142 PMID: 18408240
20. Smith NC, Bryant C, Boreham PF (1988) Possible roles for pyruvateferredoxin oxidoreductase and thiol-dependent peroxidase and reductase activities in resistance to nitroheterocyclic drugs in *Giardia intestinalis*. Int J Parasitol 18: 991–997. PMID: 3225121
21. Townson SM, Boreham PF, Upcroft P, Upcroft JA (1994) Resistance to the nitroheterocyclic drugs. Acta Tropica 56: 173–194. PMID: 8203303
22. Lindley TA, Chakraborty PR, Edlind TD (1988) Heat shock and stress response in *Giardia lamblia*. Mol Biochem Parasitol 28: 135–143. PMID: 2452980
23. Spycher C, Herman EK, Morf L, Qi W, Rehrauer H, Aquino Fournier C, et al. (2013) An ER-directed transcriptional response to unfolded protein stress in the absence of conserved sensor-transducer proteins in *Giardia lamblia*. Mol Microbiol 88: 754–771. doi: 10.1111/mmi.12218 PMID: 23617761

24. Ringqvist E, Avesson L, Söderbom F, Svärd SG (2011) Transcriptional changes in *Giardia* during host-parasite interactions. Int J Parasitol 41: 277–285. doi: 10.1016/j.ijpara.2010.09.011 PMID: 21074536

25. Ma'ayeh SY, Brook-Carter PT (2012) Representational difference analysis identifies specific genes in the interaction of *Giardia duodenalis* with the murine intestinal epithelial cell line, IEC-6. Int J Parasitol 42: 501–509. doi: 10.1016/j.ijpara.2012.04.004 PMID: 22561399

26. Tolba MEM, Kobayashi S, Imada M, Suzuki Y, Sugano S (2013) *Giardia lamblia* Transcriptome Analysis Using TSS-Seq and RNA-Seq. PLoS ONE 8: e76184. doi: 10.1371/journal.pone.0076184 PMID: 24116096

27. Franzén O, Jerlström-Hultqvist J, Einarsson E, Ankarklev J, Ferella M, Andersson B, et al. (2013) Transcriptome Profiling of *Giardia intestinalis* Using Strand-specific RNA-Seq. PLoS Comput Biol 9: e1003000. doi: 10.1371/journal.pcbi.1003000 PMID: 23555231

28. Ma'ayeh SY, Knörr L, Svärd SG (2015) Transcriptional profiling of *Giardia intestinalis* in response to oxidative stress. Int J Parasitol in press

29. Einarsson E, Svärd SG, Troell K (2015) UV irradiation responses in *Giardia intestinalis*. Exp Parasitol 154: 25–32. doi: 10.1016/j.exppara.2015.03.024 PMID: 25825252

30. Roy A, Kucukural A, Zhang Y (2010) I-TASSER a unified platform for automated protein structure and function prediction. Nat Protoc 5: 725–738. doi: 10.1038/nprot.2010.5 PMID: 20360767

31. Capon AG, Upcroft JA, Boreham PFL, Cottis LE, Bundesen PG (1989) Similarities of *Giardia* antigens derived from human and animal sources. Int J Parasitol 19: 91–98. PMID: 2651342

32. Svärd SG, Lujan HD, editors (2011) *Giardia*—A Model Organism. Springer, Vienna.

33. Lohse M, Bolger AM, Nagel A, Fernie AR, Lunn JE, Stitt M, et al. (2012) RobiNA a user-friendly, integrated software solution for RNA-Seq-based transcriptomics. Nucleic Acids Res 40: W622–W627. doi: 10.1093/nar/gks540 PMID: 22684630

34. Morrison HG, McArthur AG, Gillin FD, Aley SB, Adam RD, Olsen GJ, et al. (2007) Genomic minimalism in the early diverging intestinal parasite *Giardia lamblia*. Science 317: 1921–1926. PMID: 17901334

35. Li B, Dewey CN (2011) RSEM accurate transcript quantification fromRNA-Seq data with or without a reference. BMC Bioinformatics 12: 323. doi: 10.1186/1471-2105-12-323 PMID: 21816040

36. Leng N, Dawson JA, Thomson JA, Ruotti V, Rissman AI, Smits BMG, et al. (2013) EBSeq an empirical Bayes hierarchical model for inference in RNA-seq experiments. Bioinformatics 29: 1035–1043. doi: 10.1093/bioinformatics/btt087 PMID: 23428641

37. Garcia-Alcalde F, Okonechnikov K, Carbonell J, Cruz LM, Gotz S, Tarazona S, et al. (2012) Qualimap evaluating next-generation sequencing alignment data. Bioinformatics 28: 2678–2679. doi: 10.1093/bioinformatics/bts503 PMID: 22914218

38. Altschul SF, Madden TL, Schäffer AA, Zhang J, Zhang Z, Miller W, et al. (1997) Gapped BLAST and PSI-BLAST a new generation of protein database search programs. Nucleic Acids Res 25: 3389–3402. PMID: 9254694

39. Botstein D, Cherry JM, Ashburner M, Ball CA, Blake JA, Butler H, et al. (2000) Gene Ontology tool for the unification of biology. Nat Genet 25: 25–29. PMID: 10802651

40. Bailey TL (2011) DREME motif discovery in transcription factor ChIP-seq data. Bioinformatics 27: 1653–1659. doi: 10.1093/bioinformatics/btr261 PMID: 21543442

41. Xu F, Jerlström-Hultqvist J, Einarsson E, Ástvaldsson Á, Svärd SG, Andersson JO (2014) The Genome of Spironucleus salmonicida Highlights a Fish Pathogen Adapted to Fluctuating Environments. PLoS Genet 10: e1004053. doi: 10.1371/journal.pgen.1004053 PMID: 24516394

42. Gupta S, Stamatoyannopoulos JA, Bailey TL, Noble W (2007) Quantifying similarity between motifs. Genome Biol 8: R24. PMID: 17324271

43. Maere S, Heymans K, Kuiper M (2005) BiNGO a Cytoscape plugin to assess overrepresentation of Gene Ontology categories in Biological Networks. Bioinformatics 21: 3448–3449. PMID: 15972284

44. Shannon P, Markiel A, Ozier O, Baliga NS, Wang JT, Ramage D, et al. (2003) Cytoscape a software environment for integrated models of biomolecular interaction networks. Genome Res 13: 2498–2504. PMID: 14597658

45. Brown DM, Upcroft JA, Upcroft P (1996) A H2O-Producing NADH Oxidase from the Protozoan Parasite *Giardia duodenalis*. Eur J Biochem 241: 155–161. PMID: 8898901

46. Di Matteo A, Scandurra FM, Testa F, Forte E, Sarti P, Brunori M, et al. (2007) The O2-scavenging Flavodiiron Protein in the Human Parasite *Giardia intestinalis*. J Biol Chem 283: 4061–4068. PMID: 18077462

47. Vicente JB, Testa F, Mastronicola D, Forte E, Sarti P, Teixeira M, et al. (2009) Archives of Biochemistry and Biophysics. Arch Biochem Biophys 488: 9–13. doi: 10.1016/j.abb.2009.06.011 PMID: 19545535

48. Su L-H, Pan Y-J, Huang Y-C, Cho C-C, Chen C-W, Huang S-W, et al. (2011) A novel E2F-like protein involved in transcriptional activation of cyst wall protein genes in *Giardia lamblia*. J Biol Chem 286: 34101–34120. doi: 10.1074/jbc.M111.280206 PMID: 21835923

49. Paget TA, jarroll EL, Manning P, Lindmark DG, Lloyd D (1989) Respiration in the cysts and trophozoites of *Giardia* muris. J Gen Microbiol 135: 145–154. PMID: 2778428

50. Paget TA, Kelly ML, jarroll EL, Lindmark DG, Lloyd D (1993) The effects of oxygen on fermentation in *Giardia lamblia*. Mol Biochem Parasitol 57: 65–71. PMID: 8093974

51. Dan M, Wang AL, Wang CC (2000) Inhibition of pyruvate-ferredoxin oxidoreductase gene expression in *Giardia lamblia* by a virus-mediated hammerhead ribozyme. Mol Microbiol 36: 447–456. PMID: 10792730

52. Pineda E, Encalada R, Rodríguez-Zavala JS, Olivos-García A, Moreno-Sánchez R, Saavedra E (2010) Pyruvateferredoxin oxidoreductase and bifunctional aldehyde-alcohol dehydrogenase are essential for energy metabolism under oxidative stress in *Entamoeba* histolytica. FEBS J 277: 3382–3395. doi: 10.1111/j.1742-4658.2010.07743.x PMID: 20629749

53. Ansell BRE, McConville MJ, Ma'ayeh SY, Dagley MJ, Gasser RB, Svärd SG, et al. (2015) Drug resistance in *Giardia duodenalis*. Biotechnol Adv 33: 888–901. doi: 10.1016/j.biotechadv.2015.04.009 PMID: 25922317

54. Lloyd D, CC HJ, maroulis S, A BG, Wadley RB, Turner MP, et al. (2000) The microaerophilic flagellate *Giardia intestinalis* oxygen and its reaction products collapse membrane potential and cause cytotoxicity. Microbiology 146: 3109–3118. PMID: 11101669

55. Mastronicola D, Falabella M, Testa F, Pucillo LP, Teixeira M, Sarti P, et al. (2014) Functional Characterization of Peroxiredoxins from the Human Protozoan Parasite *Giardia intestinalis*. PLoS Negl Trop Dis 8: e2631. doi: 10.1371/journal.pntd.0002631 PMID: 24416465

56. Espey MG (2013) Role of oxygen gradients in shaping redox relationships between the human intestine and its microbiota. Free Radic Biol Med 55: 130–140. doi: 10.1016/j.freeradbiomed.2012.10.554 PMID: 23127782

57. Imlay JA (2006) Iron-sulphur clusters and the problem with oxygen. Mol Microbiol 59: 1073–1082. PMID: 16430685

58. Shang F, Taylor A (2011) Free Radical Biology & Medicine. Free Radic Biol Med 51: 5–16. doi: 10.1016/j.freeradbiomed.2011.03.031 PMID: 21530648

59. Davids BJ, Reiner DS, Birkeland SR, Preheim SP, Cipriano MJ, McArthur AG, et al. (2006) A New Family of *Giardia*l Cysteine-Rich Non-VSP Protein Genes and a Novel Cyst Protein. PLoS ONE 1: e44. PMID: 17183673

60. Emery SJ, Lacey E, Haynes PA (2015) Quantitative proteomics analysis of *Giardia duodenalis*Assemblage A—a baseline for host, assemblage and isolate variation. Proteomics 15: 2281–2285. doi: 10.1002/pmic.201400434 PMID: 25728068

61. Nash TE, Herrington DA, Levine MM, Conrad JT, Merritt JW (1990) Antigenic variation of *Giardia lamblia* in experimental human infections. J Immunol 144: 4362–4369. PMID: 2341723

62. Nash TE, Merritt JW, Conrad JT (1991) Isolate and epitope variability in susceptibility of *Giardia lamblia* to intestinal proteases. Infect Immun 59: 1334–1340. PMID: 1706319

63. Adam RD (2001) Biology of *Giardia lamblia*. Clin Microbiol Rev 14: 447–475. PMID: 11432808

64. Lindmark DG (1980) Energy metabolism of the anaerobic protozoon *Giardia lamblia*. Mol Biochem Parasitol 1: 1–12. PMID: 6108507

65. Mendis AH, Thompson RC, Reynoldson JA, Armson A, Meloni BP, Gunsberg S (1992) The uptake and conversion of L-[U14C-] aspartate and L-[U14C-] alanine to 14CO2 by intact trophozoites of *Giardia duodenalis*. Comp Biochem Physiol, B 102: 235–239. PMID: 1617934

66. Koeth RA, Wang Z, Levison BS, Buffa JA, Org E, Sheehy BT, et al. (2013) Intestinal microbiota metabolism of l-carnitine, a nutrient in red meat, promotes atherosclerosis. Nat Med 19: 576–585. doi: 10.1038/nm.3145 PMID: 23563705

67. Pal D, Banerjee S, Cui J, Schwartz A, Ghosh SK, Samuelson J (2009) *Giardia*, *Entamoeba*, and *Trichomonas* enzymes activate metronidazole (nitroreductases) and inactivate metronidazole (nitroimidazole reductases). Antimicrob Agents Chemother 53: 458–464. doi: 10.1128/AAC.00909-08 PMID: 19015349

68. Nixon JEJ, Wang A, Field J, Morrison HG, McArthur AG, Sogin ML, et al. (2002) Evidence for lateral transfer of genes encoding ferredoxins, nitroreductases, NADH oxidase, and alcohol dehydrogenase 3 from anaerobic prokaryotes to *Giardia lamblia* and *Entamoeba histolytica*. Eukaryot Cell 1: 181–190. PMID: 12455953

69. Husain A, Sato D, Jeelani G, Soga T, Nozaki T (2012) Dramatic Increase in Glycerol Biosynthesis upon Oxidative Stress in the Anaerobic Protozoan Parasite *Entamoeba histolytica*. PLoS Negl Trop Dis 6: e1831. doi: 10.1371/journal.pntd.0001831 PMID: 23029590

70. Manning G, Reiner DS, Lauwaet T, Dacre M, Smith A, Zhai Y, et al. (2011) The minimal kinome of *Giardia lamblia* illuminates early kinase evolution and unique parasite biology. Genome Biology 12: R66. doi: 10.1186/gb-2011-12-7-r66 PMID: 21787419

71. Gao R, Stock AM (2009) Biological Insights from Structures of Two-Component Proteins. Annu Rev Microbiol 63: 133–154. doi: 10.1146/annurev.micro.091208.073214 PMID: 19575571

72. Thomason P, Kay R (2000) Eukaryotic signal transduction via histidine-aspartate phosphorelay. J Cell Sci 113: 3141–3150. PMID: 10954413

73. Koretke KK, Lupas AN, Warren PV, Rosenberg M, Brown JR (2000) Evolution of two-component signal transduction. Mol Biol Evol 17: 1956–1970. PMID: 11110912

74. Wolanin PM, Thomason PA, Stock JB (2002) Histidine protein kinases key signal transducers outside the animal kingdom. Genome Biology 3: REVIEWS3013. PMID: 12372152

75. Wuichet K, Cantwell BJ, Zhulin IB (2015) Evolution and phyletic distribution of two-component signal transduction systems. Curr Opin Microbiol 1–7: 0.

76. Routh MD, Zalucki Y, Su C-C, Zhang Q, Shafer WM, Yu EW (2011) Efflux pumps of the resistance-nodulation-division family: A perspective of their structure, function, and regulation in gram-negative bacteria. Adv Enzymol Relat Area Mol Biol 77: 109–146.

77. Teodorovic S, Walls CD, Elmendorf HG (2007) Bidirectional transcription is an inherent feature of *Giardia lamblia* promoters and contributes to an abundance of sterile antisense transcripts throughout the genome. Nucleic Acids Res 35: 2544–2553. PMID: 17403692

78. Yee J, Mowatt MR, Dennis PP, Nash TE (2000) Transcriptional analysis of the glutamate dehydrogenase gene in the primitive eukaryote, *Giardia lamblia*. J Biol Chem 275: 11432–11439. PMID: 10753960

79. Huang YC, Su LH, Lee GA, Chiu PW, Cho CC, Wu JY, et al. (2008) Regulation of Cyst Wall Protein Promoters by Myb2 in *Giardia lamblia*. J Biol Chem 283: 31021–31029. doi: 10.1074/jbc.M805023200 PMID: 18768462

80. Sun C-H, Palm D, McArthur AG, Svärd SG, Gillin FD (2002) A novel Myb-related protein involved in transcriptional activation of encystation genes in *Giardia lamblia*. Mol Microbiol 46: 971–984. PMID: 12421304

81. Pan YJ, Cho CC, Kao YY, Sun CH (2009) A Novel WRKY-like Protein Involved in Transcriptional Activation of Cyst Wall Protein Genes in *Giardia lamblia*. J Biol Chem 284: 17975–17988. doi: 10.1074/jbc.M109.012047 PMID: 19423705

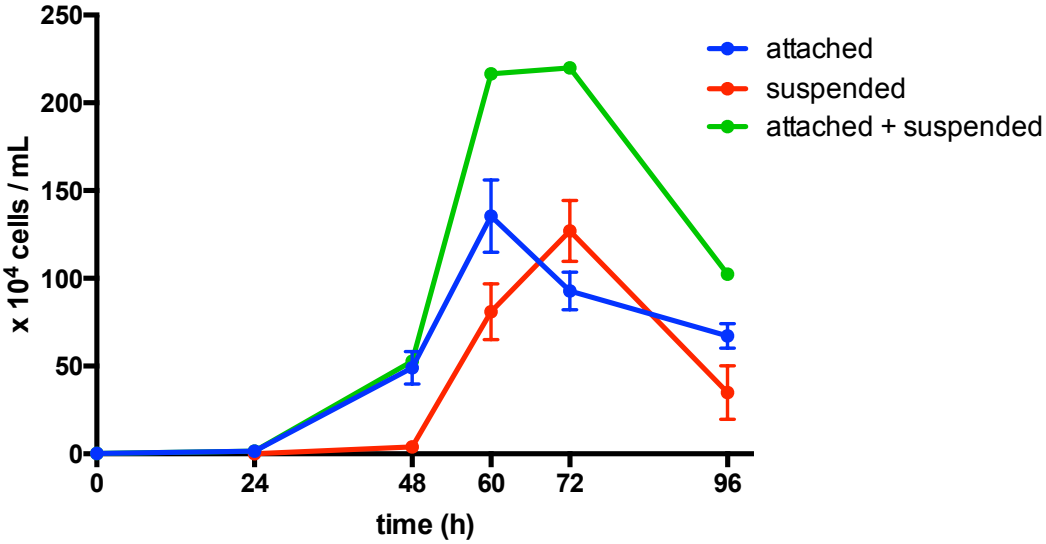
82. Sun C-H, Su L-H, Gillin FD (2006) Novel plant-GARP-like transcription factors in *Giardia lamblia*. Mol Micro Parasitol 146: 45–57.

83. Goralska M, Harned J, Fleisher LN, McGahan MC (1998) The effect of ascorbic acid and ferric ammonium citrate on iron uptake and storage in lens epithelial cells. Exp Eye Res 66: 687–697. PMID: 9657901

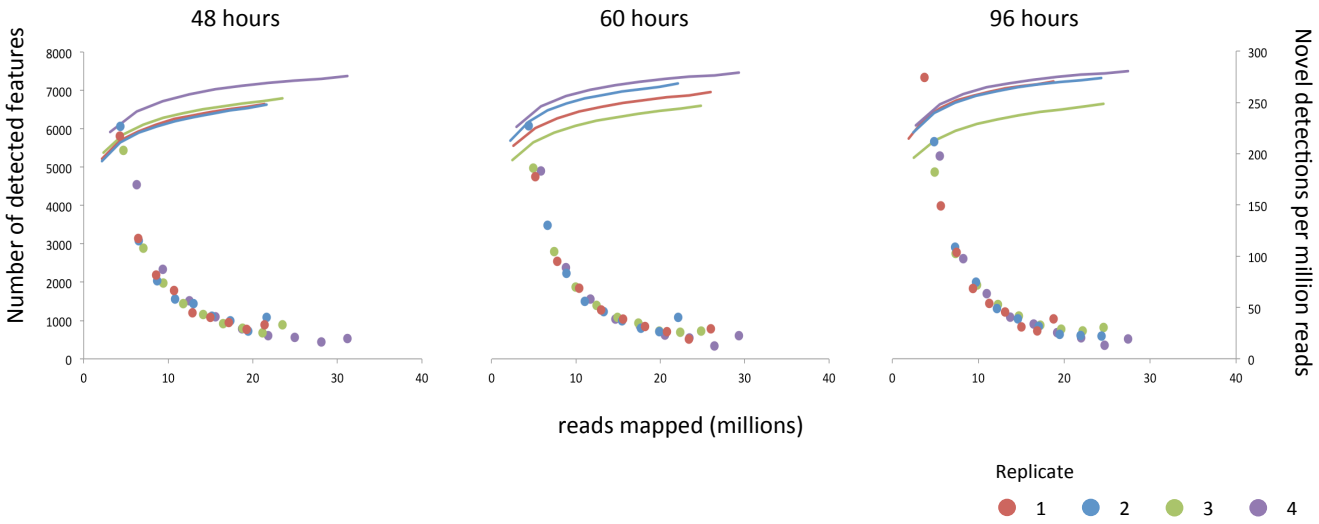
84. Franzén O, Jerlström-Hultqvist J, Castro E, Sherwood E, Ankarklev J, Reiner DS, et al. (2009) Draft genome sequencing of *Giardia intestinalis* assemblage B isolate GS is human *Giardia*sis caused by two different species? PLoS Pathog. PLoS Path 5: e1000560.

85. Jerlström-Hultqvist J, Franzén O, Ankarklev J, Xu F, Nohýnková E, Andersson JO, et al. (2010) Genome analysis and comparative genomics of a *Giardia intestinalis* assemblage E isolate. BMC Genomics 11: 543. doi: 10.1186/1471-2164-11-543 PMID: 20929575

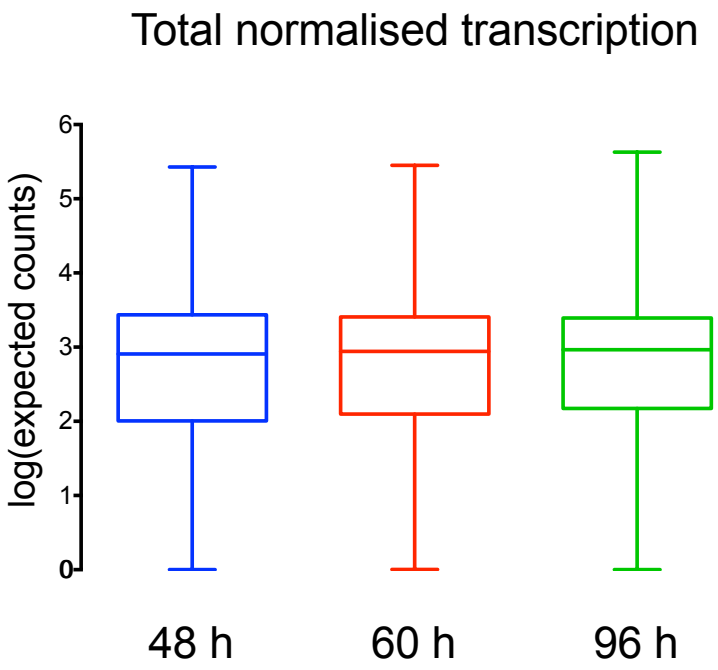
86. Müller J, Rout S, Leitsch D, Vaithilingam J, Hehl A, Müller N (2015) Comparative characterisation of two nitroreductases from *Giardia lamblia* as potential activators of nitro compounds. Int J Parasitol Drugs Drug Resist 5: 37–43.



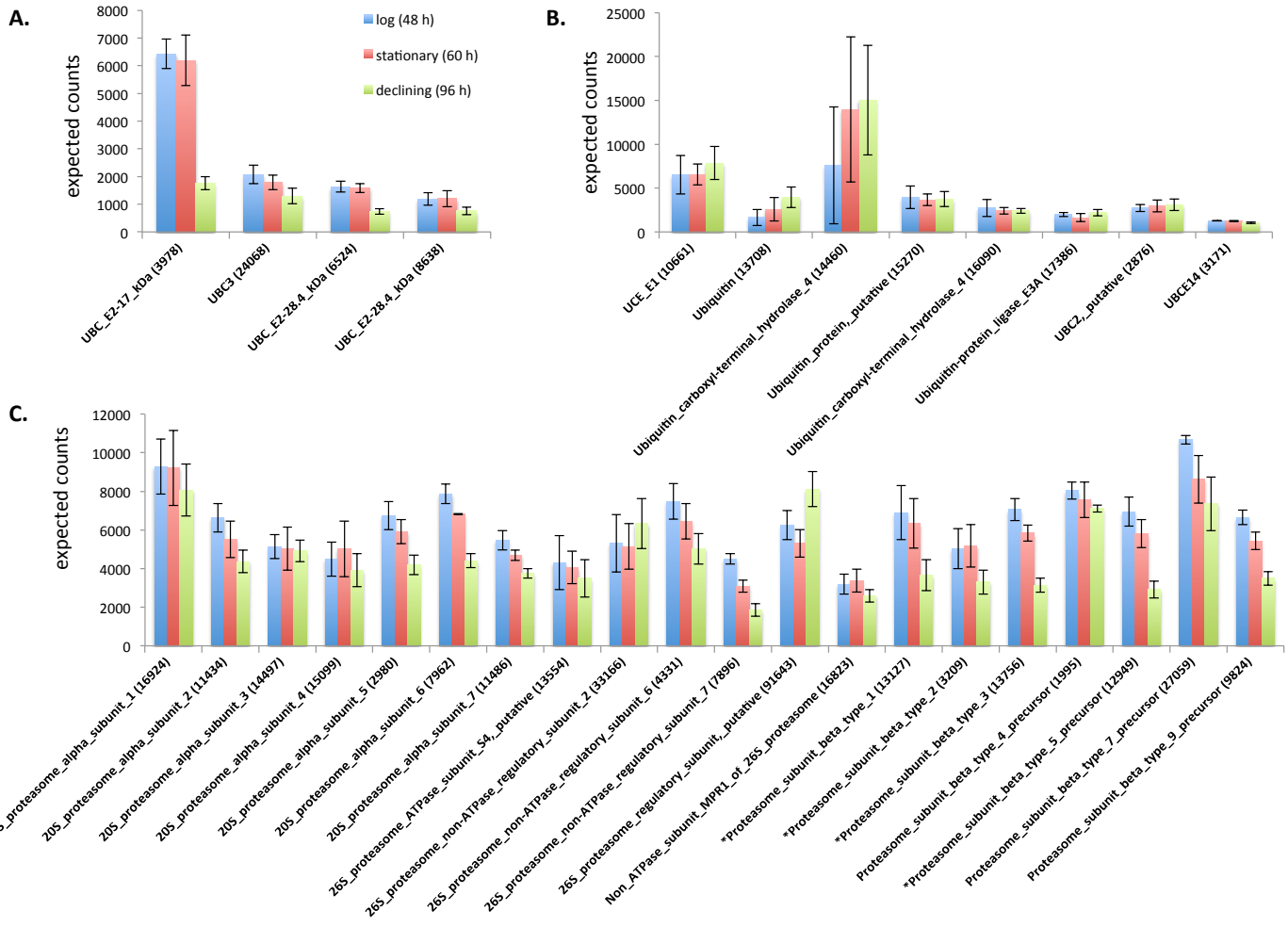
S1 Fig. Attached, suspended and total *Giardia duodenalis* trophozoite numbers over 96 hours of axenic culture. Flasks were seeded with 105 trophozoites. The decline in total cell number is due to the omission of the pellet of dead and dying cells from the cell count. Error bars represent ± 1 SD, n = 3.



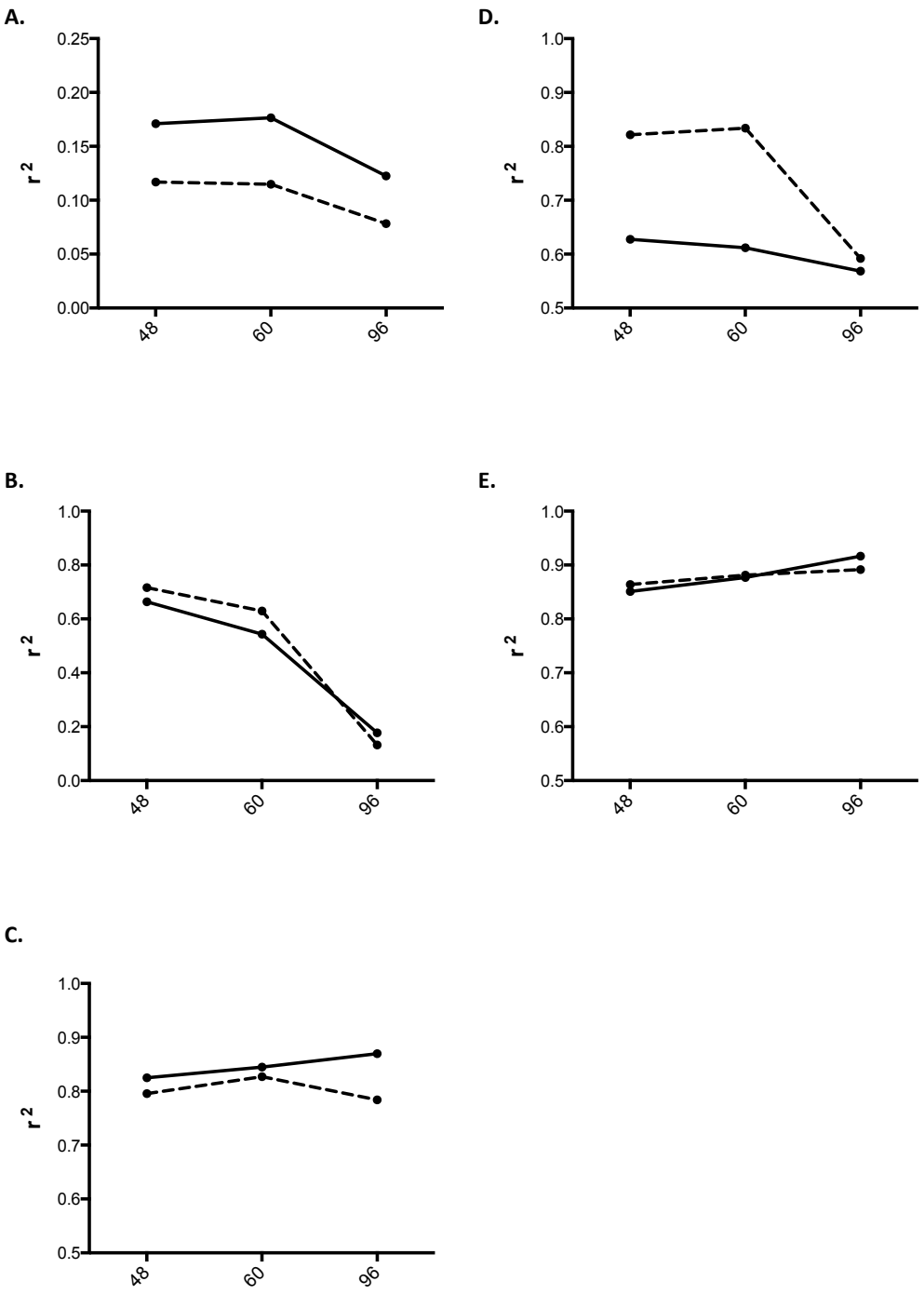
S2 Fig. Total and novel transcript detection as a function of mapped reads for replicate filtered RNA-seq read libraries representing the log, stationary, and declining phases of axenic *Giardia duodenalis* trophozoites.



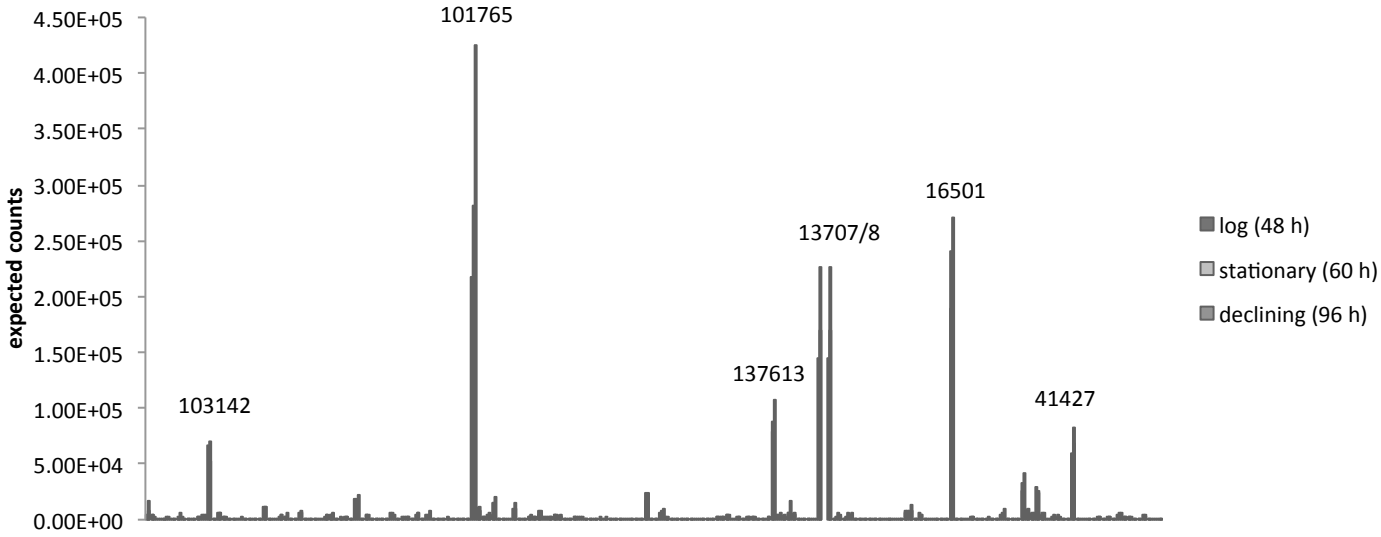
S3 Fig. Distribution of median-normalized transcriptional abundance for all genes at three growth phases.



S4 Fig. Transcriptional profiles for ubiquitinylation and proteasomal enzymes. Transcriptional profiles for down-regulated ubiquitinylation enzymes (A); ubiquitinylation enzymes that were not significantly differentially transcribed (B); and proteasome component proteins (C). Significantly differentially transcribed genes encoding proteasome components. Error bars represent ± 1 SEM. UCE: ubiquitin-conjugating enzyme.



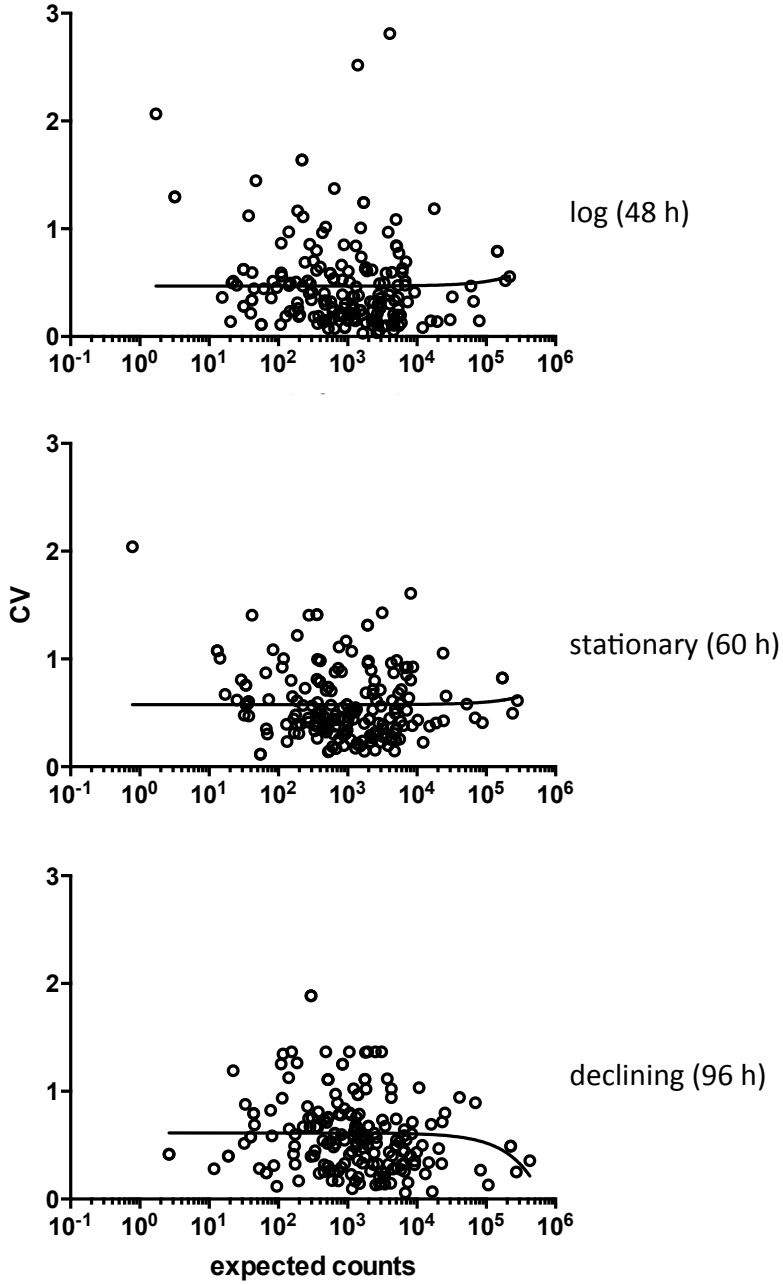
S5 Fig. Pearson correlations for transcriptional abundance in the log, stationary and declining growth phases (corresponding to 48, 60 and 96 h; x axis), and transcriptional pro- files for WB trophozoites cultured under aerobic (perforated line) and anaerobic conditions (unbroken line) as reported by Ma'ayeh et al. (2015). Correlation between all transcribed genes (A); annotated antioxidant genes (B); annotated glycolytic genes (C); and glycolytic genes encoding proteins involved in glycolysis upstream- (D) and downstream (E) of pyruvate (see Fig 4).



S6 Fig. Transcriptional abundance for variant-specific surface proteins (VSPs) at three growth phases. Gene accession numbers (GL50803) are displayed above the seven most abundant genes.

Gene ID	48 hours				60 hours				96 hours				Average rank
GL50803_101765	1	2	1	1	1	2	2	1	1	1	1	1	1.3
GL50803_16501	2	1	2	2	2	1	1	2	2	2	2	4	1.9
GL50803_137707	3	3	3	3	3	3	3	3	3	3	3	2	2.9
GL50803_137708	4	4	4	4	4	4	4	4	4	4	4	3	3.9
GL50803_137613	5	6	5	6	5	5	6	6	5	5	6	6	5.5
GL50803_41472	7	7	7	5	7	6	7	5	6	6	8	5	6.3
GL50803_103142	6	5	6	10	6	8	5	10	8	8	5	10	7.3
GL50803_13194	12	15	12	7	11	7	13	7	7	7	23	7	10.7
GL50803_113024	10	10	9	14	9	13	10	14	10	11	11	11	11.0
GL50803_40591	8	9	10	8	10	15	9	8	21	21	9	18	12.2
GL50803_38901	9	8	8	25	8	23	8	24	12	16	7	22	14.2
GL50803_11521	14	17	15	11	14	12	15	15	16	10	15	17	14.3
GL50803_115047	11	11	11	22	12	19	11	20	15	15	10	16	14.4
GL50803_111933	13	12	13	17	13	14	12	19	31	22	12	34	17.7
GL50803_14586	16	30	14	27	16	18	17	21	19	14	14	19	18.8
GL50803_134710	17	25	18	19	20	16	35	18	20	18	24	14	20.3
GL50803_137618	24	24	20	30	25	26	19	29	11	13	13	12	20.5
GL50803_101010	46	59	34	13	18	10	52	11	9	9	61	8	27.5
GL50803_34357	29	50	21	32	19	28	37	30	13	19	38	23	28.3
GL50803_11470	129	120	107	9	59	9	162	9	14	12	165	9	67.0

S7 Fig. Top 20 variant-specific surface proteins (VSPs), ranked by transcriptional abundance for each replicate.



S8 Fig. Transcriptional variation relative to mean transcriptional abundance for variant-specific surface proteins (VSPs) at three growth phases. Transcriptional variation between replicates for the same growth phase is expressed as the coefficient of variation (CV; standard deviation ÷ average; y axis). Note the x axis (mean transcriptional abundance) is log. Linear regression lines are displayed.

Chapter 6. Divergent transcriptional responses to physiological and xenobiotic stress in *Giardia duodenalis*

Brendan R E Ansell, Malcolm J. McConville, Louise Baker, Pasi K. Korhonen, Samantha J. Emery, Staffan G. Svärd, Robin B. Gasser, Aaron R. Jex. *Antimicrobial Agents and Chemotherapy* 07/2016; 60(10). DOI: 10.1128/AAC.00977-16

AMERICAN SOCIETY FOR MICROBIOLOGY | Antimicrobial Agents and Chemotherapy

Divergent Transcriptional Responses to Physiological and Xenobiotic Stress in *Giardia duodenalis*

Brendan R. E. Ansell,[a] Malcolm J. McConville,[b] Louise Baker,[a,c] Pasi K. Korhonen,[a] Samantha J. Emery,[c] Staffan G. Svärd,[d] Robin B. Gasser,[a] Aaron R. Jex[a,c]

Faculty of Veterinary and Agricultural Sciences, University of Melbourne, Melbourne, Victoria, Australia[a]; Bio21 Molecular Science and Biotechnology Institute, University of Melbourne, Melbourne, Victoria, Australia[b]; Population Health and Immunity, Walter and Eliza Hall Institute of Medical Research, Melbourne, Victoria, Australia[c]; Department of Cell and Molecular Biology, Uppsala University, Uppsala, Sweden[d]

Understanding how parasites respond to stress can help to identify essential biological processes. *Giardia duodenalis* is a parasitic protist that infects the human gastrointestinal tract and causes 200 to 300 million cases of diarrhea annually. Metronidazole, a major antigiardial drug, is thought to cause oxidative damage within the infective trophozoite form. However, treatment efficacy is suboptimal, due partly to metronidazole-resistant infections. To elucidate conserved and stress-specific responses, we calibrated sublethal metronidazole, hydrogen peroxide, and thermal stresses to exert approximately equal pressure on trophozoite growth and compared transcriptional responses after 24 h of exposure. We identified 252 genes that were differentially transcribed in response to all three stressors, including glycolytic and DNA repair enzymes, a mitogen-activated protein (MAP) kinase, high-cysteine membrane proteins, flavin adenine dinucleotide (FAD) synthetase, and histone modification enzymes. Transcriptional responses appeared to diverge according to physiological or xenobiotic stress. Downregulation of the antioxidant system and α-giardins was observed only under metronidazole-induced stress, whereas upregulation of GARP-like transcription factors and their subordinate genes was observed in response to hydrogen peroxide and thermal stressors. Limited evidence was found in support of stress-specific response elements upstream of differentially transcribed genes; however, antisense derepression and differential regulation of RNA interference machinery suggest multiple epigenetic mechanisms of transcriptional control.

Giardia duodenalis (synonyms, *Giardia lamblia* and *Giardia intestinalis*) is a parasitic protist of the vertebrate gastrointestinal tract and the most common parasite of humans (1). The vegetative life cycle stage (trophozoite) infects around 1 billion people and causes 200 to 300 million cases of diarrheal disease (giardiasis) each year (1). Infection with *G. duodenalis* is also associated with the development of chronic diseases such as irritable bowel syndrome, chronic fatigue, and diabetes (2). At present, only two major drug classes are available to treat giardiasis: nitroimidazoles, primarily metronidazole (Mtz), and benzimidazoles, such as albendazole (3, 4). Resistance to Mtz is documented in treatment-resistant clinical isolates (5–8), and resistant lines can be generated *in vitro* (reviewed in reference 9).

The mechanism of action of Mtz is relatively poorly understood. This compound is thought to diffuse into *G. duodenalis* trophozoites as an inactive prodrug, whereupon it is enzymatically reduced (activated), yielding reactive intermediates. Mtz intermediates are thought to kill trophozoites by oxidizing proteins, lipids, and DNA (10, 11); however, the relative importance of damage to different biomolecules for Mtz-induced cytotoxicity is contested (10, 12). Resistance to Mtz involves changes in enzyme expression which limit drug activation. Nitroreductase-1, thioredoxin reductase, and pyruvate-ferredoxin oxidoreductase (PFOR) and its redox partner ferredoxin are implicated in activating Mtz and are variously downregulated in resistant lines (reviewed in reference 9). Upregulation of a putative Mtz detoxification enzyme, nitroreductase-2, is also reported in resistant lines (13), suggesting that resistance involves both avoiding drug activation and enhancing enzymatic detoxification. Understanding the initial molecular response to Mtz can yield insight into the mode of action of this drug and illuminate the cellular states that may prime the development of higher levels of resistance. Previous studies (14, 15) in which *G. duodenalis* trophozoites were subjected to sublethal concentrations of Mtz reported heightened histone 2A phosphorylation (a marker of DNA damage) and downregulation of nitroreductase 1. However, there is a paucity of system-level investigations into the response of *G. duodenalis* to Mtz-induced stress.

The nature of the Mtz response in *G. duodenalis* is of interest in the context of cellular responses to other stressors. In a natural infection, trophozoites adhere to the intestinal villi, where they are exposed to spatiotemporal fluctuations in dissolved oxygen (16) and other oxidants, including hydrogen peroxide (H_2O_2) and reactive nitrogen species, which are secreted by the host against intestinal microbes (17–20). Trophozoites may also experience anaerobic conditions before the host feeds, after secretion of antioxidant-rich bile, and close to the luminal midpoint when the cells detach to divide (16). Aside from variations in oxidant con-

Received 5 May 2016 **Returned for modification** 27 May 2016
Accepted 19 July 2016

Accepted manuscript posted online 25 July 2016

Citation Ansell BRE, McConville MJ, Baker L, Korhonen PK, Emery SJ, Svärd SG, Gasser RB, Jex AR. 2016. Divergent transcriptional responses to physiological and xenobiotic stress in *Giardia duodenalis*. Antimicrob Agents Chemother 60:6034–6045. doi:10.1128/AAC.00977-16.

Address correspondence to Brendan R. E. Ansell, bransell@unimelb.edu.au.

Supplemental material for this article may be found at http://dx.doi.org/10.1128/AAC.00977-16.

Copyright © 2016, American Society for Microbiology. All Rights Reserved.

Downloaded from http://aac.asm.org/ on October 4, 2016 by University of Melbourne

centrations, these parasites may also be exposed to temperatures as high as 40°C during fever in the host (21). Since *G. duodenalis* has evolved over millions of years in the vertebrate gut, we expect that this parasite can sense thermal stress and fluctuating intracellular redox conditions and mount molecular responses to restore homeostasis. The cellular stress response is conserved across all kingdoms of life and is characterized by four main processes: (i) cell cycle arrest, (ii) transcriptional induction or posttranslational activation of molecular chaperones, including heat shock proteins (HSPs), (iii) DNA repair, and (iv) proteasomal degradation of cellular debris (22). However, *G. duodenalis* is vastly distinct, both genetically and metabolically, from other model eukaryotes (23–25). Therefore, defining a conserved stress response in this parasite is of interest for identifying novel therapeutic targets, for understanding the evolution of drug resistance and immune evasion, and for determining the redundancy of the stress response across the eukaryotic kingdom.

The first comparison of molecular stress responses in *G. duodenalis* identified four proteins of expected molecular weights for HSPs, which were induced in response to ethanol exposure (mimicking anaerobiosis), cysteine deprivation (mimicking host malnutrition), and thermal stress (20-min exposure to 43°C) (26). Conversely, exposure to dissolved oxygen (1 h), H_2O_2 (0.1 to 1 mM; 30 min), or Mtz (58 and 580 μM; 6.5 h) elicited little HSP induction. The authors concluded that *G. duodenalis* could mount a relatively redundant response to certain stressors but lacked stress-specific responses. However, recent work has challenged this notion. For instance, trophozoites from different *G. duodenalis* genotypes (assemblages A and B) (27) were shown to downregulate HSP-coding genes (GL_98054 and GL_88765) upon exposure to H_2O_2 (28), suggesting that HSP suppression might be part of a H_2O_2-specific stress response. Furthermore, a microarray-based study revealed 11 genes that were uniquely induced in response to thermal stress and 24 that were unique to protein unfolding stress, while only a single gene was induced under both conditions (29). Promoter regions upstream of genes that were uniquely induced under thermal or unfolding stress were then shown to drive luciferase expression only in response to that stressor, suggesting that *G. duodenalis* can differentiate thermal and protein unfolding stresses (29).

A limitation of previous stress response studies in *G. duodenalis* is the failure to control for different magnitudes and durations of stress, which may confound the discovery of conserved stress responses. In the present study, we calibrated Mtz and H_2O_2 concentrations and elevated temperatures to achieve an approximate 25% reduction in trophozoite growth over 24 h. Because dissolved oxygen is evidenced to compromise the efficacy of Mtz (30, 31) and to form intracellular H_2O_2 (9, 28), we established anaerobic conditions prior to and during experimental stress exposure. As Mtz is thought to oxidize biomolecules, we hypothesized that the molecular response to this drug would be more similar to that mounted against H_2O_2, a general oxidant. Here, we present the first comprehensive comparison of transcriptional responses to different therapeutic and physiological stressors in *G. duodenalis*.

MATERIALS AND METHODS

Cell culture and reagents. *Giardia duodenalis* trophozoites (WB strain, assemblage A) were cultured in TYI-S33 medium (32) modified to contain 6 mM glucose (hereafter, TYI medium) (33). Metronidazole (Sigma-Aldrich) was dissolved to 100 mM in dimethyl sulfoxide (DMSO) and stored at 4°C. Hydrogen peroxide (H_2O_2; 30%, wt/wt, in H_2O) (HA154; Chem Supply) was diluted to 200 mM in TYI medium. Reconstituted CellTiter-Glo reagent (Promega) was stored at −20°C and thawed to room temperature ([RT] 22 to 24°C) 30 min prior to use.

Stress calibration. To compare the effect of different stressors, we incubated trophozoites for 24 h in a range of concentrations of Mtz or H_2O_2 or under various elevated temperatures to achieve an approximate 25% reduction in cell number relative to that of the controls. Trophozoites from confluent flasks were chilled on wet ice, pelleted by centrifugation (680 × *g* for 5 min at 4°C), diluted in fresh TYI medium, and added in 40-μl aliquots to wells of a 96-well clear-bottom plate (3610; Corning) to achieve 10^4 cells per well. A 200-μl aliquot of sterile water was added to the peripheral wells to limit evaporation. Plates were equilibrated at 37°C in a GasPak EZ anaerobe pouch system (260683; BD) to allow trophozoite attachment and sparging of dissolved oxygen in the medium. Serial dilutions of Mtz and H_2O_2 were prepared in TYI medium and added in 10-μl aliquots in duplicate to wells containing trophozoites. The wells of the resultant plates contained approximately 10^4 trophozoites in a total volume of 50 μl and either Mtz (2.5 to 1,000 μM), H_2O_2 (500 to 5,000 μM), 1% DMSO, or TYI medium (negative controls). Plates were incubated at 37°C in GasPak EZ anaerobe pouches with new anaerobic sachets for 24 h. To test the effect of elevated temperatures, trophozoites were added to wells in 50 μl of TYI medium and allowed to equilibrate as described above. GasPak EZ pouches were then opened, and fresh anaerobic sachets were added to replicate the procedure for Mtz and H_2O_2 exposures. On different days, plates were incubated at temperatures from 39 to 44°C, and control plates were simultaneously incubated at 37°C. To quantify cell numbers, 50 μl of CellTitre-Glo reagent was added to wells containing trophozoites, and plates were incubated for 15 min at RT with shaking. Luminescence (corresponding to the number of live cells/well) was measured using a luminometer (BioTek) and converted to a percentage of the negative-control values. For Mtz and H_2O_2 optimization, data from at least two experiments were normalized to values of the negative (1% DMSO and TYI medium) and positive (1 mM Mtz or 5 mM H_2O_2) controls, and Hill plots were fitted using the log(inhibitor) versus normalized response—variable slope module, in Prism (GraphPad). Hill equations were solved for x when the y value was 75 (i.e., 25% decrease in ATP relative to the control).

Sample generation and mRNA sequencing. For each stress condition, samples were generated in six replicates in two separate experiments (a total of 12 replicates per condition). Flat-sided tubes (Nunclon Delta) were seeded with 1.78×10^4 trophozoites in 10 ml of fresh TYI medium and incubated for 60 h, at which time trophozoites formed a confluent monolayer on the tube wall. The spent medium and suspended trophozoites were discarded, 10 ml of fresh TYI medium was added, and tubes were incubated for 2.5 h at 37°C, standing open in a GasPak EZ large incubation container (260672; BD) with three large anaerobic sachets (260678; BD) to allow sparging of dissolved oxygen. The container was briefly opened, and Mtz (20 mM stock in TYI medium) or H_2O_2 (200 mM stock in TYI medium) was added. Fresh anaerobic sachets were inserted, and tubes were incubated standing open for 24 h at 37°C. For thermal stress exposure, tubes were prepared as described above and incubated at 39°C. After incubation, tubes were capped and inverted, and a 20-μl aliquot of trophozoite suspension was deposited on a glass slide (Menzl Glazer) with a coverslip for video-microscopy (see the supplemental methods). Tubes were incubated on ice-water to allow detachment of trophozoites, which were then pelleted (680 × *g*, 5 min, 4°C), dissolved in 1 ml of TriPure reagent (Roche), and stored at −80°C. Biological replicates were thawed and randomly divided into three pairs. Aliquots of 250 μl from both members of two pairs were combined, yielding three tubes with 1 ml of dissolved trophozoite material, representing inter- and intra-experimental variation (see Fig. S1 in the supplemental material). RNA was extracted according to the manufacturer's protocol within 4 weeks of sample preparation.

The dried RNA pellet was resuspended in reverse-osmosis deionized

Downloaded from http://aac.asm.org/ on October 4, 2016 by University of Melbourne

water and treated with Turbo DNase (Ambion) according to the manufacturer's instructions. The quality of DNase-treated RNA was ascertained using a BioAnalyzer (Agilent). Polyadenylated RNA was purified from 10 μg of total RNA using Sera-Mag oligo(dT) beads, fragmented to a length of 100 to 500 bases, and reverse transcribed using random hexamers. Strands were labeled using the dUTP second-strand synthesis method, end repaired and adaptor ligated, and then treated with uracil-specific excision reagent (USER; NEB) before PCR amplification. Products were purified over a MinElute column (Qiagen), and single-ended strand-specific sequencing was performed using an Illumina HiSeq 2500 system (YourGene Biosciences, Taiwan).

Data processing and analysis. Raw reads were trimmed using Trimmomatic (34) (sliding window, 4 nt; minimum average PHRED quality, 20; leading and trailing, 3 nt; minimum read length, 40 nt) and mapped as single-ended reads to the accepted *G. duodenalis* coding domains (assemblage A genome, release 25) (23; http://giardiadb.org/giardiadb/) using RSEM (35), with the "forward-prob 0" flag which discards any reads that map with <100% confidence to the reverse complement of a predicted transcript (RNA-seq reads generated using the dUTP method represent the first cDNA strand, i.e., the reverse complement of the extracted RNA). Reads that did not map under these conditions were likely to include antisense transcripts. To quantify antisense transcription, unmapped reads were mapped with the "forward-prob 1" flag.

RSeQC (36) was used to calculate read mapping statistics (bam_stat module) and to confirm the orientation of mapped reads (infer_experiment module). Feature detection was calculated as a function of read mapping depth, using the counts module in Qualimap (version 1.0) (37) with the "k 10" flag, denoting a minimum mapped read threshold of 10. Saturation plots were displayed in Excel (Microsoft). Expected counts generated by RSEM were submitted to edgeR (38), and genes represented by fewer than 1 count per million counts (CPM) in fewer than three replicates were discarded. Sample libraries were normalized (trimmed mean of *M* values [TMM] method), and transcriptional abundance values were rescaled before fitting (general linear model) and identification of differentially transcribed genes (DTGs) under each condition relative to the control (false discovery rate [FDR] of 0.01). Comparisons between DTG groups required values for the number of transcripts per million transcripts (TPM), calculated by dividing the TMM-normalized CPM value for each gene by the effective gene length. Pearson correlations with previously published data (39) were facilitated by adjusting expected count data for all replicates by library size and TMM normalization to generate comparable CPM values. The number of reads per kilobase per million reads (RPKM) was used for correlations with RNA-seq data from other laboratories (28).

Gene ontology (GO) terms for the predicted *G. duodenalis* proteome were retrieved from GiardiaDB.org (release 25), and sensitive structure-based homology searches were performed for DTGs encoding hypothetical proteins, using the I-TASSER suite (40, 41) as described previously (39). Briefly, I-TASSER integrates amino acid sequence homology searching, with secondary and *de novo* structure prediction and molecular dynamics simulation, to generate a putative three-dimensional structure for a primary amino acid query. The predicted structure is compared against solved crystal structures in the Protein Data Bank (PDB) to allow functional inference (40). Protein structures were visualized using UCSF Chimera software (42). For promoter motif analysis, genes with at least 20 nucleotides of nonoverlapping (i.e., noncoding on opposite strand) sequence upstream and downstream of the start codon were curated using the genomic colocation tool at GiardiaDB.org. To accurately assess correlations between sense and antisense transcription, analysis was limited to protein-coding genes that did not overlap other genes.

DREME software (50) was used to detect overrepresented DNA motifs in noncoding promoters in DTG groups, and Fisher tests of independence were used to identify enriched molecular function and biological process GO terms among DTGs for each stress condition, relative to a curated background of GO terms for all DTGs. For brevity in this paper, the *G. duodenalis* WB strain gene accession prefix GL50803 is abbreviated to GL.

Accession number. RNA-seq reads have been deposited in the NCBI Sequence Read Archive under BioProject number PRJNA322403.

Data availability. Relevant data are given within the paper and in its supporting files in the supplemental material except for the raw RNA-seq reads, which are available through the NCBI Sequence Read Archive.

RESULTS

Stress calibration and read mapping. Based on stress calibration experiments, 7 μM Mtz and 1.15 mM H_2O_2 were determined to exert approximately equal effects on trophozoite growth over 24 h (Fig. 1A and B). This agrees with previously published data suggesting that exposure to 5 to 10 μM Mtz induces a 25% reduction in cell growth over 24 h (15) and that 1 mM is a physiologically relevant concentration of H_2O_2 (43, 44). Incubation at either 39 or 41°C resulted in an approximate 30% reduction in cell number; however, as incubation at 42°C was highly detrimental, 39°C was selected as the more conservative condition for further experimentation (Fig. 1C). This agrees with a previous finding that *G. duodenalis* can survive prolonged exposure to temperatures of up to 40°C with little loss of viability (29). Motile and adherent cells were visible in aliquots from all replicate flasks after 24 h, indicating cellular integrity and viability prior to RNA extraction (see the video at http://gasser-research.vet.unimelb.edu.au/AAC00977-16_Supplementary_video/AAC00977-16_Supplementary_video.pptx). Based on this, we assume that the transcriptional changes associated with our stress conditions promote survival. An average of 32.8 million reads were generated for each replicate, of which at least 91% survived quality control. Approximately 90% of surviving reads mapped uniquely to predicted coding domains in the sense orientation. An average of 2.7 million unmapped reads could be mapped to the same gene models in the inverse orientation, consistent with antisense transcripts (see Table S1 in the supplemental material). The read mapping depth for all replicates was sufficient to detect transcripts from at least 5,000 coding domains (see Fig. S2 in the supplemental material). There was little difference in median CPM values for all conditions (29.2 to 34.44 CPM); however, there was a greater spread of transcriptional abundance values under thermal stress (interquartile ratio [IQR], 5.1 to 104.6 CPM) than under other conditions (IQR, ~6 to 95 CPM) (see Fig. S3).

Differential transcription statistics and stress validation. After filtering for minimum transcriptional abundance and correcting for multiple comparisons, we identified 6,273 genes that were differentially transcribed under at least one stress condition. The proportions of up- and downregulated genes were similar for each condition, with the greatest number of differentially transcribed genes (DTGs) observed under thermal stress (5,523 genes), followed by H_2O_2- and Mtz-induced stress (3,020 and 2,087 genes, respectively). The majority of Mtz-induced DTGs were unique to that condition, whereas the majority of H_2O_2 stress-induced DTGs overlapped with the thermal stress-induced DTGs (Fig. 1D and E; see also Fig. S4 in the supplemental material). When the top 100 DTGs by fold change were compared between each condition, at most approximately 10% of genes from any two groups were shared, of which many were deprecated or hypothetical (see Fig. S5). Normalized sense and antisense transcriptional abundance and fold change statistics are provided for all genes (see Tables S2

Downloaded from http://aac.asm.org/ on October 4, 2016 by University of Melbourne

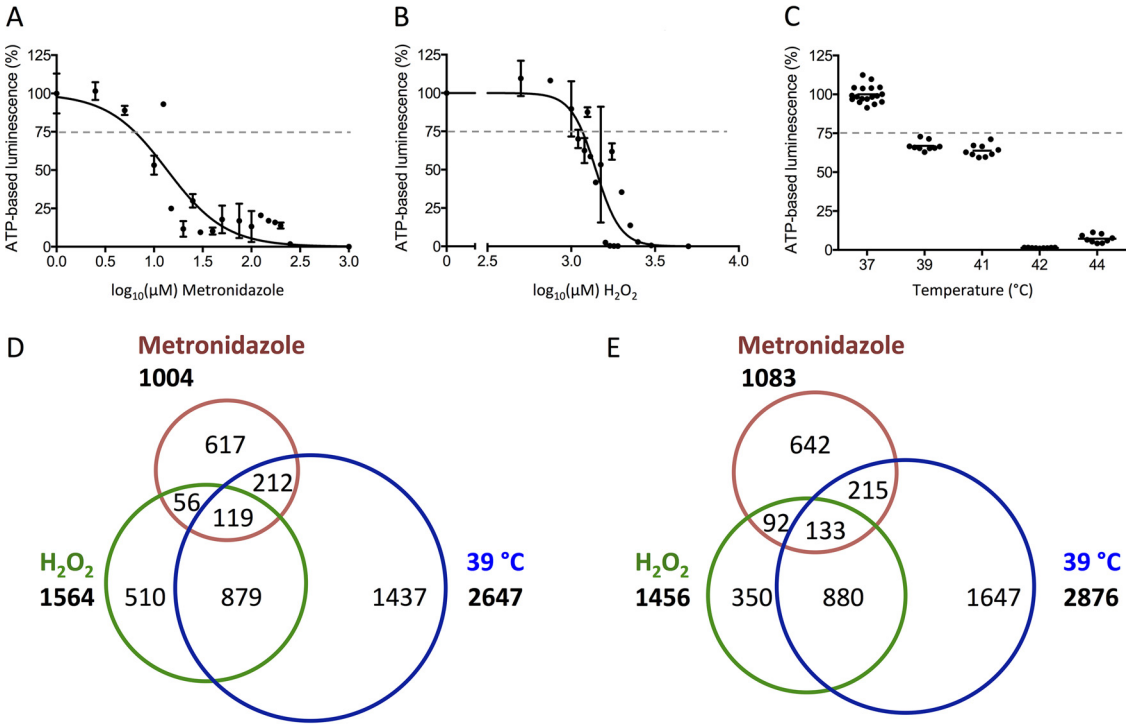


FIG 1 Stress optimization and differentially transcribed genes. Dose-response curves for *G. duodenalis* trophozoites exposed to serial dilutions of metronidazole (A), hydrogen peroxide (B), or elevated temperature (C) over 24 h. Solid lines represent Hill functions, intersected by perforated lines defining the 25% inhibitory concentration (IC_{25}) value. Venn diagrams represent significantly upregulated (D) and downregulated (E) genes at an FDR threshold of 0.01 after a 24-h exposure to each stress. Bold text indicates the total number of differentially transcribed genes under each condition.

and S3). Fold change and functional descriptions for DTGs under Mtz, H_2O_2, and thermal stress are provided in Tables S4 to S6 in the supplemental material.

In broad agreement with previous data, H_2O_2- and thermal stress-induced transcriptomes correlated equally with a previously published set of the 100 most highly transcribed genes after exposure to 150 μM H_2O_2 for 60 min ($r^2 = 0.29$) (28). Transcriptomic results for stationary-phase trophozoites grown under standard (i.e., nonanaerobic) culture conditions (39) correlated best with the transcriptome of trophozoites under H_2O_2-induced stress ($r^2 = 0.56$), whereas correlations with the anaerobic control and Mtz and thermal stress conditions were weaker ($r^2 = 0.39$ to 0.48).

Further according with previous work, nitroreductase-1 (GL_22677) was transcriptionally downregulated under Mtz-induced stress (45) and also under thermal stress (see Fig. 3E). Nine of the 11 genes that were previously reported to be specific to the thermal stress response in *G. duodenalis* (29) were upregulated under our thermal stress conditions, as were 11 of 19 other genes with annotations relating to heat shock. Interestingly, the majority of these genes were also upregulated under Mtz-induced stress, whereas 12 heat shock-related genes were downregulated under H_2O_2-induced stress (see Table S7 in the supplemental material). A hypothetical protein (GL_15125), which was previously found to be upregulated under both thermal and reducing stress (29), was upregulated under both thermal and Mtz stress in our results and has predicted structural homology with a phosphatidylinositol (PI) binding protein (PDB accession number 4BJM (46) (Fig. 2).

Metronidazole-specific genes. Genes uniquely upregulated in response to Mtz-induced stress were enriched for GO terms relating to phosphorylation and phosphatidylinositol and DNA metabolism. Mannosyltransferase and two inositol phosphatases were implicated in upregulated phosphatidylinositol metabolism, as was a partial structural homologue of the kinase mTOR. Indeed, a number of kinases, including 22 Nek and Nek-like ki-

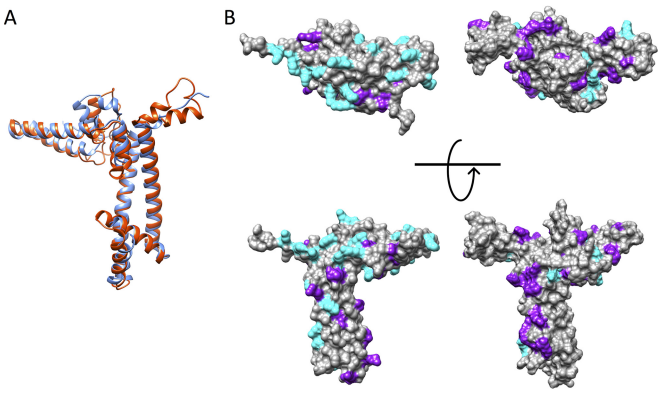


FIG 2 Comparison of the predicted structure for GL50803_15125 and the crystal structure of AvrM. (A) Predicted structure for GL50803_15125 (red), generated using I-TASSER (40), and the crystal structure of AvrM from the fungal pathogen *Melampsora lini* (blue). (B) Surface views of AvrM (left) and the predicted GL50803_15125 structure (right), with lysine (teal) and arginine (purple) residues highlighted. These residues in the AvrM N terminus (top left) are implicated in binding to phosphoinositides.

Downloaded from http://aac.asm.org/ on October 4, 2016 by University of Melbourne

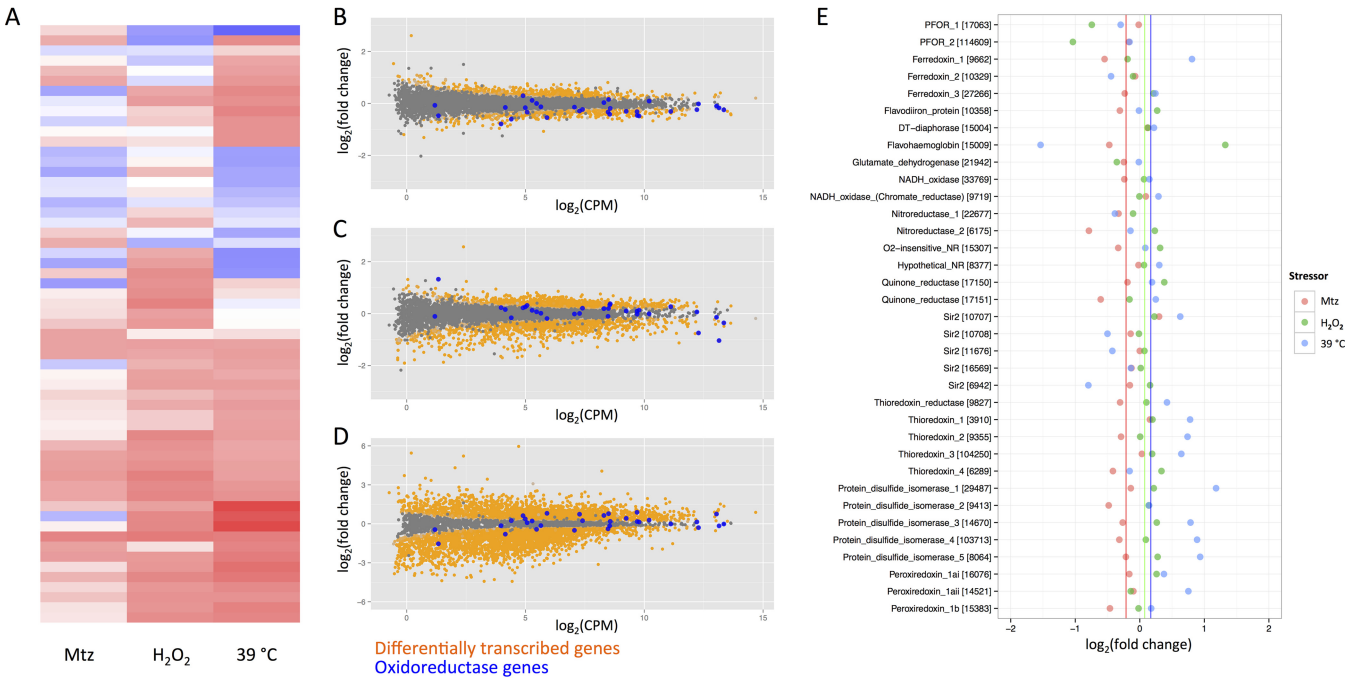


FIG 3 Antioxidant and high-cysteine membrane protein (HCMP) transcription under stress. (A) Log_2(fold change) values for HCMPs are represented in red (<0), white (0), and blue (>0), without row or column scaling. Scatter plots display differentially transcribed genes (orange) under metronidazole (B), hydrogen peroxide (C), and thermal stress (D). Antioxidant-coding genes are displayed in blue. (E) Antioxidant gene annotations including gene accession numbers (in brackets; prefix, GL50803_) and group-wise mean transcription (vertical lines) under each stress condition.

nases, were uniquely upregulated under Mtz stress. The DNA-interacting proteins Rad52, exonuclease-1, Rrm3p helicase, and PMS-1 were upregulated, as were the RNA-related proteins Dicer and pseudouridine synthase. Conversely, the vast majority of antioxidant-related genes were downregulated under Mtz-induced stress. The thioredoxin system (akin to glutathione in higher eukaryotes) and oxygen detoxification machinery were comprehensively downregulated, as were ferredoxin-1, two nitroreductases (GL_6175 and GL_15307), two putative NADPH oxidoreductases (GL_17151 and GL_17150), peroxredoxin-1b, and a glutaredoxin-related protein (Fig. 3B to E). Six Rab family members and 12 of the 21 genomically encoded α-giardins (group E annexins) (47) were also specifically downregulated, suggesting decreased vesicular trafficking and membrane fusion under Mtz stress (48, 49).

Convergent stress response genes. To identify putative general stress response genes in *G. duodenalis*, we examined genes that were up- or downregulated under all stress conditions. Enriched GO terms among 119 convergent upregulated genes related to *N*-acetyltransferase activity, ATP-dependent helicase, and cysteine-tRNA ligase activities. The genes contributing to these terms encoded glucose and histone acetyltransferases, DNA repair proteins (Rad51, TFIIH p90, and a putative ERCC-8), cysteinyl-tRNA synthetase, and a structural homologue of a catalytic aminopeptidase DIV domain. Mitogen-activated protein kinase kinase kinase (MAPKKK), flavin adenine dinucleotide (FAD) synthetase, NAD-dependent Sir2, and ubiquitin-related genes were also upregulated under all three stress conditions. Of 133 convergent downregulated genes, enriched GO terms related to molecular transport, glycolysis (specifically hexose and pyruvate metabolism), and DNA packaging. The contributing genes included ATP-binding cassette (ABC) and major facilitator superfamily (MFS) transporters, glycolytic enzymes, and several members of two gene groups that are unique to *G. duodenalis*: the high-cysteine membrane proteins (HCMPs) and 21.1-kDa ankyrin-repeat proteins (Fig. 3A).

Overlapping physiological stress response genes. A greater proportion of DTGs were shared between the thermal and H_2O_2 stress responses than between these stressors and the Mtz response (see Fig. S4 in the supplemental material), suggesting divergence in transcriptional responses according to physiological or xenobiotic stress. Investigation into the function of the 879 genes upregulated under both H_2O_2 and thermal stress conditions revealed 38 of the 68 ribosomal proteins in *G. duodenalis*, together with DNA replication enzymes, cyclin-dependent kinase 1 (51), three cyclins, and the mitotic regulator Mad2 (52). Intriguingly, three of the four GARP-like transcription factors encoded in the *G. duodenalis* genome were upregulated under both physiological stressors, as were 6 of the 17 genes with predicted GARP-binding promoter elements (53). The latter genes included the antioxidant enzymes protein disulfide isomerase 1 (PDI-1), peroxiredoxin 1a, and a Dps ferretin-like protein. Six further PDIs were also upregulated. Of the 20 Nek kinases upregulated under physiological stress, a greater proportion were predicted to be catalytically active (35%) above the background genomic prevalence of active Neks (27%) (54) (see Table S2). We found 880 downregulated genes under both H_2O_2 and thermal stressors, among which were genes encoding four cysteine proteases, a cysteine desulfurase, 17 HCMPs, and 38 Nek kinases (21% predicted active). Also downregulated were genes encoding an RNA-dependent RNA polymerase, pyruvate-ferredoxin oxidoreductase 1 (PFOR-1), three of six putative phosphatidylinositol 4,5-kinases (PI4,5Ks), and six other

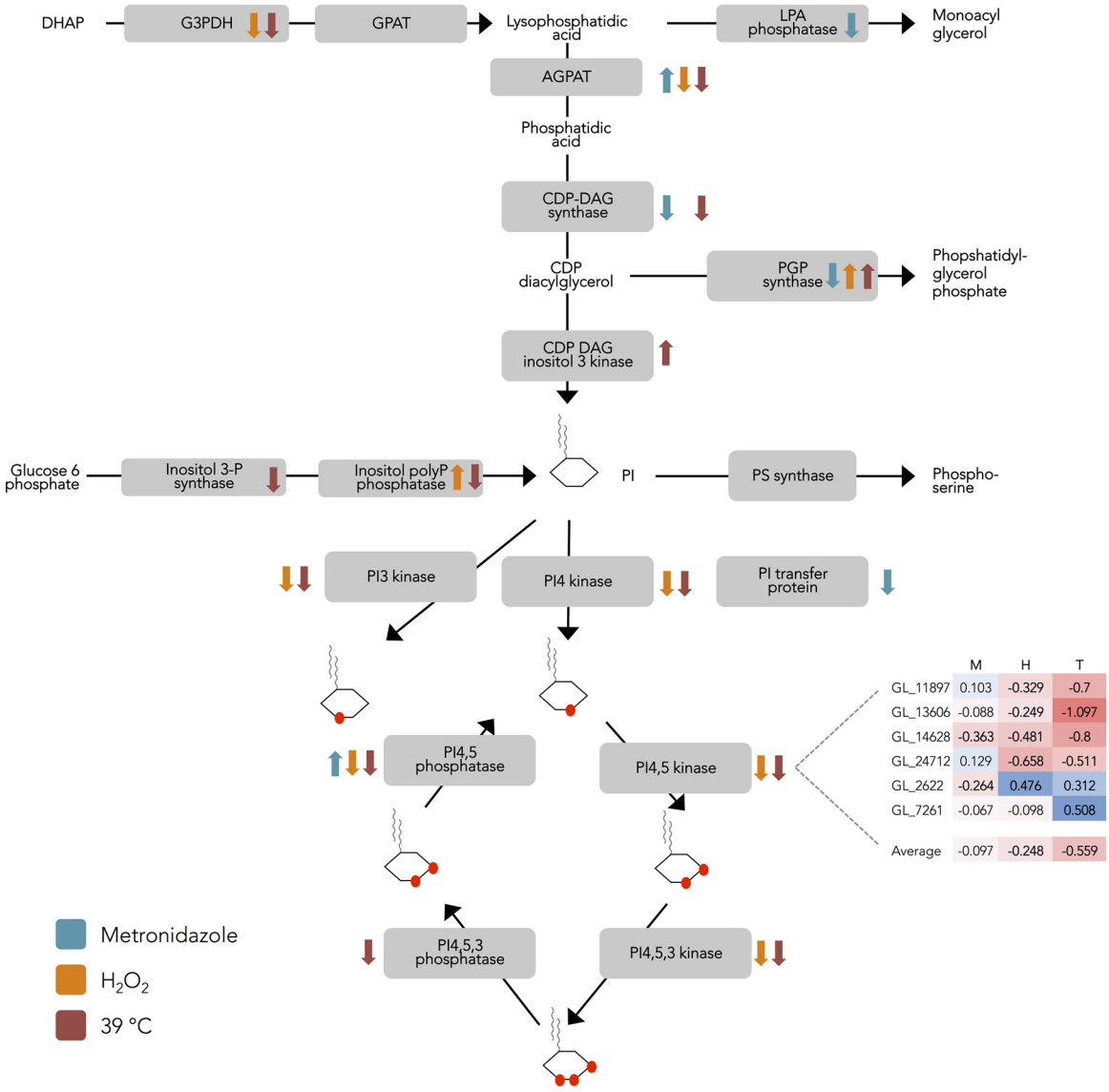


FIG 4 Differential transcription of phosphoinositide synthesis and metabolism genes under stress in *G. duodenalis*. Transcription of genes encoding enzymes involved in phosphatidylinositol (PI) metabolism appears downregulated under hydrogen peroxide and thermal stress. Trophozoites exposed to metronidazole may have a greater intracellular pool of PI4-P. Inositol phosphate is depicted as red dots. Carbon atoms in the PI ring are numbered 1 to 6 anticlockwise from the lipid moiety (wavy lines). Log_2(fold change) values for PI4,5-kinase paralogues are displayed in the table, relative to the control. Significant fold change values are displayed in bold, and average fold change for all paralogues is also indicated. Red, log_2(fold change) of <0; blue, log_2(fold change) of >0; DHAP, dihydroxyacetone phosphate; G3PDH, glyceraldehyde-3-phosphate dehydrogenase; GPAT, glycerol-3-phosphate acyltransferase; AGPAT, acyl-glycerol-3-phosphate acyltransferase; CDP-DAG, CDP diacylglycerol; PGP, phosphatidyl glycerol phosphate; polyP, polyphosphate; PS, phosphoserine.

genes involved in phosphatidylinositol synthesis and metabolism (Fig. 4). The downregulation of Dicer, together with two annotated transcription factors and five predicted structural homologues of transcriptional repressors, suggested a cessation of transcriptional repression under physiological stressors. Finally, we previously found genes encoding homologues of two-component signaling proteins that may be differentially transcribed according to dissolved oxygen tension (39). These genes also appeared to diverge transcriptionally according to physiological or xenobiotic stress. The putative MtrR repressor (GL_2338) was downregulated under Mtz stress but uniquely upregulated under H_2O_2 stress, and the putative Rap protein (GL_1979) was upregulated under both H_2O_2 and thermal stress. Comparisons of transcriptional abundance between the control and test conditions suggested that genes induced under Mtz stress were transcribed at low levels in the control, whereas genes induced under H_2O_2 and thermal stress were relatively highly transcribed in the control (see Fig. S6 in the supplemental material).

Enriched promoter motifs and antisense correlations. Given previous evidence that *G. duodenalis* may differentiate thermal and reducing stress and that stress-specific transcriptional responses might be mediated through different DNA elements (29), we searched for conserved motifs in noncoding promoters of DTGs (median length, 116 nt; IQR, 61 to 257 nt). Numerous significantly overrepresented motifs containing only A and T were identified (see Fig. S7 in the supplemental material), but more

Downloaded from http://aac.asm.org/ on October 4, 2016 by University of Melbourne

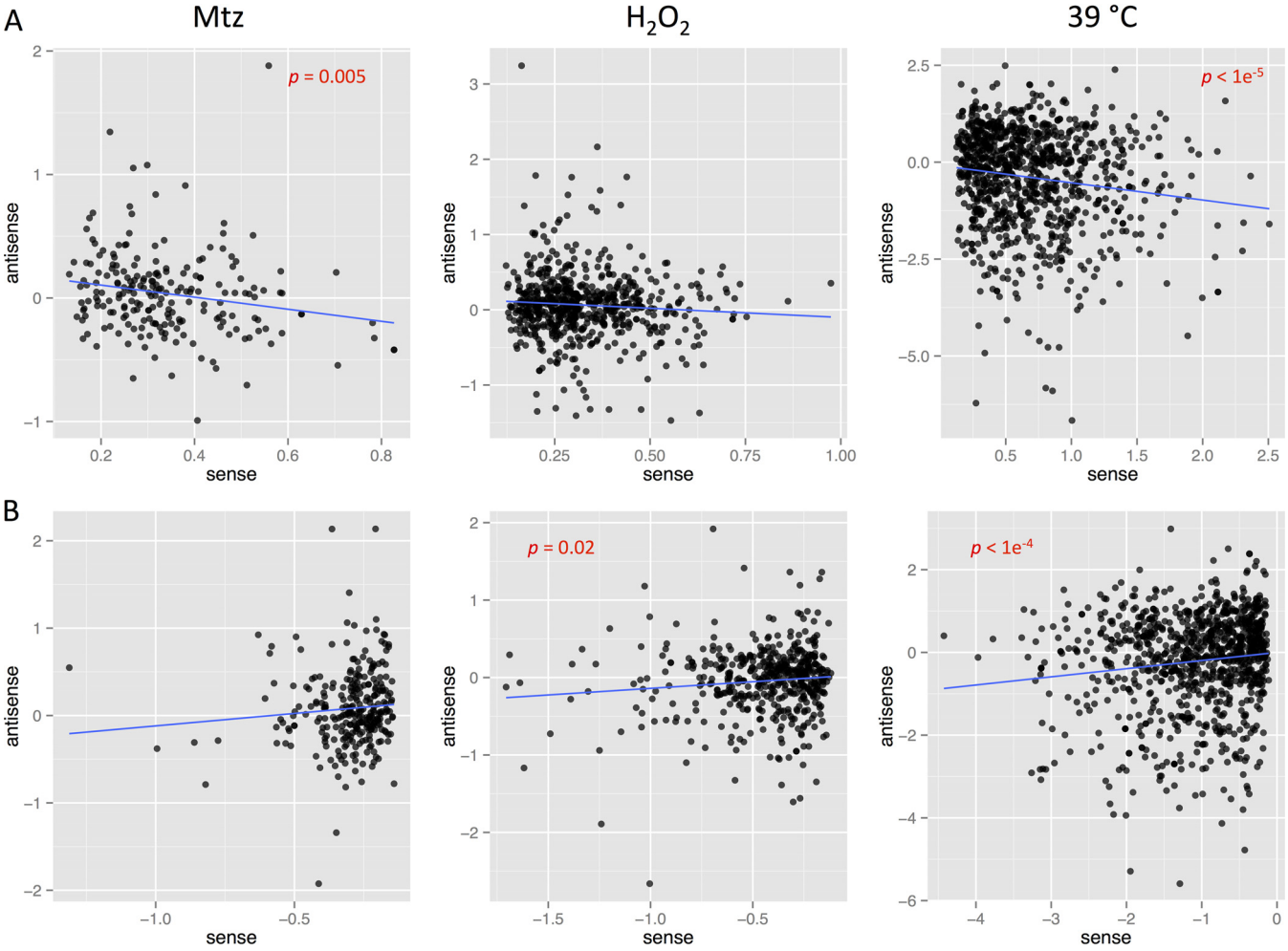


FIG 5 Change in abundance of sense and antisense transcripts from nonoverlapping differentially transcribed genes. Log_2(fold change) values for sense (*x* axis) and antisense (*y* axis) transcripts are divided according to upregulated (A) and downregulated (B) sense transcripts for each condition. Linear regression lines are shown in blue; *P* values for significant linear correlations are indicated.

complex motifs were identified upstream of genes uniquely upregulated under H_2O_2-induced stress (AGSAG), genes uniquely downregulated under Mtz stress (ADTAAA), and genes downregulated under both Mtz and thermal stresses (ACTRCC). Last, we investigated the possibility of posttranscriptional regulation by antisense transcripts under different stress conditions. Significant inverse correlation was detected between sense and antisense abundance for genes upregulated under Mtz and thermal stress, supported by relatively greater proportions of inversely differentially transcribed sense and antisense transcripts under these conditions (Mtz, 58.2%; H_2O_2, 38.4%; thermal stress, 54.0%) (see Table S8). Conversely, a positive correlation between sense and antisense transcription was observed for downregulated genes under H_2O_2 and thermal stress (Fig. 5). Significantly elevated antisense transcription from genes encoding an active Nek kinase (GL_5554), a leucine-rich repeat protein, and an ABC transporter correlated with significant suppression of sense transcripts from these genes under all stress conditions, whereas a large transcriptionally upregulated hypothetical protein (GL_34906) was associated with suppressed antisense transcription in the same manner (see Table S9). Nonoverlapping antioxidant genes tended to exhibit greater antisense transcription under Mtz stress, whereas little mean change or transcriptional suppression was observed for these genes under H_2O_2 or thermal stress, respectively (Fig. S8).

DISCUSSION

Detecting and responding to environmental stress is essential for cell survival. At the cellular level, stress can be defined as any environmental force that impairs the function of proteins, lipids, or nucleic acids and thus perturbs cellular homeostasis. Sensors that detect these perturbations generally activate signaling pathways that modulate gene activity, which, in turn, enable greater stress tolerance (22, 55). In this study, we characterized conserved and specific transcriptional responses to three different stress-inducing agents in *G. duodenalis*. Whereas previous studies did not explicitly control for differing magnitudes of stress, we optimized metronidazole (Mtz), hydrogen peroxide (H_2O_2), and thermal stressors to exert approximately equal pressure on cell growth. Previously, we reported transcriptomic evidence of oxidative stress in axenically cultured *G. duodenalis* trophozoites (39). To avoid interactions between dissolved oxygen and the stressors used in this study (30, 31), we generated anaerobic conditions

Downloaded from http://aac.asm.org/ on October 4, 2016 by University of Melbourne

prior to and during stress exposures. In similarity to previous studies of transcription in *G. duodenalis* and other microaerobic protozoa (28, 56, 57), the magnitude of change in transcript abundance for many genes was modest. However, concerted biological replication allowed the identification of many genes that were differentially transcribed at statistical significance (FDR, 0.01). Given the complexity of biological systems and gene-regulatory networks, we refrain from discounting the potential of any DTG to contribute to physiological changes in stressed cells and note numerous studies in model metazoan organisms that link modest transcriptional changes to significant physiological changes (58–60). Further exploration of these stress responses at the proteomic or metabolomic level may provide additional insight into their biological impact, notwithstanding the relatively reduced sensitivity of these techniques compared to that of RNA sequencing.

We found compelling evidence for a set of genes that are differentially transcribed in response to Mtz, H_2O_2, and thermal stress that may constitute general stress response genes in *G. duodenalis*. Downregulation of glycolysis could be interpreted as a mechanism to suppress metabolism and thereby concentrate resources on biomolecule maintenance and repair/degradation (22). Glucose conservation might also be important at times of stress as this molecule is a crucial source of reducing power. Upregulation of DNA repair enzymes and ubiquitin-related enzymes is consistent with the biomolecule repair and debris-clearing aspects of the classical stress response.

We observed transcriptional upregulation of a mitogen-activated protein kinase kinase kinase (MAPKKK) under all three stress conditions. In aerobic eukaryotes, disparate stress-inducing agents are thought to lead to the production of endogenous reactive oxygen species (ROS) (61). Particular MAPKs are activated by thioredoxin in response to endogenous ROS. When reduced, thioredoxin binds to and suppresses MAPK activity. Oxidation of reduced cysteine in thioredoxin by endogenous ROS leads to the dissociation of the thiol-MAPK complex and subsequent activation of stress response genes (62, 63). Given that our experiments were performed under anaerobic conditions, we expect low dissolved oxygen concentrations within trophozoites. Therefore, the upregulation of MAPKKK suggests that chemical and thermal stressors may converge on MAPK signaling pathways in *G. duodenalis* through mechanisms other than endogenous ROS generation. H_2O_2 and activated Mtz may converge on MAPK pathways by oxidizing thioredoxin; however, a mechanism of thermal stress-induced MAPK activation remains to be investigated. Three MAPKs are annotated in the *G. duodenalis* genome in addition to MAPKKK, and at least two of these kinases are transcriptionally upregulated under H_2O_2-induced and thermal stress. Taken together, these results suggest that MAP kinases may integrate and transduce signals from a variety of stress-inducing agents in *G. duodenalis*.

The upregulation of a redox-sensitive epigenetic regulator, Sir2, and flavin adenosine dinucleotide (FAD) synthetase also suggests perturbed redox conditions in trophozoites exposed to Mtz, H_2O_2, and thermal stressors. Sir2 NAD-dependent lysine deacetylases are stimulated by (oxidized) NAD and are thus sensitive to intracellular redox conditions. Many Sir2 enzymes are likely to deacetylate histones and may thereby coordinate transcriptional responses to oxidative stress (64, 65). The upregulation of a histone acetyltransferase under all stress conditions points to reversible and dynamic histone acetylation as an important mediator of the transcriptional response to different stressors in *G. duodenalis*. The *G. duodenalis* FAD synthetase is structurally similar to bifunctional FAD synthetases in prokaryotes, which both phosphorylate and adenylate flavin mononucleotide (FMN) (66). Interestingly, the nitroreductases implicated in Mtz activation and detoxification are FMN dependent, whereas oxidoreductases that are involved in oxygen and H_2O_2 detoxification are generally FAD dependent (reviewed in reference 9). Increased activity of FAD synthetase may therefore bias the antioxidant system toward ROS detoxification and away from Mtz activation. It is tempting to speculate that MAPK signaling or Sir2 activity might modulate the transcription of the FAD synthetase gene. Understanding the transcriptional regulation of this gene holds promise for interfering with global stress responses.

Of the *G. duodenalis*-specific protein families, high-cysteine membrane proteins (HCMPs) were comprehensively downregulated under all stress conditions. Although the role of HCMPs is poorly defined at present, these proteins may help to maintain the integrity of organellar membranes and the plasma membrane as reduced cysteine acts as an antioxidant. Disulfide bonding between oxidized cysteine residues is also important for stabilizing protein structure in harsh environments (67). Convergent downregulation of HCMPs under the stress conditions tested here is therefore counterintuitive. A possible explanation is that HCMPs may act as cysteine stores which are transcriptionally repressed under stress in order to divert cysteine to other proteins, for example, the thioredoxin/peroxiredoxin system. The concomitant upregulation of the cysteine tRNA synthase gene under all stress conditions and the overwhelming downregulation of genes encoding HCMPs under H_2O_2 stress (Fig. 3A) further support this hypothesis.

Transcriptional induction of heat shock proteins and chaperones was observed under Mtz and thermal stress to the near exclusion of H_2O_2 (see Table S4 in the supplemental material). This finding agrees in part with early work by Lindley and colleagues (26), which identified increased/sustained translation of several proteins with molecular weights corresponding to those of heat shock proteins in response to thermal stress, but not in response to oxygen or H_2O_2. The authors suggested that this discrepancy was due to *G. duodenalis* occupying an anaerobic niche *in vivo* and having little need for molecular responses against H_2O_2. However, this hypothesis is insufficient in light of recent work demonstrating spatiotemporal variation in oxygen, H_2O_2, and other oxidants in the gut (16). An alternative explanation, also supported by previous work (28), is that signaling pathways specific to the H_2O_2 response may circumvent or even suppress HSP transcription. The discrepancy in results for Mtz-induced HSP and chaperone induction between the present study and that of Lindley and colleagues (26) may also be attributed to different drug pressures (58 μM over 6 h versus 7 μM over 24 h used here). Clearly, further work is now required to establish the dynamics of gene induction in response to different stress pressures.

A key finding of this study, more broadly, is the lack of agreement between transcriptional responses to Mtz and H_2O_2. Mtz is widely hypothesized to kill microaerobic cells such as *G. duodenalis* by inducing oxidative stress, and H_2O_2 is a classical oxidizing agent. These chemicals were therefore expected to exert similar stresses in *G. duodenalis* and to produce similar changes in transcription. Contrary to this expectation, we observed upregulation or unchanged transcription of a number of antioxidant-coding

Downloaded from http://aac.asm.org/ on October 4, 2016 by University of Melbourne

genes in the presence of H_2O_2, whereas the entire antioxidant system was suppressed in the presence of Mtz. Several factors may account for this discrepancy. First, Mtz and H_2O_2 may interact with different types of biomolecules. For example, H_2O_2 is known to oxidize thiol groups in proteins such as thioredoxin (63), whereas reactive Mtz intermediates might have greater affinity for reduced cofactors (68) or nucleic acids (10). Although the importance of DNA damage in the mechanism of Mtz cytotoxicity is contested (10, 12), the increased transcription of genes encoding a pseudouridine synthase (acting to stabilize structural RNAs) (69) and several DNA repair enzymes specifically following Mtz exposure in this study suggests selective sensitivity of nucleic acids to this drug. Indeed, DNA damage may be sufficient to arrest the cell cycle, as suggested by transcriptional downregulation of the mitotic regulator Mad2 under Mtz and previous reports of H2A phosphorylation after sublethal Mtz exposure (15, 70, 71). Second, H_2O_2 requires only bivalent reduction to form H_2O, but the Mtz prodrug requires reduction with as many as six electrons until it forms an inert amine, making it more reactive (10, 72). This requirement for intracellular enzymatic reduction may, however, impose limits on the rate of Mtz activation which do not apply to H_2O_2. Yet another consequence of this difference in activation chemistry suggested in the present findings is that Mtz-induced damage can be limited by downregulating expression or activity of antioxidant enzymes, whereas H_2O_2, which is constitutively active, must be detoxified through increased/sustained antioxidant activity. Finally, while not obvious from the transcriptional results presented here, *G. duodenalis* is expected to possess mechanisms for sensing and eliciting transcriptional responses to physiologically relevant oxidants, such as dissolved oxygen, H_2O_2, and nitric oxide (16, 20, 30). Future work to identify and test the chemical specificity of these sensing mechanisms may elucidate divergent signaling pathways that could contribute to the different transcriptional responses to Mtz and H_2O_2 observed here.

It is interesting to consider how extracellular oxygen tension might influence transcriptional responses to Mtz in *G. duodenalis*. Under the anaerobic conditions used in this study, downregulation of the antioxidant system appears to be a viable transcriptional response as there is little need to combat oxidative stress. However, under higher oxygen tensions such as occur transiently *in vivo* (16), this drug evasion mechanism may not be compatible with the continued activity of antioxidant enzymes. In addition, under atmospheric oxygen tension, Mtz is rendered ineffective against *G. duodenalis* due to futile cycling between the univalently reduced nitro anion and the prodrug (reviewed in reference 9). In a metabolically related microaerophilic protozoan pathogen, *Trichomonas vaginalis*, redox-dependent constraints on gene expression are implicated in the development of different mechanisms of Mtz resistance under anaerobic and microaerobic conditions (73, 74). If similar constraints on gene expression exist under microaerobic conditions in *G. duodenalis*, it would be interesting to investigate dissolved-oxygen conditions under which the parasite might be cornered between a requirement for antioxidant activity to manage intracellular oxygen and the imperative to downregulate the same enzymes to avoid activating Mtz. Further, it is tempting to speculate that under microaerobic conditions, the cytotoxic effects of Mtz on *G. duodenalis* may be attributed to a failure to manage oxygen-derived reactive species rather than damage from Mtz-derived intermediates *per se*. Experiments exposing *G. duodenalis* to Mtz following priming with H_2O_2 or oxygen, for example, could begin to address this area (see reference 75).

A key point of difference between Mtz and physiological stressors relates to phospholipid synthesis and metabolism. Phosphorylation at different positions on membrane-linked inositol is associated with signaling for cell survival and membrane trafficking (76), and phosphoinositides are often targets of secreted effectors from bacterial and fungal pathogens (77). We observed transcriptional changes under H_2O_2 and thermal stress that suggested comprehensive downregulation of phosphatidylinositol (PI) synthesis and PI phosphorylation (PIP). Conversely, transcriptional results suggest that PI metabolism is relatively unchanged in Mtz-exposed trophozoites, wherein the PI4-P pool may increase, as suggested by upregulation of the PI4,5-phosphatase gene. PI4-P is associated with Golgi trafficking in model eukaryotes; however, the relevance of this process in the Mtz response remains to be elucidated. Differential regulation of α-giardins in Mtz and physiological stress responses is intriguing in the context of PI metabolism as particular members of this protein family, which is expanded in *G. duodenalis*, have been shown to bind both the cytoskeleton and a range of PIP species (47). Reorganization of the cytoskeleton is important for endocytosis and subsequent vesicular trafficking (78), and Rab-GTPases interact with PIPs to regulate internal organelle formation and trafficking (79). Although Mtz is thought to enter *G. duodenalis* via passive diffusion, it would be interesting to assess whether the substantial downregulation of α-giardins and Rab-GTPases observed in the presence of Mtz correlates with decreased endocytosis (80). Such suppression of communication with the extracellular environment may promote survival by further limiting the rate of Mtz internalization. Last, the importance of PI metabolism under stress in *G. duodenalis* is also supported by differential transcription of a hypothetical protein (GL_15125) with predicted structural similarity to a PI-binding effector, AvrM, from the flax rust fungus *Melampsora lini* (46). Upregulation of GL_15125 was reported under both thermal and reducing stress in a previous study (29), and we observed upregulation of the same transcript under thermal and Mtz stress. Lysine and arginine have been shown to mediate PI binding at the N terminus of AvrM (46, 81), and the predicted *G. duodenalis* protein structure exhibits similarities in the surface exposure and combined proportions of these basic residues (Fig. 2B). As the most consistently reported stress response transcript in *G. duodenalis*, the encoded hypothetical protein now clearly warrants further investigation in the context of phosphatidylinositol signaling in *G. duodenalis*.

This study provides evidence in support of a role for MAP kinase and phosphatidylinositol signaling in conserved and stress-specific responses. Multiple Nek kinases were also differentially transcribed. The Nek family is massively expanded in *G. duodenalis* although the majority of Nek proteins are predicted to be pseudokinases, many of which associate with the cytoskeleton (54). The roles of active Neks in *G. duodenalis* await experimental determination, but preferential induction of catalytically active Neks under both H_2O_2 and thermal stress suggests a role in stress-related signal transduction. Also interesting is the correlation between antisense induction and sense suppression for the predicted active Nek GL_5554, observed under all stress conditions. In this context, the experimental conditions defined here could provide a paradigm for testing the function and transcriptional regulation of active and inactive Neks in the future.

Downloaded from http://aac.asm.org/ on October 4, 2016 by University of Melbourne

Stress signaling cascades are likely to impinge on both genetic and epigenetic effectors. Although we found little evidence for stress-specific DNA response elements in this study, we cannot exclude the presence of motifs specific to smaller sets of coregulated genes that may be masked by the large number of functionally diverse DTGs identified under each stress condition. The GARP-like transcription factors upregulated under H_2O_2 and thermal stressors are particularly interesting. This protein family is recognized to be specific to plants and has not been identified in other protists to date (53). GARPs are predicted to bind upstream of genes encoding antioxidants (PDI-1), α-giardins, and calcium-binding enzymes, which were found to be upregulated under H_2O_2 and thermal stress in our results. Given the lack of GARP domains in the mammalian host and their putative role in regulating elements of the physiological stress response, these transcription factors are worthy candidates for further investigation as chemotherapeutic targets. GARP proteins are implicated in two-component signaling in plants (82), and we previously elucidated structural homologues of two-component signaling proteins in *G. duodenalis*, including an MtrR repressor, since localized in the trophozoite nucleus (85), that may be involved in oxidative stress signaling (39). The transcript encoding the MtrR homologue is downregulated under Mtz stress, further supporting the notion that the response to Mtz exposure, at least under anaerobic conditions, opposes the oxidative stress response.

Aside from differential transcription of epigenetic regulators associated with reversible histone acetylation, we also observed the upregulation of Dicer under Mtz-induced stress and downregulation of the same transcript under physiological stressors. Natural antisense-mediated epigenetic regulation of variant-specific surface protein (VSP) expression has been demonstrated to occur through reverse transcription of mRNA in the cytosol (83, 84). The transcript encoding the RNA-dependent RNA polymerase associated with this process was also downregulated under physiological stress. These findings, together with evidence of antisense derepression in upregulated, but not downregulated, genes (Fig. 5) strongly suggest that RNA interference (RNAi)-mediated transcriptional regulation plays an important role in stress responses. Finally, although results from transcriptomic studies (including the present study) tend to be interpreted as a reflection of a steady-state system, this is likely an oversimplification. Further investigation of transcript stability under stress and correlation of our findings with results from complementary proteomics approaches should yield further insight into gene-regulatory mechanisms in this basic eukaryote.

In conclusion, we calibrated Mtz, H_2O_2, and elevated temperatures to exert equivalent pressure on *Giardia duodenalis* growth and used the most sensitive techniques yet applied to investigate the resultant transcriptional changes. A core set of convergent stress response genes was identified, implicating DNA repair and protein turnover as the most highly conserved stress responses within *G. duodenalis*. A MAP kinase and a putative phosphatidylinositol binding protein may integrate signals from divergent stressors, with attendant redeployment of cysteine from membrane proteins to other thiol-containing proteins. We identified the comprehensive downregulation of antioxidant transcription under Mtz-induced stress, together with suppression of α-giardins and Rab GTPases, which was not detected under H_2O_2 or thermal stress. Under the latter two conditions, active Nek kinases and GARP-like transcription factors were induced, whereas genes involved in phosphoinositide signaling were suppressed, constituting substantial differences in transcriptional responses, which demonstrate the ability of *G. duodenalis* to differentiate physiological and xenobiotic stresses. Limited evidence for stress-specific DNA response elements may implicate epigenetic loci of transcriptional control, supported by antisense derepression and altered transcription of cytosolic RNA inference machinery. These findings reveal multiple exciting avenues for both enhancing the potency of Mtz and targeting conserved stress response genes for novel chemotherapeutic intervention.

ACKNOWLEDGMENTS

B.R.E.A. is supported by an Australian Postgraduate Award (Australian Government) and the Victorian Life Sciences Computation Initiative (Victoria, Australia). RNA sequencing was partially funded by YourGene Biosciences (Taiwan).

The funders had no role in study design, data collection and interpretation, or the decision to submit the work for publication.

FUNDING INFORMATION

This work, including the efforts of Malcolm J. McConville, was funded by Australian Research Council (ARC) (LP120200122). This work, including the efforts of Aaron R. Jex, was funded by Australian Research Council (ARC) (LP120200122).

REFERENCES

1. **Lane S, Lloyd D.** 2002. Current trends in research into the waterborne parasite *Giardia*. Crit Rev Microbiol **28:**123–147. http://dx.doi.org/10.1080/1040-840291046713.
2. **Halliez MC.** 2013. Extra-intestinal and long term consequences of *Giardia duodenalis* infections. World J Gastroenterol **19:**8974. http://dx.doi.org/10.3748/wjg.v19.i47.8974.
3. **Escobedo AA, Cimerman S.** 2007. Giardiasis: a pharmacotherapy review. Expert Opin Pharmacother **8:**1885–1902. http://dx.doi.org/10.1517/14656566.8.12.1885.
4. **Wright JM, Dunn LA, Upcroft P.** 2003. Efficacy of antigiardial drugs. Expert Opin Drug Saf **2:**529–541. http://dx.doi.org/10.1517/14740338.2.6.529.
5. **Abboud P, Lemée V, Gargala G, Brasseur P, Ballet JJ, Borsa-Lebas F, Caron F, Favennec L.** 2001. Successful treatment of metronidazole- and albendazole-resistant giardiasis with nitazoxanide in a patient with acquired immunodeficiency syndrome. Clin Infect Dis **32:**1792–1794. http://dx.doi.org/10.1086/320751.
6. **Adagu IS, Nolder D, Warhurst DC, Rossignol J-F.** 2002. In vitro activity of nitazoxanide and related compounds against isolates of *Giardia intestinalis*, *Entamoeba histolytica* and *Trichomonas vaginalis*. J Antimicrob Chemother **49:**103–111. http://dx.doi.org/10.1093/jac/49.1.103.
7. **Lemée V, Zaharia I, Nevez G, Rabodonirina M, Brasseur P, Ballet JJ, Favennec L.** 2000. Metronidazole and albendazole susceptibility of 11 clinical isolates of *Giardia duodenalis* from France. J Antimicrob Chemother **46:**819–821. http://dx.doi.org/10.1093/jac/46.5.819.
8. **McIntyre P, Boreham PF, Phillips RE, Shepherd RW.** 1986. Chemotherapy in giardiasis: clinical responses and in vitro drug sensitivity of human isolates in axenic culture. J Pediatr **108:**1005–1010. http://dx.doi.org/10.1016/S0022-3476(86)80950-7.
9. **Ansell BRE, McConville MJ, Ma'ayeh SY, Dagley MJ, Gasser RB, Svärd SG, Jex AR.** 2015. Drug resistance in *Giardia duodenalis*. Biotechnol Adv **33:**888–901. http://dx.doi.org/10.1016/j.biotechadv.2015.04.009.
10. **Edwards DI.** 1993. Nitroimidazole drugs—action and resistance mechanisms. I. Mechanisms of action. J Antimicrob Chemother **31:**9–20. http://dx.doi.org/10.1093/jac/31.1.9.
11. **Edwards DI.** 1993. Nitroimidazole drugs—action and resistance mechanisms. II. Mechanisms of resistance. J Antimicrob Chemother **31:**201–210. http://dx.doi.org/10.1093/jac/31.2.201.
12. **Leitsch D, Kolarich D, Binder M, Stadlmann J, Altmann F, Duchêne M.** 2009. *Trichomonas vaginalis*: metronidazole and other nitroimidazole drugs are reduced by the flavin enzyme thioredoxin reductase and disrupt the cellular redox system. Implications for nitroimidazole toxicity and resistance. Mol Microbiol **72:**518–536.

Downloaded from http://aac.asm.org/ on October 4, 2016 by University of Melbourne

13. **Müller J, Schildknecht P, Müller N.** 2013. Metabolism of nitro drugs metronidazole and nitazoxanide in *Giardia lamblia*: characterization of a novel nitroreductase (GlNR2). J Antimicrob Chemother **68:**1781–1789. http://dx.doi.org/10.1093/jac/dkt106.
14. **Müller J, Sterk M, Hemphill A, Müller N.** 2007. Characterization of *Giardia lamblia* WB C6 clones resistant to nitazoxanide and to metronidazole. J Antimicrob Chemother **60:**280–287. http://dx.doi.org/10.1093/jac/dkm205.
15. **Uzlikova M, Nohýnková E.** 2014. The effect of metronidazole on the cell cycle and DNA in metronidazole-susceptible and -resistant *Giardia* cell lines. Mol Biochem Parasitol **198:**75–81. http://dx.doi.org/10.1016/j.molbiopara.2015.01.005.
16. **Espey MG.** 2013. Role of oxygen gradients in shaping redox relationships between the human intestine and its microbiota. Free Radic Biol Med **55:**130–140. http://dx.doi.org/10.1016/j.freeradbiomed.2012.10.554.
17. **Arbo A, Pavía-Ruz N, Santos JI.** 2006. Opsonic requirements for the respiratory burst of neutrophils against *Giardia lamblia* trophozoites. Arch Med Res **37:**465–473. http://dx.doi.org/10.1016/j.arcmed.2005.11.002.
18. **Nathan C, Shiloh MU.** 2000. Reactive oxygen and nitrogen intermediates in the relationship between mammalian hosts and microbial pathogens. Proc Natl Acad Sci U S A **97:**8841–8848. http://dx.doi.org/10.1073/pnas.97.16.8841.
19. **Tako EA, Hassimi MF, Li E, Singer SM.** 2013. Transcriptomic analysis of the host response to *Giardia duodenalis* infection reveals redundant mechanisms for parasite control. mBio **4:**e00660-13. http://dx.doi.org/10.1128/mBio.00660-13.
20. **Pacher P, Beckman JS, Liaudet L.** 2007. Nitric oxide and peroxynitrite in health and disease. Physiol Rev **87:**315–424. http://dx.doi.org/10.1152/physrev.00029.2006.
21. **Lell B, Sovric M, Schmid D, Luckner D, Herbich K, Long HY, Graninger W, Kremsner PG.** 2001. Effect of antipyretic drugs in children with malaria. Clin Infect Dis **32:**838–841. http://dx.doi.org/10.1086/319217.
22. **Kultz D.** 2003. Evolution of the cellular stress proteome: from monophyletic origin to ubiquitous function. J Exp Biol **206:**3119–3124. http://dx.doi.org/10.1242/jeb.00549.
23. **Morrison HG, McArthur AG, Gillin FD, Aley SB, Adam RD, Olsen GJ, Best AA, Cande WZ, Chen F, Cipriano MJ, Davids BJ, Dawson SC, Elmendorf HG, Hehl AB, Holder ME, Huse SM, Kim UU, Lasek-Nesselquist E, Manning G, Nigam A, Nixon JEJ, Palm D, Passamaneck NE, Prabhu A, Reich CI, Reiner DS, Samuelson J, Svärd SG, Sogin ML.** 2007. Genomic minimalism in the early diverging intestinal parasite *Giardia lamblia*. Science **317:**1921–1926. http://dx.doi.org/10.1126/science.1143837.
24. **Nixon JEJ, Wang A, Field J, Morrison HG, McArthur AG, Sogin ML, Loftus BJ, Samuelson J.** 2002. Evidence for lateral transfer of genes encoding ferredoxins, nitroreductases, NADH oxidase, and alcohol dehydrogenase 3 from anaerobic prokaryotes to *Giardia lamblia* and *Entamoeba histolytica*. Eukaryot Cell **1:**181–190. http://dx.doi.org/10.1128/EC.1.2.181-190.2002.
25. **Pal D, Banerjee S, Cui J, Schwartz A, Ghosh SK, Samuelson J.** 2009. *Giardia*, *Entamoeba*, and *Trichomonas* enzymes activate metronidazole (nitroreductases) and inactivate metronidazole (nitroimidazole reductases). Antimicrob Agents Chemother **53:**458–464. http://dx.doi.org/10.1128/AAC.00909-08.
26. **Lindley TA, Chakraborty PR, Edlind TD.** 1988. Heat shock and stress response in *Giardia lamblia*. Mol Biochem Parasitol **28:**135–143. http://dx.doi.org/10.1016/0166-6851(88)90061-8.
27. **Monis PT, Caccio SM, Thompson RCA.** 2009. Variation in *Giardia*: towards a taxonomic revision of the genus. Trends Parasitol **25:**93–100. http://dx.doi.org/10.1016/j.pt.2008.11.006.
28. **Ma'ayeh SY, Knörr L, Svärd SG.** 2015. Transcriptional profiling of *Giardia intestinalis* in response to oxidative stress. Int J Parasitol **45:**1–14. http://dx.doi.org/10.1016/j.ijpara.2014.07.013.
29. **Spycher C, Herman EK, Morf L, Qi W, Rehrauer H, Aquino Fournier C, Dacks JB, Hehl AB.** 2013. An ER-directed transcriptional response to unfolded protein stress in the absence of conserved sensor-transducer proteins in *Giardia lamblia*. Mol Microbiol **88:**754–771. http://dx.doi.org/10.1111/mmi.12218.
30. **Gillin FD, Reiner DS.** 1982. Effects of oxygen tension and reducing agents on sensitivity of *Giardia lamblia* to metronidazole in vitro. Biochem Pharmacol **31:**3694–3697. http://dx.doi.org/10.1016/0006-2952(82)90600-1.
31. **Dan M, Wang AL, Wang CC.** 2000. Inhibition of pyruvate-ferredoxin oxidoreductase gene expression in *Giardia lamblia* by a virus-mediated hammerhead ribozyme. Mol Microbiol **36:**447–456. http://dx.doi.org/10.1046/j.1365-2958.2000.01863.x.
32. **Diamond LS, Harlow DR, Cunnick CC.** 1978. A new medium for the axenic cultivation of *Entamoeba histolytica* and other Entamoeba. Trans R Soc Trop Med Hyg **72:**431–432. http://dx.doi.org/10.1016/0035-9203(78)90144-X.
33. **Davids BJ, Gillin FD.** 2011. Methods for *Giardia* culture, cryopreservation, encystation, and excystation *in vitro*, p 381–393. *In* Svärd SG, Lujan HD (ed), *Giardia*: a model organism. Springer, Vienna, Austria.
34. **Lohse M, Bolger AM, Nagel A, Fernie AR, Lunn JE, Stitt M, Usadel B.** 2012. RobiNA: a user-friendly, integrated software solution for RNA-Seq-based transcriptomics. Nucleic Acids Res **40:**W622–W627. http://dx.doi.org/10.1093/nar/gks540.
35. **Li B, Dewey CN.** 2011. RSEM: accurate transcript quantification from RNA-Seq data with or without a reference. BMC Bioinformatics **12:**323. http://dx.doi.org/10.1186/1471-2105-12-323.
36. **Wang L, Wang S, Li W.** 2012. RSeQC: quality control of RNA-seq experiments. Bioinformatics **28:**2184–2185. http://dx.doi.org/10.1093/bioinformatics/bts356.
37. **Garcia-Alcalde F, Okonechnikov K, Carbonell J, Cruz LM, Gotz S, Tarazona S, Dopazo J, Meyer TF, Conesa A.** 2012. Qualimap: evaluating next-generation sequencing alignment data. Bioinformatics **28:**2678–2679. http://dx.doi.org/10.1093/bioinformatics/bts503.
38. **Robinson MD, McCarthy DJ, Smyth GK.** 2010. edgeR: a Bioconductor package for differential expression analysis of digital gene expression data. Bioinformatics **26:**139–140. http://dx.doi.org/10.1093/bioinformatics/btp616.
39. **Ansell BRE, McConville MJ, Baker L, Korhonen PK, Young ND, Hall RS, Rojas CAA, Svärd SG, Gasser RB, Jex AR.** 2015. Time-dependent transcriptional changes in axenic *Giardia duodenalis* trophozoites. PLoS Negl Trop Dis **9:**e0004261. http://dx.doi.org/10.1371/journal.pntd.0004261.
40. **Roy A, Kucukural A, Zhang Y.** 2010. I-TASSER: a unified platform for automated protein structure and function prediction. Nat Protoc **5:**725–738. http://dx.doi.org/10.1038/nprot.2010.5.
41. **Ashburner M, Ball CA, Blake JA, Botstein D, Butler H, Cherry JM, Davis AP, Dolinski K, Dwight SS, Eppig JT, Harris MA, Hill DP, Issel-Tarver L, Kasarskis A, Lewis S, Matese JC, Richardson JE, Ringwald M, Rubin GM, Sherlock G.** 2000. Gene ontology: tool for the unification of biology. The Gene Ontology Consortium. Nat Genet **25:**25–29.
42. **Pettersen EF, Goddard TD, Huang CC, Couch GS, Greenblatt DM, Meng EC, Ferrin TE.** 2004. UCSF Chimera—a visualization system for exploratory research and analysis. J Comput Chem **25:**1605–1612. http://dx.doi.org/10.1002/jcc.20084.
43. **Mayol JM, Adame-Navarrete Y, Alarma-Estrany P, Molina-Roldan E, Huete-Toral F, Fernandez-Represa JA.** 2006. Luminal oxidants selectively modulate electrogenic ion transport in rat colon. World J Gastroenterol **12:**5523–5527. http://dx.doi.org/10.3748/wjg.v12.i34.5523.
44. **Vicente JB, Ehrenkaufer GM, Saraiva LM, Teixeira M, Singh U.** 2009. *Entamoeba histolytica* modulates a complex repertoire of novel genes in response to oxidative and nitrosative stresses: implications for amebic pathogenesis. Cell Microbiol **11:**51–69. http://dx.doi.org/10.1111/j.1462-5822.2008.01236.x.
45. **Müller J, Wastling J, Sanderson S, Müller N, Hemphill A.** 2007. A novel *Giardia lamblia* nitroreductase, GlNR1, interacts with nitazoxanide and other thiazolides. Antimicrob Agents Chemother **51:**1979–1986. http://dx.doi.org/10.1128/AAC.01548-06.
46. **Ve T, Williams SJ, Catanzariti AM.** 2013. Structures of the flax-rust effector AvrM reveal insights into the molecular basis of plant-cell entry and effector-triggered immunity. Proc Natl Acad Sci U S A **110:**17594–17599. http://dx.doi.org/10.1073/pnas.1307614110.
47. **Weiland ME-L, McArthur AG, Morrison HG, Sogin ML, Svärd SG.** 2005. Annexin-like alpha giardins: a new cytoskeletal gene family in *Giardia lamblia*. Int J Parastiol **35:**617–626. http://dx.doi.org/10.1016/j.ijpara.2004.12.009.
48. **Vahrmann A, Šarić M, Scholze H, Koebsch I.** 2008. α14-Giardin (annexin E1) is associated with tubulin in trophozoites of *Giardia lamblia* and forms local slubs in the flagella. Parasitol Res **102:**321–326.
49. **Rescher U, Gerke V.** 2004. Annexins–unique membrane binding proteins with diverse functions. J Cell Sci **117:**2631–2639. http://dx.doi.org/10.1242/jcs.01245.

Downloaded from http://aac.asm.org/ on October 4, 2016 by University of Melbourne

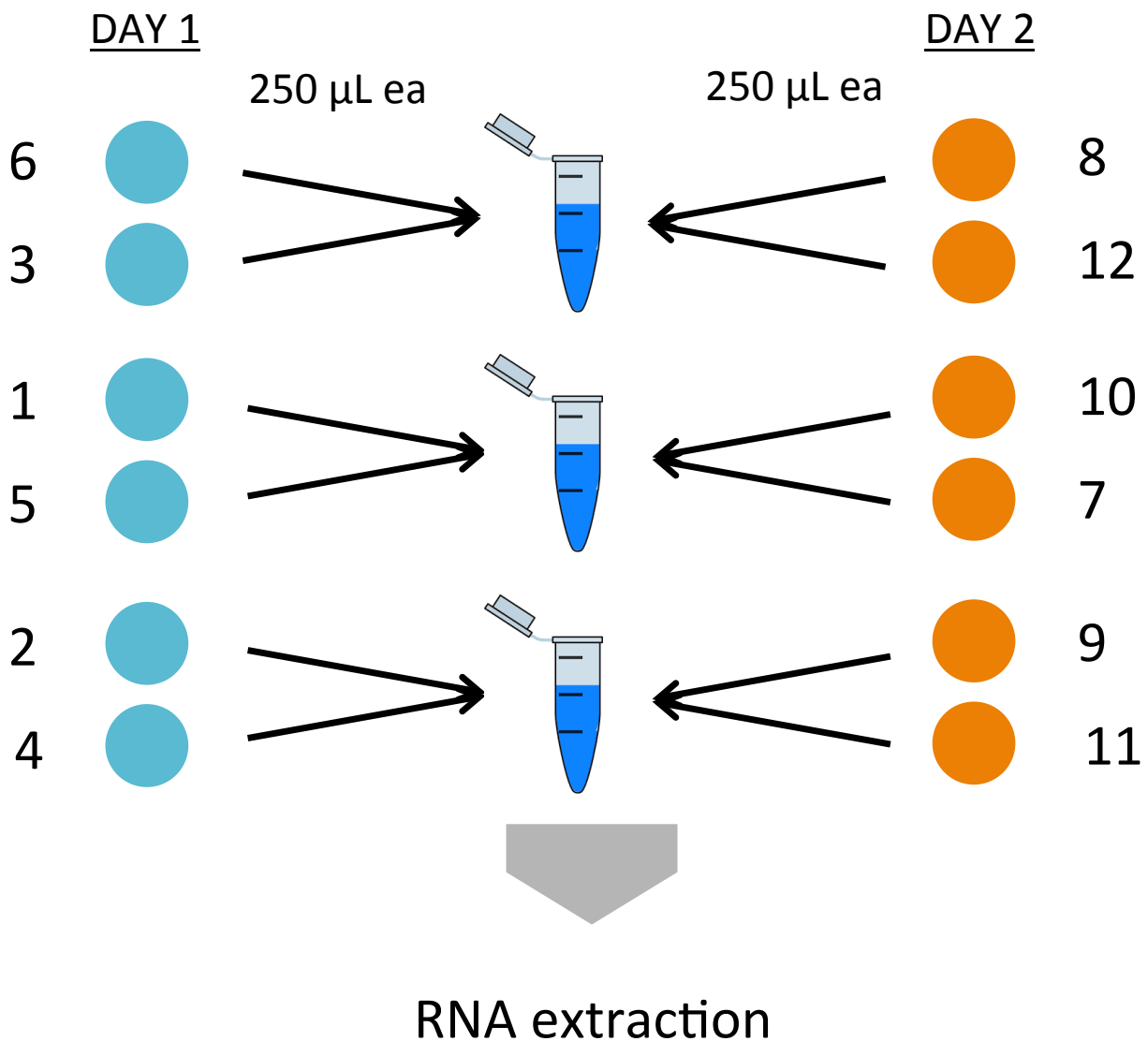
50. **Bailey TL.** 2011. DREME: motif discovery in transcription factor ChIP-seq data. Bioinformatics **27:**1653–1659. http://dx.doi.org/10.1093/bioinformatics/btr261.
51. **Gourguechon S, Holt LJ, Cande WZ.** 2013. The *Giardia* cell cycle progresses independently of the anaphase-promoting complex. J Cell Sci **126:**2246–2255. http://dx.doi.org/10.1242/jcs.121632.
52. **Vicente J-J, Cande WZ.** 2014. Mad2, Bub3 and Mps1 regulate chromosome segregation and mitotic synchrony in *Giardia intestinalis*, a binucleate protist lacking an anaphase promoting complex. Mol Biol Cell **25:**2774–2787. http://dx.doi.org/10.1091/mbc.E14-05-0975.
53. **Sun C-H, Su L-H, Gillin FD.** 2006. Novel plant-GARP-like transcription factors in *Giardia lamblia*. Mol Biochem Parasitol **146:**45–57. http://dx.doi.org/10.1016/j.molbiopara.2005.10.017.
54. **Manning G, Reiner DS, Lauwaet T, Dacre M, Smith A, Zhai Y, Svärd S, Gillin FD.** 2011. The minimal kinome of *Giardia lamblia* illuminates early kinase evolution and unique parasite biology. Genome Biol **12:**R66. http://dx.doi.org/10.1186/gb-2011-12-7-r66.
55. **Kültz D.** 2005. Molecular and evolutionary basis of the cellular stress response. Annu Rev Physiol **67:**225–257. http://dx.doi.org/10.1146/annurev.physiol.67.040403.103635.
56. **Einarsson E, Troell K, Hoeppner MP, Grabherr M, Ribacke U, Svärd SG.** 2016. Coordinated changes in gene expression throughout encystation of *Giardia intestinalis*. PLoS Negl Trop Dis **10:**e0004571. http://dx.doi.org/10.1371/journal.pntd.0004571.
57. **Tazreiter M, Leitsch D, Hatzenbichler E, Mair-Scorpio GE, Steinborn R, Schreiber M, Duchêne M.** 2008. *Entamoeba histolytica*: response of the parasite to metronidazole challenge on the levels of mRNA and protein expression. Exp Parasitol **120:**403–410. http://dx.doi.org/10.1016/j.exppara.2008.09.011.
58. **Gershman B, Puig O, Hang L, Peitzsch RM, Tatar M, Garofalo RS.** 2007. High-resolution dynamics of the transcriptional response to nutrition in *Drosophila*: a key role for dFOXO. Physiol Genomics **29:**24–34. http://dx.doi.org/10.1152/physiolgenomics.00061.2006.
59. **Benner MJ, Settles ML, Murdoch GK, Hardy RW, Robison BD.** 2013. Sex-specific transcriptional responses of the zebrafish (*Danio rerio*) brain selenoproteome to acute sodium selenite supplementation. Physiol Genomics **45:**653–666. http://dx.doi.org/10.1152/physiolgenomics.00030.2013.
60. **Toye AA, Dumas ME, Blancher C, Rothwell AR, Fearnside JF, Wilder SP, Bihoreau MT, Cloarec O, Azzouzi I, Young S, Barton RH, Holmes E, McCarthy MI, Tatoud R, Nicholson JK, Scott J, Gauguier D.** 2007. Subtle metabolic and liver gene transcriptional changes underlie diet-induced fatty liver susceptibility in insulin-resistant mice. Diabetologia **50:**1867–1879. http://dx.doi.org/10.1007/s00125-007-0738-5.
61. **Cazalé A, Rouet-Mayer M, Barbier-Brygoo H, Mathieu Y, Laurière C.** 1998. Oxidative burst and hypoosmotic stress in tobacco cell suspensions. Plant Physiol **116:**659–669. http://dx.doi.org/10.1104/pp.116.2.659.
62. **Haddad JJ, Land SC.** 2002. Redox/ROS regulation of lipopolysaccharide-induced mitogen-activated protein kinase (MAPK) activation and MAPK-mediated TNF-α biosynthesis. Br J Pharmacol **135:**520–536. http://dx.doi.org/10.1038/sj.bjp.0704467.
63. **Ray PD, Huang B-W, Tsuji Y.** 2012. Cellular signalling. Cell Signal **24:**981–990. http://dx.doi.org/10.1016/j.cellsig.2012.01.008.
64. **Fulco M, Schiltz RL, Iezzi S, King MT, Zhao P, Kashiwaya Y, Hoffman E, Veech RL, Sartorelli V.** 2003. Sir2 regulates skeletal muscle differentiation as a potential sensor of the redox state. Mol Cell **12:**51–62. http://dx.doi.org/10.1016/S1097-2765(03)00226-0.
65. **Smith JS, Brachmann CB, Celic I, Kenna MA, Muhammad S, Starai VJ, Avalos JL, Escalante-Semerena JC, Grubmeyer C, Wolberger C, Boeke JD.** 2000. A phylogenetically conserved NAD^+-dependent protein deacetylase activity in the Sir2 protein family. Proc Natl Acad Sci U S A **97:**6658–6663. http://dx.doi.org/10.1073/pnas.97.12.6658.
66. **Krupa A, Sandhya K, Srinivasan N, Jonnalagadda S.** 2003. A conserved domain in prokaryotic bifunctional FAD synthetases can potentially catalyze nucleotide transfer. Trends Biochem Sci **28:**9–12. http://dx.doi.org/10.1016/S0968-0004(02)00009-9.
67. **Davids BJ, Reiner DS, Birkeland SR, Preheim SP, Cipriano MJ, McArthur AG, Gillin FD.** 2006. A new family of giardial cysteine-rich non-VSP protein genes and a novel cyst protein. PLoS One **1:**e44. http://dx.doi.org/10.1371/journal.pone.0000044.
68. **Clarke ED, Wardman P, Goulding KH.** 1980. Anaerobic reduction of nitroimidazoles by reduced flavin mononucleotide and by xanthine oxidase. Biochem Pharmacol **29:**2684–2687. http://dx.doi.org/10.1016/0006-2952(80)90087-8.
69. **Charette M, Gray MW.** 2000. Pseudouridine in RNA: what, where, how, and why. IUBMB Life **49:**341–351. http://dx.doi.org/10.1080/152165400410182.
70. **Nakamura TM, Du LL, Redon C, Russell P.** 2004. Histone H2A phosphorylation controls Crb2 recruitment at DNA breaks, maintains checkpoint arrest, and influences DNA repair in fission yeast. Mol Cell Biol **24:**6215–6230. http://dx.doi.org/10.1128/MCB.24.14.6215-6230.2004.
71. **Vicente JB, Tran V, Pinto L, Teixeira M, Singh U.** 2012. A detoxifying oxygen reductase in the anaerobic protozoan *Entamoeba histolytica*. Eukaryot Cell **11:**1112–1118. http://dx.doi.org/10.1128/EC.00149-12.
72. **Müller J, Rout S, Leitsch D, Vaithilingam J, Hehl A, Müller N.** 2015. Comparative characterisation of two nitroreductases from *Giardia lamblia* as potential activators of nitro compounds. Int J Parastiol Drugs Drug Resist **5:**37–43. http://dx.doi.org/10.1016/j.ijpddr.2015.03.001.
73. **Kulda J.** 1999. Trichomonads, hydrogenosomes and drug resistance. Int J Parasitol **29:**199–212. http://dx.doi.org/10.1016/S0020-7519(98)00155-6.
74. **Leitsch D, Drinić M, Kolarich D, Duchêne M.** 2012. Down-regulation of flavin reductase and alcohol dehydrogenase-1 (ADH1) in metronidazole-resistant isolates of *Trichomonas vaginalis*. Mol Biochem Parasitol **183:**177–183. http://dx.doi.org/10.1016/j.molbiopara.2012.03.003.
75. **Hossain MA, Bhattacharjee S, Armin S-M, Qian P, Xin W, Li H-Y, Burritt DJ, Fujita M, Tran L-SP.** 2015. Hydrogen peroxide priming modulates abiotic oxidative stress tolerance: insights from ROS detoxification and scavenging. Front Plant Sci **6:**420. http://dx.doi.org/10.3389/fpls.2015.00420.
76. **Vanhaesebroeck B, Stephens L, Hawkins P.** 2012. PI3K signalling: the path to discovery and understanding. Nat Rev Mol Cell Biol **13:**195–203. http://dx.doi.org/10.1038/nrm3290.
77. **Pizarro-Cerdá J, Cossart P.** 2004. Subversion of phosphoinositide metabolism by intracellular bacterial pathogens. Nat Cell Biol **6:**1026–1033. http://dx.doi.org/10.1038/ncb1104-1026.
78. **Smythe E, Ayscough KR.** 2006. Actin regulation in endocytosis. J Cell Sci **119:**4589–4598. http://dx.doi.org/10.1242/jcs.03247.
79. **Jean S, Kiger AA.** 2012. Coordination between RAB GTPase and phosphoinositide regulation and functions. Nat Rev Mol Cell Biol **13:**463–470. http://dx.doi.org/10.1038/nrm3379.
80. **Somsel Rodman J, Wandinger-Ness A.** 2000. Rab GTPases coordinate endocytosis. J Cell Sci **113:**183–192.
81. **Gan PHP, Rafiqi M, Ellis JG, Jones DA, Hardham AR, Dodds PN.** 2010. Lipid binding activities of flax rust AvrM and AvrL567 effectors. Plant Signal Behav **5:**1272–1275. http://dx.doi.org/10.4161/psb.5.10.13013.
82. **Hosoda K, Imamura A, Katoh E, Hatta T, Tachiki M, Yamada H, Mizuno T, Yamazaki T.** 2002. Molecular structure of the GARP family of plant Myb-related DNA binding motifs of the *Arabidopsis* response regulators. Plant Cell **14:**2015–2029. http://dx.doi.org/10.1105/tpc.002733.
83. **Prucca CG, Lujan HD.** 2009. Antigenic variation in *Giardia lamblia*. Cell Microbiol **11:**1706–1715. http://dx.doi.org/10.1111/j.1462-5822.2009.01367.x.
84. **Prucca CG, Slavin I, Quiroga R, Elías EV, Rivero FD, Saura A, Carranza PG, Lujan HD.** 2008. Antigenic variation in *Giardia lamblia* is regulated by RNA interference. Nature **456:**750–754. http://dx.doi.org/10.1038/nature07585.
85. **Nosala C, Dawson SC.** 2015. The critical role of the cytoskeleton in the pathogenesis of *Giardia*. Curr Clin Micro Rep http://dx.doi.org/10.1007/s40588-015-0026-y.

Downloaded from http://aac.asm.org/ on October 4, 2016 by University of Melbourne

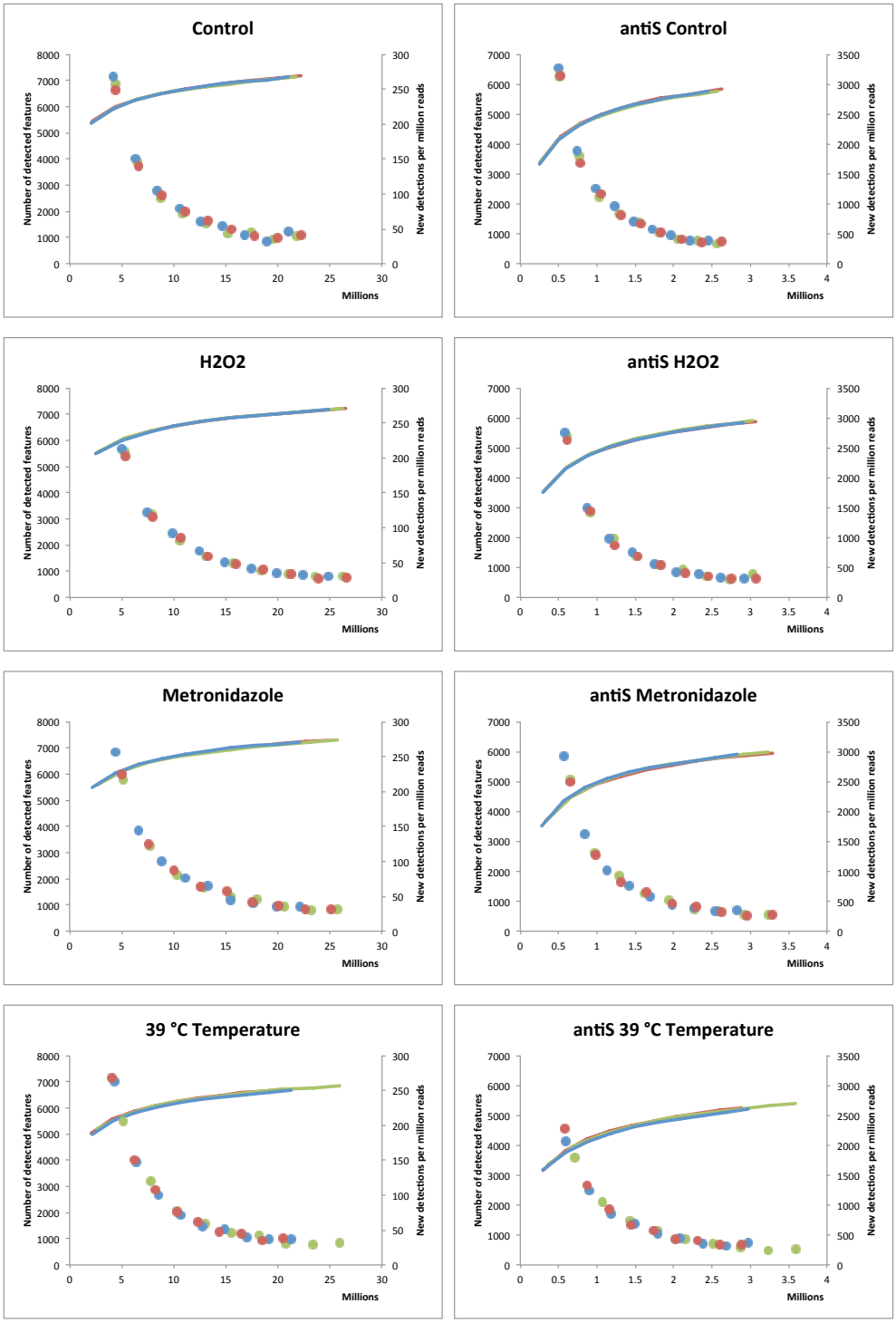
Supplementary Methods

Videomicroscopy

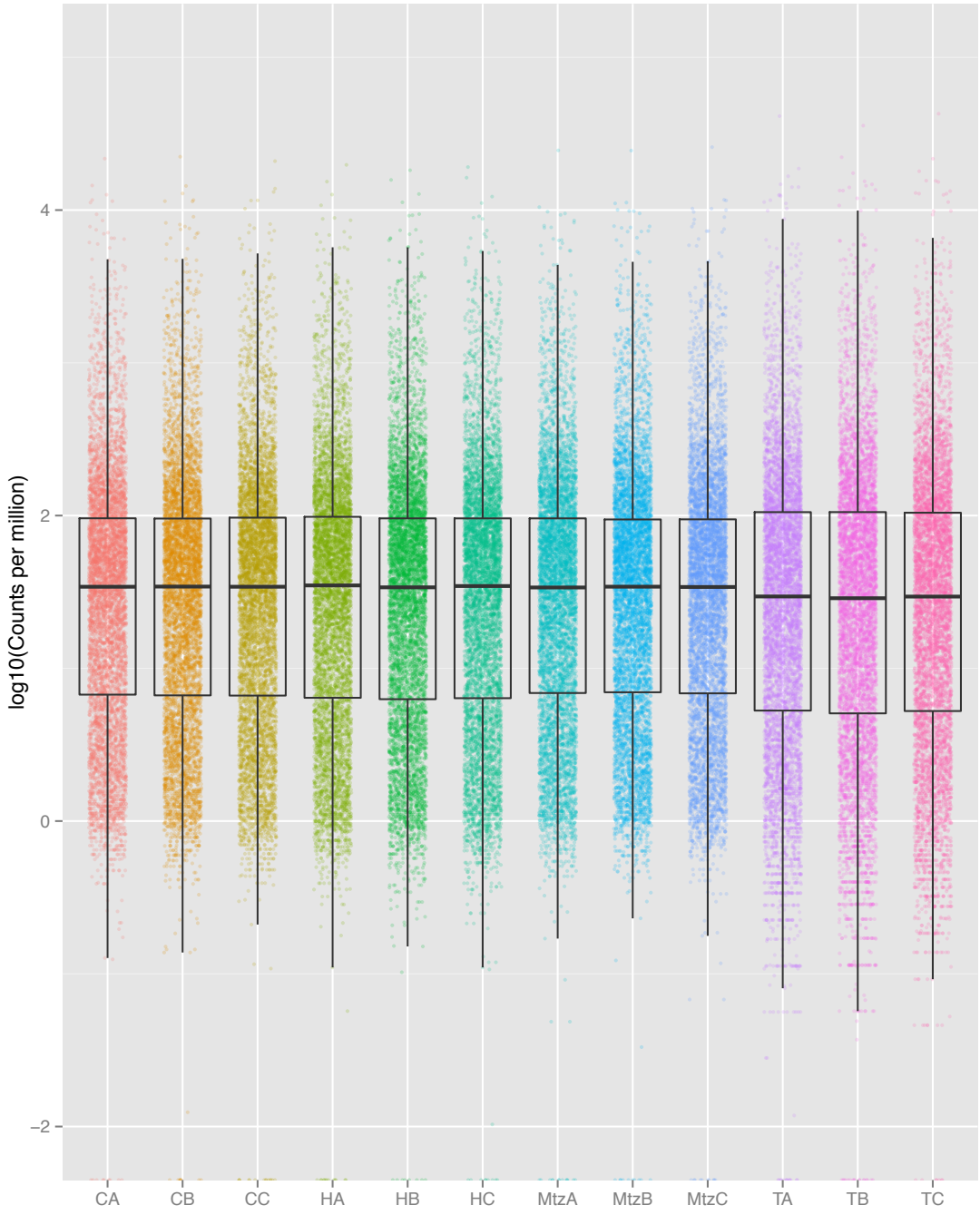
Trophozoites were filmed for at least 200 frames under a compound microscope (Olympus CX41 with DP26 video camera; 10x zoom, Ph1 phase contrast) using CellSense software with the following settings: 612x480 (binning 4x4); exposure: auto; ISO: 100; 2448x1920 snap.



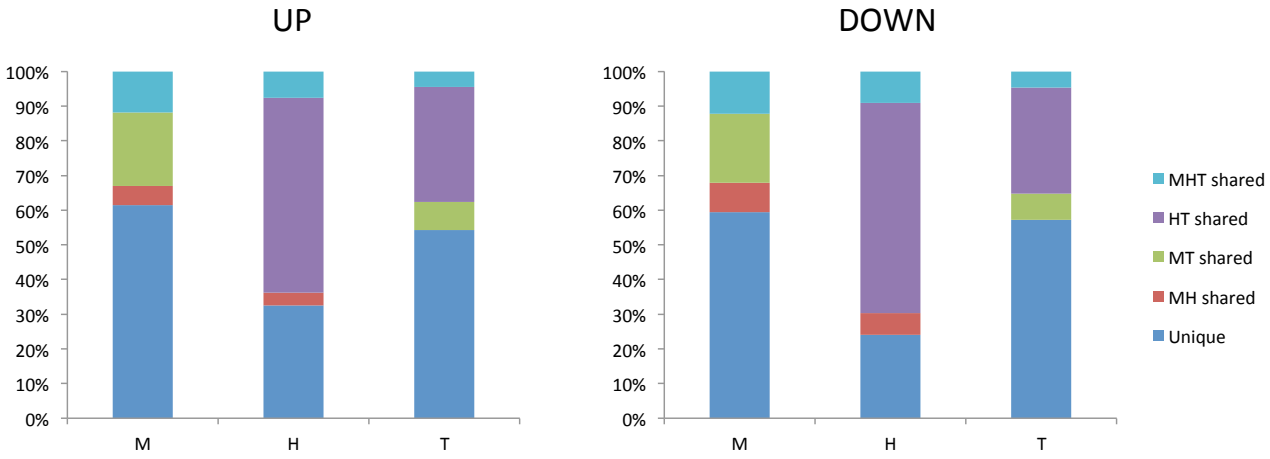
Supplementary Figure 1. Sample generation and consolidation scheme. Samples were generated in sextuplicate on two separate days, then pooled into triplicates representing inter- and intra-experimental variation, prior to RNA extraction.



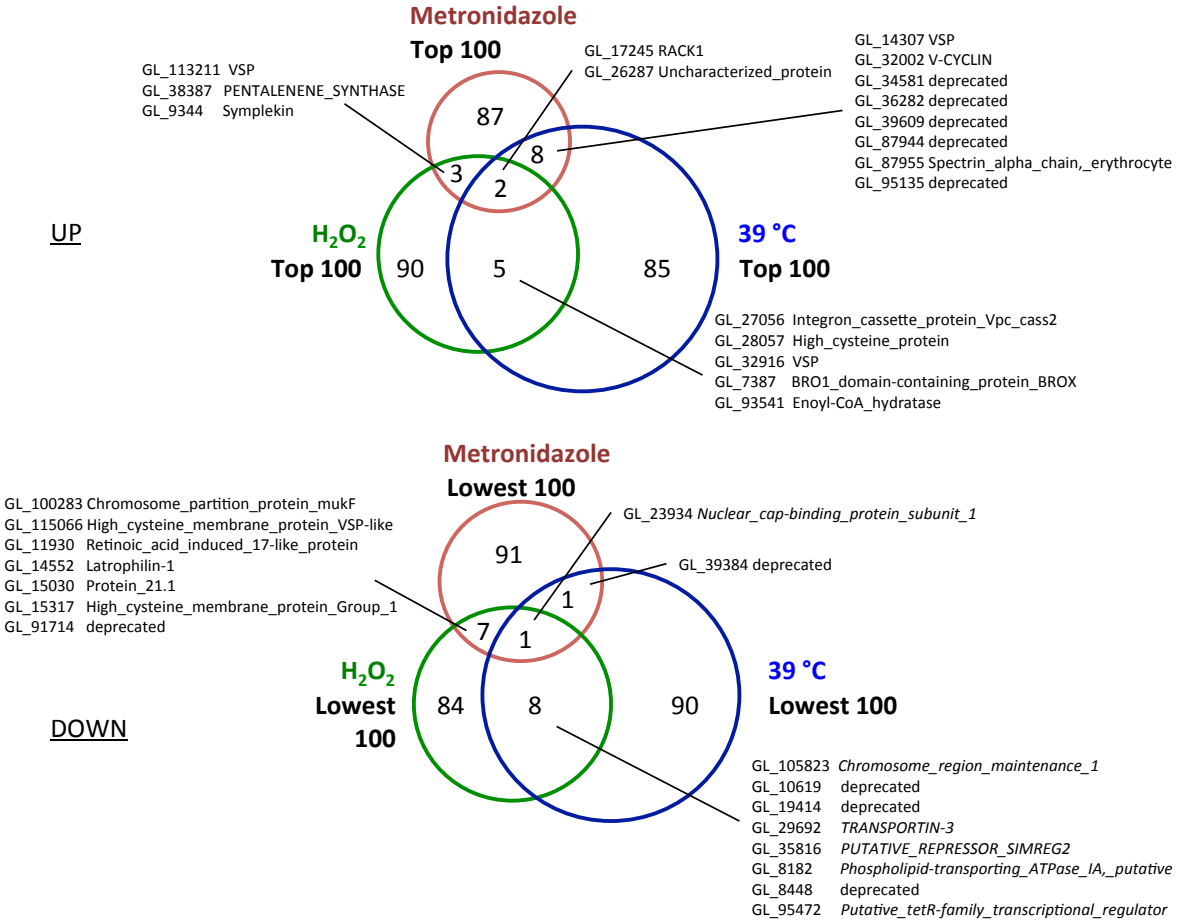
Supplementary Figure 2. Cumulative (left y axis) and novel (right y axis) feature detection as a function of sequencing depth (x) for reads mapped in forward (sense) and reverse orientation (antisense; antiS) relative to annotated transcripts (GiardiaDB.org; release 25).



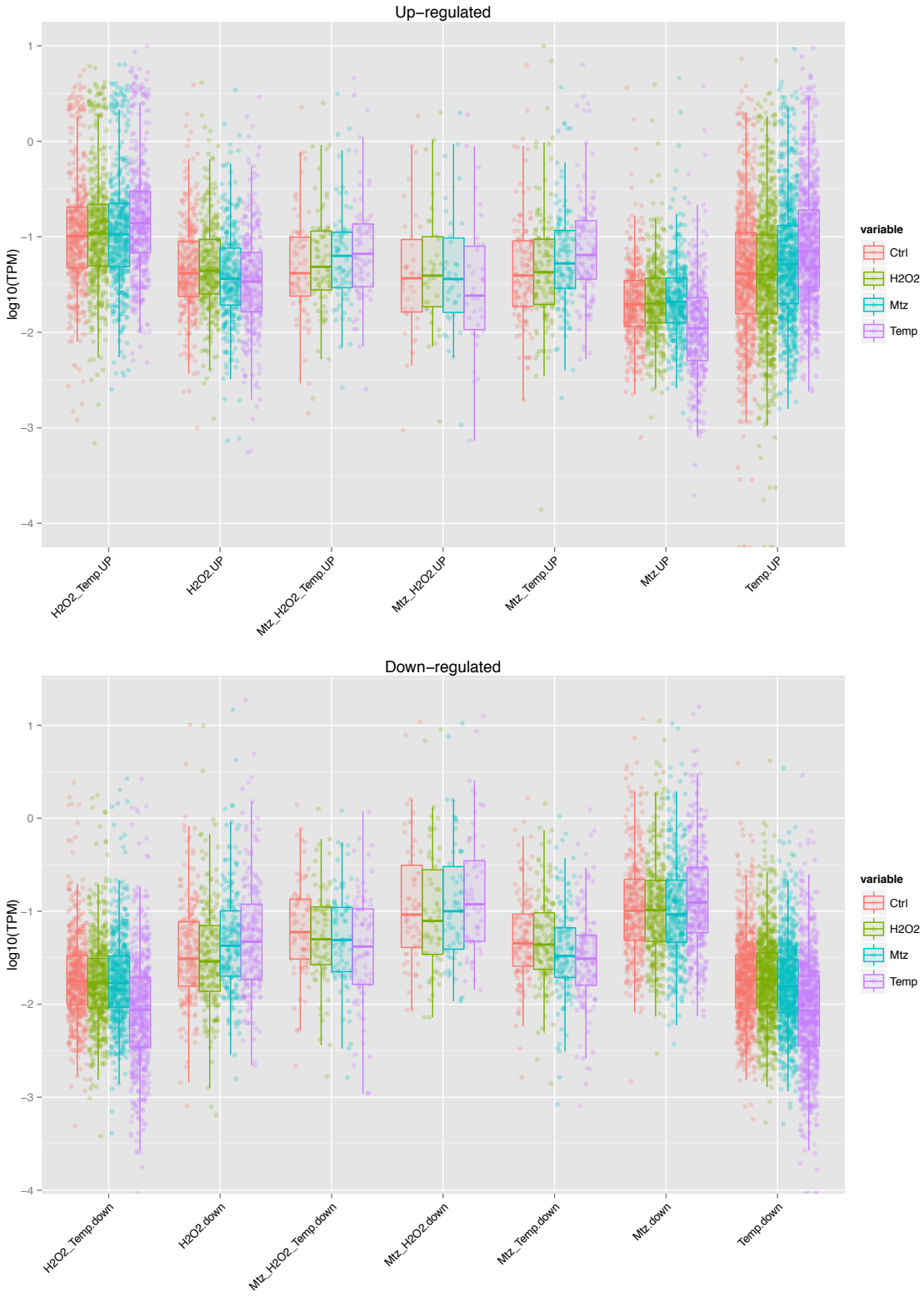
Supplementary Figure 3. TMM-normalized transcriptional abundance for genes with ≥1 count per million counts in at least three replicates.



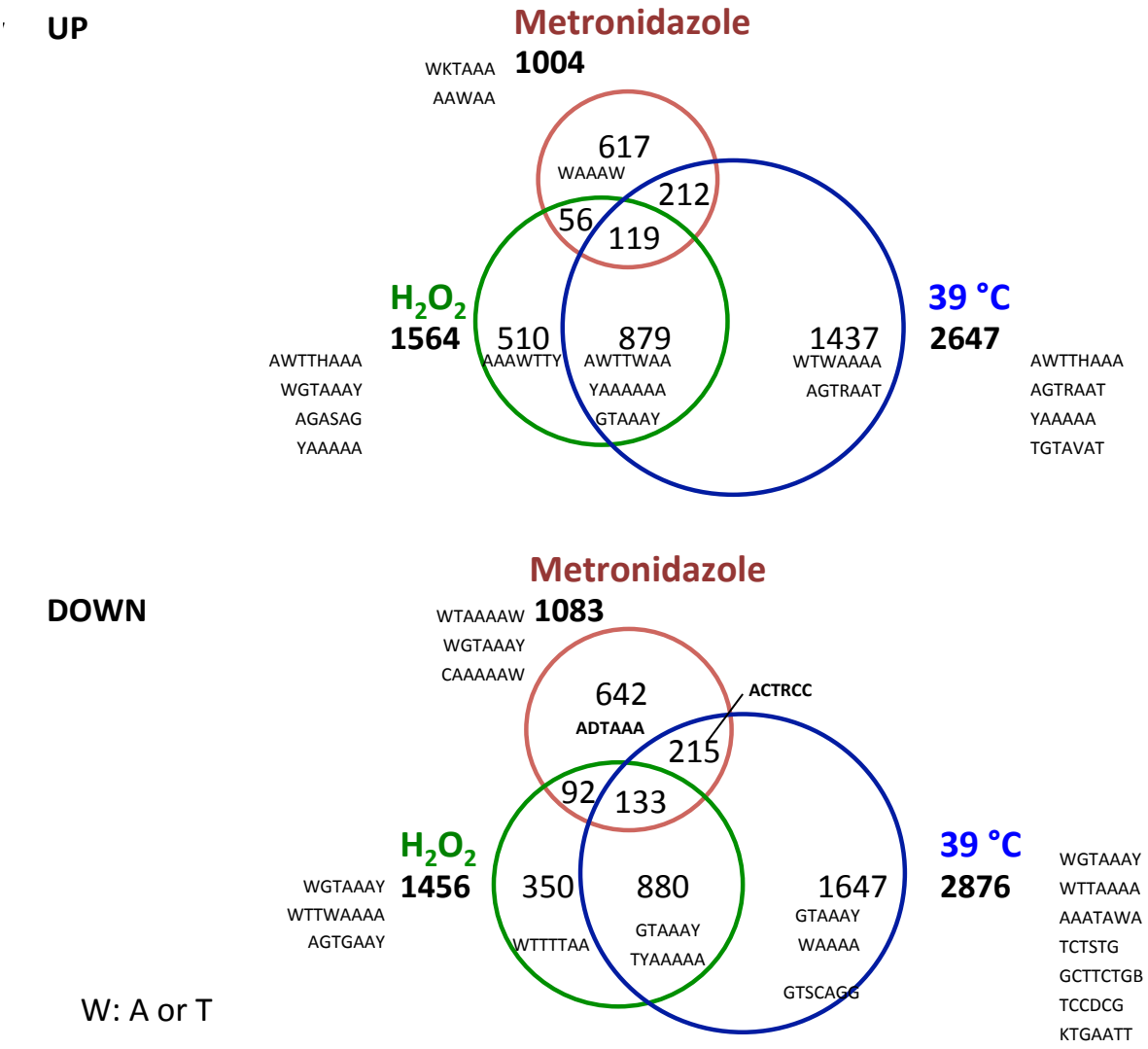
Supplementary Figure 4. Shared and stress-specific differentially transcribed genes. M: Metronidazole; H: hydrogen peroxide; T: thermal stress.



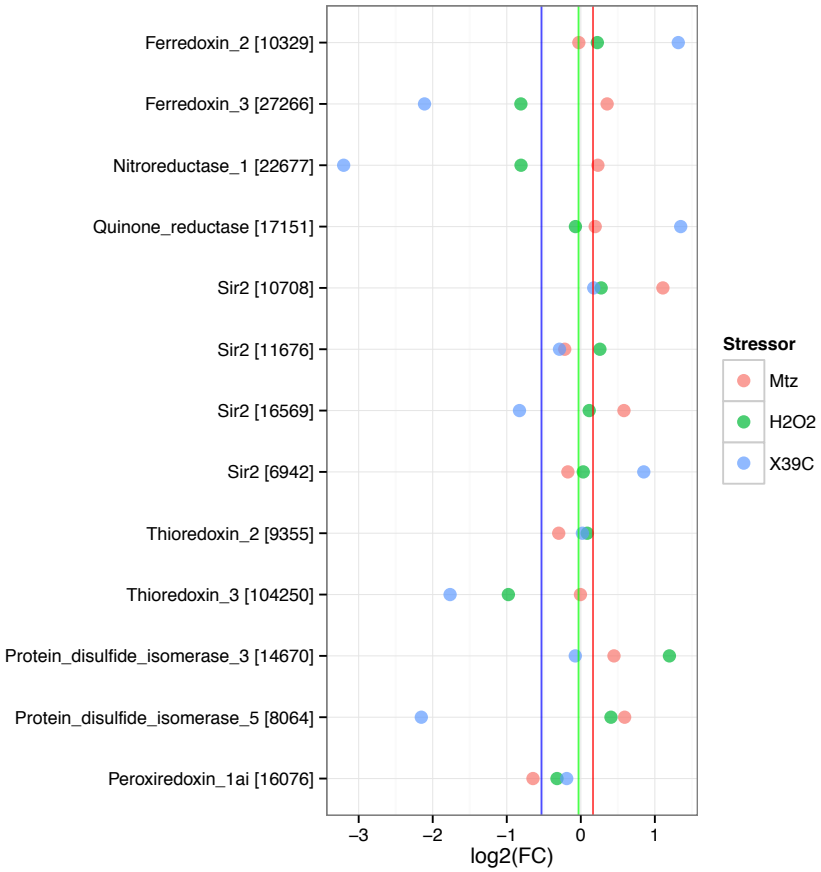
Supplementary Figure 5. Overlap in the 100 most highly differentially transcribed up- and down-regulated genes. Genes shared between two or more conditions are annotated.



Supplementary Figure 6. Length-normalized transcriptional abundance (TPM) for genes in control and stress conditions, grouped by Venn overlap segment.



Supplementary Figure 7. Significantly over-represented motifs in non-overlapping promoters upstream of differentially transcribed genes.



Supplementary Figure 8. Log_2(fold change) in antisense transcriptional abundance for non-overlapping genes related to the antioxidant system. Mean transcriptional abundance displayed as vertical lines.

Chapter 7. Transcriptomics indicates active and passive metronidazole resistance mechanisms in three seminal *Giardia* lines

Brendan R E Ansell, Louise Baker, Samantha J. Emery, Malcolm J. McConville, Staffan G. Svärd, Robin B. Gasser, Aaron R. Jex. *Frontiers in Microbiology* 02/2017; 8(398). DOI: 10.3389/fmicb.2017.00398

frontiers in Microbiology

ORIGINAL RESEARCH
published: 17 March 2017
doi: 10.3389/fmicb.2017.00398

Transcriptomics Indicates Active and Passive Metronidazole Resistance Mechanisms in Three Seminal *Giardia* Lines

Brendan R. E. Ansell[1], Louise Baker[2], Samantha J. Emery[2], Malcolm J. McConville[3], Staffan G. Svärd[4], Robin B. Gasser[1] and Aaron R. Jex[1,2]*

[1] Faculty of Veterinary and Agricultural Sciences, The University of Melbourne, Melbourne, VIC, Australia, [2] Population Health and Immunity Division, Walter and Eliza Hall Institute of Medical Research, Melbourne, VIC, Australia, [3] Bio21 Molecular Science and Biotechnology Institute, The University of Melbourne, Melbourne, VIC, Australia, [4] Department of Cell and Molecular Biology, Uppsala University, Uppsala, Sweden

Giardia duodenalis is an intestinal parasite that causes 200–300 million episodes of diarrhoea annually. Metronidazole (Mtz) is a front-line anti-giardial, but treatment failure is common and clinical resistance has been demonstrated. Mtz is thought to be activated within the parasite by oxidoreductase enzymes, and to kill by causing oxidative damage. In *G. duodenalis*, Mtz resistance involves active and passive mechanisms. Relatively low activity of iron-sulfur binding proteins, namely pyruvate:ferredoxin oxidoreductase (PFOR), ferredoxins, and nitroreductase-1, enable resistant cells to passively avoid Mtz activation. Additionally, low expression of oxygen-detoxification enzymes can allow passive (non-enzymatic) Mtz detoxification via futile redox cycling. In contrast, active resistance mechanisms include complete enzymatic detoxification of the pro-drug by nitroreductase-2 and enhanced repair of oxidized biomolecules via thioredoxin-dependent antioxidant enzymes. Molecular resistance mechanisms may be largely founded on reversible transcriptional changes, as some resistant lines revert to drug sensitivity during drug-free culture *in vitro*, or passage through the life cycle. To comprehensively characterize these changes, we undertook strand-specific RNA sequencing of three laboratory-derived Mtz-resistant lines, 106-2ID$_{10}$, 713-M3, and WB-M3, and compared transcription relative to their susceptible parents. Common up-regulated genes encoded variant-specific surface proteins (VSPs), a high cysteine membrane protein, calcium and zinc channels, a Mad-2 cell cycle regulator and a putative fatty acid α-oxidase. Down-regulated genes included nitroreductase-1, putative chromate and quinone reductases, and numerous genes that act proximal to PFOR. Transcriptional changes in 106-2ID$_{10}$ diverged from those in 713-r and WB-r ($r \leq 0.2$), which were more similar to each other ($r = 0.47$). In 106-2ID$_{10}$, a nonsense mutation in nitroreductase-1 transcripts could enhance passive resistance whereas increased transcription of nitroreductase-2, and a MATE transmembrane pump system, suggest active drug detoxification and efflux, respectively. By contrast, transcriptional changes in 713-M3 and WB-M3 indicated a higher oxidative stress load, attributed to Mtz- and oxygen-derived radicals, respectively. Quantitative comparisons of orthologous gene

OPEN ACCESS

Edited by:
Dimitris G. Hatzinikolaou, National and Kapodistrian University of Athens, Greece

Reviewed by:
Anja Joachim, Veterinärmedizinische Universität, Austria
Jozsef Soki, University of Szeged, Hungary

***Correspondence:**
Brendan R. E. Ansell
bansell@student.unimelb.edu.au

Specialty section:
This article was submitted to Systems Microbiology, a section of the journal Frontiers in Microbiology

Received: *08 December 2016*
Accepted: *27 February 2017*
Published: *17 March 2017*

Citation:
Ansell BRE, Baker L, Emery SJ, McConville MJ, Svärd SG, Gasser RB and Jex AR (2017) Transcriptomics Indicates Active and Passive Metronidazole Resistance Mechanisms in Three Seminal Giardia Lines. Front. Microbiol. 8:398. doi: 10.3389/fmicb.2017.00398

transcription between Mtz-resistant *G. duodenalis* and *Trichomonas vaginalis*, a closely related parasite, revealed changes in transcripts encoding peroxidases, heat shock proteins, and FMN-binding oxidoreductases, as prominent correlates of resistance. This work provides deep insight into Mtz-resistant *G. duodenalis*, and illuminates resistance-associated features across parasitic species.

Keywords: messenger RNA, RNA sequencing (RNA-Seq), Giardia, metronidazole resistance, oxidoreductases, single nucleotide polymorphism, Trichomonas

INTRODUCTION

Giardia duodenalis (syn. *G. lamblia*, *G. intestinalis*) is a parasitic protist of the human gastrointestinal tract that causes 200–300 million clinical cases of diarrheal disease annually (Lane and Lloyd, 2002). The nitroheterocyclic drug metronidazole (Mtz) is routinely used in treatment of microaerophilic parasites including *G. duodenalis*, *Trichomonas vaginalis* and *Entamoeba histolytica*, and is also used against the anaerobic bacterial pathogens *Helicobacter pylori* and *Clostridium difficile* (Samuelson, 1999; Petri, 2003; Löfmark et al., 2010). Mtz is thought to enter cells as an inactive pro-drug, which is reduced by oxidoreductase enzymes to form cytotoxic intermediates (radicals) that oxidize biomolecules. The low reduction potential of this drug makes it selectively active against microaerophilic and anaerobic organisms, which maintain highly reduced, oxygen-poor intracellular environments. The aerobic host is protected from Mtz cytotoxicity, as any reduced Mtz is spontaneously re-oxidized to the inactive pro-drug form, termed futile cycling (Edwards, 1993). Clinical Mtz resistance has been attributed to increased Mtz tolerance in *G. duodenalis* isolated from patients who failed Mtz therapy (Lemée et al., 2000; Adagu et al., 2001). Similar clinical resistance is reported in *T. vaginalis* (Cudmore et al., 2004) and *H. pylori* (Bereswill et al., 2003; Mirzaei et al., 2014). In addition to studies in clinical isolates, Mtz resistant *G. duodenalis* lines can be derived in the laboratory, which allows genetically controlled (i.e., isogenic) investigation of resistance mechanisms. Such lines are generally created through chronic exposure of drug-susceptible trophozoites to progressively increasing concentrations of Mtz over a period of months (Boreham et al., 1988).

Molecular Mtz resistance mechanisms can be classified as passive or active. Down-regulation of enzymes that reduce Mtz to toxic intermediates, constitute passive resistance mechanisms. Up-regulation of enzymes that detoxify Mtz directly or manage Mtz-induced damage, are considered active mechanisms. Ferredoxin family enzymes, which bind iron-sulfur (Fe-S) clusters, are strongly implicated in both passive and active resistance mechanisms. A well-established passive resistance mechanism centres on pyruvate:ferredoxin oxidoreductase (PFOR) and its electron acceptor ferredoxin. PFOR transfers glycolytic electrons via bound Fe-S clusters to soluble ferredoxin, which can, in turn, activate Mtz (Ellis et al., 1993). Accordingly, lower PFOR and ferredoxin enzyme activities are reported in laboratory-derived resistant lines, relative to their susceptible parents; and PFOR activity correlates with Mtz sensitivity in clinical isolates (Smith et al., 1988; Ellis et al., 1993; Leitsch et al., 2011). Nitroreductase-1, a ferredoxin-nitroreductase chimera, activates Mtz in recombinant enzyme assays, and is transcriptionally down-regulated in resistant lines (Müller et al., 2007b, 2013). Over-expression of nitroreductase-1 in susceptible trophozoites also increases Mtz sensitivity (Nillius et al., 2011). A less direct, passive resistance mechanism involves down-regulation of oxygen detoxification enzymes, which allows intracellular oxygen to accumulate and to inactivate Mtz via futile redox cycling (Ellis et al., 1993). This reaction creates reactive oxygen species, however, which require active detoxification (Testa et al., 2011). In contrast, nitroreductase-2, a paralog of nitroreductase-1, is thought to detoxify Mtz by reducing the Mtz pro-drug directly to an inert amine, thus bypassing the reactive intermediates (Müller et al., 2013, 2015). Transcriptional up-regulation of nitroreductase-2 in particular resistant lines is consistent with an active resistance mechanism. Regulation of thioredoxin reductase (TrxR), a major thiol-cycling enzyme in *G. duodenalis*, is inconsistent in resistant lines. This enzyme provides reducing power to thioredoxins and peroxiredoxins to manage oxidative stress. Over-expression of TrxR in susceptible trophozoites increases Mtz sensitivity, suggesting a role in drug activation (Leitsch et al., 2016); however, increased thiol reductase activity (attributable to TrxR) is reported in some resistant lines, suggesting a protective role (Smith et al., 1988). These conflicting results may be due to the antioxidant activity of TrxR outweighing its detrimental Mtz-activating effects in lines selected for resistance. Reversion to drug sensitivity in formerly resistant lines after passage through the life cycle (i.e., encystation-excystation) or in drug-free culture medium suggests that Mtz resistance is relatively unstable. That nitroreductase-1 and PFOR-1 transcription are restored in revertant excysted trophozoites, further suggests that transcriptional plasticity contributes prominently to Mtz resistance (Müller et al., 2008).

Three well-characterized Mtz-resistant lines are BRIS/83/HEPU/106-2ID$_{10}$ (referred to hereafter as 106-r), BRIS/83/HEPU/713-M3 (713-r), and WB-M3 (WB-r), which were derived in the 1980s through chronic exposure to Mtz. 713-r and WB-r were also exposed to ultraviolet (UV) irradiation prior to selection (Boreham et al., 1988; Townson et al., 1992). Lower PFOR and ferredoxin activities are reported in 106-r, 713-r, and WB-r relative to their susceptible parents (Smith et al., 1988; Townson et al., 1996; Liu et al., 2000; Leitsch et al., 2011), with one study failing to detect any PFOR activity in 106-r (Leitsch et al., 2011). Nitroreductase-1 transcription is down-regulated in 713-r, and nitroreductase-2 is up-regulated both this line and 106-r, indicating that passive and active resistance mechanisms can co-occur within resistant lines (Müller et al.,

2013). Chromosomal aberrations are also reported for all three resistant lines, but have not been resolved in detail (Upcroft et al., 1992; Townson et al., 1994; Chen et al., 1995; Upcroft and Upcroft, 1999; Upcroft et al., 2010). Further, 106-r remains infective in suckling mice, whereas 713-r lacks any infective capacity (Tejman-Yarden et al., 2011).

Variation in the infectivity and molecular phenotypes of these resistant *G. duodenalis* lines (reviewed in Ansell et al., 2015b) suggest that multiple molecular resistance phenotypes are possible, each of which could comprise changes in the genetic sequence, transcription level and functional regulation of multiple proteins. Indeed, the extent and variability of molecular phenotypes that confer resistance are far from understood. Some obvious candidates that are yet to be investigated in resistant *G. duodenalis* lines include a canonical nitroreductase NTR-1, that is similar to the RdxA of *H. pylori* and activates Mtz *in vitro* (Nixon et al., 2002; Pal et al., 2009); and several under-characterized NADPH-dependent oxidoreductases that might account for the decreased flavin reductase activity reported in certain lines (Ellis et al., 1993; Leitsch et al., 2011). Further, as we have argued previously (Ansell et al., 2015b), enzymes that produce and consume the substrates and cofactors of oxidoreductase enzymes may thereby modulate their function, which potentially implicates a host of metabolic enzymes in Mtz metabolism and resistance. Recent whole genome and transcriptome sequencing has refined and expanded the complement of genes associated with Mtz resistance in *H. pylori* (Binh et al., 2015) and *T. vaginalis* (Bradic et al., 2016), among which hitherto under-characterized flavin reductases, ribosomal proteins, and canonical nitroreductases feature prominently.

In order to better understand the transcriptional correlates of Mtz resistance in *G. duodenalis* and to probe the features of laboratory-derived resistant lines that may be clinically relevant, the present study used RNA sequencing to compare transcriptional changes in 106-r, 713-r, and WB-r relative to their susceptible parental lines. In addition to identifying differentially transcribed genes (DTGs) and gene sets, we documented single-nucleotide polymorphisms in transcripts that may affect protein function and identified genes that may be negatively regulated by antisense transcription. A core set of resistance-associated genes is discussed in the context of isotype-specific changes that may augment resistance and account for differences in growth rate and infectivity. Central roles for heat shock proteins, peroxidase enzymes and FMN-dependent oxidoreductases in Mtz resistance are underscored via quantitative comparisons of orthologous gene transcription in *T. vaginalis*. This work represents the first genetically controlled, transcriptome-wide investigation of Mtz resistance in any pathogen.

MATERIALS AND METHODS

Cell Culture

Giardia duodenalis trophozoites were generously provided by Professor Jacqueline Upcroft and Professor Peter Upcroft. Metronidazole (Mtz)-sensitive trophozoites (BRIS/83/HEPU/106, BRIS/87/HEPU/713, and WB1B; referred to hereafter as 106-s, 713-s, and WB-s) were maintained in flat-sided 10 mL tubes (Nunclon delta) filled with 10 mL of complete TYI-S33 medium (Davids and Gillin, 2011) and sub-cultured twice weekly. The standard medium contains 55 mM glucose, which is well in excess of the concentration required to sustain trophozoites throughout a four-day culture passage. As such, with a view to correlating transcriptomic results with future metabolomics results (in which glucose can saturate spectral profiles), the TYI-S33 medium was modified to contain 6 mM glucose (designated "TYI medium"). Mtz-resistant lines (BRIS/83/HEPU/106-2ID$_{10}$, BRIS/83/HEPU/713-M3 and WB1B-M3; hereafter 106-r, 713-r, and WB-r) were maintained under the same conditions with Mtz (Sigma Aldrich; 100 mM stock dissolved in dimethyl sulfoxide) added to a final concentration of 30 μM. References describing the original axenization of these lines and resistance selection methods are provided in **Table 1**.

Growth Rate and Drug Sensitivity Testing

Trophozoites from confluent flasks were chilled on wet ice (5 min), pelleted (680 × *g*, 5 min, 4°C), diluted in fresh TYI medium to 5 × 10^4 cells/mL (susceptible lines) or 1.5 × 10^5 cells/mL (resistant lines; cf Tejman-Yarden et al., 2011), and added in 40 μL volumes to wells of a 96-well clear-bottom plate (Corning #3610). 200 μL of sterile water was added to the peripheral wells to limit evaporation. Serial dilutions of Mtz were created in TYI medium and added to wells containing trophozoites, in duplicate. The wells of the resulting plates contained ∼2,000 (susceptible) or 6,000 (resistant) trophozoites in a 50 μL volume, and either Mtz (2.5–200 μM) or 1% DMSO in TYI medium (negative control). Plates were incubated at 37°C within GasPak EZ anaerobe pouches, with fresh anaerobic sachets for 48 h. Reconstituted CellTiter-Glo reagent (Promega)

TABLE 1 | Metronidazole sensitivity and generation times for isogenic lines.

Strain	Abbreviation	References	Mtz IC_{50} (μM)	IC_{50} fold increase	Doubling time (hours)	Doubling time fold increase
106	106-s	Boreham et al., 1984	9.39	–	5.48	–
106-2ID10	106-r	Boreham et al., 1988	23.99	2.55	6.36	1.16
713	713-s	Capon et al., 1989	7.79	–	5.27	–
713-M3	713-r	Townson et al., 1992	42.33	5.43	7.46	1.41
WB1B	WB-s	Capon et al., 1989	8.28	–	5.28	–
WB1B-M3	WB-r	Townson et al., 1992	22.79	2.75	13.8	2.62

was stored at −20°C and thawed to room temperature (22–24°C; RT) 30 min prior to use; 50 μL of reagent were added to wells containing trophozoites, and plates were incubated for 15 min, shaking, at RT. ATP-based luminescence (corresponding to live cells/well) was measured using a luminometer (BioTek), and transformed to a proportion of the negative control value. Prism software (GraphPad) was used to fit Hill plots to dose-response data and to calculate IC_{50} values, via the "log(inhibitor) vs. normalized response—variable slope" module. In order to estimate generation times, standard curves relating ATP luminescence and trophozoite numbers were created for Mtz-susceptible and -resistant lines, and found to be log-linear within 5×10^4–10^6 cells per well. Trophozoite numbers in the negative control wells of dose-response experiments were interpolated from the standard curve, and generation times were calculated according to Boreham et al. (1984).

Sample Generation and mRNA Sequencing

For Mtz-susceptible lines, samples for mRNA sequencing were generated in triplicate. Falcon t25 flasks were seeded with 10^5 trophozoites in 56 mL of fresh TYI medium and incubated at 37°C for ∼60 h, at which time trophozoites formed a confluent monolayer on the flask walls. For Mtz-resistant lines, up to 8 flasks were seeded with 1.5–3 × 10^6 trophozoites (according to growth-rate), and Mtz was added to a final concentration of 30 μM. After incubation, flasks were inverted, and supernatant and suspended trophozoites (likely to contain dead/dying and dividing cells, which could confound the mRNA integrity and comparative transcription analyses, respectively), were decanted to waste; 50 mL of ice-cold complete TYI medium were added and flasks were incubated on ice-water for 10 min to detach trophozoites. The suspended cells were transferred to 50 mL falcon tubes and pelleted (680 × *g*, 5 mins, 4°C). Supernatant was removed, and pellets were re-suspended, transferred to UV-irradiated 1.5 mL microfuge tubes, and pelleted (720 × *g*, 2 mins, RT). Samples from Mtz-resistant lines were consolidated into three microfuge tubes. Supernatant was removed and pellets were dissolved in 1 mL of TriPure reagent (Roche), incubated at RT for 5 min and stored at −80°C.

RNA was extracted according to the TriPure manufacturer's protocol within 4 weeks of sample preparation. The dried RNA pellet was re-suspended in reverse-osmosis deionized water (H_2O) and treated with Turbo DNAse (Ambion) according to the manufacturer's instructions. RNA concentration was estimated by fluorometry (Qubit), and quality control was performed using a BioAnalyzer (Agilent). Polyadenylated RNA was purified from 10 μg of total RNA using Sera-mag oligo(dT) beads, fragmented to a length of 100–500 bases, and reverse transcribed using random hexamers. Strands were labeled using the dUTP second-strand synthesis method, end-repaired and adaptor-ligated, and then treated with uracil-specific excision reagent (USER; NEB) before amplification by PCR. Products were purified over a MinElute column (Qiagen) and single-end sequencing was performed using an Illumina HiSeq 2500 (YourGene Biosciences, Taiwan). Raw RNA sequencing reads are available through the NCBI Sequence Read Archive (http://www.ncbi.nlm.nih.gov/sra/SRP075868).

Data Processing and Analysis

Raw reads were trimmed using Trimmomatic (Lohse et al., 2012) (sliding window: 4 nt; minimum average PHRED quality: 20; leading and trailing: 3 nt; minimum read length: 40 nt), and mapped as single-ended reads to the accepted *G. duodenalis* gene models (assemblage A genome release 25; giardiaDB.org; Morrison et al., 2007) using RSEM (Li and Dewey, 2011) with the -forward-prob 0 flag. The locus encoding superoxide reductase (Testa et al., 2011) was added to the reference genome. Reads that did not map under these conditions were likely to include antisense transcripts. To quantify antisense transcription, unmapped reads were submitted to RSEM with the –forward-prob 1 flag, which discards any reads that map with <100% confidence to the coding strand. The RSeQC bam_stats.py module (Wang et al., 2012) was used to calculate read mapping statistics; and infer_experiment.py was used to confirm read mapping orientation. Feature detection was calculated as a function of read mapping depth using the Qualimap counts module (v1.0; García-Alcalde et al., 2012) with the −k 10 flag, denoting a minimum mapped read threshold of 10. Saturation plots were displayed in Excel (Microsoft) (**Supplementary Figure 1**).

Expected counts from RSEM were submitted to edgeR (Robinson et al., 2009). For preliminary clustering analyses, low abundance genes (fewer than one count per million counts; CPM) were discarded before library re-scaling and TMM normalization. For each susceptible and resistant pair, sample normalization was performed as above and differentially transcribed genes were determined at a false discovery rate of 0.01. CPM-values were multiplied by 1,000 and divided by the reference transcript length to give transcripts per kilobase per million transcripts (TPM), suitable for comparing the transcriptional abundance of different genes across samples. Romer (Wu et al., 2010) was used to test enrichment of KEGG pathways and Gene Ontology (GO) terms among up- and down-regulated genes in resistant lines, and to test enrichment of curated gene sets specific to *G. duodenalis* (significance threshold: corrected $p < 0.05$; **Supplementary Table 9**). Hypothetical *G. duodenalis* proteins of interest were selected for tertiary structure prediction using a stand-alone implementation of the I-TASSER software suite (v3.0) generously provided by Professor Yang Zhang, as described previously (Ansell et al., 2016). It must be noted that the output from the stand-alone implementation of this software can differ from that available through the online server (zhanglab.ccmb.med.umich.edu/I-TASSER) due to computational resource constraints on the server. As such, the output from the stand-alone software should be more robust. GO terms associated with high-confidence structures (TM score > 0.5; GO confidence score > 0.5) were included in gene set testing. Structural similarity searching was performed using TM-align (Zhang and Skolnick, 2005), and protein structures were visualized using UCSF Chimera (Pettersen et al., 2004). Read coverage data were normalized by total library size (calculated in edgeR), and transcriptional abundance plots and heat maps were generated in R (ggplot2 and gplots packages).

RNA reads mapping in the sense orientation were submitted to mpileup and bcftools (SAMtools suite; Li et al., 2009) to identify single nucleotide polymorphisms (SNPs) using conservative thresholds (≥100× read coverage for the alternative allele, constituting ≥20% of nucleotides mapped at that position). Selected SNPs were visually confirmed using Integrative Genomics Viewer (Robinson et al., 2011), and amino acid substitutions (products of non-synonymous SNPs), were predicted using getORF (Rice et al., 2000) and custom scripts. For comparative transcriptomics between species, published RNA transcript count data for Mtz-susceptible and –resistant *T. vaginalis* (Bradic et al., 2016) were submitted to edgeR in a two-sample comparison of transcript abundance. Count data for resistant and susceptible *G. duodenalis* lines generated in this study were compared using the same design, and orthologous genes (defined in OrthoMCL-DB; Chen, 2006) that were differentially transcribed in the same direction in both species, were retained for further analysis.

RESULTS

Growth Rates and Metronidazole Susceptibility

All Mtz-susceptible lines exhibited generation times of ∼5 h. The generation time for WB-r was 13.85 h, indicating a marked growth defect compared to 106-r and 713-r, for which generation times were 6.36 and 7.46 h, respectively. For susceptible lines, Mtz IC_{50} concentrations ranged from 7.8 to 9.4 μM. Each resistant line showed significantly greater Mtz tolerance than its susceptible parent (two-sample comparison of fits; $p < 0.001$; **Figure 1A**). Specifically, WB-r and 106-r exhibited an approximate 2.6-fold increase in Mtz tolerance relative to their susceptible parents, whereas 713-r was 5.4-fold more tolerant than 713-s, and also more tolerant than the other resistant lines (713-r vs. WB-r: $p = 0.027$; vs. 106-r: $p = 0.004$; **Table 1**).

Clustering and Differential Transcription

RNA sequencing of six cell lines in biological triplicate produced a total of 641 million single-ended reads, with an average of 35.6 million reads per sample. The vast majority of reads satisfied quality control (mean = 93.5%; range = 92.4–94.7%), of which 80% were mapped to the accepted *G. duodenalis* genes in the sense orientation (**Supplementary Tables 1**, **2**; **Supplementary Figure 1**). Around 5% of reads from each sample mapped to the reverse complement, consistent with antisense transcripts (detailed below). After filtering lowly transcribed genes, 5,792 non-deprecated coding domains were detected in all isotypes. Transcripts from a further 231 coding domains were detected in either one or two isotypes (**Supplementary Table 3**). Using transcript abundance, susceptible lines clustered together

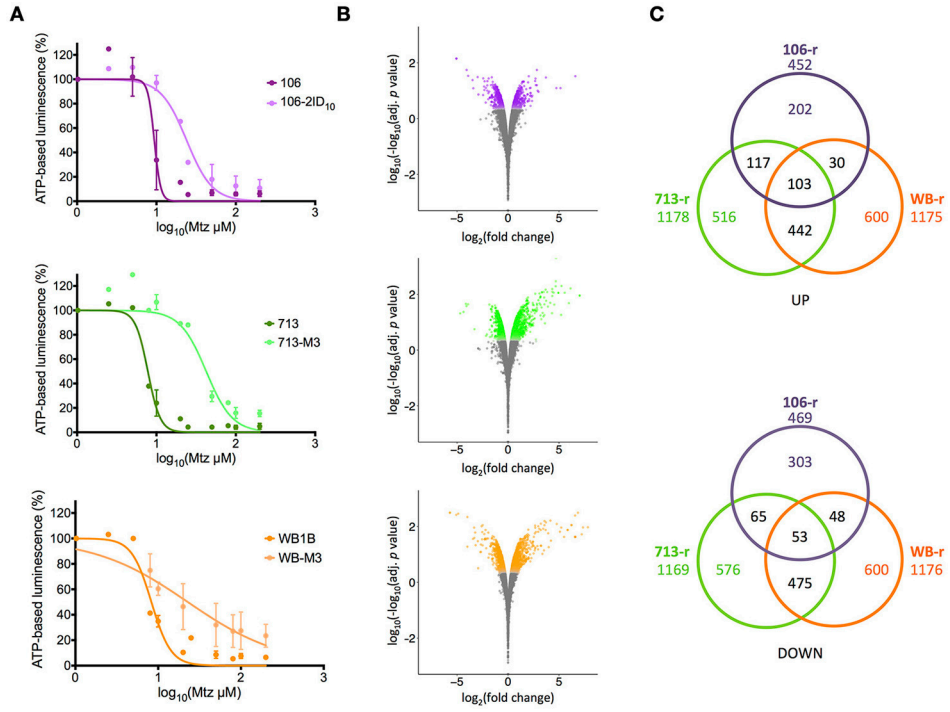


FIGURE 1 | Metronidazole dose-response and differential transcription in resistant lines. (A) Dose-response curves for metronidazole-susceptible lines (dark colors) and resistant progeny (light colors). Experiments performed in biological duplicate. Error bars represent ± 1 standard deviation. **(B)** Fold-change in transcriptional abundance in resistant lines relative to susceptible parents. Significantly differentially transcribed genes (corrected $p < 0.01$) are displayed in color. Y-axes represent log-log-transformed corrected *p* values, where higher numbers indicate greater significance. **(C)** Numbers of significantly up-regulated (top panel) and down-regulated (bottom panel) genes shared between resistant lines. The total number of differentially transcribed genes is displayed beneath the line name.

in both principal coordinate analysis and Euclidean clustering; although Pearson correlations were lower on average between susceptible lines compared with resistant lines (Pearson's $r = 0.93$ vs. 0.96). Omission of transcripts encoding VSPs improved the mean pair-wise correlation for susceptible lines ($r = 0.98$), with little effect on resistant lines ($r = 0.97$; **Supplementary Figure 2**).

Pearson correlations based on $\log_2$(fold-change) values in resistant lines, were strongest between 713-r and WB-r ($r = 0.47$). These lines also correlated with microarray-based fold-change data for 41 strongly differentially regulated genes in the previously published Mtz-resistant line WB-C4 ($0.27 < r > 0.37$; Müller et al., 2008). Transcriptional changes in 106-r diverged substantially from 713-r and WB-r ($r \leq 0.2$), and correlated negatively with WB-C4 ($r = -0.29$). Comparisons with transcriptomic data for WB-s trophozoites after exposure to sub-lethal stressors (Ansell et al., 2016) revealed strongest agreement between Mtz stress and 106-r ($r = 0.18$), and a modest correlation with 713-r ($r = 0.03$). At a false-discovery threshold of 0.01, 2,010 genes (i.e., non-deprecated coding domains) were up-regulated in at least one resistant line relative to the susceptible parent, and 2,120 genes were down-regulated (**Figure 1B**; **Supplementary Tables 4**, **5**). In 713-r, 1,178 genes were up-regulated, and 1,169 were down-regulated relative to 713-s. In WB-r, 1,175, and 1,176 genes were up- and down-regulated respectively, of which 917 were differentially transcribed in the same direction in 713-r. Comparatively few DTGs (921 in total) were identified for 106-r, supported by close clustering between the resistant and susceptible lines for this isotype (**Supplementary Figure 2B**; overlapping DTGs are displayed in **Figure 1C**). This result may also be affected by greater variance between replicates in 106 (mean biological co-efficient of variance = 0.18) compared to WB and 713 isotypes (mean BCV = 0.1). As such, the minimum change in transcript abundance for genes satisfying the statistical threshold for differential transcription in 106-r was 24%, compared to 17% in WB-r and 713-r. The 30 most strongly up- and down-regulated genes in each resistant line (excluding VSPs) are provided in **Supplementary Table 6**.

Common Differentially Transcribed Genes and Mutations

Of 156 DTGs common to all three resistant lines, 103 genes were up-regulated, and 53 were down-regulated (**Figure 1C**). Common up-regulated genes included 33 VSPs, a high-cysteine membrane protein, the mitotic regulator Mad2 (Vicente and Cande, 2014), zinc and calcium transporters, Nek and DYRK kinases, a sulfatase-like enzyme, and a putative fatty acid α-oxidase. A ParcC-like chaperone (GL_15455), and two putative mTor kinase subunits were also up-regulated (GL_6542 and GL_13469). The 53 common down-regulated genes included nitroreductase-1, putative FMN-dependent chromate and quinone oxidoreductases (GL_9719 and GL_17151), a putative calcium sensor, glutamate dehydrogenase, threonine dehydratase, acetyl co-A acetyltransferase, two α-giardins, and E1 and E2 ubiquitin-related enzymes (**Figure 2A**; **Figure 3**; **Supplementary Table 5**). Proton- and ATP-dependent transporters, a hexose transporter and a putative sugar-nucleotide transporter (GL_9036) were also down-regulated. In all resistant lines, threonine dehydratase and a small hypothetical protein (GL_104062) encoded different non-synonymous SNPs. A further 19 genes encoded identical substitutions in two of three resistant lines (**Table 2**; **Supplementary Table 7**; **Supplementary Figure 3**).

Giardia-Specific Membrane Proteins in Resistant Lines

According to previous studies, resistant lines may preferentially express certain VSPs (Chen et al., 1995; Müller et al., 2007a, 2008). As mentioned above, disparities in VSP transcription preferentially decreased the strength of correlation between susceptible lines. When the 20 most abundant VSP-coding transcripts (approximating the top decile) in each line were compared, there was greater convergence in resistant lines. Ten genes among the top decile in at least one resistant line (including GL_137617, which was in the top decile for all three resistant lines), were absent from the equivalent group in all susceptible lines. A further nine genes were among the top decile in all resistant lines, whereas only six genes were consistently highly transcribed in susceptible lines (**Supplementary Figure 4**). No VSPs were consistently suppressed in resistant- relative to susceptible lines. The VSP TSA417 (GL_113797), which was reported as transcriptionally suppressed in the Mtz-resistant lines WB-C4 and WB-C5 (Müller et al., 2007a, 2008), was among the top decile of VSPs in 713-s, and in both 106-s and 106-r. VSPAS7 (GL_137740), which was suppressed in WB-C4 (Müller et al., 2008), was in the top decile for WB-r only. CRP136 (GL_103142), was previously detected in WB-r but not WB-s (Chen et al., 1995). In this study however it was among the top VSP decile in both lines. Overall, these results show little agreement in VSP transcription between lines, and within lines over time. To test the possibility that particular VSP peptide sequences are under selection in the presence of Mtz, we investigated the proportion of clade I, II, and III VSPs among the top decile in resistant and susceptible lines (Adam et al., 2010). Clade II was over-represented in both resistant and susceptible lines, relative to the background prevalence, with little between-group difference (odds ratio = 1.44 and 1.65, respectively). Similarly, there was little difference in the number of CXXC motifs (average of 18–21 motifs), or cysteine content (9–10% cysteine) in the top decile of *vsp*s between lines (**Supplementary Table 8**). High cysteine membrane proteins are another prominent *Giardia*-specific protein family with variable numbers of cysteine motifs (Davids et al., 2006). Transcripts from 60 *hcmp*s were significantly enriched among up-regulated genes in 713-r, but not 106-r, or WB-r. A clade of six *hcmp*s whose transcription tended to increase in all resistant lines contained the only consistently up-regulated HCMP, GL_11309. Sixty-nine CXXC motifs are encoded in this gene, well above the median for the HCMP family (Davids et al., 2006). No HCMPs were consistently down-regulated (**Supplementary Figure 5**).

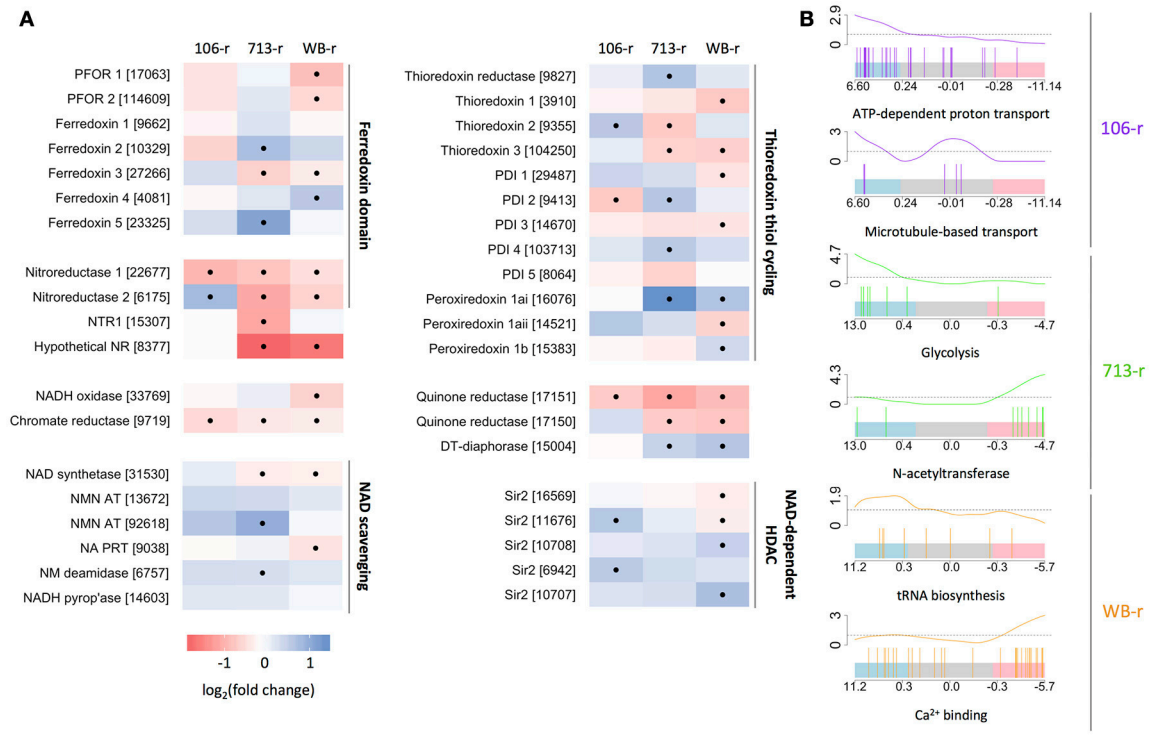


FIGURE 2 | Transcriptional changes in oxidoreductase-coding genes and related genes. (A) Color-scaled $\log_2$(fold change) values for resistant lines. Black dots indicate a statistically significant difference. Genes are grouped based on structure and/or function. Accession numbers (prefix: GL50803) appear in brackets. **(B)** Bar-code plots indicating the rank and $\log_2$(fold change) of genes (high: left, to low: right) comprising selected gene sets, below curves displaying sliding enrichment ratios. Blue and red shading indicate upper and lower quartiles, respectively.

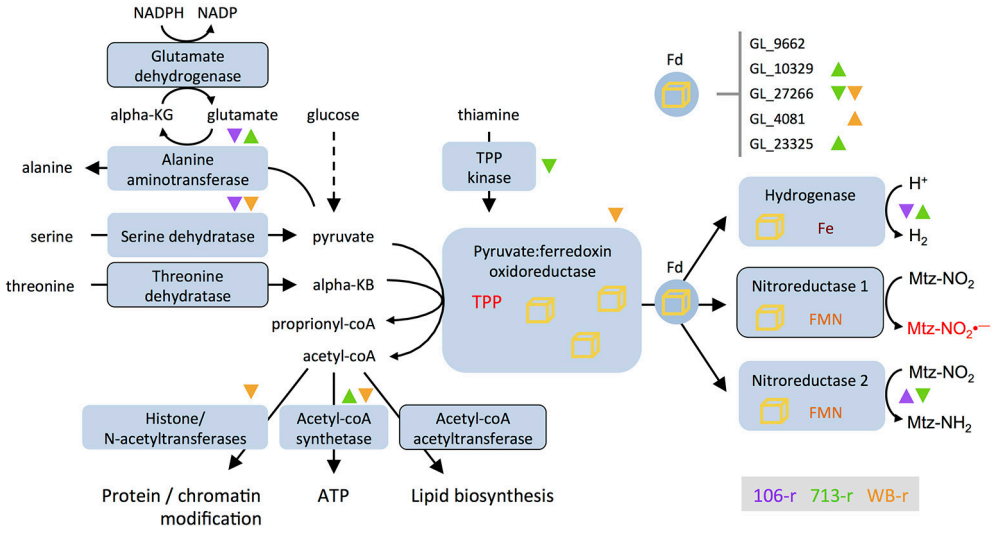


FIGURE 3 | Differential transcription of genes involved in ferredoxin-based electron transport and related processes. Nitroreductases are depicted as substrates of ferredoxin (Fd), as postulated by Ali and Nozaki (2007). The glutamate shunt consumes NADPH and cycles glutamate and α-ketoglutarate to drive the conversion of pyruvate to alanine. Enzymes encoded by genes that are down-regulated in all three resistant lines are outlined. Direction of differential transcription in different lines is indicated with color-coded up- or down-pointing triangles. Differential transcription for five ferredoxin-coding genes appears at top-right. Iron sulfur clusters are depicted as yellow cubes; Nitroreductase-1 activates metronidazole to toxic intermediates (Mtz-$NO_2^{\bullet-}$, red). Nitroreductase-2 reduces Mtz to an inert amine (Mtz-NH_2). KG, ketoglutarate; KB, ketobutyrate; coA, co-enzyme A; TPP, thiamine pyrophosphate; FMN, flavin mononucleotide; Fe, iron.

Gene Set Enrichment and Isotype-Specific DTGs in Mtz-Resistant *Giardia*

106s vs. 106-r

In agreement with previous reports, nitroreductase-2 was up-regulated in 106-r (Müller et al., 2015). Whereas, qPCR analysis had indicated non-significant down-regulation of nitroreductase-1-coding transcripts in 106-r (Müller et al., 2013), this effect was statistically significant in our data. The previously reported ablation of PFOR activity in 106-r (Leitsch et al., 2011) did not correspond to down-regulation of PFOR-coding transcripts. Gene set enrichment testing revealed increased transcription of the KEGG NAD synthesis pathway, and five NAD-dependent Sir2 enzymes in 106-r. Genes annotated with GO "ATP hydrolysis coupled proton transport," namely vacuolar ATPase components, were also up-regulated, as was GO "microtubule-based movement," contributed by dyenin- and kinesin-coding transcripts (**Figure 2B**; **Figure 4**). Conversely, gene sets encoding tRNA synthesis enzymes, protein chaperones, and FAD-binding enzymes were suppressed. The latter result derived from lower transcription of glutamate synthase, NADH oxidase (Brown et al., 1996) and dihydrouridine synthase. The KEGG arginine biosynthesis pathway was also down-regulated, contributed by lower transcription of genes in the ATP-forming arginine dihydrolase pathway (Schofield et al., 1992). A complete list of differentially transcribed gene sets is provided in **Supplementary Tables 9–12**. Among the 202 DTGs uniquely up-regulated in 106-r were a MATE-like sodium antiporter, Gmyb11 and the cell-cycle related proteins cyclin-fold protein, cell division control protein-48, and a CDK regulatory subunit. Among 303 uniquely down-regulated genes were the transcription factor Myb1, a putative Tet repressor homolog (GL_32769), iron hydrogenase, 15 high-cysteine membrane proteins, and α-giardins 8, 12, and 14. Intriguingly, a premature stop codon was identified in 29% of transcripts mapped to *nitroreductase-1* (nucleotide substitution C583T; **Supplementary Figure 6**).

713-s vs. 713-r

Nitroreductase-1 transcription was down-regulated in 713-r, in accordance with previous work. However nitroreductase-2 was not transcriptionally up-regulated as indicated previously (Müller et al., 2013). Gene sets encoding protein chaperones (HSPs, TCP-1 subunits, and peptidyl-prolyl isomerases), ABC and cation transporters, and the glycolysis pathway, were enriched among up-regulated genes in 713-r. Up-regulation of a set of genes encoding 4Fe-4S cluster-biding proteins, was founded on increased transcription of ferredoxin-2, two un-annotated ferredoxins (GL_23325 and GL_4081), and a putative glutamate synthase (GL_87577). Ferredoxin-3, which is predicted to bind iron-sulfur clusters of a 2Fe:2S geometry, was significantly down-regulated in 713-r—a finding that may relate to previous reports of suppressed ferredoxin activity

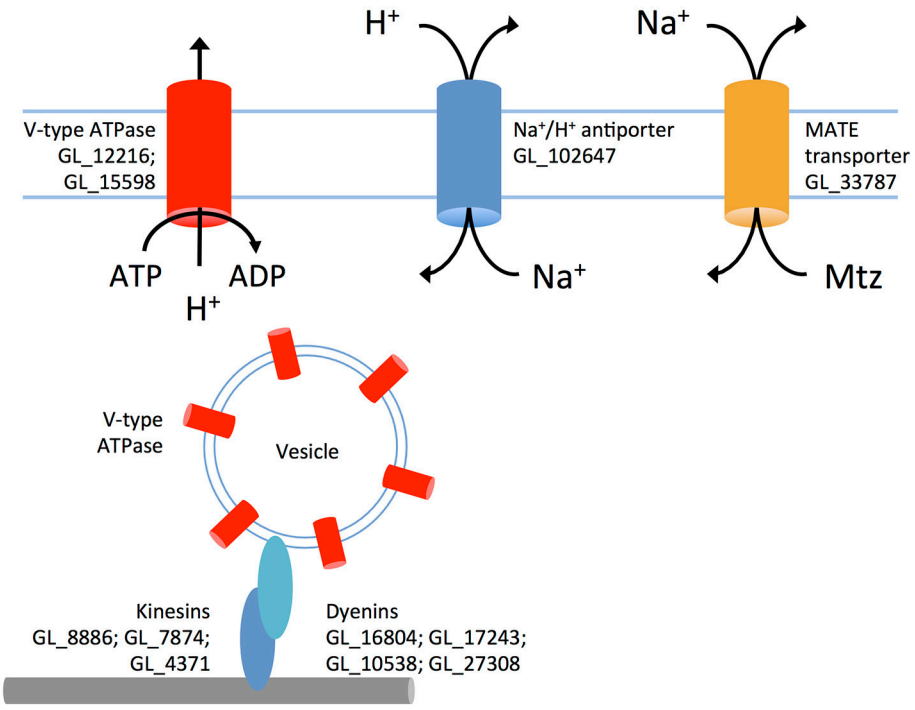


FIGURE 4 | A putative metronidazole efflux system in 106-r. V-type ATPases are inserted into vesicular membranes and transported via microtubules and dynein/kinesin motors to the plasma membrane. These pumps use ATP to transport protons out of the cytosol against the diffusion gradient. An up-regulated sodium/proton antiporter exchanges in-flowing protons for sodium, increasing the extracellular sodium concentration. The MATE transporter is proposed to expel metronidazole as sodium flows back into the cell. Up-regulated genes (prefix GL50803 abbreviated to GL) are displayed next to proteins.

(Liu et al., 2000; Leitsch et al., 2011). Gene set testing also identified down-regulated N-acetyltransferases and iron-binding proteins, the latter contributed by three putative ferretins (**Figure 2B**). A curated set of FMN-binding genes was found to be down-regulated, which included the putative quinone reductase (GL_17150), NTR-1 and the putative canonical nitroreductase GL_8377 (**Figure 2A**). Conversely, peroxiredoxin-1ai and flavohaemoglobin were strongly induced in 713-r. Predicted amino acid substitutions unique to 713-r were identified in thymidine kinase, GL_17150 (D37A) and its paralog DT-diaphorase (Y69H), CMGC and calcium/calmodulin-like kinases**,** serine dehydratase, and a putative transcription factor (GL_31921) among other proteins (summarized in **Supplementary Table 7**).

WB-s vs. WB-r

Despite relatively close agreement in the transcriptional changes observed in 713-r and WB-r detailed above, a number of unique differentially transcribed gene sets were identified in WB-r. tRNA biosynthesis genes and the KEGG N-glycan biosynthesis pathway were up-regulated, whereas a set of genes encoding calcium-binding enzymes were down-regulated, contributed by lower transcription of three calmodulins, calcineurin, five group E annexins (α-giardins), and annexins of group 6 and A2. Further, iron-binding proteins were down-regulated, incorporating four putative lipoxygenases, an Fe-S cluster scaffold, and both PFOR paralogs. The latter finding correlates with the decline in PFOR activity previously reported in WB-r (Townson et al., 1996). In addition, WB-r was the only resistant line in which the oxygen detoxification enzyme NADH oxidase (Brown et al., 1996), was significantly down-regulated. Given the markedly slower growth of WB-r compared to 106-r and 713-r, we investigated the transcripts that were differentially transcribed in 106-r and 713-r, to the exclusion of WB. Up-regulated genes in this group included a sulfatase maturating enzyme, a putative uracil DNA glycolsylase implicated in base excision repair, a ClpB chaperone, and dynein- and kinesin-related proteins. Also up-regulated were fructose bisphosphate aldolase, one of two glyceraldehyde 3-phosphate dehydrogenases (GL_6687), and the previously mentioned putative glutamate synthase (GL_87577). Genes down-regulated in 106-r and 713-r to the exclusion of WB-r included glucosamine 6-phosphate N-acetyltransferase, a MAF1-like RNA-polymerase III repressor, ubiquitin ligase E3A, and a proteasomal regulatory subunit. Further, a highly-transcribed putative tRNA methyltransferase homologue (GL_17245) was only detected in the 106 and 713 isotypes, whereas a number of short hypothetical proteins were exclusively detected in WB lines (**Supplementary Table 3**). Finally, non-synonymous mutations in transcripts encoding glucose-6-phosphate dehydrogenase (**Table 2**), and a truncation in GL_18725, were unique to 106-r and 713-r. No truncations were predicted in the WB-r proteome.

Characterization of Putative NAD(P)H Oxidases

We undertook further structural and transcriptional investigation of differentially transcribed FMN-dependent NAD(P)H oxidoreductases in resistant lines. GL_9719 and GL_17151 were down-regulated in all resistant lines. The predicted structure of GL_9719 is highly similar to the crystal structures of FMN-binding chromate reductases from *Thermus scotoductus* (Opperman et al., 2010) and *Bacillis subtilis* (Kitzing et al., 2005) (**Supplementary Figure 7**). The putative quinone reductase GL_17151 has two paralogs in assemblage A *G. duodenalis*: DT-diaphorase, which is up-regulated in 713-r and WB-r; and GL_17150, which is down-regulated in the same lines. The predicted structures of all three proteins are homologous with the KefF (K^+ efflux regulator) subunit of the *Escherichia coli* KefF/KefC complex (**Figure 5A**; Roosild et al., 2009). In *E. coli*, KefF associates with a NAD-binding KefC subunit via residues that are not conserved in the predicted *G. duodenalis* homologs. Nevertheless, we identified two hypothetical proteins (GL_8468 and GL_10682) with predicted NADP-binding pockets and structural similarity to KefC. Further, GL_8468 was down-regulated in 713-r and WB-r, in similarity to GL_17150 (**Figure 5A**). Interestingly, GL_17150 and GL_17151 are adjacent on chromosome 5, suggesting a gene duplication. Whereas these neighbours share only 43% amino acid sequence identity, GL_17150 is 86% identical to DT-diaphorase, which is encoded at a distant locus. Further, GL_17150 is vastly more highly transcribed than either GL_17151 or DT-diaphorase (∼800 vs. 40 TPM). To probe a possible mechanism of transcriptional regulation for these paralogous genes, we quantified antisense transcription from GL_17150 and GL_17151. Transcripts antisense to GL_17151 were 4-fold more abundant than those antisense to GL_17150, however the presence of a potentially confounding pseudogene antisense to GL_17150 (GL_34649), should caution the interpretation of these results (**Figure 5B**).

Antisense Transcription

We further analysed antisense transcription from 2,268 non-overlapping genes that were detected in all isotypes. A total of 792 antisense transcripts were up-regulated across resistant lines, of which 53 were identified in all lines. Alternatively, 703 down-regulated antisense transcripts were identified across resistant lines (34 in all lines; **Supplementary Tables 13**, **14**). A single antisense transcript encoding a solute transporter (GL_9036) was up-regulated in all lines and corresponded with down-regulation of the coding transcript in the same manner. When the fold change in sense and antisense transcripts from non-overlapping genes in resistant lines was compared, positive correlations were identified for 106-r ($r = 0.104$) and 713-r ($r = 0.155$; **Figure 5C**). This finding corresponds to higher proportions of directionally correlated sense and antisense DTGs in all lines (**Supplementary Table 13**).

Pan-Specific Transcriptional Correlates of Mtz-Resistance

Two-sample comparisons between Mtz-resistant and -susceptible *G. duodenalis* and *T. vaginalis* revealed orthologous heat shock protein-coding genes, peroxidases and dullard-like phosphatases that were exclusively up-regulated in resistant lines in both species (**Supplementary Table 15**; **Supplementary Figure 8**). Two large orthologous groups comprised genes encoding NEK kinase/ankyrin repeat proteins,

TABLE 2 | Predicted effects of non-synonymous SNPs in metronidazole-resistant lines.

Substitution	Accession no.	Description	106-r (aa)	713-r (aa)	WB-r (aa)	PDB chain	TM score	RMSD (Å)	Species
	GL_2834	ARF GAP		**I291V**	**I291V**				
	GL_99228	Cytochrome P450 2E1	T70A		T10I	3e6iA	0.5953	3.46	*Homo sapiens*
	GL_8682	Glucose-6-phosphate 1-dehydrogenase	G638E	T339A					
	GL_101589	High cysteine protein		N168H, N215D, R224Q	Q268K, Q269P, T270K				
	GL_102180	High cysteine protein	**I173V**		**I173V**, I175T				
	GL_103944	Nek kinase		N165S, V171I, I190M	N165S				
	GL_42657	Nek kinase		**R578H**	**R578H**				
	GL_16839	Nek kinase		**N289D**	**N289D**				
	GL_20593	Neuronal acetylcholine receptor subunit α-4		**M58V**	**M58V**	2llyA	0.7027	2.98	*Homo sapiens*
	GL_98178	Neuronal acetylcholine receptor subunit α-7	Q61H		R82H	2mawA	0.744	2.49	*Homo sapiens*
	GL_114625	Proprotein convertase precursor	**S37P, V41A, K188E, N193S, C195R**		**S37P, V41A, K188E, N193S, C195R**				
	GL_8496	Rac/Rho-like protein		**K79N**	**K79N**				
	GL_31921	Tetracycline repressor protein class D		T46M, R55S, **P57S**	**P57S**, S73G, P83Q	2o7oA	0.8263	2.37	*Escherichia coli*
	GL_12108	Threonine dehydratase (LTC)	N12D	D348H	L739P				
	GL_9121	TON 1535		**N54K**	**N54K**	3zpjA	0.8206	2.06	*Thermococcus onnurineus*
	GL_104062	Tyrosyl-tRNA synthetase	D94G	A104V, L108P	F39L	2cycA	0.6109	3.86	*Pyrococcus horikoshii*
	GL_20592	Ubiquitin conjugation factor E4	**D55N**, D56G		**D55N**	2qj0A	0.5448	4.59	*Saccharomyces cerevisiae*
	GL_101496	VSP		**E53K**, S70G, S71N, **V342A**	**E53K, V342A**				
	GL_101765	VSP		E275A, **T435A**, I544T, T560A	**T435A**				
	GL_113093	VSP	A49D, N51K		P62T, S63P				
	GL_113491	VSP	A144T	D60G, **P60T**, **A64S**	**P60T, A64S**				
	GL_137710	VSP	**T410K**, G417E	**E249D, T410K**	**E249D**				
	GL_40571	VSP		**A211S, M216I, I216V, N223T**	**A211S, M216I, I216V, N223T**				
	GL_101074	VSP		N679S	N679S				
	GL_92835	VSP		V43I, V44A	G47D, N48S, A49S, S135T, S136C				

(Continued)

TABLE 2 | Continued

Truncation	Accession no.	Description	106-r (nt)	713-r (nt)	WB-r (nt)	PDB chain	TM score	RMSD (Å)	Species
	GL_8623	Cleavage stimulation factor subunit		C91T		2ooeA	0.8828	2.3	*Mus musculus*
	GL_22677	Nitroreductase-1	C583T						
	GL_5947	Ribosomal protein L35a	A1C						
	GL_9173	Putative S/T protein kinase pkwA		C349T					
	GL_18725	Transcriptional regulator, TetR family	**C269A**	**C269A**		3eupA	0.7651	2.77	*Cytophaga hutchinsonii*
	GL_31366	Type III effector XopAI		C377A		4elnA	0.6173	3.34	*Xanthomonas citri*
	GL_42357	VP1		G1237T		3cnfB	0.8476	2.52	*Bombyx mori cypovirus 1*
	GL_111732	VSP		C111A					

Identical amino acid substitutions and nonsense mutations, are printed in bold. LTC, lateral transfer candidate. aa, amino acid; nt, nucleotide; Putative structures were predicted for hypothetical proteins. Annotations and alignment metrics are derived from the closest empirically determined structural homologues. TM score indicates overall agreement between structures (0–1); RMSD, root mean squared deviation (Å) in central carbon position between structures.

and protein transport-related molecules, that were up- and down-regulated in both species. Down-regulated orthologous groups contained threonine dehydratases, 40S and 60S ribosomal proteins, the putative *G. duodenalis* chromate reductase GL_9719 and a *T. vaginalis* putative etylmaleimide reductase (TVAG_411220), UTP glucose-phosphate metabolizing enzymes; and the previously mentioned putative quinone reductase (GL_17151) and its ortholog TVAG_311580.

DISCUSSION

Drug resistance can prevent the effective treatment of parasitic diseases in humans and animals. For neglected infectious diseases such as giardiasis, the problem of drug resistance is compounded by a limited arsenal of anti-parasitic drugs, and limited data concerning both the epidemiological extent, and biochemical mechanisms, of drug resistance. The present study used RNA sequencing to identify DTGs and gene sets, and SNPs in transcripts in Mtz-resistant *G. duodenalis* lines relative to their susceptible parents. We further increased the value of these analyses by incorporating putative structural and functional information for hypothetical proteins using the I-TASSER software suite. Of course it must be noted that predicted functions are just that, and that the true nature of the many hypothetical proteins in *Giardia* awaits experimental determination. Only two reports to date have investigated transcriptional correlates of Mtz resistance using genome-wide techniques (Müller et al., 2008; Bradic et al., 2016). In this study, in addition to sensitive genetically-controlled analyses of transcriptional changes between Mtz-resistant isotypes of *G. duodenalis*, we compared our results to these independently generated data sets to infer key transcriptional themes in Mtz resistant parasites more broadly. Transcriptional changes in lines 713-r and WB-r were relatively similar, whereas changes in 106-r were qualitatively different and comparatively modest. At the gross cellular level, however, the line WB-r grew more slowly than lines 106-r and 713-r, suggesting a higher cost of resistance. These data indicate that divergent molecular phenotypes can produce similar cellular resistance features, and *vice versa*. We attempted to reconcile the transcriptional and cellular phenotypes of the three resistant lines by analyzing both common transcriptional changes, and those unique to each line. The excellent sequencing depth attained in this study also afforded sensitive investigation of SNPs in transcripts, which can overcome the genetic idiosyncrasies of *G. duodenalis*. Namely, trophozoites contain two transcriptionally active diploid nuclei (Kabnick and Peattie, 1990), and in resistant lines, stable aneuploid states are possible (Chen et al., 1995). However, because the sum of actively transcribed alleles is manifest in the transcriptome, inferring the functional effects of SNPs at this level, should better reflect the proteome of resistant cells.

Functional Inhibition of Pyruvate:Ferredoxin Oxidoreductases

The earliest reports of Mtz-resistant *G. duodenalis* identified changed intracellular redox conditions, and perturbed enzyme

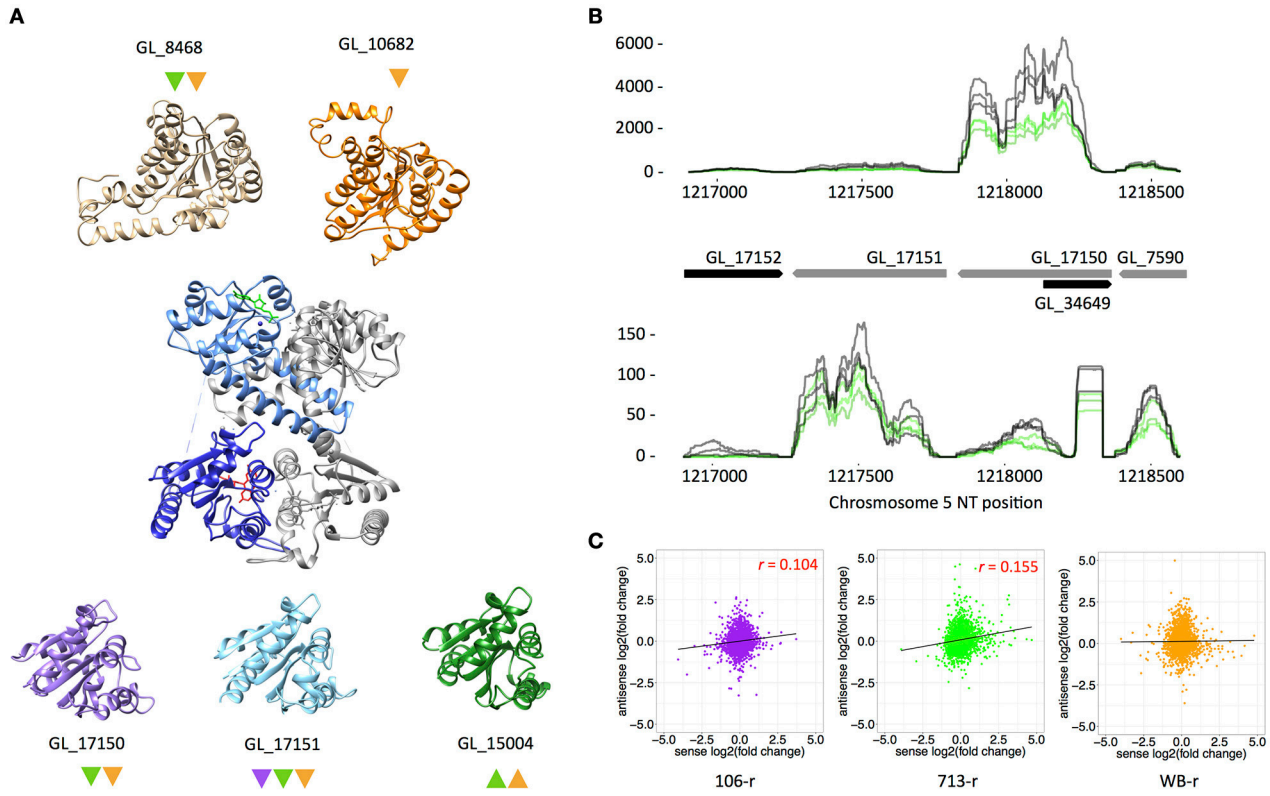


FIGURE 5 | Putative structures for FMN-dependent quinone reductases and transcriptional regulation. (A) Transcripts encoding a quinone-reductase like enzyme (GL_17151) are down-regulated in all resistant lines. Predicted structures for this enzyme and two paralogs are shown at bottom. The three predicted protein stuctures are similar to the crystal structure of KefF (PDB code 3EYW), displayed at centre. Monomers within dimers forming the Kef complex are coloured dark blue (KefF), and light blue (KefC). Two proteins with a KefC-like fold were identified (at top), of which GL_8468 shows a transcriptional profile similar to GL_17150. Differential transcription of genes encoding these proteins is indicated with color-coded up- or down-pointing triangles (purple, 106-r; green, 713-r; orange, WB-r). **(B)** Sense (top panel) and antisense (bottom panel) transcript abundance over a region in chromosome 5 encoding the paralogous putative quinone reductases, GL_17151 and GL_17150. Normalized read depth for three replicates of 713-s (gray lines) and 713-r (green lines) is displayed, and is representative of other lines. Gene models are displayed in black (forward strand) and gray (reverse strand). **(C)** Pearson correlations of $\log_2$(fold change) values for sense (x-axis) and antisense (y-axis) transcripts in metronidazole-resistant lines, relative to susceptible parent lines. Positive correlations for 106-r and 713-r are displayed in red.

activities (Gillin and Reiner, 1982; Smith et al., 1988; Ellis et al., 1993). Recurring themes have since emerged, in particular, the association of ferredoxin family proteins with resistance. PFORs operate at the interface of glycolytic, amino acid, and fatty acid metabolism in *G. duodenalis*, and supply electrons to ferredoxins that activate Mtz. Both PFOR paralogs require a thiamine pyrophosphate (TPP) catalytic co-factor, and can decarboxylate pyruvate and oxaloacetate. PFOR-2 can also catabolize α-ketobutyrate (Townson et al., 1996). Transcriptional suppression of genes that act proximal to PFORs in all lines, may impose functionally analogous limits on PFOR activity, and thus Mtz activation. Firstly, PFOR activity may be impaired by lower transcription of serine and threonine dehydratases, which produce pyruvate and α-ketobutyrate, respectively. Transcriptional suppression of thiamine pyrophosphokinase, identified in 713-r, may similarly inhibit PFOR activity by restricting supply of the TPP cofactor. That threonine dehydratase acquired non-synonymous mutations in all lines, and was consistently suppressed, may reflect the lower energetic value of its product (proprionyl-coA), which is a less preferred substrate of the ATP-forming acetyl-coA synthetase (Sanchez and Müller, 1996). Other transcriptional changes suggest that accumulation of pyruvate, which has antioxidant effects in *G. duodenalis* (Biagini et al., 2001b) may be prioritized in resistant lines. Indeed, the suppression of acetyl-coA acetyltransferase in all resistant lines, lower transcription of histone- and N-terminal acetyltransferases in 713-r, and induction of histone deacetylases in 106-r, are all consistent with acetyl-coA conservation (albeit at the cost of lipid metabolism, protein quality control, and epigenetic regulation). This in turn may promote pyruvate accumulation by inhibiting carbon flux through PFOR. In this context, lower glutamate dehydrogenase transcription in all resistant lines might further bolster the pyruvate pool by limiting its consumption through the "glutamate shunt" (Park et al., 1998; Müller, 2003). Glutamate dehydrogenase suppression would also conserve NADPH, a key source of reducing power for antioxidant enzymes such as TrxR (**Figure 3**).

FMN-Binding Oxidoreductases

Down-regulation of the ferredoxin-nitroreductase chimera, nitroreductase-1, was observed in all three lines investigated here, and is reported in the majority of Mtz-resistant *G. duodenalis* investigated to date (reviewed in Ansell et al., 2015b). Recombinant nitroreductase-1 reduces Mtz when NADH is supplied as an electron donor (Müller et al., 2015). This NADH-dependent mechanism is reminiscent of canonical nitroreductases that reduce Mtz at the NADH-binding site (Koder and Miller, 1998; Martinez-Julvez et al., 2012), and may therefore be catalytically independent of the ferredoxin domain. We contend that the toxicity of nitroreductase-1 in Mtz-exposed *G. duodenalis* could be due to an additional mechanism of drug activation that involves electron transport through the ferredoxin domain, via the FMN cofactor, to the NADH-binding site. Indeed, although *G. duodenalis* is widely claimed to lack a ferredoxin:NADH reductase (FNR), such a function has been theoretically attributed to nitroreductase-1 (Ali and Nozaki, 2007; **Figure 3**). FNR activity in nitroreductase-1 would represent a parsimonious link between pyruvate catabolism and NAD reduction under drug-free conditions (Ellis et al., 1993). By extension, in resistant lines, functional inhibition of PFOR would directly limit nitroreductase activity. The ability of ferredoxin-nitroreductases to accept electrons from PFOR or reduced ferredoxins (as is likely for Fe-hydrogenase; Mulder et al., 2011) and, thereby, to reduce NAD or Mtz, remains to be tested.

Two other putative FMN-dependent oxidoreductases were down-regulated in all resistant lines, indicating potential roles in Mtz activation. The predicted structure of the putative chromate reductase (GL_9719) is similar to that of enzymes with low substrate specificity that reduce xenobiotic electrophilic compounds such as trinitrotolulene (Blehert et al., 1999). The physiological substrates of these enzymes remain elusive, although a chromate reductase in the human gut commensal *Bacilis subtilis*, is induced after exposure to hydrogen peroxide, and proposed to reduce the unsaturated products of peroxidized lipids (oxylipins; Kitzing et al., 2005). In this context, the up-regulation of a putative fatty-acid α-oxidase in all resistant lines is particularly interesting. In plants, tissue damage or chemical insults induce oxidation of the haem co-factor bound in fatty acid α-oxidase (Zhu et al., 2013), which drives the conversion of fatty acids into oxylipins. These modified lipids are potent signaling molecules (Blée, 2002) that drive transcriptional changes (Eckardt, 2008) and are implicated in regulating growth, stage conversion and pathogenicity in numerous parasitic protists (reviewed in Noverr et al., 2003). Taken together, it may be that the down-regulation of chromate reductase in resistant lines both limits Mtz activation, and prolongs oxylipin signaling, which could, in turn, promote growth in resistant lines. To test this hypothesis, oxylipins could be added to drug-susceptible trophozoites prior to Mtz exposure, or resistant lines treated with lipoxygenase inhibitors.

A KefF-like quinone reductase encoded by GL_17151, was also down-regulated in all resistant lines investigated here, and was dynamically suppressed in a previous study after exposure of drug-sensitive trophozoites to Mtz (Ansell et al., 2016). These results strongly support a role for GL_17151 in Mtz activation. Putative structural homologs of NADP-binding KefC subunits were also found in our study. In *E. coli* the Kef system couples cytosolic oxidation with pH regulation, which can minimize oxidative damage to biomolecules (Healy et al., 2014). GL_17151 is a paralog of DT-diaphorase, an enzyme that converts oxygen to hydrogen peroxide (Sánchez et al., 2001; Li and Wang, 2006), which is up-regulated in lines 713-r and WB-r. Interestingly, an orthologous enzyme in *T. vaginalis* with H_2O_2-forming function, termed flavin reductase-1, is down-regulated in Mtz-resistant lines. Loss of this enzyme in *T. vaginalis* is proposed to confer Mtz resistance by promoting futile redox cycling (Leitsch et al., 2014). The most parsimonious explanation for the contrasting regulation of these orthologs *G. duodenalis* and *T. vaginalis* is that DT-diaphorase can detoxify Mtz, whereas the flavin reductase-1 cannot. Indeed, subtle biochemical differences in paralogous enzymes that markedly affect substrate specificity and reaction stoichiometry are well supported; in the ferredoxin nitroreductases of *G. duodenalis* (Müller et al., 2013, 2015), the canonical nitroreductases in *H. pylori* (Olekhnovich et al., 2009; Martinez-Julvez et al., 2012), and the expanded flavin reductase family in *T. vaginalis* (Leitsch et al., 2014). Effective management of functionally divergent paralogs likely requires concerted transcriptional regulation. Further to this, we found an inverse abundance of sense and antisense transcripts arising from the paralogous chromosomal neighbours GL_17150 and GL_17151, consistent with antisense interference. The role of antisense transcripts could be further probed via episomal overexpression of the pseudogene antisense to GL_17150 (**Figure 5B**), which is replicated antisense to DT-diaphorase. Transcriptional down-regulation of genes orthologous to GL_9719 and GL_17151 in Mtz-resistant *T. vaginalis*, and the established link between Mtz-resistant *H. pylori* and mutations in nitroreductase-coding genes (Sisson et al., 2002; Olekhnovich et al., 2009; Martinez-Julvez et al., 2012), demonstrate the centrality of FMN-dependent enzymes to Mtz metabolism and resistance across pathogenic species. Detailed investigation of the localization, interacting partners, substrate specificity, and reaction kinetics of these enzymes is now clearly warranted.

Cysteine-Rich Membrane Proteins

Expression of certain VSPs, the major surface antigens in *G. duodenalis*, is associated with the development of drug resistance (Chen et al., 1995; Müller et al., 2007a, 2008). These cysteine-rich molecules are proposed to protect *G. duodenalis* from environmental stresses such as stomach peptidases, and are constitutively turned over, possibly to evade the host immune system (Nash, 2002). The prominent transcription of 10 VSPs in all resistant lines, suggests positive selection from a more varied VSP population in susceptible trophozoites (**Supplementary Figure 5**). Whereas these dominant genes seem likely to confer a selective advantage in the presence of Mtz, in our investigations their functional significance has remained elusive. Specifically, we found little difference in the cysteine content and motif number between highly-transcribed VSPs in resistant and susceptible lines, and cysteine substitutions were not highly prevalent. It is possible that resistance-associated VSPs play a role that predominates antioxidant activity, for

example, in maximizing the stability and integrity of degraded plasma membranes (Touz et al., 2005). In contrast, the high proportion of CxxC motifs in the consistently up-regulated HCMP GL_11309, supports an important function in protecting membranes from oxidative damage in the presence of Mtz. Functional considerations aside, this molecule and the highly transcribed VSPs in resistant lines, could yet be explored in clinical isolates as potential biomarkers of resistance.

Isotype-Specific Resistance Mechanisms

The transcriptional changes discussed thus far are common to all three Mtz-resistant lines, and are therefore most likely to account for increased Mtz tolerance. However, it is clear in this study and others, that cellular phenotypes such as growth rate and infectivity diverge between resistant lines (Tejman-Yarden et al., 2011). Those that remain infectious may be more clinically relevant, and thus concerning, than non-infectious resistant lines. The divergent transcriptomes of 106-r and 713-r belie similar growth rates, although only 106-r can establish experimental infections (Tejman-Yarden et al., 2011). Alternatively, despite the transcriptional similarities between 713-r and WB-r, the latter line grows more slowly. Investigating the transcriptional features that are unique to each line can shed some light on the molecular bases of these different cellular phenotypes, and on transcriptional changes that may augment drug resistance.

106-r remains infective, grows relatively well and exhibits the fewest DTGs, which together suggest a highly efficient resistance phenotype. The non-sense mutation in 29% of transcripts encoding nitroreductase-1, could functionally ablate a substantial proportion of the nitroreductase-1 enzyme pool (assuming for simplicity equimolar transcript and protein concentrations), and may thus contribute to the increased Mtz tolerance of 106-r. This finding constitutes the first report of a functional mutation in a known Mtz-activating gene in *G. duodenalis*, which, combined with transcriptional suppression of the same enzyme, should substantially decrease nitroreductase-1 function in 106-r. In addition, 106-r is the only line in which the NAD scavenging pathway and the putative Mtz-detoxification enzyme, nitroreductase-2, are up-regulated. If these changes preference the flow of glycolytic electrons to nitroreductase-2, (either indirectly via NADH, or directly via the ferredoxin electron transport chain as proposed above), then 106-r may essentially use Mtz as a terminal electron acceptor in glycolysis. Such an adaptation would allow sustained PFOR activity and possibly ATP generation via acetyl-CoA, whilst negating the detrimental effects of the activated drug. Continued ATP generation might in turn decrease reliance on other sources of ATP, such as the arginine dihydrolase pathway, which is transcriptionally suppressed.

Increased NAD scavenging in 106-r might also support heightened activity of NAD-dependent Sir2 deacetylases, which are redox-responsive histone modification enzymes (Fulco et al., 2003). By contrast, transcriptional suppression of a Sir2-coding gene (GL_16569) was found in WB-r, and is previously reported in WB-C4 (Müller et al., 2008), a line whose transcriptional profile correlates negatively with 106-r but positively with 713-r and WB-r. It would be interesting to test whether chemical or genetic perturbation of Sir2 enzymes could recapitulate aspects of these divergent molecular resistance phenotypes. Further, 106-r is the only line in which a set of V-type ATPases and a MATE-like transporter are up-regulated. Like other protists, *G. duodenalis* may utilize V-type ATPases at the plasma membrane to regulate cytosolic pH (Biagini et al., 2001a). Increased transcription of dynein and kinesin-related proteins in 106-r is consistent with the recycling of such ATPases via microtubule-dependent transport of ATPase-rich vesicles, evidenced in higher eukaryotes (Breton and Brown, 2013). Active proton efflux, coupled to a sodium:proton exchanger (up-regulated in 106-r and WB-r; Biagini et al., 2001a), may decrease the cytosolic sodium concentration sufficiently to drive Mtz efflux via the MATE transporter, which is a sodium-coupled multidrug efflux pump (Du et al., 2015). Indeed, although MATE transporters are generally associated with extruding cationic compounds, the possibility of Mtz efflux through these channels is supported by experiments in *H. pylori* demonstrating increased Mtz sensitivity MATE-knockout lines (van Amsterdam et al., 2005; **Figure 4**).

The transcriptome of 713-r is similar to WB-r, despite a marked difference in growth rate. This may derive from active and passive resistance mechanisms that appear unique to 713-r. In addition to lower transcription of nitroreductase-1, a physiological role for NTR-1 in Mtz activation is supported by lower transcription of the encoding gene in this line. Similarly, marked transcriptional suppression of the putative nitroreductase GL_8377, and GL_17150, provides further evidence that several hitherto understudied FMN-binding enzymes may contribute to Mtz activation. Down-regulation of nitroreductase-2 in 713-r may, however, preclude the energetic efficiencies postulated to occur in 106-r. Induction of iron hydrogenase might compensate for lower nitroreductase-2 abundance, and sustain some PFOR activity by directing the flow of electrons to form hydrogen (Lloyd et al., 2002; **Figure 3**). Further, the marked transcriptional induction of flavohaemoglobin, might represent an alternative Mtz detoxification enzyme. Flavohaemoglobin homologs in bacteria are shown to bind to imidazole drugs (Helmick et al., 2005); and a homolog of this enzyme in the intestinal parasitic protist *Blastocystis hominis*, is postulated to contribute to Mtz resistance (Wu et al., 2014)—findings that warrant further testing of the ability of the *G. duodenalis* flavohaemoglobin to detoxify Mtz.

Despite evidence supporting passive Mtz evasion and active detoxification mechanisms in 713-r, other transcriptional features suggest that this line is under greater oxidative stress than 106-r. Up-regulation of components of the thioredoxin system including TrxR, protein disulfide isomerases-2 and -4 (previously reported in WB-C4; Müller et al., 2008), and peroxiredoxin-1ai, indicate reliance on an antioxidant system that collaterally activates Mtz. It is conceivable that Mtz-induced damage necessitates greater thioredoxin activity, creating a positive feedback loop that constitutes an indirect and metabolically burdensome Mtz detoxification system. Although we did not observe increased transcription of NADPH-forming enzymes that might assist thioredoxin reductase activity in 713-r, the functional significance of the T339A substitution predicted in glucose-6-phosphate dehydrogenase,

which catalyzes the first step in the NADPH-forming pentose-phosphate pathway, requires further investigation. Lastly in 713-r, up-regulation of protein chaperones suggests that the thioredoxin system alone is insufficient to manage Mtz-induced damage. Induction of peptidyl-prolyl isomerases, HSPs-90 and TCP-1 chaperonins, may help to maintain the structure and function of damaged proteins, although suppression of proteasomal subunits does not support concomitant recycling of highly degraded proteins. Increased activity of ATP-dependent chaperones may be serviced by induction of glycolytic genes in 713-r, especially the ATP-forming phosphoglycerate kinase. Induction of orthologous peroxidredoxins and ATP-dependent HSPs70 and 90 in Mtz-resistant *G. duodenalis* and *T. vaginalis*, may constitute universal active resistance mechanisms that complement passive down-regulation of FMN-dependent enzymes.

The transcriptional changes unique to, and uniquely lacking in WB-r may account for its slower growth. Lower transcription of iron-binding enzymes including ferredoxin-3, both PFOR paralogs, putative lipoxygenases and a Fe-S cluster scaffold protein, is intriguing given that a key oxygen detoxification enzyme, NADH oxidase (Brown et al., 1996), is down-regulated solely in WB-r. We previously reported transcriptomic results suggesting heightened oxidative stress in WB-s trophozoites at log and stationary phases of *in vitro* culture, when PFOR transcription is comparatively low (Ansell et al., 2015a). As the function of Fe-S-binding enzymes such as PFORs is sensitive to dissolved oxygen (Dan et al., 2000), together these findings suggest that WB-r may endure increased intracellular oxygen, consistent with reliance on futile redox cycling. In this context, concerted induction of genes encoding multiple tRNA biosynthesis enzymes, ribosomal proteins and translation initiation factors, may reflect heightened demand for protein synthesis in WB-r, possibly to replace oxidized proteins. Further, as outlined above, lipoxygenases initiate oxylipin signaling pathways in eukaryotes, and oxylipins, such as prostaglandins are implicated in sustaining the growth and development of other protists (Noverr et al., 2003). If the heightened oxidative stress postulated within WB-r is not compatible with sustained expression of iron-dependent lipoxygenases, then a scarcity of oxylipins may compound the observed growth defect. This phenotype may also relate to insufficient induction of important genes in WB-r, relative to the other resistant lines. For example, inorganic sulfate is liberated from sulfate esters by sulfatases, which require sulfatase maturating enzymes to become catalytically active (Bojarová and Williams, 2008). Although a sulfatase-like enzyme is up-regulated in all lines, the Fe-S-dependent maturating enzyme is only up-regulated in 106-r and 713-r. If sulfur metabolism is less efficient in WB-r as a result, then non-protein antioxidant activity could also be impaired (Brown et al., 1998). More broadly, transcripts that were exclusively detected in 106 and 713 isotypes, such as a highly transcribed putative tRNA methyltransferase which may modulate translation efficiency; or those which were only detected the WB isotype, may also contribute to the phenotypic differences between resistant lines. Future work to detail the genetic differences between these isotypes, and between the resistant and susceptible lines therein, will be necessary to differentiate those transcriptional differences based in genetic architecture, from those based purely in dynamic transcriptional regulation. Although the infectivity of WB-r has not been tested, we expect that this line would lack infectivity due to both the similarity between its transcriptional phenotype and that of the non-infective 713-r, and its retarded growth.

CONCLUDING REMARKS

The Mtz-resistant lines 106-r, 713-r, and WB-r are among the best-characterized *G. duodenalis* lines, as subjects of biochemical and genetic research over the past 30 years. The present study combined deep sequencing with protein structure prediction to profile the transcriptional foundations of the biochemical and cellular phenotypes of these seminal lines. Previously, we contended that the handful of enzymes known to metabolize Mtz, need to be considered in the context of the vast metabolic networks which support their function. We now identify networks of carbon flux, thiol cycling, and NAD synthesis, among others, which are differentially regulated in Mtz-resistant *G. duodenalis*, and propose important roles for under-studied enzymes. Passive resistance mechanisms that are common among the three resistant lines include transcriptional down-regulation of nitroreductase-1, and of enzymes that are likely to support PFOR activity. Functionally analogous changes in different resistant lines that conserve free acetyl-coA and thus pyruvate, might suppress PFOR activity and bolster pyruvate-dependent antioxidant activity. Down-regulation of hitherto under-studied FMN-binding enzymes, including putative quinone and chromate reductases as well as canonical nitroreductases, may constitute novel passive resistance mechanisms, which are emulated in *T. vaginalis*. The transcription of these enzymes appears tightly regulated, possibly via antisense interference, which may relate to subtle biochemical differences between paralogues that exert opposing effects on Mtz toxicity. Convergence among highly transcribed VSPs in resistant lines is consistent with a selective advantage in the presence of Mtz, which transcends global cysteine content or motif number. Cysteine sparging capacity may, however, be under selection in high cysteine membrane proteins.

Molecular changes are of particular interest in 106-r, as this line remains infectious. Up-regulation of nitroreductase-2, together with a nonsense mutation in nitroreductase-1, and induction of a putative MATE-like drug efflux system, together suggest a highly metabolically efficient resistance phenotype. Incidentally, the strength of correlation between transcriptional changes in trophozoites in lines 106-r, and in WB-s after exposure to sub-lethal Mtz, further highlights the potential clinical relevance of laboratory models for investigating drug response and resistance. It appears that 713-r and WB-r are more reliant on active management of Mtz- and oxygen-induced damage, respectively. The former is consistent with collateral activation of Mtz via the thioredoxin

system; the latter with Mtz inactivation through passive futile cycling. Increased glycolysis may be necessary to sustain these energetically expensive strategies, and failure to up-regulate genes encoding glycolytic or sulfur cycling enzymes, might account for the sluggish growth of WB-r. Future work to correlate transcript and protein abundances in these resistant lines should assess the contribution of post-transcriptional regulation to Mtz resistance, and reveal the functional penetrance of the amino acid mutations predicted here. Pursuing these avenues would do much to establish *G. duodenalis* as the defining model for understanding, and ultimately for preventing, Mtz resistance in microaerophilic eukaryotic pathogens.

AUTHOR CONTRIBUTIONS

BA, LB, and AJ designed experiments. BA and LB generated experimental samples. BA, SS, and AJ analyzed data. BA, SE, MM, RG, SS, and AJ wrote the manuscript.

FUNDING

This work, including the efforts of AJ and MM, was funded by Australian Research Council (ARC) (LP120200122). BA, LB, SE, and AJ are supported by the Victorian State Government Operational Infrastructure Support and Australian Government National Health and Medical Research Council Independent Research Institute Infrastructure Support Scheme. BA is supported by an Australian Postgraduate Award (Australian Government) and the Victorian Life Sciences Computation Initiative (Victoria, Australia). RNA sequencing was partially funded by YourGene Biosciences (Taiwan). The funders had no role in study design, data collection and interpretation, or the decision to submit the work for publication.

SUPPLEMENTARY MATERIAL

The Supplementary Material for this article can be found online at: http://journal.frontiersin.org/article/10.3389/fmicb.2017.00398/full#supplementary-material

Supplementary Table 1 | Sense and antisense read mapping statistics for metronidazole resistant (-R) and susceptible (-S) lines.

Supplementary Table 2 | TMM-normalized counts per million counts (CPM) values for all replicates.

Supplementary Table 3 | Coding transcripts detected in resistant and susceptible trophozoites from one or two isotypes.

Supplementary Table 4 | Transcriptional abundance, fold-change, and functional annotations for genes detected in all resistant and susceptible *Giardia* trophozoite lines.

Supplementary Table 5 | Transcriptional abundance, fold-change, and functional annotations for 156 consistently up- or down-regulated genes.

Supplementary Table 6 | Transcriptional abundance and functional annotations for the 30 most strongly up- and down-regulated genes in each resistant line, excluding variant-specific surface proteins (VSPs).

Supplementary Table 7 | Synonymous and non-synonymous single nucleotide polymorphisms (SNPs) and predicted peptide modifications in resistant lines, relative to susceptible parent lines of the same genotype.

Supplementary Table 8 | Comparative transcription and single nucleotide polymorphism (SNP) statistics for transcripts encoding variant-specific surface proteins (VSPs). Transcripts among the top decile (20) of highly transcribed VSPs in susceptible and resistant lines are identified. Clade and cysteine content information is adapted from Adam et al. (2010) doi: 10.1186/1471-2164-11-424.

Supplementary Table 9 | Curated gene sets specific to *Giardia duodenalis* and used in rotational gene enrichment testing.

Supplementary Table 10 | KEGG terms enriched among differentially transcribed genes in resistant- relative to susceptible trophozoite lines, with comparative transcriptional statistics for contributing genes.

Supplementary Table 11 | Gene Ontology (GO) Molecular Function terms enriched among differentially transcribed genes in resistant- relative to susceptible trophozoite lines, with comparative transcriptional statistics for contributing genes.

Supplementary Table 12 | Gene Ontology (GO) Biological Process terms enriched among differentially transcribed genes in resistant- relative to susceptible trophozoite lines, with comparative transcriptional statistics for contributing genes.

Supplementary Table 13 | Comparative transcription statistics for non-overlapping, non-deprecated antisense transcripts, with differential transcription statistics for the corresponding sense transcripts.

Supplementary Table 14 | Comparative transcription statistics for non-overlapping, non-deprecated antisense transcripts that are differentially transcribed in the same direction in all resistant lines.

Supplementary Table 15 | Orthologous differentially transcribed genes metronidazole-resistant *Giardia duodenalis* and *Trichomonas vaginalis*.

Supplementary Figure 1 | Saturating RNA sequencing depth. Total and novel transcript detection as a function of read depth for reads mapping in the sense orientation to accepted gene models. Different colors represent biological replicates.

Supplementary Figure 2 | Transcriptome clustering for metronidazole-resistant and -susceptible lines. (A) Primary principal co-ordinate clustering based on biological coefficient of variance (BCV) for resistant and susceptible lines. Susceptible lines are represented in in soft colors, and shaded. **(B)** Unsupervised clustering of z-scaled transcript abundance values (by row) for biological triplicates (columns). Resistant and susceptible lines cluster separately. **(C)** Mean Pearson correlation coefficients (*r*) for resistant and susceptible transcriptomes with (top), and without 200 variant-specific surface protein (VSP)-coding genes (bottom).

Supplementary Figure 3 | Single nucleotide polymorphisms and predicted amino acid substitutions. Thirty-nine non-synonymous SNPs were identified in in coding transcripts in 106-r, and 211 and 70 such SNPs were identified in 713-r and WB-r respectively, which may relate to preliminary UV mutagenesis of the latter lines. Non-synonymous SNPs were predicted to bias the proteomes of resistant lines toward alanine, cysteine and glutamine residues, and to decrease the proportion of asparagine. **(A)** Net changes in amino acid prevalence in metronidazole-resistant lines relative to susceptible parents (at left; WB-r: red; 106-r: green; 713-r: blue), and each amino acid as a proportion of all substituted amino acids in each resistant line (right). **(B)** Mapped synonymous and non-synonymous SNPs as a proportion of all nucleotides mapped at the relevant locus, when a lower threshold of 20% prevalence for the alternative allele is applied. Partial prevalence is evident for most SNPs.

Supplementary Figure 4 | Highly transcribed variant-specific surface protein-coding genes (*vsps*) in metronidazole-susceptible and -resistant *Giardia duodenalis*. (A) Overlap in the 20 most highly transcribed *vsp*s in susceptible (left) and resistant (right) lines. Ten *vsps* that are highly transcribed in all three resistant lines are marked with an asterisk in panel **(B)**. **(B)** Unsupervised

clusters formed by 32 *vsp*s that are among the top 20 most highly transcribed *vsp*s in at least one susceptible, or resistant line. Colors represent TPM values, z-scaled by row.

Supplementary Figure 5 | Transcriptional changes in genes encoding high-cysteine membrane proteins in metronidazole-resistant lines. Log_2(fold change) values are represented as colors. GL50803_11309 is the only HCMP-coding gene that is significantly up-regulated in all three lines.

Supplementary Figure 6 | Nonsense mutation in transcripts encoding nitroreductase-1 (GL50803_22677) in 106-r. Screen capture from Integrative Genomics Viewer. Triplicate tracks are shown for 106-r (top) and 106-s (bottom). Aligned reads are displayed in mauve. A single nucleotide polymorphism (C538T; red) is visible in the top tracks.

Supplementary Figure 7 | Predicted protein structure for the putative chromate reductase (GL50803_9719). The putative GL50803_9719 structure, at left, is similar to the Old Yellow Enzyme from *Thermus scotoductus* (at centre; RMSD = 1.06 Å; PDB code 3hf3; Opperman et al., 2010) and the chromate reductase from *Bacillis subtilis* (at right; RMSD = 1.32 Å; PDB code 1z48; Kitzing et al., 2005). The FMN cofactor and structural sulfate in the crystal structures, are displayed in red.

Supplementary Figure 8 | Change in transcription of orthologous genes in Mtz-resistant *Giardia duodenalis* and *Trichomonas vaginalis*. Two-sample comparisons of transcription in Mtz-resistant and –susceptible *G. duodenalis* (circles) and *T. vaginalis* (triangles) revealed differentially transcribed orthologs from eighteen different groups (key, right), with genes of interest annotated. For clarity, the orthologous group OG5_126566, which contains four *G. duodenalis* proteins and 41 *T. vaginalis* ankyrin repeat-like proteins, is omitted from the chart. Full gene descriptions for each group are provided in **Supplementary Table 15**. CPM, counts per million counts; FC, fold change; HSP, heat shock protein; UDP, uridine diphosphate.

REFERENCES

Adagu, I. S., Nolder, D., Warhurst, D. C., and Rossignol, J.-F. (2001). *In vitro* activity of nitazoxanide and related compounds against isolates of *Giardia intestinalis*, *Entamoeba histolytica* and *Trichomonas vaginalis*. *J. Antimicrob. Chemother.* 49, 103–111. doi: 10.1093/jac/49.1.103

Adam, R. D., Nigam, A., Seshadri, V., Martens, C. A., Farneth, G. A., Morrison, H. G., et al. (2010). The *Giardia lamblia* vsp gene repertoire: characteristics, genomic organization, and evolution. *BMC Genomics* 11:424. doi: 10.1186/1471-2164-11-424

Ali, V., and Nozaki, T. (2007). Current therapeutics, their problems, and sulfur-containing-amino-acid metabolism as a novel target against infections by "amitochondriate" protozoan parasites. *Clin. Microbiol. Rev.* 20, 164–187. doi: 10.1128/CMR.00019-06

Ansell, B. R. E., McConville, M. J., Baker, L., Korhonen, P. K., Emery, S. J., Svärd, S. G., et al. (2016). Divergent transcriptional responses to physiological and xenobiotic stress in *Giardia duodenalis*. *Antimicrob. Agents Chemother.* 60, AAC.00977–00916. doi: 10.1128/AAC.00977-16

Ansell, B. R. E., McConville, M. J., Baker, L., Korhonen, P. K., Young, N. D., Hall, R. S., et al. (2015a). Time-dependent transcriptional changes in axenic *Giardia duodenalis* trophozoites. *PLoS Negl. Trop. Dis.* 9:e0004261. doi: 10.1371/journal.pntd.0004261.s013

Ansell, B. R. E., McConville, M. J., Ma'ayeh, S. Y., Dagley, M. J., Gasser, R. B., Svärd, S. G., et al. (2015b). Drug resistance in *Giardia duodenalis*. *Biotech. Adv.* 33, 888–901. doi: 10.1016/j.biotechadv.2015.04.009

Bereswill, S., Krainick, C., Stähler, F., Herrmann, L., and Kist, M. (2003). Analysis of the rdxA gene in high-level metronidazole-resistant clinical isolates confirms a limited use of rdxA mutations as a marker for prediction of metronidazole resistance in *Helicobacter pylori*. *FEMS Immunol. Med. Microbiol.* 36, 193–198. doi: 10.1016/S0928-8244(03)00031-2

Biagini, G. A., Knodler, L. A., Saliba, K. J., Kirk, K., and Edwards, M. R. (2001a). Na(+)-dependent pH regulation by the amitochondriate protozoan parasite *Giardia intestinalis*. *J. Biol. Chem.* 276, 29157–29162. doi: 10.1074/jbc.M102728200

Biagini, G. A., Park, J. H., Lloyd, D., and Edwards, M. R. (2001b). The antioxidant potential of pyruvate in the amitochondriate diplomonads *Giardia intestinalis* and *Hexamita inflata*. *Microbiology* 147, 3359–3365. doi: 10.1099/00221287-147-12-3359

Binh, T. T., Suzuki, R., Trang, T. T. H., Kwon, D. H., and Yamaoka, Y. (2015). Search for novel candidate mutations for metronidazole resistance in *Helicobacter pylori* using next-generation sequencing. *Antimicrob. Agents Chemother.* 59, 2343–2348. doi: 10.1128/AAC.04852-14

Blée, E. (2002). Impact of phyto-oxylipins in plant defense. *Trends Plant Sci.* 7, 315–322. doi: 10.1016/S1360-1385(02)02290-2

Blehert, D. S., Fox, B. G., and Chambliss, G. H. (1999). Cloning and sequence analysis of two *pseudomonas* flavoprotein xenobiotic reductases. *J. Bacteriol.* 181, 2564–6263.

Bojarová, P., and Williams, S. J. (2008). Sulfotransferases, sulfatases and formylglycine-generating enzymes: a sulfation fascination. *Curr. Opp. Chem. Biol.* 12, 573–581. doi: 10.1016/j.cbpa.2008.06.018

Boreham, P. F. L., Phillips, R. E., and Shepherd, R. W. (1988). Altered uptake of metronidazole *in vitro* by stocks of *Giardia intestinalis* with different drug sensitivities. *Trans. R. Soc. Trop. Med. Hyg.* 82, 104–106. doi: 10.1016/0035-9203(88)90278-7

Boreham, P. F., Phillips, R. E., and Shepherd, R. W. (1984). The sensitivity of *Giardia intestinalis* to drugs *in vitro*. *J. Antimicrob. Chemother.* 14, 449–461. doi: 10.1093/jac/14.5.449

Bradic, M., Warring, S. D., Tooley, G. E., Scheid, P., Secor, W. E., Land, K. M., et al. (2016). Genetic indicators of drug resistance in the highly repetitive genomes of *Trichomonas vaginalis* and other trichomonads. *BiorXiv*. 1, 4–24. doi: 10.1101/076729

Breton, S., and Brown, D. (2013). Regulation of luminal acidification by the v-ATPase. *Physiology* 28, 318–329. doi: 10.1152/physiol.00007.2013

Brown, D. M., Upcroft, J. A., Edwards, M. R., and Upcroft, P. (1998). Anaerobic bacterial metabolism in the ancient eukaryote *Giardia duodenalis*. *Int. J. Parasitol.* 28, 149–164. doi: 10.1016/S0020-7519(97)00172-0

Brown, D. M., Upcroft, J. A., and Upcroft, P. (1996). A h2o-producing NADH oxidase from the protozoan parasite *Giardia duodenalis*. *Eur. J. Biochem.* 241, 155–161. doi: 10.1111/j.1432-1033.1996.0155t.x

Capon, A. G., Upcroft, J. A., Boreham, P. F., Cottis, L. E., and Bundesen, P. G. (1989). Similarities of *Giardia* antigens derived from human and animal sources. *Int. J. Parasitol.* 19, 91–98.

Chen, F. (2006). OrthoMCL-db: querying a comprehensive multi-species collection of ortholog groups. *Nucleic Acids Res.* 34, D363–D368. doi: 10.1093/nar/gkj123

Chen, N., Upcroft, J. A., and Upcroft, P. (1995). A *Giardia duodenalis* gene encoding a protein with multiple repeats of a toxin homologue. *Parasitology* 111(Pt 4), 423–431. doi: 10.1017/S0031182000065926

Cudmore, S. L., Delgaty, K. L., Hayward-McClelland, S. F., Petrin, D. P., and Garber, G. E. (2004). Treatment of infections caused by metronidazole-resistant *Trichomonas vaginalis*. *Clin. Microbiol. Rev.* 17, 783–793. doi: 10.1128/CMR.17.4.783-793.2004

Dan, M., Wang, A. L., and Wang, C. C. (2000). Inhibition of pyruvate-ferredoxin oxidoreductase gene expression in *Giardia lamblia* by a virus-mediated hammerhead ribozyme. *Mol. Microbiol.* 36, 447–456. doi: 10.1046/j.1365-2958.2000.01863.x

Davids, B. J., and Gillin, F. D. (2011). "Methods for *Giardia* culture, cryopreservation, encystation, and excystation *in vitro*," in *Giardia: a model organism*, eds S. G. Svärd and H. D. Lujan (Vienna: Springer), 381–394.

Davids, B. J., Reiner, D. S., Birkeland, S. R., Preheim, S. P., Cipriano, M. J., McArthur, A. G., et al. (2006). A new family of *Giardial* cysteine-rich non-VSP protein genes and a novel cyst protein. *PLoS ONE* 1:e44. doi: 10.1371/journal.pone.0000044.s003

Du, D., van Veen, H. W., Murakami, S., Pos, K. M., and Luisi, B. F. (2015). Structure, mechanism and cooperation of bacterial multidrug

transporters. *Curr. Opp. Struct. Biol.* 33, 76–91. doi: 10.1016/j.sbi.2015.07.015

Eckardt, N. A. (2008). Oxylipin signaling in plant stress responses. *Plant Cell* 20, 495–497. doi: 10.1105/tpc.108.059485

Edwards, D. I. (1993). Nitroimidazole drugs–action and resistance mechanisms. I. Mechanisms of action. *J. Antimicrob. Chemother.* 31, 9–20. doi: 10.1093/jac/31.1.9

Ellis, J. E., Wingfield, J. M., Cole, D., Boreham, P. F., and Lloyd, D. (1993). Oxygen affinities of metronidazole-resistant and-sensitive stocks of *Giardia intestinalis*. *Int. J. Parasitol.* 23, 35–39. doi: 10.1016/0020-7519(93)90095-G

Fulco, M., Schiltz, R. L., Iezzi, S., King, M. T., Zhao, P., Kashiwaya, Y., et al. (2003). Sir2 regulates skeletal muscle differentiation as a potential sensor of the redox state. *Mol. Cell* 12, 51–62. doi: 10.1016/S1097-2765(03)00226-0

García-Alcalde, F., Okonechnikov, K., Carbonell, J., Cruz, L. M., Götz, S., Tarazona, S., et al. (2012). Qualimap: evaluating next-generation sequencing alignment data. *Bioinformatics* 28, 2678–2679. doi: 10.1093/bioinformatics/bts503

Gillin, F. D., and Reiner, D. S. (1982). Effects of oxygen tension and reducing agents on sensitivity of *Giardia lamblia* to metronidazole *in vitro*. *Biochem. Pharmacol.* 31, 3694–3697. doi: 10.1016/0006-2952(82)90600-1

Healy, J., Ekkerman, S., Pliotas, C., Richard, M., Bartlett, W., Grayer, S. C., et al. (2014). Understanding the structural requirements for activators of the Kef bacterial potassium efflux system. *Biochemistry* 53, 1982–1992. doi: 10.1021/bi5001118

Helmick, R. A., Fletcher, A. E., Gardner, A. M., Gessner, C. R., Hvitved, A. N., Gustin, M. C., et al. (2005). Imidazole antibiotics inhibit the nitric oxide dioxygenase function of microbial flavohemoglobin. *Antimicrob. Agents Chemother.* 49, 1837–1843. doi: 10.1128/AAC.49.5.1837-1843.2005

Kabnick, K. S., and Peattie, D. A. (1990). *In situ* analyses reveal that the two nuclei of *Giardia lamblia* are equivalent. *J. Cell Sci.* 95(Pt 3), 353–360.

Kitzing, K., Fitzpatrick, T. B., Wilken, C., Sawa, J., Bourenkov, G. P., Macheroux, P., et al. (2005). The 1.3 A Crystal Structure of the flavoprotein YqjM reveals a novel class of old yellow enzymes. *J. Biol. Chem.* 280, 27904–27913. doi: 10.1074/jbc.M502587200

Koder, R. L., and Miller, A. F. (1998). Steady-state kinetic mechanism, stereospecificity, substrate and inhibitor specificity of *Enterobacter cloacae* nitroreductase. *Biochim. Biophys. Acta* 1387, 395–405. doi: 10.1016/S0167-4838(98)00151-4

Lane, S., and Lloyd, D. (2002). Current trends in research into the waterborne parasite *Giardia*. *Crit. Rev. Microbiol.* 28, 123–147. doi: 10.1080/1040-840291046713

Leitsch, D., Burgess, A. G., Dunn, L. A., Krauer, K. G., Tan, K., Duchene, M., et al. (2011). Pyruvate:ferredoxin oxidoreductase and thioredoxin reductase are involved in 5-nitroimidazole activation while flavin metabolism is linked to 5-nitroimidazole resistance in *Giardia lamblia*. *J. Antimicrob. Chemother.* 66, 1756–1765. doi: 10.1093/jac/dkr192

Leitsch, D., Janssen, B. D., Kolarich, D., Johnson, P. J., and Duchene, M. (2014). *Trichomonas vaginalis* flavin reductase 1 and its role in metronidazole resistance. *Mol. Microbiol.* 91, 198–208. doi: 10.1111/mmi.12455

Leitsch, D., Müller, J., and Müller, N. (2016). Evaluation of *Giardia lamblia* thioredoxin reductase as drug activating enzyme and as drug target. *Int. J. Parasitol. Drugs Drug Res.* 6, 148–153. doi: 10.1016/j.ijpddr.2016.07.003

Lemée, V., Zaharia, I., Nevez, G., Rabodonirina, M., Brasseur, P., Ballet, J. J., et al. (2000). Metronidazole and albendazole susceptibility of 11 clinical isolates of *Giardia duodenalis* from France. *J. Antimicrob. Chemother.* 46, 819–821. doi: 10.1093/jac/46.5.819

Li, B., and Dewey, C. N. (2011). RSEM: accurate transcript quantification from RNA-seq data with or without a reference. *BMC Bioinformatics* 12:323. doi: 10.1186/1471-2105-12-323

Li, H., Handsaker, B., Wysoker, A., Fennell, T., Ruan, J., Homer, N., et al. (2009). The sequence alignment/map format and SAMtools. *Bioinformatics* 25, 2078–2079. doi: 10.1093/bioinformatics/btp352

Li, L., and Wang, C. C. (2006). A likely molecular basis of the susceptibility of *Giardia lamblia* towards oxygen. *Mol. Microbiol.* 59, 202–211. doi: 10.1111/j.1365-2958.2005.04896.x

Liu, S. M., Brown, D. M., O'Donoghue, P., Upcroft, P., and Upcroft, J. A. (2000). Ferredoxin involvement in metronidazole resistance of *Giardia duodenalis*. *Mol. Biochem. Parasitol.* 108, 137–140. doi: 10.1016/S0166-6851(00)00194-8

Lloyd, D., Ralphs, J. R., and Harris, J. C. (2002). *Giardia intestinalis*, a eukaryote without hydrogenosomes, produces hydrogen. *Microbiology* 148, 727–733. doi: 10.1099/00221287-148-3-727

Löfmark, S., Edlund, C., and Nord, C. E. (2010). Metronidazole is still the drug of choice for treatment of anaerobic infections. *Clin. Infect. Dis.* 50, S16–S23. doi: 10.1086/647939

Lohse, M., Bolger, A. M., Nagel, A., Fernie, A. R., Lunn, J. E., Stitt, M., et al. (2012). Robina: a user-friendly, integrated software solution for RNA-seq-based transcriptomics. *Nucleic Acids Res.* 40, W622–W627. doi: 10.1093/nar/gks540

Martinez-Julvez, M., Rojas, A. L., Olekhnovich, I., Angarica, V. E., Hoffman, P. S., and Sancho, J. (2012). Structure of RdxA - an oxygen-insensitive nitroreductase essential for metronidazole activation in *Helicobacter pylori*. *FEBS J.* 279, 4306–4317. doi: 10.1111/febs.12020

Mirzaei, N., Poursina, F., Moghim, S., Rahimi, E., and Safaei, H. G. (2014). The mutation of the rdxA gene in metronidazole-resistant *Helicobacter pylori* clinical isolates. *Adv. Biomed. Res.* 3:90. doi: 10.4103/2277-9175.128469

Morrison, H. G., McArthur, A. G., Gillin, F. D., Aley, S. B., Adam, R. D., Olsen, G. J., et al. (2007). Genomic minimalism in the early diverging intestinal parasite *Giardia lamblia*. *Science* 317, 1921–1926. doi: 10.1126/science.1143837

Mulder, D. W., Shepard, E. M., Meuser, J. E., Joshi, N., King, P. W., Posewitz, M. C., et al. (2011). Insights into [FeFe]-hydrogenase structure, mechanism, and maturation. *Structure* 19, 1038–1052. doi: 10.1016/j.str.2011.06.008

Müller, J., Ley, S., Felger, I., Hemphill, A., and Müller, N. (2008). Identification of differentially expressed genes in a *Giardia lamblia* WB C6 clone resistant to nitazoxanide and metronidazole. *J. Antimicrob. Chemother.* 62, 72–82. doi: 10.1093/jac/dkn142

Müller, J., Rout, S., Leitsch, D., Vaithilingam, J., Hehl, A., and Müller, N. (2015). Comparative characterisation of two nitroreductases from *Giardia lamblia* as potential activators of nitro compounds. *Int. J. Parasitol. Drugs Drug Resist.* 5, 37–43. doi: 10.1016/j.ijpddr.2015.03.001

Müller, J., Schildknecht, P., and Müller, N. (2013). Metabolism of nitro drugs metronidazole and nitazoxanide in *Giardia lamblia*: characterization of a novel nitroreductase (GlNR2). *J. Antimicrob. Chemother.* 68, 1781–1789. doi: 10.1093/jac/dkt106

Müller, J., Sterk, M., Hemphill, A., and Müller, N. (2007a). Characterization of *Giardia lamblia* WB C6 clones resistant to nitazoxanide and to metronidazole. *J. Antimicrob. Chemother.* 60, 280–287. doi: 10.1093/jac/dkm205

Müller, J., Wastling, J., Sanderson, S., Müller, N., and Hemphill, A. (2007b). A novel *Giardia lamblia* nitroreductase, GlNR1, interacts with nitazoxanide and other thiazolides. *Antimicrob. Agents Chemother.* 51, 1979–1986. doi: 10.1128/AAC.01548-06

Müller, M. (2003). "Energy metabolism. Part I: anaerobic protozoa," in *Molecular Medical Parasitology,* eds J. J. Marr, T. W. Nilsen, and R. Komuniecki (London: Academic Press), 125–139.

Nash, T. E. (2002). Surface antigenic variation in *Giardia lamblia*. *Mol. Microbiol.* 45, 585–590. doi: 10.1046/j.1365-2958.2002.03029.x

Nillius, D., Müller, J., and Müller, N. (2011). Nitroreductase (GlNR1) increases susceptibility of *Giardia lamblia* and *Escherichia coli* to nitro drugs. *J. Antimicrob. Chemother.* 66, 1029–1035. doi: 10.1093/jac/dkr029

Nixon, J. E. J., Wang, A., Field, J., Morrison, H. G., McArthur, A. G., Sogin, M. L., et al. (2002). Evidence for lateral transfer of genes encoding ferredoxins, nitroreductases, NADH oxidase, and alcohol dehydrogenase 3 from anaerobic prokaryotes to *Giardia lamblia* and *Entamoeba histolytica*. *Euk. Cell* 1, 181–190. doi: 10.1128/EC.1.2.181-190.2002

Noverr, M. C., Erb-Downward, J. R., and Huffnagle, G. B. (2003). Production of eicosanoids and other oxylipins by pathogenic eukaryotic microbes. *Clin. Microbiol. Rev.* 16, 517–533. doi: 10.1128/CMR.16.3.517-533.2003

Olekhnovich, I. N., Goodwin, A., and Hoffman, P. S. (2009). Characterization of the NAD(P)H oxidase and metronidazole reductase activities of the RdxA nitroreductase of *Helicobacter pylori*. *FEBS J.* 276, 3354–3364. doi: 10.1111/j.1742-4658.2009.07060.x

Opperman, D. J., Sewell, B. T., Litthauer, D., Isupov, M. N., Littlechild, J. A., and van Heerden, E. (2010). Structure of a thermostable old yellow enzyme

from *Thermus scotoductus* SA-01. *Biochem. Biophys. Res. Comm.* 393, 426–431. doi: 10.1016/j.bbrc.2010.02.011

Pal, D., Banerjee, S., Cui, J., Schwartz, A., Ghosh, S. K., and Samuelson, J. (2009). *Giardia, Entamoeba,* and *Trichomonas* enzymes activate metronidazole (nitroreductases) and inactivate metronidazole (nitroimidazole reductases). *Antimicrob. Agents Chemother.* 53, 458–464. doi: 10.1128/AAC.00909-08

Park, J.-H., Schofield, P. J., and Edwards, M. R. (1998). *Giardia intestinalis*: characterization of a NADP-dependent glutamate dehydrogenase. *Exp. Parasitol.* 88, 131–138. doi: 10.1006/expr.1998.4199

Petri, W. A. (2003). Therapy of intestinal protozoa. *Trends Parasitol.* 19, 523–526. doi: 10.1016/j.pt.2003.09.003

Pettersen, E. F., Goddard, T. D., Huang, C. C., Couch, G. S., Greenblatt, D. M., Meng, E. C., et al. (2004). UCSF Chimera a visualization system for exploratory research and analysis. *J. Comput. Chem.* 25, 1605–1612. doi: 10.1002/jcc.20084

Rice, P., Longden, I., and Bleasby, A. (2000). EMBOSS: the European molecular biology open software suite. *Trends Genet.* 16, 276–277. doi: 10.1016/S0168-9525(00)02024-2

Robinson, J. T., Thorvaldsdóttir, H., Winckler, W., Guttman, M., Lander, E. S., Getz, G., et al. (2011). Integrative genomics viewer. *Nat. Biotech.* 29, 24–26. doi: 10.1038/nbt0111-24

Robinson, M. D., McCarthy, D. J., and Smyth, G. K. (2009). EdgeR: a bioconductor package for differential expression analysis of digital gene expression data. *Bioinformatics* 26, 139–140. doi: 10.1093/bioinformatics/btp616

Roosild, T. P., Castronovo, S., Miller, S., Li, C., Rasmussen, T., Bartlett, W., et al. (2009). KTN (RCK) domains regulate K^+ channels and transporters by controlling the dimer-hinge conformation. *Structure* 17, 893–903. doi: 10.1016/j.str.2009.03.018

Samuelson, J. (1999). Why metronidazole is active against both bacteria and parasites. *Antimicrob. Agents Chemother.* 43, 1533–1541.

Sánchez, L. B., Elmendorf, H., Nash, T. E., and Müller, M. (2001). NAD(P)H:menadione oxidoreductase of the amitochondriate eukaryote *Giardia lamblia*: a simpler homologue of the vertebrate enzyme. *Microbiology* 147, 561–570. doi: 10.1099/00221287-147-3-561

Sanchez, L. B., and Müller, M. (1996). Purification and characterization of the acetate forming enzyme, acetyl-coA synthetase (ADP-forming) from the amitochondriate protist, *Giardia lamblia*. *FEBS Lett.* 378, 240–244. doi: 10.1016/0014-5793(95)01463-2

Schofield, P. J., Edwards, M. R., Matthews, J., and Wilson, J. R. (1992). The pathway of arginine catabolism in *Giardia intestinalis*. *Mol. Biochem. Parasitol.* 51, 29–36. doi: 10.1016/0166-6851(92)90197-R

Sisson, G., Goodwin, A., Raudonikiene, A., Hughes, N. J., Mukhopadhyay, A. K., Berg, D. E., et al. (2002). Enzymes associated with reductive activation and action of nitazoxanide, nitrofurans, and metronidazole in *Helicobacter pylori*. *Antimicrob. Agents Chemother.* 46, 2116–2123. doi: 10.1128/AAC.46.7.2116-2123.2002

Smith, N. C., Bryant, C., and Boreham, P. F. (1988). Possible roles for pyruvate:ferredoxin oxidoreductase and thiol-dependent peroxidase and reductase activities in resistance to nitroheterocyclic drugs in *Giardia intestinalis*. *Int. J. Parasitol.* 18, 991–997. doi: 10.1016/0020-7519(88)90183-X

Tejman-Yarden, N., Millman, M., Lauwaet, T., Davids, B. J., Gillin, F. D., Dunn, L., et al. (2011). Impaired parasite attachment as fitness cost of metronidazole resistance in *Giardia lamblia*. *Antimicrob. Agents Chemother.* 55, 4643–4651. doi: 10.1128/AAC.00384-11

Testa, F., Mastronicola, D., Cabelli, D. E., Bordi, E., Pucillo, L. P., Sarti, P., et al. (2011). The superoxide reductase from the early diverging eukaryote *Giardia intestinalis*. *Free Radic. Biol. Med.* 51, 1567–1574. doi: 10.1016/j.freeradbiomed.2011.07.017

Touz, M. C., Conrad, J. T., and Nash, T. E. (2005). A novel palmitoyl acyl transferase controls surface protein palmitoylation and cytotoxicity in *Giardia lamblia*. *Mol. Microbiol.* 58, 999–1011. doi: 10.1111/j.1365-2958.2005.04891.x

Townson, S. M., Boreham, P. F., Upcroft, P., and Upcroft, J. A. (1994). Resistance to the nitroheterocyclic drugs. *Acta Trop.* 56, 173–194. doi: 10.1016/0001-706X(94)90062-0

Townson, S. M., Laqua, H., Upcroft, P., Boreham, P. F., and Upcroft, J. A. (1992). Induction of metronidazole and furazolidone resistance in *Giardia*. *Trans. R. Soc. Trop. Med. Hyg.* 86, 521–522. doi: 10.1016/0035-9203(92)90095-T

Townson, S. M., Upcroft, J. A., and Upcroft, P. (1996). Characterisation and purification of pyruvate: ferredoxin oxidoreductase from *Giardia duodenalis*. *Mol. Biochem. Parasitol.* 79, 183–193. doi: 10.1016/0166-6851(96)02661-8

Upcroft, J. A., Healey, A., Murray, D. G., Boreham, P. F., and Upcroft, P. (1992). A gene associated with cell division and drug resistance in *Giardia duodenalis*. *Parasitology* 104(Pt 3), 397–405. doi: 10.1017/S0031182000063642

Upcroft, J. A., Krauer, K. G., and Upcroft, P. (2010). Chromosome sequence maps of the *Giardia lamblia* assemblage A isolate WB. *Trends Parasitol.* 26, 484–491. doi: 10.1016/j.pt.2010.07.002

Upcroft, P., and Upcroft, J. A. (1999). Organization and structure of the *Giardia genome*. *Protist* 150, 17–23. doi: 10.1016/S1434-4610(99)70005-2

van Amsterdam, K., Bart, A., and van der Ende, A. (2005). A *Helicobacter pylori* TolC efflux pump confers resistance to metronidazole. *Antimicrob. Agents Chemother.* 49, 1477–1482. doi: 10.1128/AAC.49.4.1477-1482.2005

Vicente, J.-J., and Cande, W. Z. (2014). Mad2, Bub3 and Mps1 regulate chromosome segregation and mitotic synchrony in *Giardia intestinalis*, a binucleate protist lacking an anaphase promoting complex. *Mol. Biol. Cell.* doi: 10.1091/mbc.E14-05-0975

Wang, L., Wang, S., and Li, W. (2012). RSeQC: quality control of RNA-seq experiments. *Bioinformatics* 28, 2184–2185. doi: 10.1093/bioinformatics/bts356

Wu, D., Lim, E., Vaillant, F., Asselin-Labat, M. L., Visvader, J. E., and Smyth, G. K. (2010). ROAST: rotation gene set tests for complex microarray experiments. *Bioinformatics* 26, 2176–2182. doi: 10.1093/bioinformatics/btq401

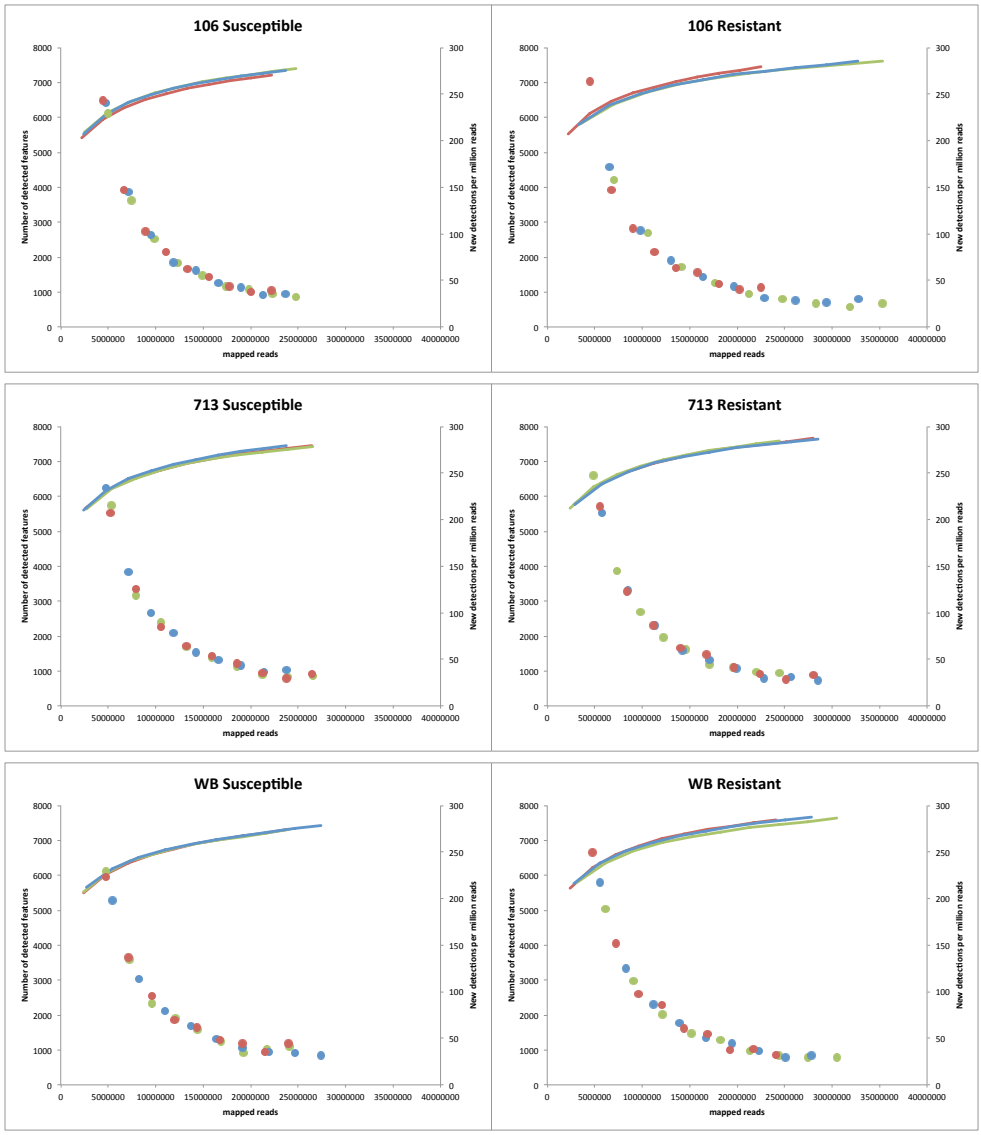
Wu, Z., Mirza, H., and Tan, K. S. W. (2014). Intra-subtype variation in enteroadhesion accounts for differences in epithelial barrier disruption and is associated with metronidazole resistance in Blastocystis subtype-7. *PLoS Negl. Trop. Dis.* 8:e2885. doi: 10.1371/journal.pntd.0002885.s005

Zhang, Y., and Skolnick, J. (2005). TM-align: a protein structure alignment algorithm based on the tm-score. *Nucleic Acids Res.* 33, 2302–2309. doi: 10.1093/nar/gki524

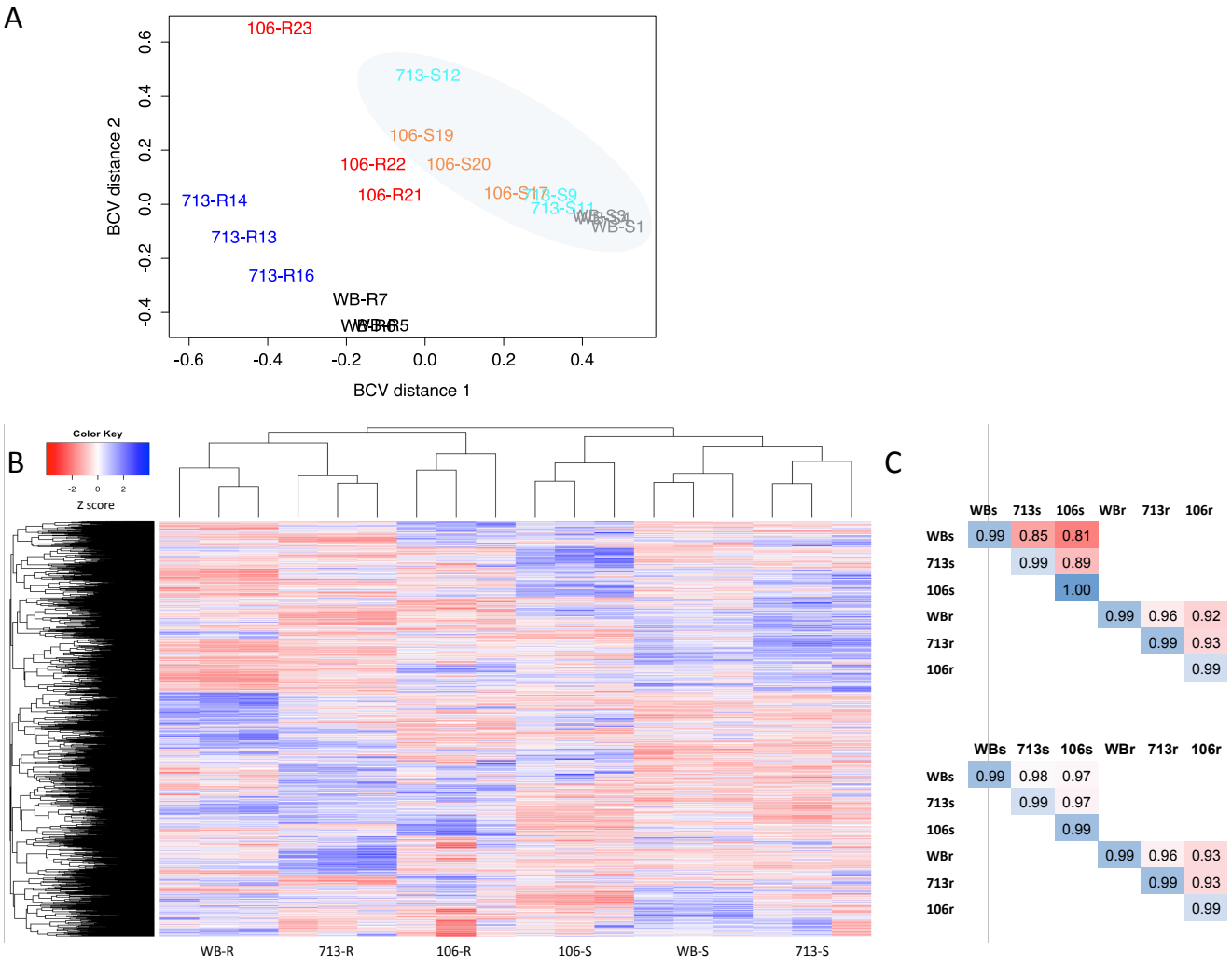
Zhu, G., Koszelak-Rosenblum, M., and Malkowski, M. G. (2013). Crystal structures of α-dioxygenase from *Oryza sativa*: insights into substrate binding and activation by hydrogen peroxide. *Protein Sci.* 22, 1432–1438. doi: 10.1002/pro.2327

Conflict of Interest Statement: The authors declare that the research was conducted in the absence of any commercial or financial relationships that could be construed as a potential conflict of interest.

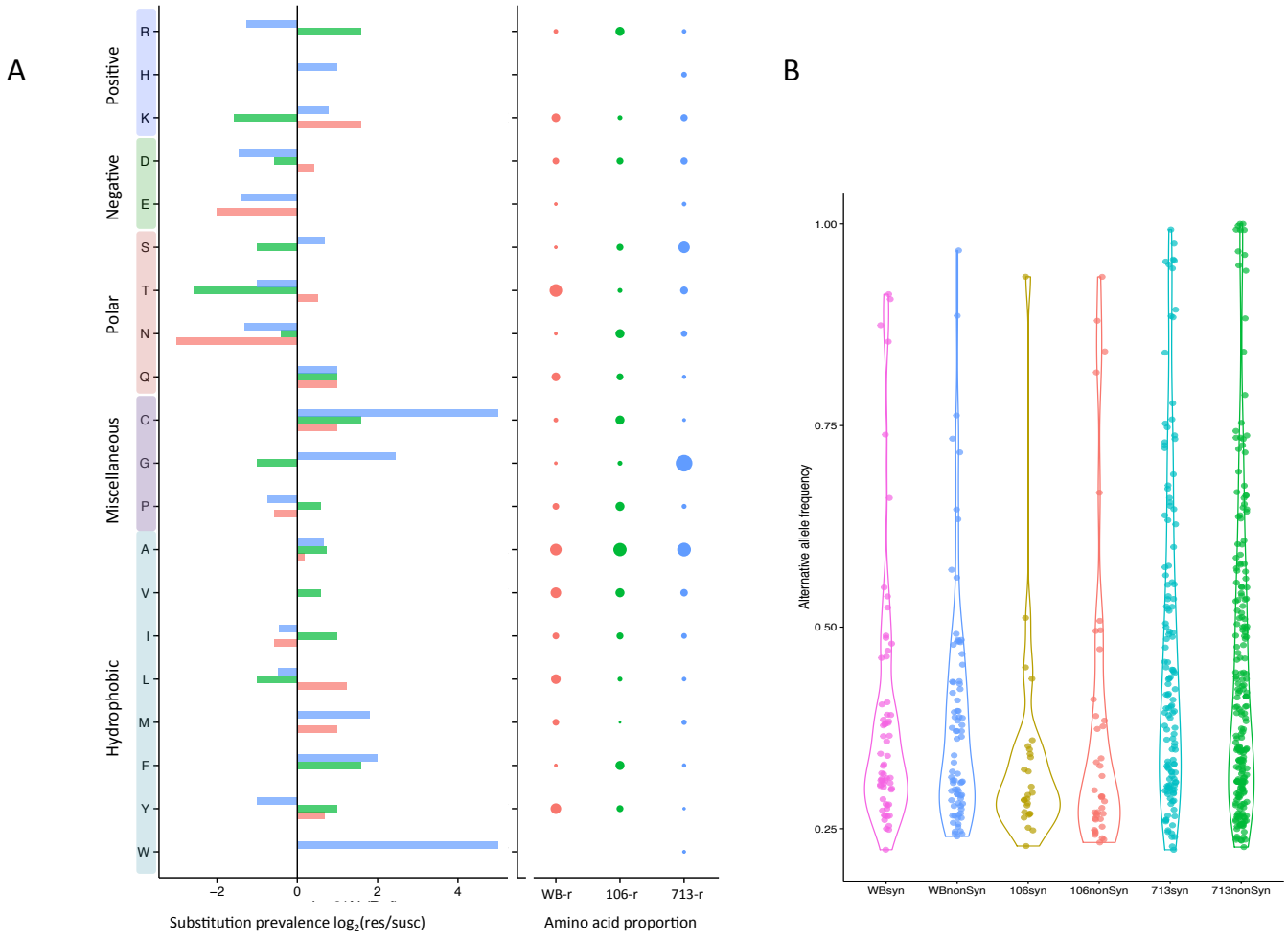
Copyright © 2017 Ansell, Baker, Emery, McConville, Svärd, Gasser and Jex. This is an open-access article distributed under the terms of the Creative Commons Attribution License (CC BY). The use, distribution or reproduction in other forums is permitted, provided the original author(s) or licensor are credited and that the original publication in this journal is cited, in accordance with accepted academic practice. No use, distribution or reproduction is permitted which does not comply with these terms.



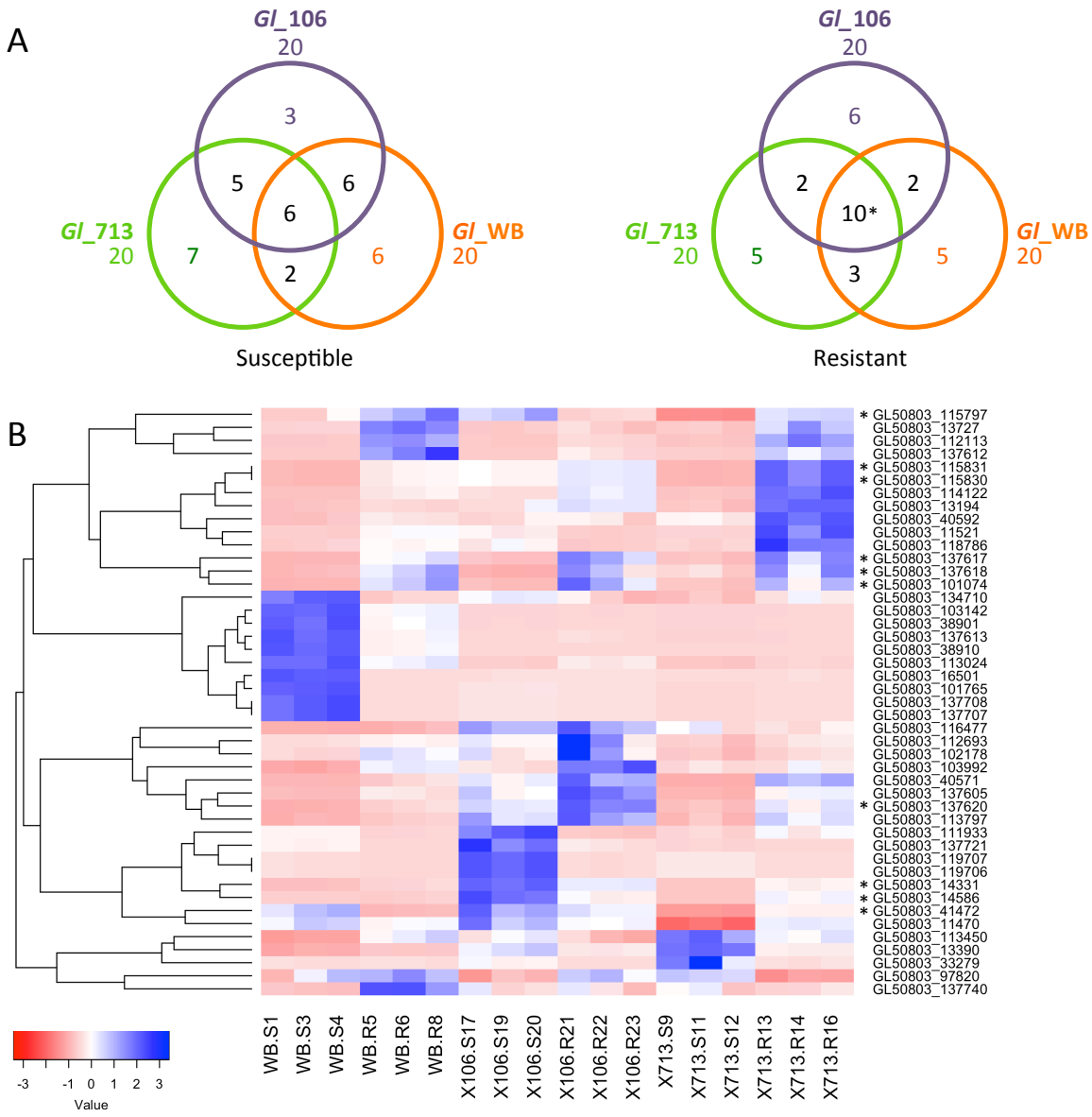
Supplementary Figure 1. Saturating RNA sequencing depth. Total and novel transcript detection as a function of read depth for reads mapping in the sense orientation to accepted gene models. Different colors represent biological replicates.



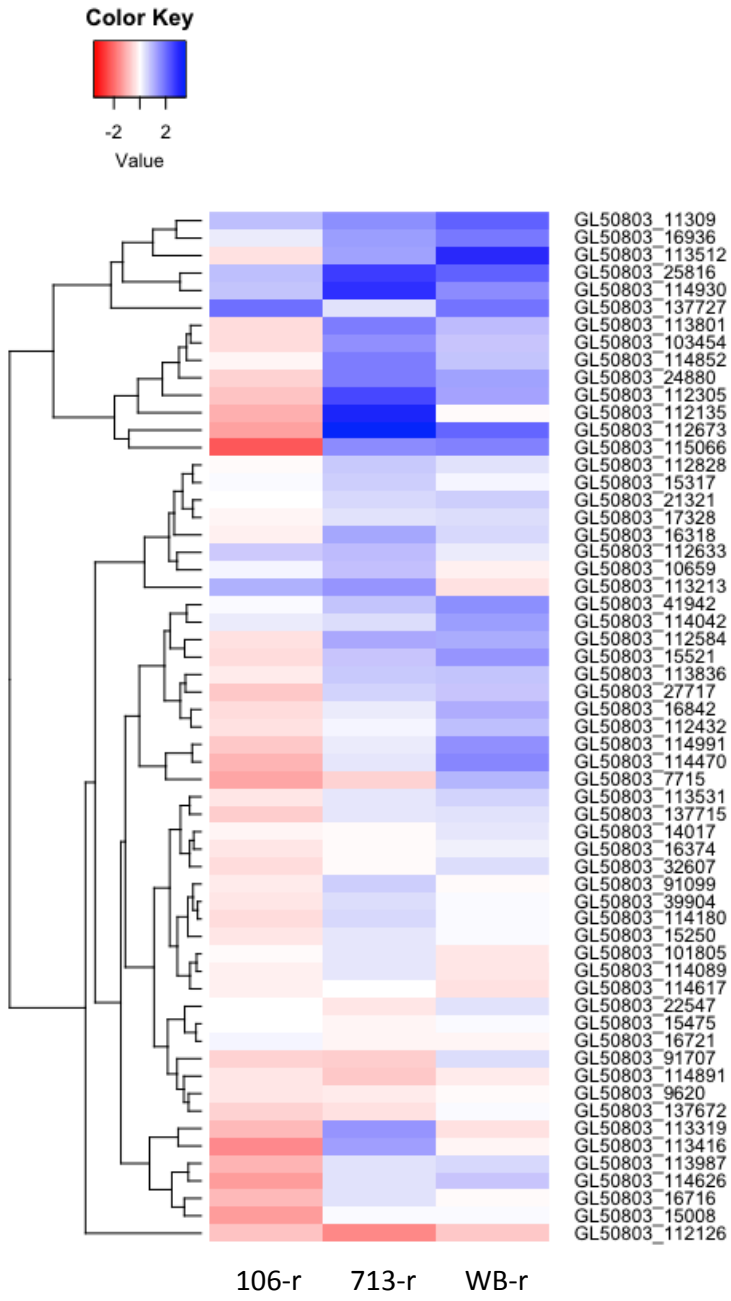
Supplementary Figure 2. Transcriptome clustering for metronidazole-resistant and -susceptible lines. A) Primary principal co-ordinate clustering based on biological coefficient of variance (BCV) for resistant and susceptible lines. Resistant lines are represented in in soft colors, and shaded. B) Unsupervised clustering of z-scaled transcript abundance values (by row) for biological triplicates (columns). Resistant and susceptible lines cluster separately. C. Mean Pearson correlation scores (*r*) for resistant and susceptible transcriptomes with (top), and without 200 variant-specific surface protein (VSP)-coding genes (bottom).



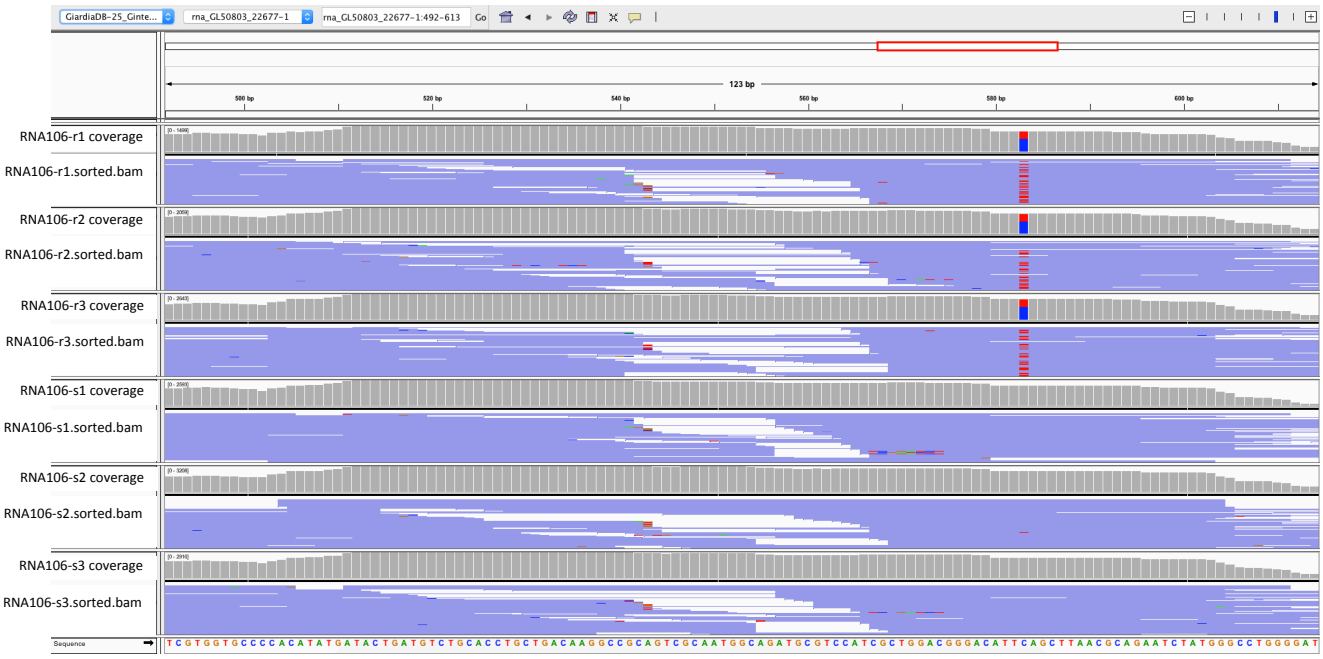
Supplementary Figure 3. Single nucleotide polymorphisms and predicted amino acid substitutions. Thirty-nine non-synonymous SNPs were identified in in coding transcripts in 106-r, and 211 and 70 such SNPs were identified in 713-r and WB-r respectively, which may relate to preliminary UV mutagenesis of the latter lines. Non-synonymous SNPs were predicted to bias the proteomes of resistant lines towards alanine, cysteine and glutamine residues, and to decrease the proportion of asparagine. A) Net changes in amino acid prevalence in metronidazole-resistant lines relative to susceptible parents (at left; WB-r: red; 106-r: green; 713-r: blue), and each amino acid as a proportion of all substituted amino acids in each resistant line (right). B) Mapped synonymous and non-synonymous SNPs as a proportion of all nucleotides mapped at the relevant locus, when a lower threshold of 20% prevalence for the alternative allele is applied. Partial prevalence is evident for most SNPs.



Supplementary Figure 4. Highly transcribed variant-specific surface protein-coding genes (*vsps*) in metronidazole-susceptible and -resistant *G. duodenalis*. A) Overlap in the 20 most highly transcribed *vsps* in susceptible (left) and resistant (right) lines. Ten *vsps* that are highly transcribed in all three resistant lines are marked with an asterisk in panel B. B) Unsupervised clusters formed by 32 *vsps* that are among the top 20 most highly transcribed *vsps* in at least one susceptible, or resistant line. Colors represent TPM values, z-scaled by row.



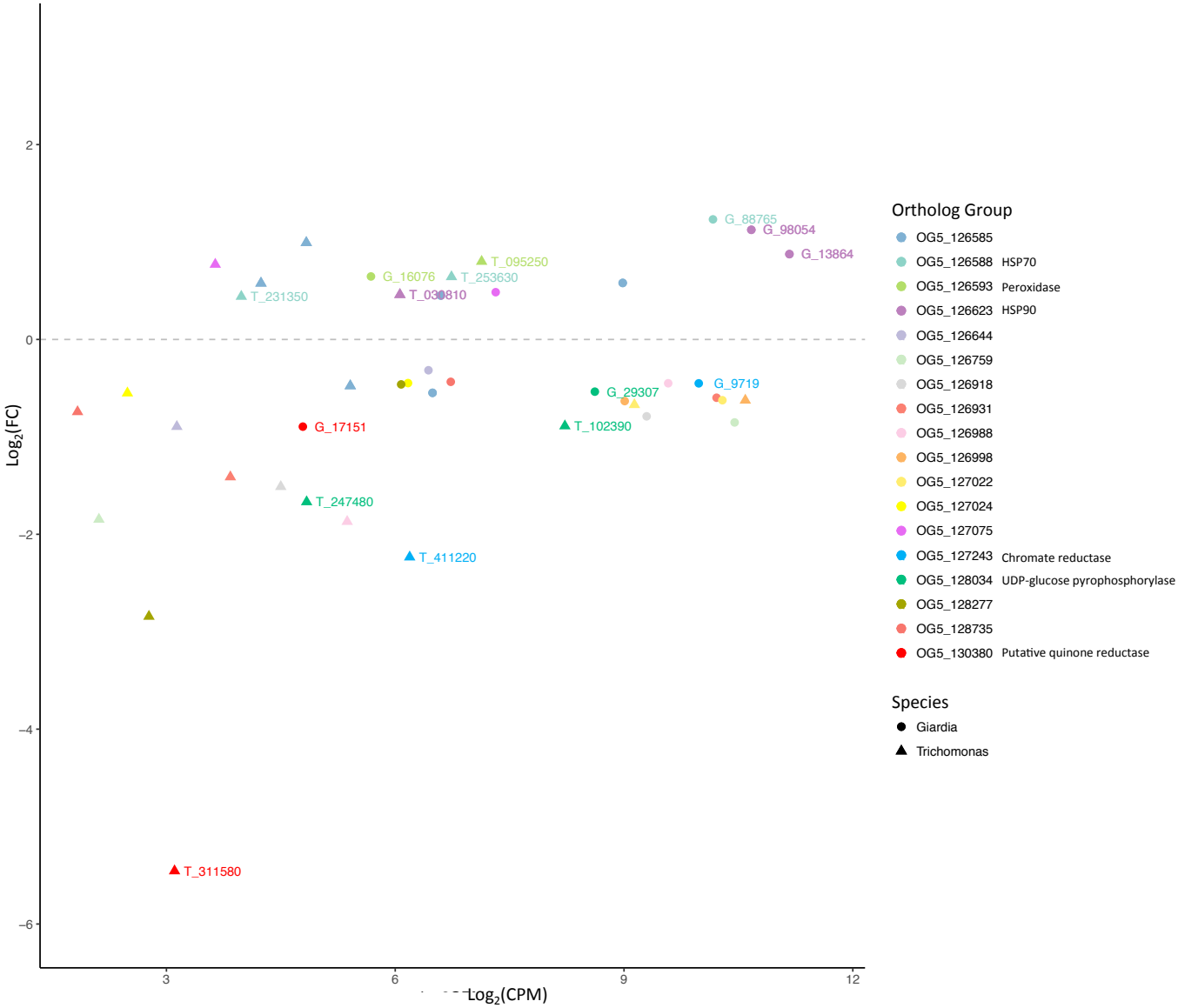
Supplementary Figure 5. Change in genes encoding high-cysteine membrane proteins in metronidazole-resistant lines. Log_2(fold change) values are represented as colors. GL50803_11309 is the only HCMP-coding gene that is significantly up-regulated in all three lines.



Supplementary Figure 6. Nonsense mutation in nitroreductase-1 coding transcripts arising from GL50803_22677 in 106-r. Screen capture from Integrative Genomics Viewer. Triplicate tracks are shown for 106-r (top) and 106-s (bottom). Aligned reads are displayed in mauve. A single nucleotide polymorphism (C538T; red) is visible in the top tracks.



Supplementary Figure 7. Predicted protein structure for the putative chromate reductase (GL50803_9719). The putative GL50803_9719 structure, at left, is similar to the Old Yellow Enzyme from *Thermus scotoductus* (at centre; RMSD=1.06 Å; PDB code 3hf3; Opperman et al., 2010) and the chromate reductase from *Bacillis subtilis* (at right; RMSD=1.32 Å; PDB code 1z48; Kitzing 2005). The FMN cofactor and structural sulfate in the crystal structures, are displayed in red.



Supplementary Figure 8. Change in transcription of orthologous genes in Mtz-resistant *Giardia duodenalis* and *Trichomonas vaginalis*. Two-sample comparisons of transcription in Mtz-resistant and –susceptible *G. duodenalis* (circles) and *T. vaginalis* (triangles) revealed differentially transcribed orthologs from eighteen different groups (key, right), with genes of interest annotated. For clarity, the orthologous group OG5_126566, which contains four *G. duodenalis* proteins and 41 *T. vaginalis* ankyrin repeat-like proteins, is omitted from the chart. Full gene descriptions for each group are provided in Supplementary Table 15. CPM: counts per million counts; FC: fold change; HSP: heat shock protein; UDP: uridine diphosphate.

Chapter 8. General discussion

This chapter includes some text and ideas published in Brendan R. E. Ansell, Malcolm J. McConville, Showgy Y. Ma'ayeh, Michael J. Dagley, Robin B. Gasser, Staffan G. Svärd, Aaron R. Jex. Drug resistance in *Giardia duodenalis*. *Biotechnology Advances* 2015;33:888-901.
See preface for author contributions, and Appendix I for full text.

Giardia duodenalis is an ancient eukaryote and parasitic protist that causes diarrhoeal disease in hundreds of millions of people each year. Metronidazole (Mtz) is one of only two major anti-giardial drugs, however the mechanism of action of Mtz, and mechanisms of response and resistance in *G. duodenalis* are incompletely understood. Elucidating these mechanisms is particularly important because metronidazole is an essential drug for treating multiple protozoan and bacterial pathogens that feature microaerobic metabolism (Löfmark et al., 2010). Further, clinical resistance to Mtz is documented in patients infected with *G. duodenalis* (detailed in Chapter 1), and *Trichomonas vaginalis* (Cudmore et al., 2004) and *Helicobacter pylori* (Samuelson, 1999). Wide-spread resistance to the drug in any of these pathogens would thus have devastating effects on global health.

Several studies, reviewed in Chapter 1, have suggested that Mtz resistance in *G. duodenalis* may be largely based in the dynamic suppression of so-called 'suicide enzymes' that activate the drug. Such enzymes include thioredoxin reductase, and ferredoxin family enzymes including nitroreductase-1. Previous work in this area used enzymology or microarray technology to investigate aspects of molecular resistance phenotypes, and produced conflicting results in some cases. Therefore in this thesis I aimed to investigate the full extent of transcriptional changes in response to Mtz, and in fully Mtz-resistant lines, using high-resolution whole-transcriptome sequencing. I also sought to characterize the contributions of putative oxidoreductases to Mtz metabolism via experimental over-expression.

Informatic and experimental characterization of oxidoreductases

In order to maximise the informative value of our transcriptomic and experimental reverse genetics studies, I undertook high-throughput *in silico* protein structure prediction and structural homology searching, and assigned putative functions to some 4,680 un-annotated genes in *G. duodenalis*. Further, I devised a scalable approach to independently validate predicted structures, whereby agreement between sequence-derived annotations for predicted and experimentally-determined structural homologues was treated as a proxy for close structural alignment. The alignment features that best predicted agreement in sequence-based annotations were used to identify a second tier of high-confidence-like structures that were otherwise beyond the reach of informatic validation. This approach vastly expanded the functional information available for the hypothetical proteome in *G. duodenalis*, and provided valuable leads in the search for elusive enzymes related to electron transport and drug detoxification.

For example, ferredoxin:NAD reductase activity is assumed to occur in *Giardia* and to link pyruvate catabolism with NAD(P)H formation, but is yet to be identified. Experimental data from *E. histolytica* combined with predicted structures for non-cannonical FNRs in that organism, support an annotated and a putative glutamate synthase in *G. duodenalis* as likely FNR candidates. Furthermore, cytochrome P450-mediated monoxygenation reactions are central to drug detoxification in higher eukaryotes (Zanger and Schwab, 2013) but not evidenced in *G. duodenalis* to date. This is despite experimental evidence of multiple cytochromes b5 (accessories to cytochromes P450), and two likely cytochrome P450 reductases in the parasite. The increased sensitivity of the random forest classifier created in Chapter 3 facilitated the identification of a putative cytochrome P450 among high-confidence-like structures.

In addition to comprehensive *in silico* investigations, I assessed the contributions of two uncharacterized nitroreductase-like enzymes to Mtz metabolism. Over-expression of the canonical nitroreductase NTR1, previously shown to metabolise Mtz *in vitro* (Pal et al., 2009), increased the Mtz tolerance of transgenic trophozoites (Chapter 4). This is consistent with a role in Mtz detoxification. The presence of potentially redox-active cysteine residues within the FAD-binding domains of both this enzyme, and ferredoxin-nitroreductases, may account for their ability to reduce Mtz despite its exceptionally low redox potential. These findings demonstrate the power of protein structure prediction in combination with reverse genetics for elucidating the biology of putative drug targets and resistance mediators in *G. duodenalis*.

Transcriptional responses to nutrient depletion and exogenous stress

The first transcriptomic study in this thesis sought to infer the metabolic priorities of trophozoites over time in axenic culture. I posited that the heightened transcription of enzymes that sequester iron, and that sparge reactive oxygen species, at early stages (48- and 60 hours post-inoculation) of *in vitro* culture, indicate potentially detrimental levels of dissolved oxygen in the culture medium. Conversely, at later stages in culture (96 hours p-i), transcriptional induction of anaerobic glycolytic enzymes, specifically oxygen-sensitive pyruvate:ferredoxin oxidoreductases (PFORs), and declining transcription of antioxidant enzymes, suggested a decline in dissolved oxygen and increased reliance on fermentative metabolism. This shift corresponded with transcriptional changes in two putative structural homologs of bacterial transcription factors. MtrR and a complement of transcripts potentially

constituting a two-component signaling system, were highly transcribed at early time points. Conversely, a transcript up-regulated at 96 hours p-i encodes a putative GntR family transcriptional repressor, involved in regulating NADPH production. Given the propensity for *G. duodenalis* to acquire genes horizontally from bacteria, further investigation of these proteins as transcriptional effectors of change in glycolytic intermidiates and intracellular redox conditions, is now warranted. More broadly, these data demonstrate the transcriptional flexibility of trophozoites over time under standard conditions and suggest that the transcriptional programme may be largely shaped by the intracellular redox status. Moreover, findings from this study strongly suggest that dissolved oxygen should be controlled during experimentats involving Mtz, given that the two oxidants are likely to interact within trophozoites, and to compete for electrons from the same enzymes (expanded below).

In order to explore the nature of the Mtz response relative to physiological-type stressors, and to assess the ability of the parasite to differentiate exogenous stimuli at the transcriptional level, I next compared the transcriptional response of *G. duodenalis* trophozoites to sub-lethal concentrations of Mtz and hydrogen peroxide (H_2O_2), and sub-lethal thermal stress (Chapter 6). In accordance with the conclusions from Chapter 5, I established anaerobic conditions prior to experimentation, and carefully calibrated each stress condition to ensure comparability in the transcriptional response. In this work, Mtz and H_2O_2 were hypothesized to induce similar transcriptional responses because both agents are accepted to cause intracellular oxidative stress. Interestingly however, the response to Mtz diverged substantially from that to H_2O_2 and thermal stress. Of note was the concerted down-regulation of antioxidant enzymes in trophozoites exposed to Mtz, whereas under H_2O_2, transcripts encoding antioxidant enzymes exhibited little overall change. Exceptions were the marked suppression of PFOR transcription, and induction of flavohaemoglobin in cells exposed to H_2O_2. Under thermal stress, thiol cycling enzymes were strongly induced among antioxidant transcripts, although the basis of this oxidative stress-like response is unclear given the anaerobic background.

Clustering analysis over the entire transcriptome supported the marked differences in transcriptional responses to physiological and xenobiotic stress, illustrated in the antioxidant system. These findings agree with previous reports that *G. duodenalis* can differentiate exogenous stress stimuli. Spycher and colleagues (2013) reported clearly distinguishable responses to protein unfolding stress (induced via the reducing agent DTT) and thermal

stress; and identified a protein folding stress-response element upstream of genes uniquely induced by DTT. Similarly, in our study, GARP-like transcription factors and their sub-ordinate genes were induced under H_2O_2 and thermal stress but not Mtz stress, and represent starting points for investigating putative regulators of physiological stress responses in *G. duodenalis*. Conversely, Spycher and colleagues identified a transcript (GL_15125) that was up-regulated under both reducing and thermal stress, which was also up-regulated under Mtz and thermal stress in our study. This transcript, encoding a putative phosphoinositide-interacting protein, now represents the most consistently reported general stress-response-like transcript in *G. duodenalis*.

A model of drug-oxygen interactions

I argued that the divergent transcriptional responses to Mtz and H_2O_2, support the possibility that Mtz efficacy varies according to the ambient concentrations of oxygen and reactive oxygen species (ROS). The interaction of Mtz with dissolved oxygen and ROS (i.e., superoxide, H_2O_2, and hydroxyl radicals) may operate as follows. As reviewed in Chapter 1, Mtz requires enzymatic reduction to cytotoxic intermediates via certain oxidoreductase enzymes that are also key components of the antioxidant system. Under anaerobic conditions in the presence of Mtz, results from Chapter 6 suggest that the parasite may be able to suppress the transcription of antioxidant enzymes that would otherwise be required to combat ROS. This could allow trophozoites to avoid activating the pro-drug. Unpublished observations (M. J. Dagley & M. J. McConville) that trophozoites growing in oxidized media are more susceptible to Mtz than those growing in fresh media, may be due to induction of antioxidant enzymes in oxidized media, which cause strong collateral Mtz activation. This molecular phenotype could be an exaggeration of that inferred in trophozoites growing in oxygenated media in the early stages of axenic passage (Chapter 5).

At higher oxygen concentrations, activated Mtz is spontaneously re-oxidized via 'futile redox cycling'. Indeed, impaired Mtz potency under atmospheric oxygen tension was demonstrated in the earliest experiments in this field (Gillin and Reiner, 1982). Parasites that can tolerate exceptionally high intracellular oxygen may benefit from passive detoxification of Mtz via futile redox cycling, although this likely entails a high ROS-derived oxidative stress load, and attendant detrimental effects (detailed below). Longer periods of elevated oxygen pressure will saturate the parasite antioxidant system and lead to ROS-induced cell death (Lloyd et al., 2000). The effects on trophozoite viability of the interaction between Mtz and oxygen hypothesized here, is represented graphically in Figure 8.1. Crucially, if the expression of

antioxidant enzymes can vary in response to Mtz in the absence of oxygen, as suggested in Chapter 6 and in response to changes in oxygen tension, then prospects for trophozoite survival in the presence of the drug may be substantially increased (Figure 8.1). Incidentally, stoichiometric descriptions of Mtz activation and detoxification, and ROS formation and degradation are published (Adolfsen and Brynildsen, 2015; Edwards, 1993a), and imply that enzymatic detoxification of Mtz, which requires six electrons, is more metabolically expensive than reduction of superoxide and H_2O_2 to water, requiring four (Figure 1.2; Table 8.1). These variables could be incorporated into an electron flux model together with likely reaction stoichiometries for parasite oxidoreductases, and solved under varying oxygen concentrations in order to predict drug-oxygen interaction effects.

Resistance drivers and constraints

In conjunction with controlled experiments on Mtz-susceptible trophozoites, I charted transcriptional changes in three seminal Mtz-resistant lines, derived via chronic sub-lethal exposure in the 1980s (Chapter 7). The resistant line 106-r was derived without initial UV mutagenesis, whereas 713-r and WB-r were mutagenized prior to drug exposure. Importantly, isogenic comparison of each resistant line to its susceptible parent, enriched for transcriptional changes associated with the resistant state. Excellent sequencing depth also enabled the identification of non-synonymous single nucleotide polymorphisms in transcripts that could affect protein behaviour. This study represents the first genetically-controlled transcriptome-wide profile of genetic lesions at single nucleotide resolution in any Mtz-resistant pathogen to our knowledge. The line 106-r featured transcriptional suppression of the key drug-activating enzyme nitroreductase-1, potentially enhanced by a nonsense mutation in 30% of encoding transcripts. Further, up-regulation of a putative drug efflux system in this line may represent a novel Mtz resistance mechanism. In all resistant lines, enzymes that provide substrates to, and metabolize products from PFORs, were differentially transcribed. This indicates that modulation of ferredoxin-based electron transport chains may be a universal feature of Mtz resistance. Interestingly however, 713-r exhibited heightened transcription of thioredoxin cycling enzymes (which activate Mtz), and heat shock proteins, consistent with an 'active' resistance phenotype that activates the drug and must then repair damage to biomolecules. In WB-r, a transcriptional signature consistent with oxidative stress (down-regulation of PFORs, and of the oxygen-reducing NADH oxidase), indicate that this line may tolerate heightened intracellular oxygen in order to benefit from futile redox cycling. This resistance mechanism may come at a substantial metabolic cost, however, as suggested by the retarded growth of WB-r relative to other resistant lines.

The lines 713-r and WB-r were both mutagenized prior to induction of resistance, and created in the same laboratory (Townson et al., 1992). However, around half of all differentially transcribed genes (DTGs) in each line were unique. Assuming these lines were treated in a similar manner *in vitro*, such results prompt us to question the relative contribution of genetic and environmental factors to producing Mtz resistance. It may be that resistance is conferred by a handful of driver genes that are differentially transcribed in all three lines. More probably, resistance is a polygenic phenomenon produced by changes in expression or activity of enzymes that directly interact with Mtz, and others that affect cofactor supply, glucose consumption and intracellular oxygen concentrations, as proposed in Chapter 7. In the latter case, it may be that pre-existing genetic differences in drug-susceptible parental trophozoites, or stochastic changes in gene expression, constrain the repertoire of resistance phenotypes available to trophozoites when Mtz is introduced. For example, elevated expression of oxygen-sensitive PFORs in a susceptible line, might predispose against the development of aerobic-like resistance (Dan et al., 2000). As reviewed in Chapter 1, changes in the expression and sequence of resistance-associated enzymes, are proposed to occur hierarchically as Mtz resistance develops in *T. vaginalis* and *H. pylori*.

Indeed, similar dependencies in *G. duodenalis* might account for the disagreement between results of differential transcription analyses (Chapter 7) and reverse genetic perturbation of putative nitroreductases (Chapter 4). Specifically, the transcripts encoding putative nitroreductases GL_15307 and GL_8377, were down-regulated in 713-r, and 713-r and WB-r respectively (Chapter 7). Based on these results one might postulate that these enzymes are involved in Mtz activation, as their expression appears to be detrimental in trophozoites in the presence of the drug. However, results from Chapter 4 suggest little role for GL_8377 in metabolizing Mtz, and that over-expression of GL_15307 has a protective effect. In order to validate these findings, enzyme abundance should be determined both in the WB-C6 transfectants, and in the lines assayed in Chapter 7. If validated, the conflict might be explained by the acquisition of multiple changes in enzyme expression/activity in trophozoites in response to chronic Mtz exposure, which are not recapitulated when certain genes are perturbed in isolation. For example prior up-regulation of a drug detoxification enzyme such as NR-2 could conceivably increase demand for NAD(P)H, which might necessitate the suppression of other NAD(P)H-dependent enzymes such as GL_15307. To further explore the possibility of contingencies in gene expression as resistance develops, expression profiles in parasites displaying intermediate levels of resistance could be

compared with those in highly resistant, and susceptible lines. In order to pinpoint drivers of resistance, and to prove the existence of any contingencies, however, more comprehensive description of molecular systems is required, including technologies to create sequential gene deletions (see below).

Redox-responsive epigenetic regulators and cofactor supply

The transcriptional plasticity of *G. duodenalis* trophozoites in response to sub-lethal Mtz exposure (Chapter 6) together with observations that restored transcription of drug-activating enzymes accompanies reversion to drug sensitivity in formerly resistant lines (Müller et al., 2008; Smith et al., 1988; Tejman-Yarden et al., 2011), suggest that dynamic transcriptional changes are central to the development of Mtz resistance. Understanding how such transcriptional responses to oxidative stress are produced has the potential to reveal key drivers of Mtz resistance. Although transcriptomics in isolation cannot distinguish the drivers from the products of transcriptional regulation, transcriptional changes in redox-responsive histone modification enzymes are regularly associated with Mtz response and resistance, and are attractive candidates for further investigation.

Five Sir2 histone deacetylase enzymes are encoded in the WB genome. This class of enzymes consume NAD in the process of histone deacetylation and their activity is proposed to increase as the intracellular ratio of NAD to NADH increases (Denu 2003; Fulco et al. 2003; Guarente 2000; Smith et al. 2000). In susceptible trophozoites, exposure to both oxygen and Mtz activation are likely to stimulate NAD(P)H-dependent oxidoreductase activity, and thus to increase the relative concentration of NAD(P). This should increase Sir2 activity and modulate transcription across the genome (Jaenisch and Bird, 2003). Indeed, the first transcriptomic assay of Mtz-resistant *G. duodenalis* found that the Sir2-coding gene GL_16569 was down-regulated (Müller et al., 2008). The same transcript was down-regulated in WB-r in Chapter 7. Conversely, a paralogous enzyme GL_10707 was transcriptionally up-regulated in WB-r (Chapter 7), and in drug-sensitive trophozoites under Mtz, H_2O_2 and thermal stress (Chapter 6). GL_16569, GL_10707, and two other Sir2 enzymes, were recently localized to the nucleus/nuclear periphery in trophozoites (Carranza et al., 2016; Wang et al., 2016). Further, treatment of trophozoites with a canonical Sir2 inhibitor, trichostatin A, decreased the rate of encystation — a process evidenced to involve epigenetic changes (Carranza et al., 2016; Sonda et al., 2010). In 106-r, transcriptional induction of the NAD scavenging pathway may reflect a greater demand for NAD, consistent with increased transcription of the Sir2 gene family (Chapter 7). More broadly, increased transcription of FAD synthetase under all stress

conditions tested in Chapter 6; and amino acid substitutions in enzymes in the NADPH-producing pentose phosphate pathway in 713-r (Chapter 7), indicate that changes in systems that supply electron transport cofactors to drug-interacting oxidoreductases, may be important global effectors of Mtz response and resistance, as is demonstrated in other pathogens (Alsford et al., 2013).

Clinical infections and resistance

It is interesting to consider whether conditions in the host gut can pre-dispose *G. duodenalis* to Mtz resistance. The first suggestions of this are found in the history of the genome strain WB, which was isolated from a patient refractory to Mtz treatment, but showed normal Mtz sensitivity in axenic culture (Smith et al., 1982). Oxygen concentrations vary considerably over time and space in the mammalian gut (Espey, 2013), and early experiments demonstrated increased Mtz tolerance in trophozoites in the presence of oxygen *in vitro* (Gillin and Reiner, 1982). Could more chronic exposure to oxidative stress induce, or select for, molecular phenotypes that also render trophozoites resistant to Mtz? This hypothesis is informed by reports of increased gut oxidation in malnourished children with infectious diarrhoea (Khaled, 1994), and systemic oxidative stress in children with giardiasis (Soto-Méndez et al., 2014). An inverse correlation between PFOR activity and Mtz tolerance is reported in isolates from diagnostic duodenal biopsies for which prior Mtz exposure is not reported (Smith et al., 1988). Interestingly, loss of PFOR may have relatively little cost for parasites *in vivo*, as artificial suppression of *pfor-1* in *G. duodenalis* correlated with more rapid growth in the presence of dO_2 (Dan et al., 2000), and 106-r remains infective in suckling mice, despite lacking detectable PFOR activity (Leitsch et al., 2011; Tejman-Yarden et al., 2011). Taken together, these data are consistent with a model of oxygen-dependent Mtz resistance that may stem from chronic gut oxidation attendant with malnutrition and decreased bile quality. Long term exposure to oxidizing conditions may select for altered expression of glycolytic and/or antioxidant enzymes in order to tolerate oxidative stress, which might inadvertently increase parasite tolerance towards Mtz (Figure 8.1). Furthermore, resistance-associated phenotypes such as the retarded growth observed in WB-r, may yet have clinical relevance. In *Mycobacterium tuberculosis*, slow-growing drug-resistant strains are rarely detected in clinical isolates, but contribute disproportionately to treatment refractivity (Bradley et al., 2015). In the context of a natural *Giardia* infection, it is conceivable that susceptible trophozoites could be induced to drug resistance during Mtz treatment, at the cost of slower growth. Therefore although this feature would likely preclude laboratory-dervied

resistant lines from establishing an experimental infection, similar phenotypes may be viable if produced *in vivo*.

Lastly in terms of clinical considerations, if Mtz resistance is based in dynamic changes in antioxidant expression and reverts relatively quickly in the absence of drug and in treatment-refractory clinical isolates (reviewed in Chapter 1), then this phenomenon may have little genetic basis and thus low heritability. Consequently, Mtz resistance may be arise *de novo* in each refractory clinical infection. If so, it is possible that much clinical Mtz resistance may be undetectable using standard axenization and drug susceptibility testing approaches. This may account for the relative dearth of experimentally validated reports of drug resistance in clinical isolates, despite reported rates of treatment refractivity near 30% (Solaymani-Mohammadi et al., 2010). With this troubling possibility in mind, we turn to prospects for improving anti-giardial drug chemotherapy.

Prospects for metronidazole combination therapies

Suppression of Mtz-activating enzymes, constituting 'passive' resistance mechanisms, are more consistently reported in Mtz-resistant lines than are 'active' resistance mechanisms such as detoxification and biomolecule repair (Chapters 1 and 7). This presents obstacles for preventing or reversing resistance. Compounds that target transcriptional regulation may hold the most promise for preventing down-regulation of enzymes that are essential for Mtz activation. Although no transcriptional regulators were consistently differentially transcribed in resistant lines in Chapter 7, the substantial transcriptional differences between Mtz-resistant and -susceptible lines reported therein may be due to the action of multiple, potentially functionally analogous, transcriptional regulators. Further elucidation of the genes regulated by differentially transcribed Gmybs, TATA-binding proteins and putative Tet repressors identified in Chapter 7, may yet reveal targets for preventing or reversing resistance-associated transcriptional changes. In addition, signaling pathways are barely described in *G. duodenalis*, and are likely important for establishing and maintaining drug-resistant molecular phenotypes. Kinases, which mediate phosphorylation-based signaling, are particularly tractable targets for anti-parasitic chemotherapy (Doerig, 2004; Manning et al., 2011; Naula et al., 2005). Similarly, sodium-proton antiporters such as the putative MATE-like efflux system which is up-regulated in 106-r, are essential and druggable in other protists (Spillman and Kirk, 2015), and could be experimentally inhibited to test the importance of Mtz efflux in resistant lines, with a view to increasing Mtz potency and potentially reversing resistance.

Systems biology and future directions

This project has produced the first whole-transcriptomic data for *Giardia duodenalis* with multiple biological replicates, which enabled controlled and statistically robust investigation into mechanisms of response and resistance to the key anti-giardial drug Mtz. These experiments built on sound foundations in the form of decades of work from the laboratory of Professors Jacqueline and Peter Upcroft (QIMR) that provided fundamental insights into Mtz resistance mechanisms, and other seminal studies of stress responses (Lindley et al., 1988), genomics (Chen et al., 1995; Morrison et al., 2007) and transcriptomics (Müller et al., 2008; Teodorovic et al., 2007) in this unique eukaryote. I described with hitherto unmatched breadth and resolution, a multitude of transcriptional changes in trophozoites during the standard culture cycle, under physiological and xenobiotic stress, and in highly Mtz resistant states. In order to increase the informative value of transcriptomics experiments, I undertook high-throughput *in silico* protein structure prediction and structural homology searching, and generated putative functions for some 4,680 un-annotated genes. This work provides the foundation for a fuller description of the biology of *Giardia* in conjunction with high-resolution genomic, proteomic and metabolomic investigations (cf Lasonder et al., 2016). Several key areas remain to be investigated in the context of Mtz response and resistance. A major conclusion from this discussion is that in order to fully understand the kinetics of redox-active drugs and attendant molecular responses, experiments must be performed under a range of redox conditions. Future systems-level studies should test responses to Mtz under progressively increasing oxygen tensions, in order to fully capture the interactions between these oxidants, and the molecular phenotypes that they produce. Such considerations are particularly important for extrapolating drug action in the host gut, where oxygen tension can vary substantially as mentioned above.

Three complementary avenues could be persued to identify drivers of the transcriptional response to Mtz. Firstly, the original description of nitroreductase-1 as a Mtz-activating enzyme, reported dynamic repression of the encoding transcript in susceptible trophozoites after three hours of exposure to the drug (Müller et al., 2007b). The same transcript was suppressed in our study after 24 hours of exposure to a sub-lethal concentration of Mtz (Chapter 6), and was down-regulated in all three Mtz-resistant lines (Chapter 7). These data suggest that NR-1 suppression may represent a consistant and dynamic transcriptional reponse to Mtz exposure. If so, transfection of drug-sensitive trophozoites with an episome containing segments of the NR-1 promoter upstream of a luciferase-coding gene, could be

used to investigate the presence of a Mtz-response element that may control NR-1 expression. Specifically, a decline in luciferase signal in the presence of Mtz would constitute a change in reporter activity, which should be ablated when the binding site for a Mtz-induced transcriptional repressor is excised from the NR-1 promoter. Similar approaches have successfully identified essential motifs in the glutamate dehydrogenase promoter (Yee et al., 2000), binding sites for GARP-like transcription factors upstream of the cyst wall protein 1 gene (CWP-1; Sun et al., 2006), and a general stress-response element upstream of heat-shock protein genes (Spycher et al., 2013).

Secondly, chromatin-linked immunoprecipitation DNA sequencing (ChIP-seq) would provide genome-wide data to complement targeted experimentation. For example, previous studies transfected yeast and mammalian cells with myc-tagged Sir2 enzymes (Li et al., 2013; Motta et al., 2004), which allowed the use of a commercially available anti-myc antibody to profile Sir2-associated DNA (Li et al., 2013). The transfection technique used in Chapter 4 could be adapted to create *G. duodenalis* lines expressing myc-tagged Sir2 enzymes, in order to assay Sir2 dynamics in the presence of Mtz and trichostatin A. Indeed, the latter compound is already reported to decrease encystation efficiency *in vitro* (Carranza et al., 2016). If TSA can be shown to perturb Mtz-induced transcriptional changes, then this drug class could be further investigated as a partner therapy with Mtz that might both minimize the development of Mtz resistance, and independently decrease disease transmission.

Thirdly, gene interaction networks have powerful potential for illuminating 'hub' genes that drive changes across the transcriptome. In lieu of targeted gene perturbation technologies such as CRISPR/Cas9, vectors similar to those used in Chapter 4 could be generated to create a panel of lines over-expressing native, or catalytically dead components of the antioxidant system (cf Leitsch et al., 2016). The transcriptomic profiles of such lines could be analysed in combination to to identify those genes whose perturbation modulates large numbers of others (i.e., driver genes). Simultaneous quantification of small non-coding RNAs would provide another layer of insight into transcriptional regulation (cf Ragan et al., 2011). Such work would constitute the first major step toward elucidating the gene interaction network in *G. duodenalis*.

Beyond genomics and transcriptomics, other aspects of the phenotype of resistant lines require close attention. For example, the changes in enzyme function may occur in resistant lines due to amino acid substitutions and postulated changes in co-factor availability. Heavy

carbon labeling and metabolic flux analysis can allow inferences about the overall activity of pathways such as glycolysis and fatty acid synthesis (Husain et al., 2012), based on the relative concentration of enzyme substrates and products. Post-translational protein modifications including histone acetylation and methylation await investigation in resistant lines, and would be crucial to validate hypothesized changes in Sir2 activity. Recent developments in mass spectrometry technologies to quantify NAD synthesis (Trammell and Brenner, 2013) and redox dynamics (Rühl et al., 2012), further present exciting opportunities to describe molecular Mtz resistance phenotypes at multiple biochemical levels.

Finally, whereas this thesis has focused on the best-characterized assemblage A *G. duodenalis* genotypes, *Giardia* likely comprises a species complex, wherein genetic diversity manifests as variation in host preferences and drug susceptibility. The full extent of biochemical differences between assemblages remains to be elucidated, and will inform prospects for enhancing, or superseding Mtz-based chemotherapy. Similarly, this drug represents the prototypical nitroheterocyclic from which numerous active derivatives have been created, including the clinically approved compounds nitazoxanide and furazolidone (Chapter 1; Dunn et al., 2010; Miyamoto et al., 2013). Comparisons of response and resistance mechanisms between chemotypes are now required to determine the fundamental requirements for, and genetic drivers of nitroheterocyclic resistance. I hope that the data and hypotheses generated here will help to advance on these important goals.

Table 8.1. Estimated stoichiometry of oxidation-reduction reactions in *Giardia duodenalis* trophozoites in the presence of oxygen and metronidazole.

	Substrates (n)			Products (n)				
Enzymatic reactions							**References**	**Notes**
PFOR		pyruvate	2 Fd (ox)		acetyl CoA	2 Fd (red)	(Kerscher and Oesterhelt, 1981; Townson et al., 1996)	
Ferredoxin		Fd (red)	Mtz		Fd (ox)	Mtz^{-}	(Leitsch et al., 2011; Liu et al., 2000)	
		Fd (red)	Mtz^{-}		Fd (ox)	Mtz^{2-}		
Acetyl-Co synthase		acetyl CoA	ADP		acetate	ATP	(Sanchez et al., 2000)	
Alcohol dehydrogenase E		acetyl CoA	NADH		ethanol	NAD	(Sánchez, 1998)	
NADH oxidase		O_2	2 NADH		H_2O	2 NAD	(Brown et al., 1996)	
Flavodriiron protein		O_2	2 Rrx (red)		H_2O	2 Rrx (ox)	(Testa et al., 2011a)	
DT-diaphorase		O_2	2 NADH		H_2O_2	2 NAD	(Li and Wang, 2006; Sánchez et al., 2001)	
		O_2	NADH		O_2^{-}	NAD		
Superoxide reductase		O_2^{-}	NADH		H_2O_2	NAD	(Testa et al., 2011b)	
Peroxiredoxin		H_2O_2	Trx-SH		H_2O	Trx-SS	(Mastronicola et al., 2014)	
Nitroreductase-1		NADH	Mtz		NAD	Mtz^{-}	(Müller et al., 2015; 2013; 2007; Nillius et al., 2011)	
	2	Fd (red)	NAD	2	Fd (ox)	NADH	(Ali and Nozaki, 2007)	Postulated
Nitroreductase-2	3	NADH	Mtz	3	NAD	3 $Mtz\text{-}NH_2$	(Müller et al., 2007; 2013; 2015)	
	2	Fd (red)	NAD	2	Fd (ox)	NADH	(Ali and Nozaki, 2007)	Postulated
Thioredoxin reductase	2	NADPH	Trx-SH	2	NADP	Trx-SS	(Leitsch et al., 2011; 2016)	
	2	NADPH	PDI-SS	2	NADP	PDI-SH		
		NADPH	Mtz		NADP	Mtz^{-}		
Protein disulfide isomerase		PDI-SH	protein-SS		PDI-SS	protein-SH		
Heat shock protein		Protein unstable	ATP		Protein stable	ADP		
NAD kinase		NAD	ATP		NADP	ADP		
Enzyme-free reactions		Mtz^{-}	O_2		Mtz	O_2^{-}		
		Mtz^{-}	protein-SH		Mtz^{2-}	protein-SS		
		Mtz^{-}	thymine		Mtz^{2-}	thymine+	(Edwards, 1993)	
		O_2	Fe^{2+}		O_2^{-}	Fe^{3+}		
		O_2^{-}	Fe^{2+}		H_2O_2	Fe^{3+}		
		H_2O_2	Fe^{2+}		$OH^{-\bullet}$	Fe^{3+}		
		$OH^{-\bullet}$	protein-SH		H_2O	protein-SS		
		$OH^{-\bullet}$	thymine		H_2O	$thymine^{+}$		

PFOR: Pyruvate:ferredoxin oxidoreductase; Rrx: Rubredoxin (not described in *Giardia duodenalis*; see Table 1.1). Stoichiometry is estimated only. Molar ratios are 1 unless otherwise specified.

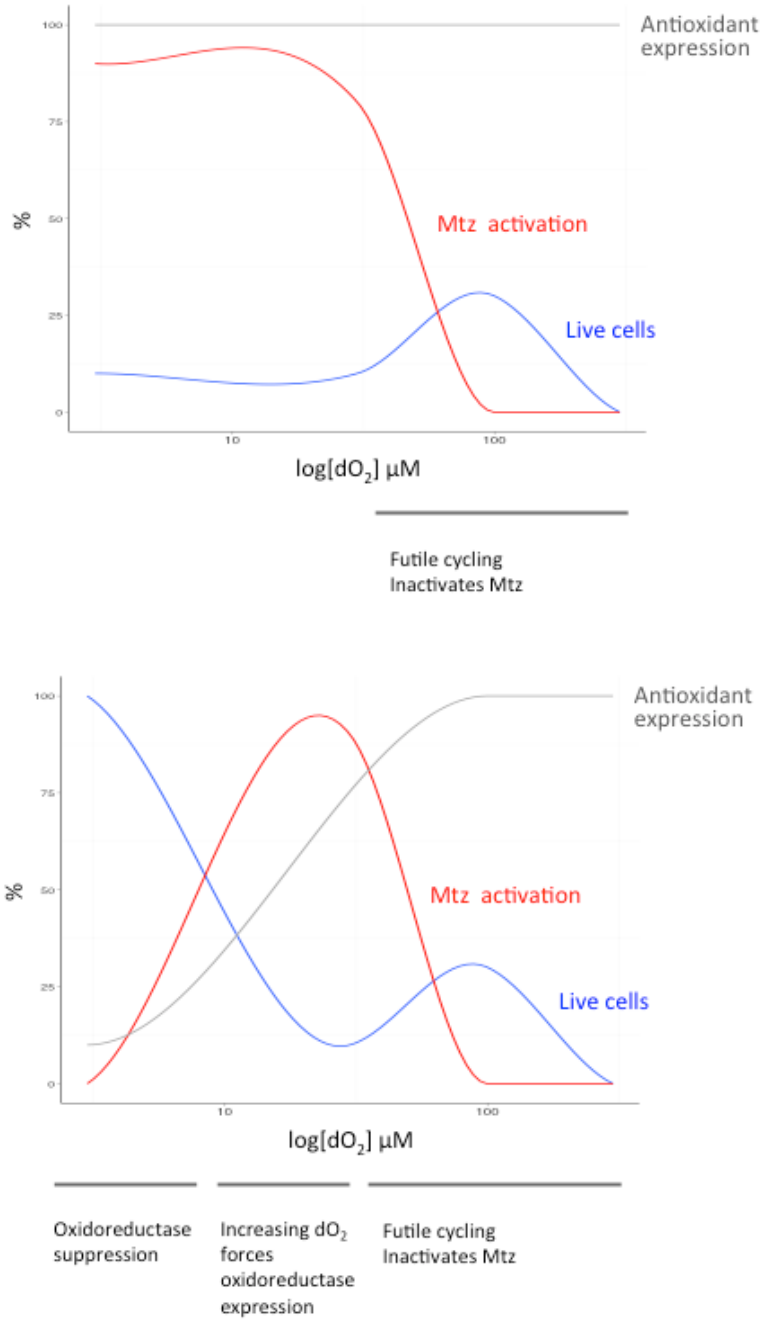


Figure 8.1. Models of metronidazole cytotoxicity in *Giardia duodenalis* trophozoites under varying dissolved oxygen concentrations. When expression of drug-activating antioxidant enzymes is unresponsive to ambient oxygen concentrations, and a single maximum of increased trophozoite viability (low drug efficacy) at high oxygen concentrations is hypothesized to exist (Top panel). If antioxidant expression can be suppressed at low oxygen concentrations in the presence of metronidazole, then a second local maximum of trophozoite viability may exist (Bottom panel).

Bibliography

Abboud, P., Lemée, V., Gargala, G., Brasseur, P., Ballet, J.J., Borsa-Lebas, F., Caron, F., and Favennec, L. (2001). Successful treatment of metronidazole- and albendazole-resistant giardiasis with nitazoxanide in a patient with acquired immunodeficiency syndrome. Clin. Infect. Dis. *32*, 1792–1794.

Adagu, I.S., Nolder, D., Warhurst, D.C., and Rossignol, J.-F. (2001). In vitro activity of nitazoxanide and related compounds against isolates of *Giardia intestinalis*, *Entamoeba histolytica* and *Trichomonas vaginalis*. J. Antimicrob. Chemother. *49*, 103–111.

Adam, R.D. (2001). Biology of *Giardia lamblia*. Clinical Microbiology Reviews *14*, 447–475.

Adam, R.D., Yang, Y.M., and Nash, T.E. (1992). The cysteine-rich protein gene family of *Giardia lamblia*: loss of the CRP170 gene in an antigenic variant. Mol. Cell. Biol. *12*, 1194–1201.

Adolfsen, K.J., and Brynildsen, M.P. (2015). A Kinetic Platform to Determine the Fate of Hydrogen Peroxide in Escherichia coli. PLoS Comput Biol *11*, e1004562.

Alam, S., Yee, J., Couture, M., Takayama, S.-I.J., Tseng, W.-H., Mauk, A.G., and Rafferty, S. (2012). Cytochrome b5 from *Giardia lamblia*. Metallomics *4*, 1255.

Albert, T.J., Dailidiene, D., Dailide, G., Norton, J.E., Kalia, A., Richmond, T.A., Molla, M., Singh, J., Green, R.D., and Berg, D.E. (2005). Mutation discovery in bacterial genomes: metronidazole resistance in Helicobacter pylori. Nat Meth *2*, 951–953.

Ali, V., and Nozaki, T. (2007). Current Therapeutics, Their Problems, and Sulfur-Containing-Amino-Acid Metabolism as a Novel Target against Infections by "Amitochondriate" Protozoan Parasites. Clinical Microbiology Reviews *20*, 164–187.

Alsford, S., Eckert, S., Baker, N., Glover, L., Sanchez-Flores, A., Leung, K.F., Turner, D.J., Field, M.C., Berriman, M., and Horn, D. (2013). High-throughput decoding of antitrypanosomal drug efficacy and resistance. Nature *482*, 232–236.

Altschul, S.F., Madden, T.L., Schäffer, A.A., Zhang, J., Zhang, Z., Miller, W., and Lipman, D.J. (1997). Gapped BLAST and PSI-BLAST: a new generation of protein database search programs. Nucleic Acids Research *25*, 3389–3402.

Andersson, J.O., and Roger, A.J. (2002). Evolutionary Analyses of the Small Subunit of Glutamate Synthase: Gene Order Conservation, Gene Fusions, and Prokaryote-to- Eukaryote Lateral Gene Transfers. Eukaryotic Cell *1*, 304–310.

Ankarklev, J., Franzén, O., Peirasmaki, D., Jerlström-Hultqvist, J., Lebbad, M., Andersson, J., Andersson, B., and Svärd, S.G. (2015). Comparative genomic analyses of freshly isolated *Giardia intestinalis* assemblage A isolates. BMC Genomics 1–14.

Ankarklev, J., Jerlström-Hultqvist, J., Ringqvist, E., Troell, K., and Svärd, S.G. (2010). Behind the smile: cell biology and disease mechanisms of Giardia species. Nature Publishing Group *8*, 413–422.

Ankarklev, J., Svärd, S.G., and Lebbad, M. (2012). Allelic sequence heterozygosity in single Giardia parasites. BMC Microbiol *12*, 65.

Arbo, A., Pavía-Ruz, N., and Santos, J.I. (2006). Opsonic Requirements for the Respiratory Burst of Neutrophils against *Giardia lamblia* Trophozoites. Archives of Medical Research *37*, 465–473.

Bartelt, L.A., Roche, J., Kolling, G., Bolick, D., Noronha, F., Naylor, C., Hoffman, P., Warren, C.,

Singer, S., and Guerrant, R. (2013). Persistent G. lamblia impairs growth in a murine malnutrition model. J. Clin. Invest. *123*, 2672–2684.

Bentley, D.R., Balasubramanian, S., Swerdlow, H.P., Smith, G.P., Milton, J., Brown, C.G., Hall, K.P., Evers, D.J., Barnes, C.L., Bignell, H.R., et al. (2008). Accurate whole human genome sequencing using reversible terminator chemistry. Nature *456*, 53–59.

Biagini, G.A., Park, J.H., Lloyd, D., and Edwards, M.R. (2001). The antioxidant potential of pyruvate in the amitochondriate diplomonads *Giardia intestinalis* and Hexamita inflata. Microbiology *147*, 3359–3365.

Bittencourt-Silvestre, J., Lemgruber, L., and de Souza, W. (2010). Encystation process of *Giardia lamblia*: morphological and regulatory aspects. Arch. Microbiol. *192*, 259–265.

Boreham, P.F.L., Phillips, R.E., and Shepherd, R.W. (1988). Altered uptake of metronidazole in vitro by stocks of *Giardia intestinalis* with different drug sensitivities. Trans. R. Soc. Trop. Med. Hyg. *82*, 104–106.

Boucher, S.E., and Gillin, F.D. (1990). Excystation of in vitro-derived *Giardia lamblia* cysts. Infection and Immunity *58*, 3516–3522.

Bradic, M., Warring, S.D., Tooley, G.E., Scheid, P., Secor, W.E., Land, K.M., Huang, P.-J., Chen, T.-W., Lee, C.-C., Tang, P., et al. (2016). Genetic indicators of drug resistance in the highly repetitive genomes of *Trichomonas vaginalis* and other trichomonads.

Bradley, P., Gordon, N.C., Walker, T.M., Dunn, L., Heys, S., Huang, B., Earle, S., Pankhurst, L.J., Anson, L., de Cesare, M., et al. (2015). Rapid antibiotic-resistance predictions from genome sequence data for *Staphylococcus aureus* and *Mycobacterium tuberculosis*. Nature Communications *6*, 1–14.

Brown, D.M., Upcroft, J.A., and Upcroft, P. (1993). Cysteine is the major low-molecular weight thiol in *Giardia duodenalis*. Molecular & Biochemical Parasitology *61*, 155–158.

Brown, D.M., Upcroft, J.A., and Upcroft, P. (1995). Free radical detoxification in *Giardia duodenalis*. Molecular & Biochemical Parasitology *72*, 47–56.

Brown, D.M., Upcroft, J.A., and Upcroft, P. (1996a). A thioredoxin reductase-class of disulphide reductase in the protozoan parasite *Giardia duodenalis*. Molecular & Biochemical Parasitology *83*, 211–220.

Brown, D.M., Upcroft, J.A., Edwards, M.R., and Upcroft, P. (1998). Anaerobic bacterial metabolism in the ancient eukaryote *Giardia duodenalis*. International Journal for Parasitology *28*, 149–164.

Brown, D.M., Upcroft, J.A., and Upcroft, P. (1996b). A H2O-Producing NADH Oxidase from the Protozoan Parasite Giardia Duodenalis. Eur. J. Biochem. *241*, 155–161.

Cacciò, S.M., and Sprong, H. (2011). Epidemiology of Giardiasis in Humans. In *Giardia*: A Model Organism, H.D. Lujan, and S.G. Svärd, eds. (Vienna: Springer Vienna).

Carpenter, B.M., Gilbreath, J.J., Pich, O.Q., McKelvey, A.M., Maynard, E.L., Li, Z.Z., and Merrell, D.S. (2013). Identification and Characterization of Novel Helicobacter pylori apo-Fur-Regulated Target Genes. J. Bacteriol. *195*, 5526–5539.

Carranza, P.G., Gargantini, P.R., Prucca, C.G., Torri, A., Saura, A., Svärd, S., and Lujan, H.D. (2016). Specific histone modifications play critical roles in the control of encystation and antigenic

variation in the early-branching eukaryote *Giardia lamblia*. Int. J. Biochem. Cell Biol. *81*, 32–43.

Chabriere, E. (2001). Crystal Structure of the Free Radical Intermediate of Pyruvate:Ferredoxin Oxidoreductase. Science *294*, 2559–2563.

Chapman, A., Linstead, D.J., and Lloyd, D. (1999). Hydrogen peroxide is a product of oxygen consumption by *Trichomonas vaginalis*. Journal of Biosciences *24*, 339.

Chen, N., Upcroft, J.A., and Upcroft, P. (1994). Physical map of a 2 Mb chromosome of the intestinal protozoan parasite *Giardia duodenalis*. Chromosome Res. *2*, 307–313.

Chen, N., Upcroft, J.A., and Upcroft, P. (1995). A *Giardia duodenalis* gene encoding a protein with multiple repeats of a toxin homologue. Parasitology *111 (Pt 4)*, 423–431.

Coombs, G.H., Westrop, G.D., Suchan, P., Puzova, G., Hirt, R.P., Embley, T.M., Mottram, J.C., and Muller, S. (2004). The Amitochondriate Eukaryote *Trichomonas vaginalis* Contains a Divergent Thioredoxin-linked Peroxiredoxin Antioxidant System. Journal of Biological Chemistry *279*, 5249–5256.

Crozet, M.D., Botta, C., Gasquet, M., Curti, C., REmusat, V., Hutter, S., Chapelle, O., Azas, N., De MEo, M., and Vanelle, P. (2009). Lowering of 5-nitroimidazole's mutagenicity: Towards optimal antiparasitic pharmacophore. European Journal of Medicinal Chemistry *44*, 653–659.

Cudmore, S.L., Delgaty, K.L., Hayward-McClelland, S.F., Petrin, D.P., and Garber, G.E. (2004). Treatment of Infections Caused by Metronidazole-Resistant *Trichomonas vaginalis*. Clinical Microbiology Reviews *17*, 783–793.

Dan, M., Wang, A.L., and Wang, C.C. (2000). Inhibition of pyruvate-ferredoxin oxidoreductase gene expression in *Giardia lamblia* by a virus-mediated hammerhead ribozyme. Molecular Microbiology *36*, 447–456.

Davids, B.J., and Gillin, F.D. (2011). Methods for *Giardia* culture, cryopreservation, encystation, and excystation in vitro. In *Giardia*: A Model Organism, H.D. Lujan, and S.G. Svärd, eds. (Vienna: Springer Vienna).

Davids, B.J., Reiner, D.S., Birkeland, S.R., Preheim, S.P., Cipriano, M.J., McArthur, A.G., and Gillin, F.D. (2006). A New Family of Giardial Cysteine-Rich Non-VSP Protein Genes and a Novel Cyst Protein. PLoS ONE *1*, e44.

Dawson, S.C., and House, S.A. (2010). Imaging and Analysis of the Microtubule Cytoskeleton in (Elsevier Inc.).

Demmer, J.K., Huang, H., Wang, S., Demmer, U., Thauer, R.K., and Ermler, U. (2015). Insights into Flavin-based Electron Bifurcation via the NADH-dependent Reduced Ferredoxin:NADP Oxidoreductase Structure. Journal of Biological Chemistry *290*, 21985–21995.

Di Matteo, A., Scandurra, F.M., Testa, F., Forte, E., Sarti, P., Brunori, M., and Giuffre, A. (2007). The O2-scavenging Flavodiiron Protein in the Human Parasite *Giardia intestinalis*. Journal of Biological Chemistry *283*, 4061–4068.

Diawara, A., Halpenny, C.M., Churcher, T.S., Mwandawiro, C., Kihara, J., Kaplan, R.M., Streit, T.G., Idaghdour, Y., Scott, M.E., Basáñez, M.-G., et al. (2013). Association between Response to Albendazole Treatment and β-Tubulin Genotype Frequencies in Soil-transmitted Helminths. PLoS Negl Trop Dis *7*, e2247.

Doerig, C. (2004). Protein kinases as targets for anti-parasitic chemotherapy. Biochimica Et Biophysica Acta (BBA) - Proteins and Proteomics *1697*, 155–168.

Duchene, M. (2015). Metronidazole and the Redox Biochemistry of *Entamoeba histolytica*. In Amebiasis, T. Nozaki, and A. Bhattacharya, eds. (Amebiasis).

Dunn, L.A., Burgess, A.G., Krauer, K.G., Eckmann, L., Vanelle, P., Crozet, M.D., Gillin, F.D., Upcroft, P., and Upcroft, J.A. (2010). A new-generation 5-nitroimidazole can induce highly metronidazole-resistant *Giardia lamblia* in vitro. Int. J. Antimicrob. Agents *36*, 37–42.

Ebneter, J.A., Heusser, S.D., Schraner, E.M., Hehl, A.B., and Faso, C. (2016). Cyst-Wall-Protein-1 is fundamental for Golgi-like organelle neogenesis and cyst-wall biosynthesis in *Giardia lamblia*. Nature Communications *7*, 1–10.

Edwards, D.I. (1993a). Nitroimidazole drugs--action and resistance mechanisms. I. Mechanisms of action. J. Antimicrob. Chemother. *31*, 9–20.

Edwards, D.I. (1993b). Nitroimidazole drugs--action and resistance mechanisms. II. Mechanisms of resistance. J. Antimicrob. Chemother. *31*, 201–210.

Einarsson, E., Ástvaldsson, À., Hultenby, K., Andersson, J.O., Svärd, S.G., and Jerlstrom-Hultqvist, J. (2015). Comparative cell biology and evolution of Annexins in Diplomonads.

Ellis, J.E., Wingfield, J.M., Cole, D., Boreham, P.F., and Lloyd, D. (1993). Oxygen affinities of metronidazole-resistant and-sensitive stocks of *Giardia intestinalis*. International Journal for Parasitology *23*, 35–39.

Erickson, M.C., and Ortega, Y.R. (2006). Inactivation of protozoan parasites in food, water, and environmental systems. J. Food Prot. *69*, 2786–2808.

Escobedo, A.A., and Cimerman, S. (2007). Giardiasis: a pharmacotherapy review. Expert Opin. Pharmacother. *8*, 1885–1902.

Espey, M.G. (2013). Role of oxygen gradients in shaping redox relationships between the human intestine and its microbiota. Free Radic. Biol. Med. *55*, 130–140.

Eswar, N., Webb, B., Marti-Renom, M.A., Madhusudhan, M.S., Eramian, D., Shen, M.-Y., Pieper, U., and Sali, A. (2006). Comparative protein structure modeling using MODELLER. Curr Protoc Bioinformatics *Chapter 5*, Unit5.6.

Farthing, M.J. (1996). Giardiasis. Gastroenterol. Clin. North Am. *25*, 493–515.

Feng, Y., and Xiao, L. (2011). Zoonotic potential and molecular epidemiology of Giardia species and giardiasis. Clinical Microbiology Reviews *24*, 110–140.

Fisher, B.S., Estraño, C.E., and Cole, J.A. (2013). Modeling Long-Term Host Cell-*Giardia lamblia* Interactions in an In Vitro Co-Culture System. PLoS ONE *8*, e81104.

Franzén, O., Jerlström-Hultqvist, J., Castro, E., Sherwood, E., Ankarklev, J., Reiner, D.S., Palm, D., Andersson, J.O., Andersson, B., and Svärd, S.G. (2009). Draft genome sequencing of *Giardia intestinalis* assemblage B isolate GS: is human giardiasis caused by two different species? PLoS Pathog. *5*, e1000560.

Franzén, O., Jerlström-Hultqvist, J., Einarsson, E., Ankarklev, J., Ferella, M., Andersson, B., and Svärd, S.G. (2013). Transcriptome profiling of *Giardia intestinalis* using strand-specific RNA-seq.

PLoS Comput Biol *9*, e1003000.

Galkin, A., Kulakova, L., Lim, K., Chen, C.Z., Zheng, W., Turko, I.V., and Herzberg, O. (2014). Structural Basis for Inactivation of *Giardia lamblia* Carbamate Kinase by Disulfiram. Journal of Biological Chemistry.

Gillin, F.D., and Diamond, L.S. (1981). *Entamoeba histolytica* and *Giardia lamblia*: effects of cysteine and oxygen tension on trophozoite attachment to glass and survival in culture media. Experimental Parasitology *52*, 9–17.

Gillin, F.D., and Reiner, D.S. (1982). Effects of oxygen tension and reducing agents on sensitivity of *Giardia lamblia* to metronidazole in vitro. Biochem. Pharmacol. *31*, 3694–3697.

Gillin, F.D., Hagblom, P., Harwood, J., Aley, S.B., Reiner, D.S., McCaffery, M., So, M., and Guiney, D.G. (1990). Isolation and expression of the gene for a major surface protein of *Giardia lamblia*. Proc. Natl. Acad. Sci. U.S.a. *87*, 4463–4467.

Gilman, R.H., Marquis, G.S., Miranda, E., Vestegui, M., and Martinez, H. (1988). Rapid reinfection by *Giardia lamblia* after treatment in a hyperendemic Third World community. Lancet *1*, 343–345.

Goodwin, A., Kersulyte, D., Sisson, G., Veldhuyzen van Zanten, S.J.O., Berg, D.E., and Hoffman, P.S. (1998). Metronidazole resistance in Helicobacter pylori is due to null mutations in a gene (rdxA) that encodes an oxygen-insensitive NADPH nitroreductase. Molecular Microbiology *28*, 383–393.

Gottstein, B., Harriman, G.R., Conrad, J.T., and Nash, T.E. (1990). Antigenic variation in *Giardia lamblia*: cellular and humoral immune response in a mouse model. Parasite Immunol. *12*, 659–673.

Guerrant, R.L., DeBoer, M.D., Moore, S.R., Scharf, R.J., and Lima, A.A.M. (2012). The impoverished gut—a triple burden of diarrhoea, stunting and chronic disease. Nature Reviews Gastroenterology & Hepatology 1–10.

Haas, C.N., and Aturaliye, D.N. (1999). Kinetics of electroporation-assisted chlorination of Giardia muris. Water Research *33*, 1761–1766.

Hagen, K.D., Hirakawa, M.P., House, S.A., Schwartz, C.L., Pham, J.K., Cipriano, M.J., La Torre, De, M.J., Sek, A.C., Du, G., Forsythe, B.M., et al. (2011). Novel Structural Components of the Ventral Disc and Lateral Crest in *Giardia intestinalis*. PLoS Negl Trop Dis *5*, e1442.

Halliez, M.C. (2013). Extra-intestinal and long term consequences of *Giardia duodenalis* infections. World J. Gastroenterol. *19*, 8974.

Hamdane, D., Xia, C., Im, S.C., Zhang, H., and Kim, J. (2009). Structure and function of an NADPH-cytochrome P450 oxidoreductase in an open conformation capable of reducing cytochrome P450. Journal of Biological ….

Han, J., and Collins, L.J. (2012). Reconstruction of Sugar Metabolic Pathways of *Giardia lamblia*. International Journal of Proteomics *2012*, 1–9.

Hausen, M.A., Freitas, J.C.M., Jr., and Monteiro-Leal, L.H. (2006). The effects of metronidazole and furazolidone during Giardia differentiation into cysts. Experimental Parasitology *113*, 135–141.

Hoffman, P.S., Sisson, G., Croxen, M.A., Welch, K., Harman, W.D., Cremades, N., and Morash, M.G. (2007). Antiparasitic drug nitazoxanide inhibits the pyruvate oxidoreductases of Helicobacter

pylori, selected anaerobic bacteria and parasites, and Campylobacter jejuni. Antimicrob. Agents Chemother. *51*, 868–876.

House, S.A., Richter, D.J., Pham, J.K., and Dawson, S.C. (2011). Giardia Flagellar Motility Is Not Directly Required to Maintain Attachment to Surfaces. PLoS Pathog. *7*, e1002167.

Huang, Y.J., Mao, B., Aramini, J.M., and Montelione, G.T. (2014). Assessment of template-based protein structure predictions in CASP10. Proteins *82*, 43–56.

Hubbard, P.A., Shen, A.L., Paschke, R., Kasper, C.B., and Kim, J.J. (2001). NADPH-cytochrome P450 oxidoreductase. Structural basis for hydride and electron transfer. J. Biol. Chem. *276*, 29163–29170.

Husain, A., Sato, D., Jeelani, G., Soga, T., and Nozaki, T. (2012). Dramatic Increase in Glycerol Biosynthesis upon Oxidative Stress in the Anaerobic Protozoan Parasite *Entamoeba histolytica*. PLoS Negl Trop Dis *6*, e1831.

Illergård, K., Ardell, D.H., and Elofsson, A. (2009). Structure is three to ten times more conserved than sequence-A study of structural response in protein cores. Proteins *77*, 499–508.

Isaac-Renton, J.L., Cordeiro, C., Sarafis, K., and Shahriari, H. (1993). Characterization of *Giardia duodenalis* isolates from a waterborne outbreak. J Infect Dis *167*, 431–440.

Jaenisch, R., and Bird, A. (2003). Epigenetic regulation of gene expression: how the genome integrates intrinsic and environmental signals. Nat Genet *33*, 245–254.

Jedelský, P.L., Doležal, P., Rada, P., Pyrih, J., Smíd, O., Hrdy, I., Šedinová, M., Marcinčiková, M., Voleman, L., Perry, A.J., et al. (2011). The Minimal Proteome in the Reduced Mitochondrion of the Parasitic Protist *Giardia intestinalis*. PLoS ONE *6*, e17285.

Jeelani, G., Husain, A., Sato, D., Ali, V., Suematsu, M., Soga, T., and Nozaki, T. (2010). Two Atypical L-Cysteine-regulated NADPH-dependent Oxidoreductases Involved in Redox Maintenance, L-Cystine and Iron Reduction, and Metronidazole Activation in the Enteric Protozoan *Entamoeba histolytica*. Journal of Biological Chemistry *285*, 26889–26899.

Jeelani, G., and Nozaki, T. (2014). Metabolomic analysis of *Entamoeba*: applications and implications. Curr. Opin. Microbiol. *20*, 118–124.

Jerlstrom-Hultqvist, J., Stadelmann, B., Birkestedt, S., Hellman, U., and Svärd, S.G. (2012). Plasmid Vectors for Proteomic Analyses in *Giardia*: Purification of Virulence Factors and Analysis of the Proteasome. Eukaryotic Cell *11*, 864–873.

Jerlström-Hultqvist, J., Franzén, O., Ankarklev, J., Xu, F., Nohýnková, E., Andersson, J.O., Svärd, S.G., and Andersson, B. (2010). Genome analysis and comparative genomics of a *Giardia intestinalis* assemblage E isolate. BMC Genomics *11*, 543.

Jiménez-Cardoso, E., Eligio-García, L., Cortés-Campos, A., Flores-Luna, A., Valencia-Mayoral, P., and Lozada-Chávez, I. (2009). Changes in β-giardin sequence of *Giardia intestinalis* sensitive and resistant to albendazole strains. Parasitol. Res. *105*, 25–33.

Jones, P., Binns, D., Chang, H.Y., Fraser, M., Li, W., McAnulla, C., McWilliam, H., Maslen, J., Mitchell, A., Nuka, G., et al. (2014). InterProScan 5: genome-scale protein function classification. Bioinformatics *30*, 1236–1240.

Kabnick, K.S., and Peattie, D.A. (1990). In situ analyses reveal that the two nuclei of *Giardia*

lamblia are equivalent. J. Cell. Sci. *95 (Pt 3)*, 353–360.

Karplus, K., Barrett, C., and Hughey, R. (1998). Hidden Markov models for detecting remote protein homologies. Bioinformatics *14*, 846–856.

Kazmier, F.J. (1976). A significant interaction between metronidazole and warfarin. Mayo Clin Proc *51*, 782–784.

Khaled, M.A. (1994). Oxidative stress in childhood malnutrition and diarrhoeal diseases. J Diarrhoeal Dis Res *12*, 165–172.

Kim, D.E., Chivian, D., and Baker, D. (2004). Protein structure prediction and analysis using the Robetta server. Nucleic Acids Research *32*, W526–W531.

Kosek, M., Bern, C., and Guerrant, R.L. (2003). The global burden of diarrhoeal disease, as estimated from studies published between 1992 and 2000. Bull. World Health Organ. *81*, 197–204.

Kudo, T., Endo, Y., Taguchi, R., Yatsu, M., and Ito, K. (2014). Metronidazole reduces the expression of cytochrome P450 enzymes in HepaRG cells and cryopreserved human hepatocytes. Xenobiotica *45*, 413–419.

Kulakova, L., Singer, S.M., Conrad, J., and Nash, T.E. (2006). Epigenetic mechanisms are involved in the control of *Giardia lamblia* antigenic variation. Molecular Microbiology *61*, 1533–1542.

Kulda, J. (1999). Trichomonads, hydrogenosomes and drug resistance. International Journal for Parasitology *29*, 199–212.

Kumar, M., Adhikari, S., and Hurdle, J.G. (2014). Action of nitroheterocyclic drugs against Clostridium difficile. Int. J. Antimicrob. Agents *44*, 314–319.

Kyes, S.A., Kraemer, S.M., and Smith, J.D. (2007). Antigenic Variation in Plasmodium falciparum: Gene Organization and Regulation of the var Multigene Family. Eukaryotic Cell *6*, 1511–1520.

Lane, S., and Lloyd, D. (2002). Current trends in research into the waterborne parasite *Giardia*. Crit. Rev. Microbiol. *28*, 123–147.

Larocque, R., Nakagaki, K., Lee, P., Abdul-Wahid, A., and Faubert, G.M. (2003). Oral Immunization of BALB/c Mice with *Giardia duodenalis* Recombinant Cyst Wall Protein Inhibits Shedding of Cysts. Infection and Immunity *71*, 5662–5669.

Lasek-Nesselquist, E., Welch, D.M., and Sogin, M.L. (2010). The identification of a new *Giardia duodenalis* assemblage in marine vertebrates and a preliminary analysis of G. duodenalis population biology in marine systems. International Journal for Parasitology *40*, 1063–1074.

Lasonder, E., Rijpma, S.R., van Schaijk, B.C.L., Hoeijmakers, W.A.M., Kensche, P.R., Gresnigt, M.S., Italiaander, A., Vos, M.W., Woestenenk, R., Bousema, T., et al. (2016). Integrated transcriptomic and proteomic analyses of P. falciparumgametocytes: molecular insight into sex-specific processes and translational repression. Nucleic Acids Research *44*, 6087–6101.

Leger, M.M., Kolísko, M., Kamikawa, R., Stairs, C.W., Kume, K., Čepička, I., Silberman, J.D., Andersson, J.O., Xu, F., Yabuki, A., et al. (2017). Organelles that illuminate the origins of Trichomonas hydrogenosomes and Giardia mitosomes. Nature Publishing Group *1*, 1–7.

Leitsch, D., Burgess, A.G., Dunn, L.A., Krauer, K.G., Tan, K., Duchene, M., Upcroft, P., Eckmann, L.,

and Upcroft, J.A. (2011). Pyruvate:ferredoxin oxidoreductase and thioredoxin reductase are involved in 5-nitroimidazole activation while flavin metabolism is linked to 5-nitroimidazole resistance in *Giardia lamblia*. Journal of Antimicrobial Chemotherapy *66*, 1756–1765.

Leitsch, D., Drinić, M., Kolarich, D., and Duchêne, M. (2012a). Molecular & Biochemical Parasitology. Molecular & Biochemical Parasitology *183*, 177–183.

Leitsch, D., Kolarich, D., Binder, M., Stadlmann, J., Altmann, F., and Duchêne, M. (2009). *Trichomonas vaginalis*: metronidazole and other nitroimidazole drugs are reduced by the flavin enzyme thioredoxin reductase and disrupt the cellular redox system. Implications for nitroimidazole toxicity and resistance. Molecular Microbiology *72*, 518–536.

Leitsch, D., Müller, J., and Müller, N. (2016). Evaluation of *Giardia lamblia* thioredoxin reductase as drug activating enzyme and as drug target. International Journal for Parasitology: Drugs and Drug Resistance *6*, 148–153.

Leitsch, D., Schlosser, S., Burgess, A., and Duchêne, M. (2012b). Nitroimidazole drugs vary in their mode of action in the human parasite *Giardia lamblia*. International Journal for Parasitology: Drugs and Drug Resistance *2*, 166–170.

Lemée, V., Zaharia, I., Nevez, G., Rabodonirina, M., Brasseur, P., Ballet, J.J., and Favennec, L. (2000). Metronidazole and albendazole susceptibility of 11 clinical isolates of *Giardia duodenalis* from France. J. Antimicrob. Chemother. *46*, 819–821.

Levin, J.Z., Yassour, M., Adiconis, X., Nusbaum, C., Thompson, D.A., Friedman, N., Gnirke, A., and Regev, A. (2010). Comprehensive comparative analysis of strand-specific rnA sequencing methods. Nat Meth *7*, 709–715.

Li, H., Handsaker, B., Wysoker, A., Fennell, T., Ruan, J., Homer, N., Marth, G., Abecasis, G., Durbin, R., 1000 Genome Project Data Processing Subgroup (2009). The Sequence Alignment/Map format and SAMtools. Bioinformatics *25*, 2078–2079.

Li, H., and Durbin, R. (2009). Fast and accurate short read alignment with Burrows-Wheeler transform. Bioinformatics *25*, 1754–1760.

Li, L., and Wang, C.C. (2006). A likely molecular basis of the susceptibility of *Giardia lamblia* towards oxygen. Molecular Microbiology *59*, 202–211.

Li, L., Stoeckert, C.J., and Roos, D.S. (2003). OrthoMCL: identification of ortholog groups for eukaryotic genomes. Genome Research *13*, 2178–2189.

Li, M., Valsakumar, V., Poorey, K., Bekiranov, S., and Smith, J.S. (2013). Genome-wide analysis of functional sirtuin chromatin targets in yeast. Genome Biology *14*, R48.

Li, Y., Luo, J., Zhou, H., Liao, J.Y., Ma, L.M., Chen, Y.Q., and Qu, L.H. (2008). Stress-induced tRNA-derived RNAs: a novel class of small RNAs in the primitive eukaryote *Giardia lamblia*. Nucleic Acids Research *36*, 6048–6055.

Lindley, T.A., Chakraborty, P.R., and Edlind, T.D. (1988). Heat shock and stress response in *Giardia lamblia*. Molecular & Biochemical Parasitology *28*, 135–143.

Lindmark, D.G. (1980). Energy metabolism of the anaerobic protozoon *Giardia lamblia*. Molecular & Biochemical Parasitology *1*, 1–12.

Linstead, D.J., and Bradley, S. (1988). The purification and properties of two soluble reduced

nicotinamide: acceptor oxidoreductases from *Trichomonas vaginalis*. Elsevier B.v. *27*, 125–133.

Liu, S.M., Brown, D.M., O'Donoghue, P., Upcroft, P., and Upcroft, J.A. (2000). Ferredoxin involvement in metronidazole resistance of *Giardia duodenalis*. Molecular & Biochemical Parasitology *108*, 137–140.

Lloyd, D. (2004). The plasma membrane of microaerophilic protists: oxidative and nitrosative stress. Microbiology *150*, 1183–1190.

Lloyd, D., CC, H.J., maroulis, S., A, B.G., Wadley, R.B., Turner, M.P., and Edwards, M.R. (2000). The microaerophilic flagellate *Giardia intestinalis*: oxygen and its reaction products collapse membrane potential and cause cytotoxicity. Microbiology *146 Pt 12*, 3109–3118.

Lloyd, D., Harris, J.C., Biagini, G.A., Maroulis, S., Edwards, M.R., Turner, M.P., Ralphs, J.R., Hann, A.C., Wadley, R.B., Ellis, J., et al. (2002). Oxygen homeodynamics in *Giardia* (CABI Publishing).

Lohse, M., Bolger, A.M., Nagel, A., Fernie, A.R., Lunn, J.E., Stitt, M., and Usadel, B. (2012). RobiNA: a user-friendly, integrated software solution for RNA-Seq-based transcriptomics. Nucleic Acids Research *40*, W622–W627.

Löfmark, S., Edlund, C., and Nord, C.E. (2010). Metronidazole Is Still the Drug of Choice for Treatment of Anaerobic Infections. Clin. Infect. Dis. *50*, S16–S23.

Lundström, J., and Holmgren, A. (1990). Protein disulfide-isomerase is a substrate for thioredoxin reductase and has thioredoxin-like activity. J. Biol. Chem. *265*, 9114–9120.

Ma'ayeh, S.Y. (2013). Molecular and cellular interactions of four giardia duodenalis isolates with the murine intestinal epithelial cell line IEC-6 in vitro.

Ma'ayeh, S.Y., and Brook-Carter, P.T. (2012). Representational difference analysis identifies specific genes in the interaction of *Giardia duodenalis* with the murine intestinal epithelial cell line, IEC-6. International Journal for Parasitology *42*, 501–509.

Manning, G., Reiner, D.S., Lauwaet, T., Dacre, M., Smith, A., Zhai, Y., Svärd, S., and Gillin, F.D. (2011). The minimal kinome of *Giardia lamblia* illuminates early kinase evolution and unique parasite biology. Genome Biology *12*, R66.

Martínez-Júlvez, M., Rojas, A.L., Olekhnovich, I., Angarica, V.E., Hoffman, P.S., and Sancho, J. (2012). Structure of RdxA - an oxygen-insensitive nitroreductase essential for metronidazole activation in *Helicobacter pylori*. Febs J. *279*, 4306–4317.

Mastronicola, D., Falabella, M., Testa, F., Pucillo, L.P., Teixeira, M., Sarti, P., Saraiva, L.M., and Giuffrè, A. (2014). Functional Characterization of Peroxiredoxins from the Human Protozoan Parasite *Giardia intestinalis*. PLoS Negl Trop Dis *8*, e2631.

Mastronicola, D., Giuffrè, A., Testa, F., Mura, A., Forte, E., Bordi, E., Pucillo, L.P., Fiori, P.L., and Sarti, P. (2011). *Giardia intestinalis* escapes oxidative stress by colonizing the small intestine: A molecular hypothesis. IUBMB Life *63*, 21–25.

Mastronicola, D., Testa, F., Forte, E., Bordi, E., Pucillo, L.P., Sarti, P., and Giuffrè, A. (2010). Flavohemoglobin and nitric oxide detoxification in the human protozoan parasite *Giardia intestinalis*. Biochemical and Biophysical Research Communications *399*, 654–658.

McArthur, A.G., Knodler, L.A., Silberman, J.D., Davids, B.J., Gillin, F.D., and Sogin, M.L. (2001). The evolutionary origins of eukaryotic protein disulfide isomerase domains: new evidence from the

amitochondriate protist *Giardia lamblia*. Molecular Biology and Evolution *18*, 1455–1463.

McCormick, B.J. (2014). Frequent symptomatic or asymptomatic infections may have long-term consequences on growth and cognitive development. In Old Herborn University Seminar Monographs, P.J. Heitdt, D. Lang, M.S. Riddle, R.I. Walker, and Rusch V, eds. (Institute for Microbiology und Biochemistry, Herborn, Germany).

McIntyre, P., Boreham, P.F., Phillips, R.E., and Shepherd, R.W. (1986). Chemotherapy in giardiasis: clinical responses and in vitro drug sensitivity of human isolates in axenic culture. J. Pediatr. *108*, 1005–1010.

Mendis, A.H., Thompson, R.C., Reynoldson, J.A., Armson, A., Meloni, B.P., and Gunsberg, S. (1992). The uptake and conversion of L-[U14C-] aspartate and L-[U14C-] alanine to 14CO2 by intact trophozoites of *Giardia duodenalis*. Comp. Biochem. Physiol., B *102*, 235–239.

Miyamoto, Y., Kalisiak, J., and Korthals, K. (2013). Expanded therapeutic potential in activity space of next-generation 5-nitroimidazole antimicrobials with broad structural diversity.

Monis, P.T., Caccio, S.M., and Thompson, R.C.A. (2009). Variation in Giardia: towards a taxonomic revision of the genus. Trends in Parasitology *25*, 93–100.

Morokutti, A., Lyskowski, A., Sollner, S., Pointner, E., Fitzpatrick, T.B., Kratky, C., Gruber, K., and Macheroux, P. (2005). Structure and Function of YcnD from *Bacillus subtilis*, a Flavin-Containing Oxidoreductase. Biochemistry *44*, 13724–13733.

Morrison, H.G., McArthur, A.G., Gillin, F.D., Aley, S.B., Adam, R.D., Olsen, G.J., Best, A.A., Cande, W.Z., Chen, F., Cipriano, M.J., et al. (2007). Genomic minimalism in the early diverging intestinal parasite *Giardia lamblia*. Science *317*, 1921–1926.

Mortazavi, A., Williams, B.A., McCue, K., Schaeffer, L., and Wold, B. (2008). Mapping and quantifying mammalian transcriptomes by RNA-Seq. Nat Meth *5*, 621–628.

Motta, M.C., Divecha, N., Lemieux, M., Kamel, C., Chen, D., Gu, W., Bultsma, Y., McBurney, M., and Guarente, L. (2004). Mammalian SIRT1 represses forkhead transcription factors. Cell *116*, 551–563.

Mustacich, D., and Powis, G. (2000). Thioredoxin reductase. Biochem. J *346*, 1–8.

Müller, J., Ley, S., Felger, I., Hemphill, A., and Müller, N. (2008). Identification of differentially expressed genes in a *Giardia lamblia* WB C6 clone resistant to nitazoxanide and metronidazole. Journal of Antimicrobial Chemotherapy *62*, 72–82.

Müller, J., Rout, S., Leitsch, D., Vaithilingam, J., Hehl, A., and Müller, N. (2015). Comparative characterisation of two nitroreductases from *Giardia lamblia* as potential activators of nitro compounds. International Journal for Parasitology: Drugs and Drug Resistance *5*, 37–43.

Müller, J., Schildknecht, P., and Müller, N. (2013). Metabolism of nitro drugs metronidazole and nitazoxanide in *Giardia lamblia*: characterization of a novel nitroreductase (GlNR2). Journal of Antimicrobial Chemotherapy *68*, 1781–1789.

Müller, J., Sterk, M., Hemphill, A., and Müller, N. (2007a). Characterization of *Giardia lamblia* WB C6 clones resistant to nitazoxanide and to metronidazole. J. Antimicrob. Chemother. *60*, 280–287.

Müller, J., Wastling, J., Sanderson, S., Müller, N., and Hemphill, A. (2007b). A Novel *Giardia lamblia* Nitroreductase, GlNR1, Interacts with Nitazoxanide and Other Thiazolides. Antimicrob. Agents

Chemother. *51*, 1979–1986.

Müller, M. (2003). Energy metabolism. Part I: anaerobic protozoa. In Molecular Medical Parasitology, J.J. Marr, T.W. Nilsen, and R. Komuniecki, eds. (London: Academic Press), pp. 125–139.

Mørch, K., Hanevik, K., Rivenes, A.C., Bødtker, J.E., Næss, H.N., Stubhaug, B., Wensaas, K.-A., Rortveit, G., Eide, G.E., Hausken, T., et al. (2013). Chronic fatigue syndrome 5 years after giardiasis: differential diagnoses, characteristics and natural course. BMC Gastroenterology *13*, 1–1.

Nash, T.E., Herrington, D.A., Levine, M.M., Conrad, J.T., and Merritt, J.W. (1990). Antigenic variation of *Giardia lamblia* in experimental human infections. J. Immunol. *144*, 4362–4369.

Nash, T.E., Merritt, J.W., and Conrad, J.T. (1991). Isolate and epitope variability in susceptibility of *Giardia lamblia* to intestinal proteases. Infection and Immunity.

Nash, T.E. (2002). Surface antigenic variation in *Giardia lamblia*. Molecular Microbiology *45*, 585–590.

Nathan, C., and Shiloh, M.U. (2000). Reactive oxygen and nitrogen intermediates in the relationship between mammalian hosts and microbial pathogens. Proc. Natl. Acad. Sci. U.S.a. *97*, 8841–8848.

Naula, C., Parsons, M., and Mottram, J.C. (2005). Protein kinases as drug targets in trypanosomes and Leishmania. Biochimica Et Biophysica Acta (BBA) - Proteins and Proteomics *1754*, 151–159.

Nillius, D., Müller, J., and Müller, N. (2011). Nitroreductase (GlNR1) increases susceptibility of *Giardia lamblia* and *Escherichia coli* to nitro drugs. Journal of Antimicrobial Chemotherapy *66*, 1029–1035.

Nixon, J.E.J., Wang, A., Field, J., Morrison, H.G., McArthur, A.G., Sogin, M.L., Loftus, B.J., and Samuelson, J. (2002). Evidence for lateral transfer of genes encoding ferredoxins, nitroreductases, NADH oxidase, and alcohol dehydrogenase 3 from anaerobic prokaryotes to *Giardia lamblia* and *Entamoeba histolytica*. Eukaryotic Cell *1*, 181–190.

Nolan, M.J., Jex, A.R., Upcroft, J.A., Upcroft, P., and Gasser, R.B. (2011). Barcoding of *Giardia duodenalis* isolates and derived lines from an established cryobank by a mutation scanning-based approach. Electrophoresis *32*, 2075–2090.

Olekhnovich, I.N., Goodwin, A., and Hoffman, P.S. (2009). Characterization of the NAD(P)H oxidase and metronidazole reductase activities of the RdxA nitroreductase of Helicobacter pylori. Febs J. *276*, 3354–3364.

Pacher, P., Beckman, J.S., and Liaudet, L. (2007). Nitric Oxide and Peroxynitrite in Health and Disease. Physiological Reviews *87*, 315–424.

Paget, T.A., Macechko, P.T., and jarroll, E.L. (1998). Metabolic changes in *Giardia intestinalis* during differentiation. J. Parasitol. *84*, 222–226.

Paget, T., Maroulis, S., Mitchell, A., Edwards, M.R., Jarroll, E.L., and Lloyd, D. (2004). Menadione kills trophozoites and cysts of *Giardia intestinalis*. Microbiology *150*, 1231–1236.

Pal, D., Banerjee, S., Cui, J., Schwartz, A., Ghosh, S.K., and Samuelson, J. (2009). *Giardia*, *Entamoeba*, and *Trichomonas* enzymes activate metronidazole (nitroreductases) and inactivate

metronidazole (nitroimidazole reductases). Antimicrob. Agents Chemother. *53*, 458–464.

Pathuri, P., Nguyen, E.T., Ozorowski, G., Svärd, S.G., and Luecke, H. (2009). Apo and Calcium-Bound Crystal Structures of Cytoskeletal Protein Alpha-14 Giardin (Annexin E1) from the Intestinal Protozoan Parasite *Giardia lamblia*. Journal of Molecular Biology *385*, 1098–1112.

Pays, E., Vanhamme, L., and Pérez-Morga, D. (2004). Antigenic variation in Trypanosoma brucei: facts, challenges and mysteries. Curr. Opin. Microbiol. *7*, 369–374.

Pazdzior, R., Yang, Z.A., Mesbahuddin, M.S., Yee, J., van der Est, A., and Rafferty, S. (2015). Low reduction potential cytochrome b_5 isotypes of *Giardia intestinalis*. Experimental Parasitology *157*, 197–201.

Pettersen, E.F., Goddard, T.D., Huang, C.C., Couch, G.S., Greenblatt, D.M., Meng, E.C., and Ferrin, T.E. (2004). UCSF Chimera — A visualization system for exploratory research and analysis. J. Comput. Chem. *25*, 1605–1612.

Pineda, E., Encalada, R., Rodríguez-Zavala, J.S., Olivos-García, A., Moreno-Sánchez, R., and Saavedra, E. (2010). Pyruvate:ferredoxin oxidoreductase and bifunctional aldehyde-alcohol dehydrogenase are essential for energy metabolism under oxidative stress in Entamoeba histolytica. FEBS Journal *277*, 3382–3395.

Poxleitner, M.K., Carpenter, M.L., Mancuso, J.J., Wang, C.J.R., Dawson, S.C., and Cande, W.Z. (2008). Evidence for Karyogamy and Exchange of Genetic Material in the Binucleate Intestinal Parasite *Giardia intestinalis*. Science *319*, 1530–1533.

Prucca, C.G., and Lujan, H.D. (2009). Antigenic variation in *Giardia lamblia*. Cell. Microbiol. *11*, 1706–1715.

Prucca, C.G., Slavin, I., Quiroga, R., Elías, E.V., Rivero, F.D., Saura, A., Carranza, P.G., and Lujan, H.D. (2008). Antigenic variation in *Giardia lamblia* is regulated by RNA interference. Nature *456*, 750–754.

Pyrih, J., Harant, K., Martincová, E., Sutak, R., Lesuisse, E., Hrdy, I., and Tachezy, J. (2014). *Giardia intestinalis* incorporates heme into cytosolic cytochrome b_5. Eukaryotic Cell *13*, 231–239.

Rafferty, S., Luu, B., March, R.E., and Yee, J. (2010). *Giardia lamblia* encodes a functional flavohemoglobin. Biochemical and Biophysical Research Communications *399*, 347–351.

Ragan, C., Zuker, M., and Ragan, M.A. (2011). Quantitative Prediction of miRNA-mRNA Interaction Based on Equilibrium Concentrations. PLoS Comput Biol *7*, e1001090.

Ringqvist, E., Avesson, L., Söderbom, F., and Svärd, S.G. (2011). Transcriptional changes in Giardia during host-parasite interactions. International Journal for Parasitology *41*, 277–285.

Ringqvist, E., Palm, J.E.D., Skarin, H., Hehl, A.B., Weiland, M., Davids, B.J., Reiner, D.S., Griffiths, W.J., Eckmann, L., Gillin, F.D., et al. (2008). Release of metabolic enzymes by *Giardia* in response to interaction with intestinal epithelial cells. Molecular & Biochemical Parasitology *159*, 85–91.

Roberts, A., Goff, L., Pertea, G., Kim, D., Kelley, D.R., Pimentel, H., Salzberg, S.L., Rinn, J.L., Pachter, L., and Trapnell, C. (2012). Differential gene and transcript expression analysis of RNA-seq experiments with TopHat and Cufflinks. Nat Protoc *7*, 562–578.

Robertson, L.J., Hanevik, K., Escobedo, A.A., Mørch, K., and Langeland, N. (2010). Giardiasis–why do the symptoms sometimes never stop? Trends in Parasitology *26*, 75–82.

Robinson, M.D., McCarthy, D.J., and Smyth, G.K. (2009). edgeR: a Bioconductor package for differential expression analysis of digital gene expression data. Bioinformatics *26*, 139–140.

Rost, B. (1999). Twilight zone of protein sequence alignments. Protein Eng. *12*, 85–94.

Roy, A., Kucukural, A., and Zhang, Y. (2010). I-TASSER: a unified platform for automated protein structure and function prediction. Nat Protoc *5*, 725–738.

Rühl, M., Le Coq, D., Aymerich, S., and Sauer, U. (2012). ^{13}C-flux analysis reveals NADPH-balancing transhydrogenation cycles in stationary phase of nitrogen-starving *Bacillus subtilis*. Journal of Biological Chemistry *287*, 27959–27970.

Samuelson, J. (1999). Why metronidazole is active against both bacteria and parasites. Antimicrob. Agents Chemother. *43*, 1533–1541.

Saraiya, A.A., and Wang, C.C. (2008). snoRNA, a novel precursor of microRNA in *Giardia lamblia*. PLoS Pathog. *4*, e1000224.

Saraiya, A.A., Li, W., Wu, J., Chang, C.H., and Wang, C.C. (2014). The microRNAs in an Ancient Protist Repress the Variant-Specific Surface Protein Expression by Targeting the Entire Coding Sequence. PLoS Pathog. *10*, e1003791.

Savioli, L., Smith, H., and Thompson, A. (2006). Giardia and Cryptosporidium join the 'Neglected Diseases Initiative'. Trends in Parasitology *22*, 203–208.

Sánchez, L.B., Elmendorf, H., Nash, T.E., and Müller, M. (2001). NAD(P)H:menadione oxidoreductase of the amitochondriate eukaryote *Giardia lamblia*: a simpler homologue of the vertebrate enzyme. Microbiology (Reading, Engl.) *147*, 561–570.

Schenkman, J.B., and Jansson, I. (2003). The many roles of cytochrome b5. Pharmacology and Therapeutics *97*, 139–152.

Schofield, P.J., Costello, M., Edwards, M.R., and O'Sullivan, W.J. (1990). The arginine dihydrolase pathway is present in *Giardia intestinalis*. International Journal for Parasitology *20*, 697–699.

Schofield, P.J., Edwards, M.R., Matthews, J., and Wilson, J.R. (1992). The pathway of arginine catabolism in *Giardia intestinalis*. Molecular & Biochemical Parasitology *51*, 29–36.

Sisson, G., Jeong, J.Y., Goodwin, A., Bryden, L., Rossler, N., Lim-Morrison, S., Raudonikiene, A., Berg, D.E., and Hoffman, P.S. (2000). Metronidazole Activation Is Mutagenic and Causes DNA Fragmentation in Helicobacter pylori and in Escherichia coli Containing a Cloned H. pylori rdxA+ (Nitroreductase) Gene. J. Bacteriol. *182*, 5091–5096.

Smith, N.C., Bryant, C., and Boreham, P.F. (1988). Possible roles for pyruvate:ferredoxin oxidoreductase and thiol-dependent peroxidase and reductase activities in resistance to nitroheterocyclic drugs in *Giardia intestinalis*. International Journal for Parasitology *18*, 991–997.

Smith, P.D., Gillin, F.D., Spira, W.M., and Nash, T.E. (1982). Chronic giardiasis: studies on drug sensitivity, toxin production, and host immune response. Ygast *83*, 797–803.

Solaymani-Mohammadi, S., Genkinger, J.M., Loffredo, C.A., and Singer, S.M. (2010). A meta-analysis of the effectiveness of albendazole compared with metronidazole as treatments for infections with *Giardia duodenalis*. PLoS Negl Trop Dis *4*, e682.

Sonda, S., Morf, L., Bottova, I., Baetschmann, H., Rehrauer, H., Caflisch, A., Hakimi, M.-A., and Hehl,

A.B. (2010). Epigenetic mechanisms regulate stage differentiation in the minimized protozoan *Giardia lamblia*. Molecular Microbiology *76*, 48–67.

Soto-Méndez, M., Aguilera, C., Mesa, M., Campaña-Martín, L., Martín-Laguna, V., Solomons, N., Schümann, K., and Gil, A. (2014). Relationship between oxidative stress biomarkers in urine and erythrocytes, and to estimates of fecal *Giardia intestinalis* intensity in Guatemalan preschool children with a common menu offering (639.3). The FASEB Journal *28*.

Spillman, N.J., and Kirk, K. (2015). International Journal for Parasitology:Drugs and Drug Resistance. International Journal for Parasitology: Drugs and Drug Resistance *5*, 149–162.

Spycher, C., Herman, E.K., Morf, L., Qi, W., Rehrauer, H., Aquino Fournier, C., DACKS, J.B., and Hehl, A.B. (2013). An ER-directed transcriptional response to unfolded protein stress in the absence of conserved sensor-transducer proteins in *Giardia lamblia*. Molecular Microbiology *88*, 754–771.

Sun, C.-H., Su, L.-H., and Gillin, F.D. (2006). Novel plant-GARP-like transcription factors in *Giardia lamblia*. Molecular & Biochemical Parasitology *146*, 45–57.

Svärd, S.G., Meng, T.-C., Hetsko, M.L., McCaffery, J.M., and Gillin, F.D. (1998). Differentiation-associated surface antigen variation in the ancient eukaryote *Giardia lamblia*. Molecular Microbiology *30*, 979–989.

Tai, C.-H., Bai, H., Taylor, T.J., and Lee, B. (2013). Assessment of template-free modeling in CASP10 and ROLL. Proteins *82*, 57–83.

Tako, E.A., Hassimi, M.F., Li, E., and Singer, S.M. (2013). Transcriptomic Analysis of the Host Response to *Giardia duodenalis* Infection Reveals Redundant Mechanisms for Parasite Control. *4*, e00660–13–e00660–13.

Tejman-Yarden, N., Miyamoto, Y., Leitsch, D., Santini, J., Debnath, A., Gut, J., McKerrow, J.H., Reed, S.L., and Eckmann, L. (2013). A Reprofiled Drug, Auranofin, Is Effective against Metronidazole-Resistant *Giardia lamblia*. Antimicrob. Agents Chemother. *57*, 2029–2035.

Tejman-Yarden, N., Millman, M., Lauwaet, T., Davids, B.J., Gillin, F.D., Dunn, L., Upcroft, J.A., Miyamoto, Y., and Eckmann, L. (2011). Impaired parasite attachment as fitness cost of metronidazole resistance in *Giardia lamblia*. Antimicrob. Agents Chemother. *55*, 4643–4651.

Tekwani, B.L., and Mehlotra, R.K. (1999). Molecular basis of defence against oxidative stress in *Entamoeba histolytica* and *Giardia lamblia*. Microbes and Infection *1*, 385–394.

Teodorovic, S., Walls, C.D., and Elmendorf, H.G. (2007). Bidirectional transcription is an inherent feature of *Giardia lamblia* promoters and contributes to an abundance of sterile antisense transcripts throughout the genome. Nucleic Acids Research *35*, 2544–2553.

Testa, F., Giuffrè, A., Mastronicola, D., Forte, E., and Sarti, P. (2011a). Enzymatic detoxification of O2 and NO in the human parasite, *Giardia intestinalis*: A mini review. Indian Journal of Biotechnology *10*, 404–409.

Testa, F., Mastronicola, D., Cabelli, D.E., Bordi, E., Pucillo, L.P., Sarti, P., Saraiva, L.M., Giuffrè, A., and Teixeira, M. (2011b). The superoxide reductase from the early diverging eukaryote *Giardia intestinalis*. Free Radic. Biol. Med. *51*, 1567–1574.

Tolba, M.E.M., Kobayashi, S., Imada, M., Suzuki, Y., and Sugano, S. (2013). *Giardia lamblia* Transcriptome Analysis Using TSS-Seq and RNA-Seq. PLoS ONE *8*, e76184.

Touz, M.C., Rópolo, A.S., Rivero, M.R., Vranych, C.V., Conrad, J.T., Svard, S.G., and Nash, T.E. (2008). Arginine deiminase has multiple regulatory roles in the biology of *Giardia lamblia*. J. Cell. Sci. *121*, 2930–2938.

Townson, S.M., Boreham, P.F., Upcroft, P., and Upcroft, J.A. (1994a). Resistance to the nitroheterocyclic drugs. Acta Tropica *56*, 173–194.

Townson, S.M., Hanson, G.R., Upcroft, J.A., and Upcroft, P. (1994b). A purified ferredoxin from *Giardia duodenalis*. Eur. J. Biochem. *220*, 439–446.

Townson, S.M., Laqua, H., Upcroft, P., Boreham, P.F., and Upcroft, J.A. (1992). Induction of metronidazole and furazolidone resistance in *Giardia*. Trans. R. Soc. Trop. Med. Hyg. *86*, 521–522.

Townson, S.M., Upcroft, J.A., and Upcroft, P. (1996). Characterisation and purification of pyruvate: ferredoxin oxidoreductase from *Giardia duodenalis*. Molecular & Biochemical Parasitology *79*, 183–193.

Trammell, S.A., and Brenner, C. (2013). Targeted, LCMS-based Metabolomics for Quantitative Measurement of NAD(+) Metabolites. Comput Struct Biotechnol J *4*, e201301012.

Tsugawa, H., Suzuki, H., Satoh, K., Hirata, K., Matsuzaki, J., Saito, Y., Suematsu, M., and Hibi, T. (2011). Two amino acids mutation of ferric uptake regulator determines Helicobacter pylori resistance to metronidazole. Antioxidants & Redox Signaling *14*, 15–23.

Upcroft, J.A., Healey, A., Murray, D.G., Boreham, P.F., and Upcroft, P. (1992). A gene associated with cell division and drug resistance in *Giardia duodenalis*. Parasitology *104 (Pt 3)*, 397–405.

Upcroft, J.A., Upcroft, P., and Boreham, P.F.L. (1990). Drug resistance in *Giardia intestinalis*. International Journal for Parasitology *20*, 489–496.

Upcroft, J.A., Mitchel, R., Chen, N., and Upcroft, P. (1996). Albendazole resistance in Giardia is correlated with cytoskeletal changes but not with a mutation at amino acid 200 in beta-tubulin. Microb Drug Resist *2*, 303–308.

Upcroft, P., and Upcroft, J.A. (2001). Drug Targets and Mechanisms of Resistance in the Anaerobic Protozoa. Clinical Microbiology Reviews *14*, 150–164.

Uzlikova, M., and Nohýnková, E. (2014). The effect of metronidazole on the cell cycle and DNA in metronidazole-susceptible and -resistant Giardia cell lines. Molecular & Biochemical Parasitology *198*, 75–81.

Verdu, E.F., and Riddle, M.S. (2012). Chronic gastrointestinal consequences of acute infectious diarrhea: evolving concepts in epidemiology and pathogenesis. Am. J. Gastroenterol. *107*, 981–989.

Vicente, J.B., Testa, F., Mastronicola, D., Forte, E., Sarti, P., Teixeira, M., and Giuffrè, A. (2009). Archives of Biochemistry and Biophysics. Archives of Biochemistry and Biophysics *488*, 9–13.

Wagner, G., and Levin, R. (1978). Oxygen tension of the vaginal surface during sexual stimulation in the human. Fertil Steril *30*, 50–53.

Wampfler, P.B., Faso, C., and Hehl, A.B. (2014). The Cre/loxP system in *Giardia lamblia*: genetic manipulations in a binucleate tetraploid protozoan. International Journal for Parasitology *44*, 497–506.

Wang, C.H., Su, L.H., and Sun, C.H. (2007). A novel ARID/Bright-like protein involved in transcriptional activation of cyst wall protein 1 gene in *Giardia lamblia*. Journal of Biological Chemistry.

Wang, Y.-H., Zheng, G.-X., and Li, Y.-J. (2016). *Giardia duodenalis* GlSir2.2, homolog of SIRT1, is a nuclear-located and NAD(+)-dependent deacethylase. Experimental Parasitology *169*, 28–33.

Weiland, M.E.-L., McArthur, A.G., Morrison, H.G., Sogin, M.L., and Svärd, S.G. (2005). Annexin-like alpha giardins: a new cytoskeletal gene family in *Giardia lamblia*. International Journal for Parasitology *35*, 617–626.

Woodruff, B.K., Wijdicks, E.F.M., and Marshall, W.F. (2002). Reversible metronidazole-induced lesions of the cerebellar dentate nuclei. N Engl J Med *346*, 68–69.

Wright, J.M., Dunn, L.A., and Upcroft, P. (2003). Efficacy of antigiardial drugs. Expert Opinion on Drug Safety *2*, 529–541.

Wu, S., Skolnick, J., and Zhang, Y. (2007). Ab initio modeling of small proteins by iterative TASSER simulations. BMC Biol *5*, 17.

Yang, Z.A., Pazdzior, R., Yee, J., and Rafferty, S. (2016). Reduction potential and heme-pocket polarity in low potential cytochrome b5 of *Giardia intestinalis*. J. Inorg. Biochem.

Yee, J., Mowatt, M.R., Dennis, P.P., and Nash, T.E. (2000). Transcriptional analysis of the glutamate dehydrogenase gene in the primitive eukaryote, *Giardia lamblia*. Identification of a primordial gene promoter. J. Biol. Chem. *275*, 11432–11439.

Zanger, U.M., and Schwab, M. (2013). Pharmacology & Therapeutics. Pharmacology and Therapeutics *138*, 103–141.

Zhang, Y., and Skolnick, J. (2005). TM-align: a protein structure alignment algorithm based on the TM-score. Nucleic Acids Research *33*, 2302–2309.

Appendix I: Ansell et al. (2015) *Biotechnology Advances*

Biotechnology Advances 33 (2015) 888–901

Contents lists available at ScienceDirect

Biotechnology Advances

journal homepage: www.elsevier.com/locate/biotechadv

Research review paper

Drug resistance in *Giardia duodenalis*

Brendan R.E. Ansell [a,*], Malcolm J. McConville [b], Showgy Y. Ma'ayeh [c], Michael J. Dagley [b], Robin B. Gasser [a], Staffan G. Svärd [c], Aaron R. Jex [a]

[a] Faculty of Veterinary and Agricultural Sciences, University of Melbourne, Cnr Park Dr and Flemington Rd, Parkville, VIC 3010, Australia
[b] Bio21 Institute, University of Melbourne, 30 Flemington Rd, Parkville, VIC 3010, Australia
[c] Department of Cell and Molecular Biology, Biomedical Center, Uppsala University, Box 596, SE-751 24 Uppsala, Sweden

ARTICLE INFO

Article history:
Received 20 February 2015
Received in revised form 21 April 2015
Accepted 21 April 2015
Available online 25 April 2015

Keywords:
Giardia
Nitroheterocyclic
Drug resistance
Metronidazole
Nitazoxanide
Furazolidone
NAD(P)H oxidoreductase
Sir2 NAD-dependent histone deacetylase
Treatment failure

ABSTRACT

Giardia duodenalis is a microaerophilic parasite of the human gastrointestinal tract and a major contributor to diarrheal and post-infectious chronic gastrointestinal disease world-wide. Treatment of *G. duodenalis* infection currently relies on a small number of drug classes. Nitroheterocyclics, in particular metronidazole, have represented the front line treatment for the last 40 years. Nitroheterocyclic-resistant *G. duodenalis* have been isolated from patients and created in vitro, prompting considerable research into the biomolecular mechanisms of resistance. These compounds are redox-active and are believed to damage proteins and DNA after being activated by oxidoreductase enzymes in metabolically active cells. In this review, we explore the molecular phenotypes of nitroheterocyclic-resistant *G. duodenalis* described to date in the context of the protist's unusual glycolytic and antioxidant systems. We propose that resistance mechanisms are likely to extend well beyond currently described resistance-associated enzymes (i.e., pyruvate ferredoxin oxidoreductases and nitroreductases), to include NAD(P)H- and flavin-generating pathways, and possibly redox-sensitive epigenetic regulation. Mechanisms that allow *G. duodenalis* to tolerate oxidative stress may lead to resistance against both oxygen and nitroheterocyclics, with implications for clinical control. The present review highlights the potential for systems biology tools and advanced bioinformatics to further investigate the multifaceted mechanisms of nitroheterocyclic resistance in this important pathogen.

© 2015 Elsevier Inc. All rights reserved.

Contents

1. Introduction . . . 889
2. The microaerophilic lifestyle of *G. duodenalis* . . . 889
   2.1. The antioxidant system . . . 889
   2.2. Electron transport cofactors and the energetic advantage of oxygen . . . 892
3. Nitroheterocyclic resistance in *G. duodenalis* . . . 893
   3.1. Metronidazole . . . 893
      3.1.1. Chemistry, cytotoxicity and metabolism . . . 893
      3.1.2. Resistance markers and cross-resistance . . . 894
      3.1.3. Other nitroheterocyclics . . . 894
      3.1.4. Functional enzyme regulation by cofactor modulation . . . 895
4. Epigenetic regulation in nitroheterocyclic-resistant *G. duodenalis* . . . 896
   4.1. Redox-sensitive epigenetic regulators . . . 896
5. A link between gut conditions and treatment failure? . . . 896
6. Systems biology for understanding drug resistance . . . 897
7. Nitroheterocyclic activation and resistance in other microaerophiles . . . 897
8. Conclusion . . . 898
Acknowledgments . . . 898
Appendix A. Supplementary data . . . 898
References . . . 898

* Corresponding author.
E-mail address: bransell@unimelb.edu.au (B.R.E. Ansell).

http://dx.doi.org/10.1016/j.biotechadv.2015.04.009
0734-9750/© 2015 Elsevier Inc. All rights reserved.

1. Introduction

Giardia duodenalis (syn. *Giardia lamblia* or *Giardia intestinalis*) is a gastrointestinal parasitic protist that infects approximately one billion people world-wide and causes 200–300 million cases of disease (giardiasis) each year (Lane and Lloyd, 2002). Infection may be acute or chronic, and symptoms include nausea, vomiting, diarrhea and dehydration (Farthing, 1996; Robertson et al., 2010). *G. duodenalis* infection has been reported in approximately 15% of children aged 0–24 months in the developing world (McCormick, 2014) and contributes to the global burden of diarrheal diseases that collectively constitute the second-leading cause of death in children under five years of age (Kosek et al., 2003; Savioli et al., 2006). Infection can also cause malabsorption syndrome and failure to thrive. Indeed, as few as 3 episodes of chronic (>2 week duration) diarrheal disease per year in the first 24 months of life is associated with significant reductions in height (approximately 10 cm) and IQ (10 points) by 7–9 years of age (Guerrant et al., 2013). *G. duodenalis* infection induces physical stunting and modified gut physiology in laboratory animals (Bartelt et al., 2013). In humans, pathophysiological changes in the gut may persist long after *G. duodenalis* infection is cleared (Halliez, 2013), and so this parasite is also implicated in the etiology of major non-communicable diseases such as irritable bowel syndrome, chronic fatigue, obesity and type II diabetes (Mørch et al., 2013; Verdu and Riddle, 2012).

G. duodenalis is transmitted via environmentally resilient cysts shed in the feces of an infected individual, which are then ingested (e.g., in contaminated water or food). Upon ingestion and passage through the stomach, trophozoites emerge from cysts to colonize the small intestine. Treatment is largely limited to two drug classes: nitroheterocyclic compounds (e.g., metronidazole (MET), nitazoxanide and furazolidone) and benzimidazoles (e.g., albendazole (ALB) and mebendazole) (Escobedo and Cimerman, 2007; Wright et al., 2003). Paromomycin and quinacrine are also occasionally used to treat giardiasis, but pose problems due to low efficacy and high toxicity respectively (Escobedo and Cimerman, 2007). Treatment efficacy is 73–100% for MET, and 79–100% for ALB (Gardner and Hill, 2001; Solaymani-Mohammadi et al., 2010), suggesting that initial treatment failure is relatively common. Although non-compliance or immune deficiency may contribute to treatment failures, isolates from patients who were unsuccessfully treated with either MET or ALB have demonstrated resistance to the prescribed drug in the laboratory (Abboud et al., 2001; Adagu et al., 2002; Lemée et al., 2000; McIntyre et al., 1986). Whereas relatively few studies have focused on benzimidazole resistance in *G. duodenalis* (Argüello-García et al., 2009; Jiménez-Cardoso et al., 2004, 2009; Paz-Maldonado et al., 2012; Upcroft et al., 1996), nitroheterocyclic resistance has been extensively studied (Boreham et al., 1991; Gillin and Reiner, 1982; Smith et al., 1988; Townson et al., 1994a; Upcroft and Upcroft, 2001) and is thus the focus of the present review. Nitroheterocyclics enter the cell through passive diffusion, are generally activated by oxidoreductase enzymes and appear to induce oxidative stress, leading to protein and DNA damage (Edwards, 1993a; Leitsch et al., 2012a). Investigation of laboratory-derived nitroheterocyclic-resistant lines (Townson et al., 1992) has linked resistance to differential regulation of oxidoreductase enzymes (Leitsch et al., 2011; Müller et al., 2007a, 2008, 2013; Tejman-Yarden et al., 2011), and certain clinical isolates appear naturally resistant to nitroheterocyclics prior to treatment (Smith et al., 1988; Townson et al., 1994a). The present review considers the implications of differential oxidoreductase activity in the context of the multifaceted antioxidant system in *G. duodenalis*, and identifies points of convergence between the mechanisms of response and resistance to nitroheterocyclic compounds, and oxygen and its reactive metabolites. This work provides a timely consolidation of our understanding of nitroheterocyclic resistance in *G. duodenalis*, and highlights key areas and technologies for further exploration.

2. The microaerophilic lifestyle of *G. duodenalis*

G. duodenalis belongs to a phylogenetically diverse 'group' of microaerophilic protists and bacteria, which thrive in environments with low dissolved oxygen (dO_2) of approximately 5–80 μM, but fail to survive under atmospheric dO_2 concentrations (298 μM) (Krieg and Hoffman, 1986; Lane and Lloyd, 2002). Other medically important microaerophiles include the parasitic protists *Trichomonas vaginalis* and *Entamoeba histolytica*, and bacteria such as *Helicobacter pylori* and *Campylobacter jejuni* (Lloyd, 2004; Lloyd et al., 1989). The microaerophilic metabolism of *G. duodenalis* appears to have been shaped by fluctuating oxygen levels and commensal bacteria in the host intestine. In natural infections, *G. duodenalis* trophozoites attach to the intestinal mucosa, and detach periodically, especially during division. Concentrations of dO_2 in this environment fluctuate from 0–80 μM depending on the metabolic activity of host enterocytes; the oxygen affinity of other commensal microbes (Espey, 2013); the antioxidant richness of host bile, and proximity to the anoxic luminal mid-point (Espey, 2013; Mastronicola et al., 2011).

Products of lateral gene transfer (LGT) from anaerobic bacteria, allow *G. duodenalis* to maximize energy production under low dO_2 conditions (Morrison et al., 2007; Nixon et al., 2002; Pal et al., 2009). For example, the remnant mitochondria of *G. duodenalis* lack a tricarboxylic acid cycle and oxidative phosphorylation, but the organism has acquired enzymes of likely LGT origin that support fermentative glycolysis (Lindmark, 1980), the arginine dihydrolase pathway (Schofield et al., 1990, 1992) and substrate-level ATP generation (Adam, 2001; Han and Collins, 2012; Mendis et al., 1992) (Supplementary Fig. 1). Many LGT-derived *G. duodenalis* enzymes contain catalytic iron, which renders them liable to inactivation under higher dO_2 concentrations (Dan et al., 2000; Gillin and Reiner, 1982; Lloyd, 2004; Lloyd et al., 2002). Notable among these oxygen-sensitive enzymes are two pyruvate ferredoxin oxidoreductases (PFOR-1 and -2) that decarboxylate pyruvate to acetyl-CoA and shuttle the resultant electrons to ferredoxin via iron–sulfur clusters (Chabriere et al., 2011; Horner et al., 1999; Nixon et al., 2002; Townson et al., 1996) (Fig. 1). In *E. histolytica*, oxidation of PFOR iron–sulfur clusters is associated with enzyme inactivation and the generation of reactive oxygen species (ROS) (Pineda et al., 2010), which in *G. duodenalis*, can lead to disruption of the plasma membrane potential and parasite death (Lloyd et al., 2000). In contrast, other iron-dependent enzymes (aka metalloenzymes) in the antioxidant network of *G. duodenalis* (including LGT products), appear to be more resistant to dO_2 inactivation, and may therefore be involved in dO_2 detoxification processes (Goncalves et al., 2014; Mastronicola et al., 2010; Müller et al., 2013; Nixon et al., 2002; Pal et al., 2009; Rafferty et al., 2010; Testa et al., 2011; Vicente et al., 2009).

2.1. The antioxidant system

G. duodenalis lacks superoxide dismutase, catalase (Brown et al., 1995; Morrison et al., 2007), and glutathione cycling (Brown et al., 1993), but expresses at least two oxidoreductases, likely derived through LGT, that consume dO_2 and produce water. A 46 kDa enzyme termed 'NADH oxidase' was the first of these oxidoreductases to be identified, although subsequent studies showed that it preferentially utilizes NADPH as a source of electrons to reduce oxygen (Brown et al., 1996a) (see Table 1 for gene identifiers). More recently, a NADH-dependent flavodiiron protein with water-forming activity has been characterized (Di Matteo et al., 2007; Mastronicola et al., 2011). Reduction of dO_2 to water by these oxidoreductases limits the production of superoxide and hydrogen peroxide ROS (resulting from uni- and divalent reduction of dO_2, respectively). However, these systems appear to be saturated at dO_2 concentrations of ~25 μM, as indicated by progressive loss of dO_2 consumption above this concentration (Lloyd et al., 2002). In addition to inhibiting PFOR and other metalloenzymes, excessive dO_2 accumulation can stimulate ROS production by other enzymes. For example,

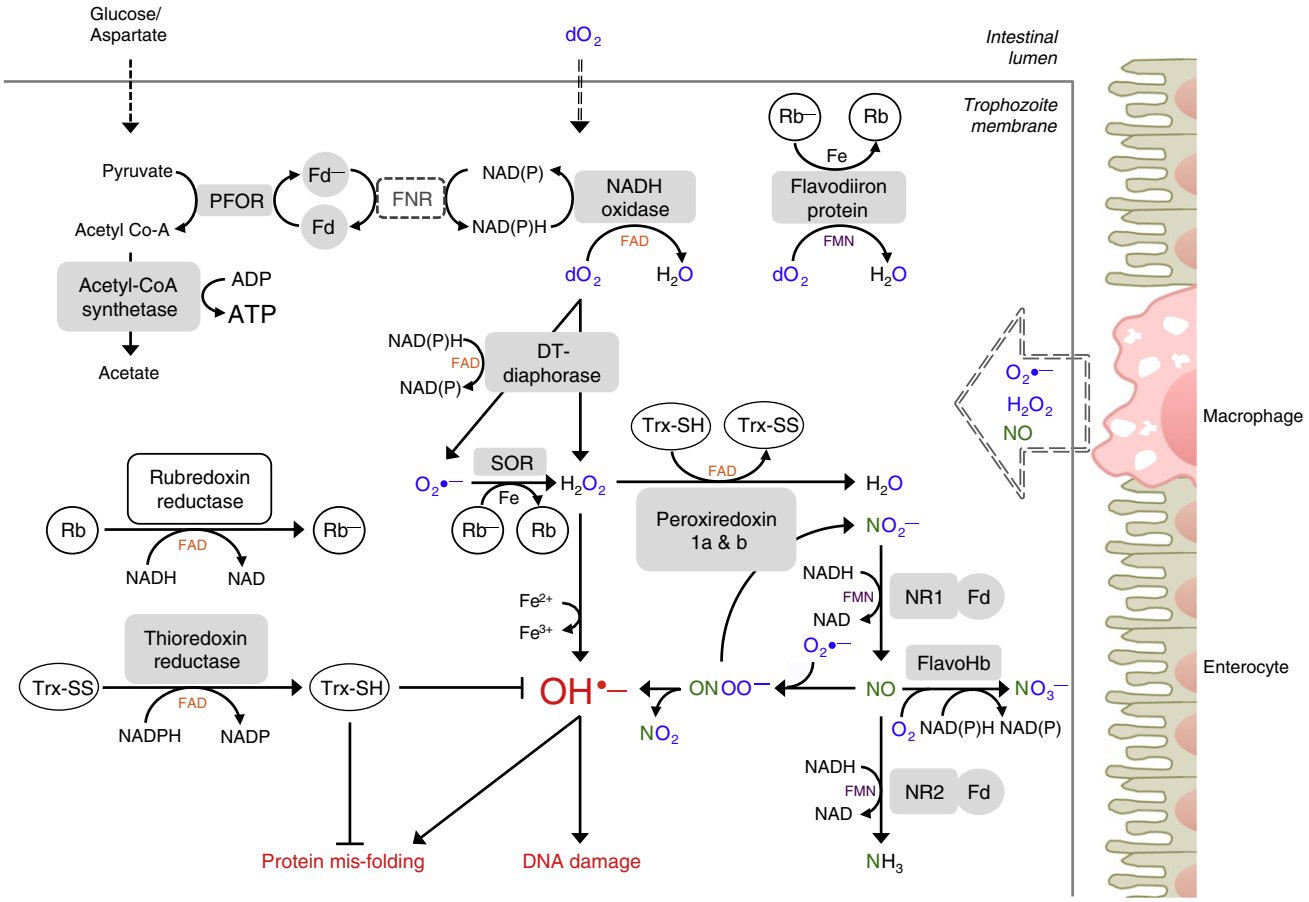


Fig 1. ATP production and the antioxidant system in *Giardia duodenalis* trophozoites in the context of a natural infection. Dissolved molecular oxygen (dO_2) and macrophage-generated hydrogen peroxide (H2O2), superoxide ($O_2^{\bullet-}$) and nitric oxide (NO), diffuse into the parasite from the intestinal lumen. NADH and/or NADPH (collectively NAD(P)H) provide electrons to reduce dO_2, NO and associated reactive oxygen- and nitrogen species. Pyruvate and acetyl-coA are therefore available for further oxidation to acetate, yielding ATP. Functionally characterized enzymes are shaded gray. Enzymes outlined in black have not been characterized in *G. duodenalis* to date but functionally analogous enzymes are inferred to exist in the parasite based on experiments using *Escherichia coli* enzymes. Enzymes for which there is neither genomic nor functional evidence are displayed with perforated outline. PFOR: pyruvate ferredoxin oxidoreductase; Fd: ferredoxin; Fe^{2+}: ferrous iron; Fe^{3+}: ferric iron; NAD(P): oxidized nicotinamide adenine dinucleotide (phosphate); FAD: flavin adenine dinucleotide; FMN: flavin mononucleotide; FNR: ferredoxin NAD(P) reductase; Rb: rubredoxin; SOR: superoxide reductase; Trx-SH/SS: reduced/oxidized thioredoxin; NR: nitroreductase; FlavoHb: flavohemoglobin; NO_2^-: nitrite; NO_3^-: nitrate; $ONOO^-$: peroxinitrite; $OH^{\bullet-}$: hydroxyl radical.

DT-diaphorase (aka NAD(P)H:menadione oxidoreductase) catalyses the partial reduction of dO_2 to superoxide and hydrogen peroxide, and is therefore considered to be a major contributor to oxygen sensitivity in *G. duodenalis* (Li and Wang, 2006; Lindmark, 1980; Paget et al., 2004; Sánchez et al., 2001). Superoxide accumulation may be managed by an iron-dependent superoxide reductase (SOR) that converts superoxide to hydrogen peroxide without regenerating molecular oxygen (Testa et al., 2011). Hydrogen peroxide can then be reduced to water by peroxiredoxins 1a and 1b (Mastronicola et al., 2014). If these peroxiredoxins are overwhelmed, hydrogen peroxide may react with divalent cations (e.g., Fe^{2+}, Cu^{2+}) to form the hydroxyl radical (Edwards, 1993a,1993b; Pacher et al., 2007), which is proposed to be the most cytotoxic ROS.

In addition to endogenous ROS, *G. duodenalis* may be exposed to exogenous ROS and reactive nitrogen species (RNS) produced by epithelial cells, macrophages and granulocytes in the host intestinal wall. These cells release superoxide, hydrogen peroxide and nitric oxide (NO) in response to gastrointestinal parasites (Arbo et al., 2006; Maloney et al., in press; Nathan and Shiloh, 2000; Tako et al., 2013). Superoxide can react with NO to form peroxynitrite, which decomposes to form the hydroxyl radical (Pacher et al., 2007) (Fig. 1). Extracellular and intracellular proteins are suggested to combat host-derived ROS and RNS. High-cysteine membrane proteins (HCMPs) and cysteine-rich variant-specific surface proteins (VSPs) may absorb extracellular ROS and RNS to minimize intracellular damage (Adam et al., 1992; Gillin et al., 1990; Ringqvist et al., 2011). *G. duodenalis* also secretes an arginine deiminase (ADI) that can deplete host arginine, which is required for NO synthesis (Eckmann et al., 2000; Knodler, 1998; Li et al., 2009; Ringqvist et al., 2008; Touz et al., 2008). Within the trophozoite, NO may be detoxified through conversion to nitrate, by flavohemoglobin (dO_2-dependent), or to an amine by the ferredoxin-containing nitroreductase NR-2 (Mastronicola et al., 2010; Müller et al., 2013, 2015; Rafferty et al., 2010). Conversely, another ferredoxin-containing nitroreductase, NR-1, is implicated in the production of endogenous NO through partial reduction of nitrate/nitrite, based on the finding that both the NO and DNA-damage responses are elicited in *Escherichia coli* reporter strains when transfected with this *G. duodenalis* enzyme (Müller et al., 2013). Recent evidence suggests that NR-1 and NR-2 can also reduce a range of other substrates including menadione, and act in concert as an enzyme complex (Müller et al., 2015). As a further line of defense against RNS, peroxiredoxins may detoxify peroxynitrite (Mastronicola et al., 2014) to prevent formation of the hydroxyl radical (Ma'ayeh and Brook-Carter, 2012; Pacher et al., 2007) (Fig. 1) (Table 1).

Intracellular hydroxyl radicals can be scavenged by cysteine (Brown et al., 1993), cysteine thioglycolate (a non-protein thiol) (Brown et al., 1998; Tekwani and Mehlotra, 1999), and pyruvate (Biagini et al., 2001).

Table 1
Substrates, products and cofactors for antioxidant enzymes in *Giardia duodenalis*.

Enzyme (abbreviation)	ORF no. (GL50803)	Catalytic cofactors	Electron donors	Substrates	Products	Notes	References
Pyruvate:ferredoxin oxidoreductase 1 (PFOR-1)	17063	Fe–S, thiamine pyrophosphate		Pyruvate, oxaloacetate, co-A, Fd (ox)	Acetyl co-A, Fd (red)	Named according to Müller et al. (2007a)	Leitsch et al. (2011), Townson et al. (1996)
Pyruvate:ferredoxin oxidoreductase 2 (PFOR-2)	114609	Fe–S, thiamine pyrophosphate		Pyruvate, oxaloacetate, α-ketobutyrate, co-A, Fd (ox)	Acetyl co-A, Fd (red)	Named according to Müller et al. (2007a)	Horner et al. (1999), Müller et al. (2007a), Townson et al. (1996)
Ferredoxin (Fd)	9662, 10329, 27266	Fe–S	PFOR (red)	MET–NO_2	MET–NO_2•$^-$		Leitsch et al. (2011), Liu et al. (2000), Tejman-Yarden et al. (2011), Townson et al. (1994b)
Ferredoxin:NAD(P) reductase (FNR)		FAD, FMN	Fd (red)	NAD, NADP	Fd (ox), NADH, NADPH	Existence inferred in but no genomic or enzymatic evidence to date	Brown et al. (1998), Ellis et al. (1993), Leitsch et al. (2011), Müller (2003), Nixon et al. (2002), Upcroft and Upcroft (2001)
Alcohol dehydrogenase E (ADHE)	93358		NADH	Acetyl-CoA, acetaldehyde	Ethanol	Regenerates NAD under anaerobic conditions	Sánchez (1998)
Glutamate dehydrogenase (GDH)	21942		NADPH	Ammonia, α-ketogluterate	Glutamate	Reversible, more active in NADPH oxidation/glutamate formation; regenerates NADP under anaerobic conditions	Park et al. (1998)
NADH oxidase	33769	FAD	NADH, NADPH	O_2, FAD, FMN, FUR–NO_2	H_2O, $FADH_2$, $FMNH_2$, FUR–NO_2•$^-$	Published purified enzyme activity is likely derived from this gene product	Brown et al. (1996a)
NADH oxidase	9719	FMN	NADH			Predicted FMN binding domain	Morrison et al. (2007)
NADH:rubredoxin reductase			NADH	Rubredoxin (ox)	Rubredoxin (red)	*E. coli* homologue required for recombinant assays of flavodiiron protein and SOR	Di Matteo et al. (2007), Mastronicola et al. (2011), Testa et al. (2011), Vicente et al. (2009)
Flavodiiron protein	10358	Fe, FMN	Rubredoxin (red)	O_2	H_2O	Recombinant *E. coli* NADH rubredoxin reductase and rubredoxin required for activity assays	Di Matteo et al. (2007), Mastronicola et al. (2011), Vicente et al. (2009)
Acetyl-coA synthetase	13608			ADP, acetyl-coA	ATP, acetate	Generates ATP under microaerobic conditions	Sánchez et al. (1999)
DT-diaphorase	15004	FAD	NADPH	O_2; menadione (ox)	H_2O_2 + O_2•$^-$; menadione (red)	Major contributor to ROS generation	Li and Wang (2006), Paget et al. (2004), Sánchez et al. (2001)
Superoxide reductase (SOR)	Ch1 NT 217012-216680	Fe	Rubredoxin (red)	O_2•$^-$	H_2O_2	Recombinant *E. coli* NADH rubredoxin reductase and rubredoxin required for activity assays	Testa et al. (2011)
Thioredoxin reductase (TrxR)	9827	FAD	NADPH	Thioredoxin (ox); MET–NO_2	Thioredoxin (red); MET–NO_2•$^-$	May require reduced flavins ($FADH_2$) for activity	Brown et al. (1996b), Leitsch et al. (2011)
Thioredoxin (Trx)	3910, 9355, 104250, 6829		TrxR	Oxidized protein	Reduced protein	Endogenous thioredoxin for TrxR yet to be identified	Leitsch et al. (2011), Ma′ayeh and Brook-Carter (2012)
Peroxiredoxin 1a,b	16076, 14521, 15383		Thioredoxin (red)	H_2O_2; peroxynitrite; peroxidized lipids	H_2O; NO_2^-; neutralized lipids	Recombinant *E. coli* TrxR and thioredoxin required for activity assays	Mastronicola et al. (2014)
Nitroreductase 1 (NR-1)	22677	Fe–S, FMN	NADH	NO_3^-; NO_2^-; menadione (ox); MET–NO_2; NTZ–NO_2	NO; menadione (red); MET–NO_2•$^-$; NTZ–NO_2•$^-$	Named according to Müller et al. (2007b)	Müller et al. (2007a, 2007b, 2008, 2013, 2015), Nillius et al. (2011)
Nitroreductase 2 (NR-2)	6175	Fe–S, FMN	NADH	NO_3^-; NO_2^-; menadione (ox); MET–NO_2; NTZ–NO_2	NH_3; menadione (red); MET–NH_2; NTZ–NH_2	Named according to Müller et al. (2013)	Müller et al. (2013, 2015)
Oxygen-insensitive nitroreductase 1 (NTR-1)	15307	FMN	NADH, NADPH			Lacks a ferredoxin domain	Martínez-Júlvez et al. (2012), Nixon et al. (2002), Olekhnovich et al. (2009), Pal et al. (2009)
Flavohemoglobin	15009	Fe	NADH, NADPH	NO, O_2	NO_3^-		Mastronicola et al. (2010), Rafferty et al. (2010)

Enzymes without genetic or enzymatic evidence in *Giardia duodenalis*, and cofactors/substrates inferred through homology, are displayed in gray. Mutually exclusive substrates and products are separated by ";". For simplicity, the stoichiometry of half-reactions is omitted.

In addition, a thioredoxin cycling system may repair oxidized biomolecules (Mustacich and Powis, 2000). An NADPH-dependent thioredoxin reductase (TrxR) has been identified whose activity is enhanced in the presence of an unidentified low molecular weight protein (Brown et al., 1996b). While early reports demonstrated that glutathione could act as an electron acceptor for TrxR (Brown et al., 1996b; Smith et al., 1988), it is likely that the endogenous electron acceptor is an, as yet unidentified, thioredoxin (Brown et al., 1996b; Leitsch et al., 2011). Other likely substrates of TrxR are protein disulfide isomerases that contain thioredoxin domains (Lundström and Holmgren, 1990; McArthur et al., 2001) and are important components of the cellular protein-folding machinery. Thioredoxin is also likely to provide electrons to peroxiredoxins, which are suggested to neutralize peroxidized lipids, in addition to ROS and RNS (Brown et al., 1993, 1998; Mastronicola et al., 2014) (Fig. 1) (Table 1).

2.2. Electron transport cofactors and the energetic advantage of oxygen

Whereas dO_2 is detrimental to *G. duodenalis* at high concentrations, at microaerobic concentrations it may provide an energetic advantage. Many oxidoreductases in the antioxidant network utilize NADH and/or NADPH (collectively NAD(P)H) as a source of reducing power, and thus maintain the pool of oxidized electron acceptors (i.e., NAD(P)), which are required to drive glycolysis (Fig. 2; Supplementary Fig. 2). Therefore in the presence of dO_2, glycolytic intermediates that would be diverted to facilitate the regeneration of NAD(P) under anaerobic conditions (Park et al., 1998; Sanchez et al., 1998), are available for further oxidation to generate ATP (Adam, 2001; Lindmark, 1980; Mendis et al., 1992; Muller, 2003; Paget et al., 1993; Sanchez et al., 1999). Consistent with this proposal, *G. duodenalis* trophozoites exhibit enhanced growth under microaerobic compared with anoxic (i.e., nitrogen-sparged) conditions (Gillin and Diamond, 1981).

The ability of *G. duodenalis* to thrive under varying dO_2 concentrations in the host intestine depends on the availability of essential cofactors. Nicotinamide scavenging enzymes provide the NAD backbone which is converted to NADP by NAD kinase (Mattevi, 2006; Morrison et al., 2007). NAD(P)H is produced during the catabolism of glucose, malate and glutamate (Adam, 2001; Jarroll and Paget, 1995; Mendis et al., 1992) (Fig. 2). Another vital class of electron transport cofactors are the flavins (FMN and FAD), which bind to the catalytic core of oxidoreductase enzymes and transfer electrons from NAD(P)H to the substrate (Fraaije and Mattevi, 2000). In *G. duodenalis*, flavin cofactors are likely produced from imported riboflavin by a homologue of the prokaryotic bifunctional riboflavin kinase/FAD synthetase enzyme (Krupa et al., 2003). The cofactor binding specificities of oxidoreductase enzymes in *G. duodenalis* are shown in Table 1.

In contrast to trophozoites, *G. duodenalis* cysts are exposed to atmospheric oxygen when they are shed from the host. Cysts consume oxygen, albeit at a lower rate than trophozoites, and so are not technically cryptobiotic (Paget et al., 1989, 1993, 1998). The low oxygen consumption of cysts suggests that they have low metabolic activity, which may be necessary to preserve limited endogenous carbon supplies. This also implies that intracellular dO_2 can accumulate to higher levels in cysts than trophozoites (Jarroll and Paget, 1995; Paget et al., 1998). The mechanisms via which cysts can tolerate atmospheric oxygen for long periods remain to be understood.

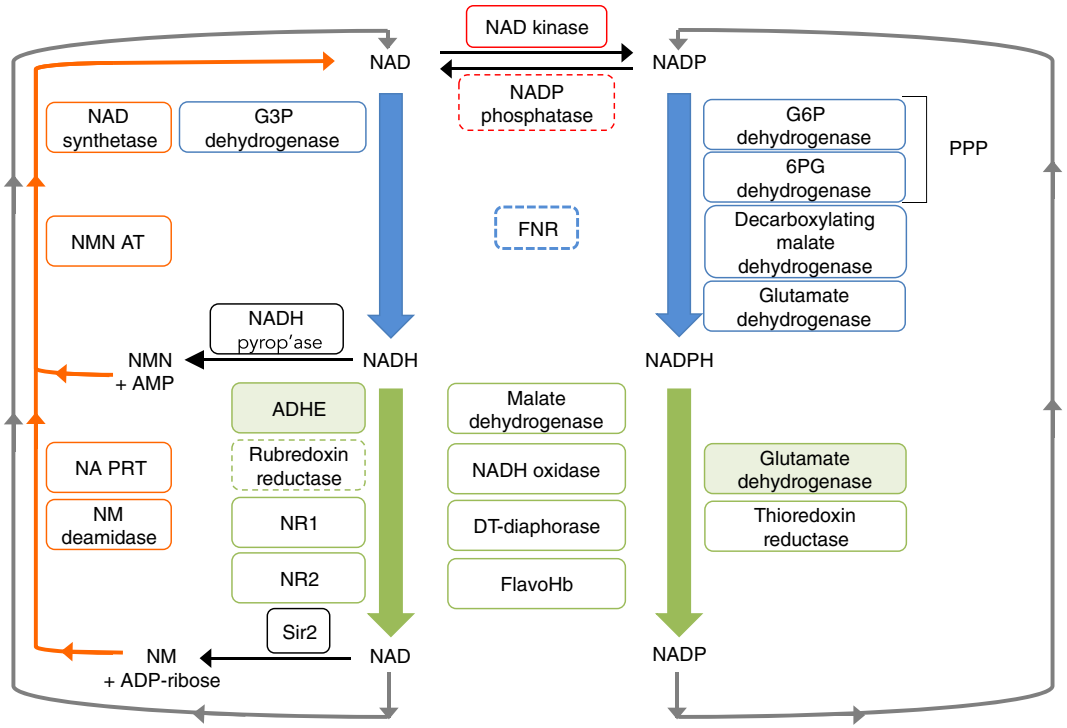


Fig 2. Mechanisms of NAD(P)H production and consumption in *Giardia duodenalis*. Modulation in NAD scavenging (orange) or NAD(P) reducing (blue) enzyme activity may functionally inhibit NAD(P)H consuming enzymes (green) that participate in nitroheterocyclic activation (e.g., NR1, thioredoxin reductase), or detoxification (NR2). NAD and NADP are interconverted by NAD kinase and NADP phosphatase (red borders). NAD-specific enzymes are displayed left of center and NADP-specific enzymes are displayed right of center. Enzymes capable of reducing both NAD and NADP are displayed in the center. Enzymes widely inferred to exist but without genetic or functional evidence in *G. duodenalis* are displayed with a perforated border. Enzymes involved in NAD(P)H oxidation under anaerobic conditions are shaded. Enzymes that degrade the NAD backbone are displayed with black borders. Recycling of NAD(P) is displayed in gray. PPP: pentose phosphate pathway; G3P: glyceraldehyde-3-phosphate; G6P: glucose-6-phosphate; 6PG: 6-phosphogluconate; pyrop'ase: pyrophosphatase; FNR: ferredoxin:NAD(P) reductase; ADHE: alcohol dehydrogenase E; NR1/2: nitroreductase 1/2; FlavoHb: flavohemoglobin; Sir2: NAD-dependent histone deacetylase; NAD(P): oxidized nicotinamide adenine dinucleotide (phosphate); NMN AT: nicotinamide mononucleotide adenyltransferase; NA PRT: nicotinic acid phosphoribosyltransferase; NM: nicotinamide.

3. Nitroheterocyclic resistance in *G. duodenalis*

The highly reduced (i.e., electron-rich) intracellular environment that *G. duodenalis* maintains to manage oxidative stress is the basis of its susceptibility to nitroheterocyclics. Anti-giardial nitroheterocyclics, all of which feature a nitro group extending from a heterocyclic backbone, include the nitroimidazoles MET, ornidazole (ORN), tinidazole (TIN), and a novel compound termed C17 (Crozet et al., 2009; Dunn et al., 2010); as well as a nitrothiazolide, nitazoxanide (NTZ), and a nitrofuran, furazolidone (FUR) (Supplementary Fig. 3). Nitroheterocyclics are 'redox-active' pro-drugs with low redox potentials (Supplementary Table 1) and are thought to enter the trophozoite via passive diffusion, before being reduced to toxic intermediate forms. The exact mechanisms of nitroheterocyclic-induced cell death are unknown, but are thought to include oxidation of biomolecules. As suppliers of reducing power, glycolytic and oxidoreductase enzymes are strongly implicated in the activation and detoxification of redox-active nitroheterocyclics (Leitsch et al., 2011; Müller et al., 2007a, 2007b, 2008, 2013, 2015; Tejman-Yarden et al., 2011). Accordingly, differential regulation of multiple gene products is evident in clinical and laboratory-derived nitroheterocyclic-resistant *G. duodenalis*. The following section focuses on resistance to MET, as this is the best-studied nitroheterocyclic drug. Subsequent sections review the proposed mechanisms of action and resistance to other nitroheterocyclics.

Here, we define *G. duodenalis* derived from patients as 'isolates', and isolates established in continuous axenic laboratory culture as 'strains.' A strain that has been cloned or selected for drug resistance will be termed a 'line' (Nolan et al., 2011). Lines that exhibit resistance to a drug that they have not been previously exposed to, of equal or greater magnitude than that for the selected drug, are considered cross-resistant.

We acknowledge that *G. duodenalis* as it is currently defined, is likely to represent a species complex composed of multiple 'assemblages' (A–G; Monis et al., 2009) that differ in genetic organization, host specificity, and ratios of allelic heterozygosity (Adam et al., 2013; Franzén et al., 2009, 2013; Jerlström-Hultqvist et al., 2010). All references to *G. duodenalis* in this work without further specification of assemblage or strain/line, are intended to refer to the complex as a whole. It is important to note however, that research into nitroheterocyclic resistance in *G. duodenalis* has focused almost exclusively on assemblage A parasites, with molecular characterization largely focused on laboratory lines derived from the WB, 106, and 713 isolates. Future work to investigate nitroheterocyclic drug resistance in other assemblages is clearly required. Indeed, even within an assemblage, the potential for pre-existing differences in the antioxidant activity of susceptible parent organisms must be considered, and may influence the trajectory of resistance development (discussed below).

3.1. Metronidazole

3.1.1. Chemistry, cytotoxicity and metabolism

The prototypic 5-nitroimidazole, MET, is a pro-drug which is activated by intracellular reduction of the nitro group (Edwards, 1993a) (Supplementary Fig. 3). Univalent reduction yields a nitro radical anion, which can be re-oxidized by dO_2 in aerobic cells due to its very low redox potential (Supplementary Table 1). Re-oxidation is termed 'futile redox cycling' (Fig. 3c) and renders MET largely non-toxic to host cells. However, under the highly reduced conditions found in the cytoplasm of *G. duodenalis* and other microaerophiles, the nitro anion radical can be further reduced to reactive nitroso- and hydroxylamine intermediates. These unstable intermediates are thought to progressively acquire electrons by oxidizing biomolecules, finally forming the inert amine MET–NH_2 (Edwards, 1993a) (Fig. 3a). MET is unequivocally mutagenic in *H. pylori* (Sisson et al., 2000), and damage to DNA via thymine dimerization is a widely accepted mechanism of cytotoxicity (Edwards, 1993a). Recent work correlating exposure to MET with histone 2A (H2A) phosphorylation (a marker of DNA damage) and arrest of cell cycle progression suggests that the drug may also damage DNA in *G. duodenalis* (Uzlikova and Nohýnková, in press). However, the relatively short time to MET-induced cytotoxicity in microaerophiles (within 4–6 hours) may be indicative of extensive oxidation of cytosolic biomolecules in addition to DNA, as DNA damage alone would be expected to result in delayed cell death (Edwards, 1993a; Leitsch et al., 2009; Uzlikova and Nohýnková, in press). Furthermore, activated MET intermediates in the cytosol would be more likely to interact with proximal biomolecules or the nuclear membrane, rather than DNA itself (Leitsch et al., 2009). Indeed, differential two-dimensional electrophoretic analysis of proteins from MET-exposed trophozoites (strain 106), indicated the existence of covalent adducts between MET and proteins including pyrophosphate-dependent pyruvate kinase, alcohol dehydrogenase E (ADHE), structural proteins and a protein translation

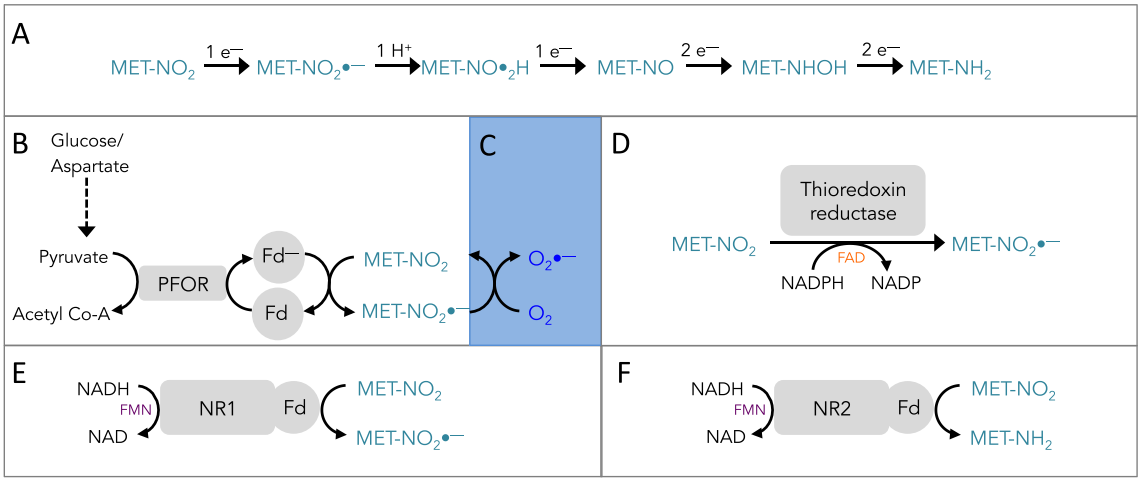


Fig 3. Mechanisms of metronidazole activation and detoxification in *Giardia duodenalis*. The metronidazole pro-drug (MET–NO_2) enters the cell via passive diffusion and requires univalent reduction by glycolytic or antioxidant enzymes to generate the nitro anion (MET–$NO_2^{\bullet-}$). Further enzymatic reduction or oxidation of biomolecules provides five additional electrons to yield the inert amine (MET–NH_2; Panel A). MET can accept electrons from ferredoxin (Fd) reduced by PFOR (Panel B), however oxygen can re-oxidize the nitro anion to the pro-drug with the concomitant production of superoxide (Panel C). Thioredoxin reductase can activate MET using NADPH as an electron donor (Panel D). Nitroreductase 1 is evidenced in activating MET to reactive intermediates (Panel E) whereas nitroreductase 2 may detoxify MET by completely reducing the pro-drug to an inert amine (Panel F). For simplicity, only the univalent reduction product is displayed in panels B, D, E & F, however these mechanisms may supply additional electrons to activated intermediates. PFOR: pyruvate:ferredoxin oxidoreductase; NR: nitroreductase.

elongation factor EF-1γ (Leitsch et al., 2012a). Although the functional implications of these interactions are yet to be determined, permanent inactivation of proteins might also contribute to MET cytotoxicity in *G. duodenalis*.

At present, three enzymes are implicated in activating MET in *G. duodenalis*. Purified ferredoxin (reduced by PFOR) and recombinant TrxR have been shown to reduce MET in vitro (Leitsch et al., 2011; Townson et al., 1994b, 1996) (Fig. 3b & d). The third enzyme, NR-1, is implicated in MET activation as its overexpression in *G. duodenalis* increased susceptibility to MET (Nillius et al., 2011). As NR-1 contains a ferredoxin domain it may activate MET in a similar manner to the PFOR–ferredoxin couple (Fig. 3e), although this is yet to be demonstrated (Müller et al., 2007b). Complete enzymatic detoxification of MET to MET–NH_2 may also occur in *G. duodenalis*. In particular, the nitroreductase NR-2, is proposed to act to detoxify MET, as over-expression of this enzyme in WB trophozoites protected against MET-induced cytotoxicity (Müller et al., 2013) (Fig. 3f). However recombinant NR-2 failed to reduce MET under aerobic conditions, possibly due to oxygen sensitivity of the ferredoxin domain (Müller et al., 2013).

3.1.2. Resistance markers and cross-resistance

MET-resistant *G. duodenalis* lines have been selected using a range of techniques including constant exposure to sub-lethal MET concentrations (lines 1062ID10 and WB-C5 (Boreham et al., 1988; Müller et al., 2007a)), and mutagenesis using ultra-violet radiation followed by exposure to moderate (WB-M1 and WB-M2 (Tejman-Yarden et al., 2011)) or high concentrations of MET (WB-M3 and 713-M3 (Townson et al., 1992)) (Table 2). The karyotypes of three of these lines have been investigated; 1062ID10, which was not mutagenized, exhibited partial deletion of chromosome 4 (Upcroft et al., 1992), and the mutagenized line WB-M3 exhibited duplication and partial deletion of chromosome 5 (Chen et al., 1994). Similar rearrangements are also claimed in the mutagenized line 713-M3, but not further described (Townson et al., 1994a). These reports suggest that MET exposure alone can produce gross genetic lesions. The translocation break-point in 1062ID10 is near a gene encoding a multidrug-resistance transporter homologue (Townson et al., 1994a), indicating that MET efflux may contribute to resistance. Further investigation of the abundance, structure and function of these membrane pumps in resistant *G. duodenalis* is therefore required.

In addition to genetic data, transcript abundance and/or enzyme activity data are available for six *G. duodenalis* lines that have been selected for MET-resistance in vitro. Comparisons of these lines with their respective MET-susceptible parents suggest that MET-resistance arises in part through decreases in PFOR, ferredoxin and NR-1 activity, in various combinations (Table 2). The behavior of these lines is highly complex and incompletely characterized, suggesting multiple avenues to MET-resistance and indicating the need for deeper study. Five lines exhibit lower PFOR activity or lower transcription of at least one of two *pfor* genes relative to their drug-sensitive parents (Ellis et al., 1993; Leitsch et al., 2011; Tejman-Yarden et al., 2011; Townson et al., 1996). Transcription of *pfor-2* appears unchanged in the line WB-M2 (Tejman-Yarden et al., 2011), however *pfor-1* transcription has not been investigated in this line. Lower ferredoxin transcription/activity may be functionally equivalent to lower PFOR activity given that the two proteins work in concert to activate MET. The transcription of *ferredoxin-1* is lower in WB-M1 and WB-M2 than in their susceptible parent (Tejman-Yarden et al., 2011), and ferredoxin activity is decreased in 713-M3 (Leitsch et al., 2011; Liu et al., 2000). Nitroreductase genes are also differentially transcribed in several resistant lines. Transcription of *nr-1* is decreased in 713-M3, WB-M1 and WB-M2, and *nr-2* transcription is up-regulated in 713-M3 and 1062ID10 (Müller et al., 2013; Tejman-Yarden et al., 2011). A positive correlation between MET resistance and glutathione reductase activity (incorporating TrxR activity), and glutathione oxidase (incorporating peroxiredoxin) activity was reported in 1062ID10 (Smith et al., 1988). Taken together, lower transcription/activity of the PFOR/ferredoxin couple is the most consistent finding in lines selected for resistance to MET, and supports the finding that artificial suppression of *pfor-1* induces MET resistance (Dan et al., 2000). Additional mechanisms of resistance may include MET detoxification by NR-2, and neutralization of activated MET intermediates and damaged biomolecules through increased thioredoxin cycling (Smith et al., 1988). Furthermore, the recent identification of constitutive H2A phosphorylation in 713-M3 and 106-2ID10 (Uzlikova and Nohýnková, in press) suggests that up-regulation of DNA repair pathways also contribute to resistance. Cross-resistance in lines selected for resistance to MET appears restricted to other 5-nitroimidazoles. 1062ID10 and WB-M2 are cross-resistant to tinidazole (TIN) and ornidazole (ORN) (Tejman-Yarden et al., 2011), suggesting that the mechanisms of action and resistance to these drugs overlap with MET. However, MET-specific resistance mechanisms must also exist, given that 713-M3 and WB-M1 show little cross-resistance to TIN, ORN or any other nitroheterocyclics (Tejman-Yarden et al., 2011) (Table 2). The molecular basis of differential cross-resistance in these lines is presently unclear.

3.1.3. Other nitroheterocyclics

Relative to MET, mechanisms of resistance to other nitroheterocyclics in *G. duodenalis* are less well characterized. Two lines have been selected for resistance to a novel 5-nitroimidazole termed C17 (Crozet et al., 2009; Dunn et al., 2010). The line 106-C17 was selected for resistance to this compound from a nitroheterocyclic-susceptible parental strain (106), whereas 713-M3-C17 was derived from the MET-resistant line 713-M3 (Dunn et al., 2010). The gene encoding NR-1 is transcriptionally down-regulated in both C17-resistant lines (Müller et al., 2013), and recombinant NR-1 appears able to reduce C17 (Müller et al., 2015). Interestingly, 106-C17 shows similar PFOR activity to its nitroheterocyclic-susceptible parent, but is cross-resistant to MET (Dunn et al., 2010; Leitsch et al., 2011). Similarly, both PFOR activity and MET resistance are higher in 713-M3-C17 than the already MET-resistant parent (Dunn et al., 2010; Leitsch et al., 2011). These data indicate that MET resistance is possible in the presence of active PFOR, and therefore lower *nr-1* transcription may contribute substantially to both C17- and MET resistance. Although there is broad agreement in the (albeit limited) enzyme transcription/activity data available for 106-C17 and 713-M3-C17, only 713-M3-C17 is also cross-resistant to TIN and ORN (Dunn et al., 2010; Tejman-Yarden et al., 2011), and the molecular basis for this difference remains to be discovered.

Nitazoxanide (NTZ) may have a range of mechanisms of action within *G. duodenalis*. Recombinant NR-1 is reported to reduce NTZ (Müller et al., 2015), and overexpression of this enzyme in the WB background increases NTZ susceptibility (Nillius et al., 2011). Furthermore, the gene encoding NR-1 is down-regulated in the two NTZ-resistant laboratory lines reported to date (WB-C4 and NTZII) (Müller et al., 2007a, 2008, 2013). Together, these data strongly suggest that NR-1 reduces NTZ to toxic intermediates within *G. duodenalis*, and that resistant lines avoid this by down-regulating *nr-1* transcription. Interestingly, NTZ may also act as a steric inhibitor of PDI and PFOR enzymes (Müller et al., 2007a; Hoffman et al., 2007). Transcription of *pdi-2*, *pdi-4* and *pfor-1* is increased in WB-C4 relative to the drug-susceptible parent (Müller et al., 2008), which may represent an attempt to compensate for chemical inhibition of the gene products. NTZ may also lead to protein misfolding in *Giardia*, as microarray analysis of WB-C4 revealed the up-regulation of genes encoding the heat-shock proteins HSP70-B2 and HSP90, and other chaperones (Müller et al., 2008). Similar to C17-resistant lines, WB-C4 is cross-resistant to MET despite marked up-regulation of *pfor-1* (Müller et al., 2008). If MET is activated in WB-C4, resistance may be partially due to the efficient management of protein oxidation by HSP chaperones.

Lastly, furazolidone (FUR)-resistant lines of *G. duodenalis* have been developed in vitro (Townson et al., 1992; Upcroft et al., 1990), and resistant clinical isolates are reported (Ellis et al., 1993; Smith et al., 1988).

Table 2
Differential activity/expression of redox-associated enzymes, and infectivity of laboratory-derived MET-resistant *G. duodenalis*.

Line	Selected resistance	Cross-resistance	Infectivity	MET activation					MET detoxification	NADPH metabolism		Protein chaperones & HDACs			References
				PFOR		Fd	TrxR	NR-1	NR-2	NADPH oxidase	GDH	PDI-2	PDI-4	Sir-2	
				PFOR-1 17063	PFOR-2 114609	Fd-1 9662	9827	22677	6175	†	21942	9413	103713	16569	
WB-M3	MET (UV)			a ↓											Townson et al. (1996)
713-M3	MET (UV)	•	0	a ↓		a ↓		t ↓*	t ↑*	a ↓					Leitsch et al. (2011), Liu et al. (2000), Müller et al. (2013), Townson et al. (1996)
WB-C5	MET			t ↓	t ↓			t -	t -		t ↓	t ↑	t -		Müller et al. (2007a), Müller et al. (2013)
1062ID$_{10}$	MET	TIN, ORN	10^5	a ↓		a -	a ↑	t -	t ↑*	a ↓					Leitsch et al. (2011), Müller et al. (2013), Smith et al. (1988), Townson et al. (1996)
WB-M1	MET (UV)	•	0		t ↓*	t ↓*	t -	t ↓*							Tejman-Yarden et al. (2011)
WB-M2	MET (UV)	TIN, ORN	10^6		t -	t ↓*	t -	t ↓*							Tejman-Yarden et al. (2011)
713-M3-C17	MET (UV), C17	TIN, ORN		a ↑		a -		t ↓*	t -	a ↓					Dunn et al. (2010), Leitsch et al. (2011), Müller et al. (2013)
106-C17	C17	MET	0	a -		a -		t ↓*	t -	a ↓					Dunn et al. (2010), Leitsch et al. (2011), Müller et al. (2013)
WB-C4	NTZ	MET		t ↑*	t -	t -	t -	t ↓*	t -	t -	t ↓	t ↑*	t ↑*	t ↓*	Müller et al. (2007a, 2008, 2013), Nillius et al. (2011)
NTZII	NTZ							t ↓*							Nillius et al. (2011)

The drug under which resistant lines were selected is underlined. Cross-resistance is reported for compounds where an equal or greater increase in resistance is observed relative the compound used to select for resistance. Infectivity in suckling mice (no. trophozoites in small intestine 4 days post-infection) is stated according to Tejman-Yarden et al. (2011). The parent of 713-M3-C17 is 713-M3, which was selected for MET resistance prior to selection for C17 resistance (Dunn et al., 2010). ORF codes for strain WB (giardiadb.org) are displayed for relevant genes. Blank spaces indicate a lack of available data. † NADPH oxidase enzyme activity was tested in cell lysates and may result from multiple enzymes including NADH oxidase, DT-diaphorase, thioredoxin reductase and glutamate dehydrogenase (see text). • cross-resistance to other nitroheterocyclics tested but not evident at similar or greater levels than for the selected drug (see text); UV: trophozoites were mutagenized using ultra-violet radiation prior to selection on MET; a: enzyme activity; t: transcription; ↑ increase; ↓ decrease; - activity/transcription was tested but not found to be different from the drug-susceptible parent strain; * a test of significance was performed, and differential transcription was found to be significant. Tests of significance are not reported for tabulated enzyme activity assays. GDH: glutamate dehydrogenase, HDAC: histone deacetylase.

As for MET, FUR-resistant lines have been created via a range of mutagenesis and exposure regimes (Townson et al., 1992). Similar to the MET-resistant line WB-M3, duplication and partial deletion of chromosome five is reported in the mutagenized FUR-resistant line BAC2-F3 (Chen et al., 1994). The appearance of this mutation in lines resistant to both MET and FUR is puzzling, and could indicate either the existence of a gene(s) whose disruption protects against exposure to both drugs; or an effect of regional chromosomal sensitivity to nitroheterocyclic- or UV-induced stress that entails little fitness cost. Purified NADH oxidase is reported to activate FUR (Brown et al., 1996a), but clinical isolates from patients who were unsuccessfully treated with this drug exhibited little difference in NADPH oxidase or PFOR activity relative to susceptible laboratory strains (Ellis et al., 1993). Similarly, no correlation between PFOR activity and FUR resistance was observed in isolates from diagnostic duodenal biopsies, but positive correlations were found for both thiol-dependent peroxidase and reductase activity (representing TrxR and peroxiredoxin enzyme activity respectively) (Smith et al., 1988). Together these data support a model of FUR resistance whereby the drug is activated by NADH oxidase and the ensuing oxidative damage is managed by elevated thioredoxin-based antioxidant activity. Cross-resistance has not been investigated in FUR-resistant *G. duodenalis* to date, but may be informed by a report of minimal cross-resistance to non-nitrofuran compounds in FUR-resistant *Clostridium difficile* (Kumar et al., 2014). Additionally, FUR inhibits cyst viability more effectively than does MET (Hausen et al., 2006), perhaps due to greater penetration through the cyst wall (Paget et al., 1998).

In summary, results from laboratory-derived nitroheterocyclic-resistant lines suggest that loss of either of the PFOR/ferredoxin couple or NR-1 can lead to MET resistance, and that resistance may be further augmented by up-regulation of NR-2 and thioredoxin cycling mechanisms. Lower transcription of the gene encoding NR-1 is implicated in resistance to MET, NTZ and C17, however cross-resistance between these compounds is not universal, indicating that factors other than the aforementioned oxidoreductases must influence resistance. In contrast to resistance mediated through down-regulation of nitroheterocyclic drug-activating oxidoreductases, FUR resistance appears to be primarily mediated through the up-regulation of thioredoxin-based antioxidant enzymes.

3.1.4. Functional enzyme regulation by cofactor modulation

The activation of nitroheterocyclics within G. duodenalis may be further regulated by the intracellular abundance and oxidation status of NAD(P)H and flavin cofactors that are required for oxidoreductase enzyme activity. A number of enzymes are involved in the synthesis, reduction and oxidation of NAD(P) and flavins (Table 1, Fig. 2), and changes in the activity/transcription of these enzymes are implicated in nitroheterocyclic drug resistance. For example, the NADPH-producing enzyme glutamate dehydrogenase (Park et al., 1998) is not directly associated with nitroheterocyclic drug activation or detoxification, but the encoding gene is transcriptionally down-regulated in the lines WB-C5 (MET-resistant), WB-C4 (NTZ/MET-resistant), and in the susceptible line WB-C6 after three hours of MET exposure (Müller et al., 2007a, 2007b). Loss of glutamate dehydrogenase activity may limit the intracellular supply of NADPH and thereby inhibit the activity of NADPH-dependent enzymes such as TrxR and NADH oxidase, which activate nitroheterocyclics (Müller et al., 2007a). Additionally, the apparent involvement of glutamate dehydrogenase in MET resistance makes *gdh* an inappropriate control gene for studies of differential transcription in resistant lines (Argüello-García et al., 2009).

Flavoenzymes including NADH oxidase and TrxR may be functionally inhibited by a lack of the FAD cofactor in some MET-resistant *G. duodenalis* lines. This 'flavin starvation' hypothesis is supported by decreased NADPH oxidase activity (attributed to enzymes including the FAD-dependent NADH oxidase) in four MET-resistant lines including 1062ID10 (Table 2) (Leitsch et al., 2011). Given that recombinant TrxR has been shown to activate MET, a scarcity of FAD ('flavin starvation') would limit the activity of this enzyme, and could account for its continued expression in several MET-resistant lines (Leitsch et al., 2011). For 1062ID10 however, this interpretation appears to conflict with a previous finding of increased thiol-dependent reductase (i.e., TrxR) activity (Smith et al., 1988), that would necessitate adequate FAD levels. Nevertheless, further support for the flavin starvation hypothesis is found in reports of MET-resistant *T. vaginalis* demonstrating that TrxR expression is unchanged, but FAD-dependent TrxR activity is decreased (Leitsch et al., 2009). More broadly, resistance to nifurtimox (a nitrofuran) in *Trypanosoma brucei* is associated with independent artificial suppression of a FMN-producing flavokinase, and a FMN-

dependent nitroreductase (Alsford et al., 2013). Global regulators of resistance in *G. duodenalis* may yet be identified through investigation of the transcription/activity of flavin- and NAD(P)H producing enzymes, and of cofactor concentrations (Trammell and Brenner 2013) in nitroheterocyclic-resistant lines.

4. Epigenetic regulation in nitroheterocyclic-resistant *G. duodenalis*

Based on the previous discussion, it is evident that differential transcription and functional regulation of enzymes involved in nitroheterocyclic drug activation, or detoxification, are likely to occur in resistant *G. duodenalis*. These mechanisms ultimately require changes in the transcription of either the enzymes that interact directly with nitroheterocyclics, or the enzymes that supply cofactors to drug-interacting enzymes. Aside from reports of chromosomal translocation in some nitroheterocyclic-resistant lines (Townson et al., 1992; Upcroft et al., 1992), mutations in promoter and coding regions of the genome have not been extensively explored. Even in light of documented genetic lesions, several features of laboratory-derived drug-resistant lines suggest that resistance may not be a stable genetic phenotype. A striking demonstration of the reversibility of nitroheterocyclic resistance is found in the NTZ and MET-resistant line WB-C4, which reverted to sensitivity to both drugs during a single passage through encystation followed by excystation (Müller et al., 2008). Concomitant with restored drug sensitivity, *nr-1* transcription was restored to levels similar to the drug-sensitive parent, and *pdi-4*, *hsp40*, *hsp70* and *hsp90* transcription decreased significantly (Müller et al., 2008). Although this could technically result from recombination at multiple heterozygotic resistance alleles during encystation (Poxleitner et al., 2008), such an event is extremely unlikely within a single generation. Epigenetic mechanisms provide a more parsimonious explanation for the rapid and complete reversion to drug sensitivity observed in excysted WB-C4 trophozoites. Epigenetic transcriptional regulation is mediated through enzymatic modification of histone proteins and DNA that change the local chromatin binding affinity to modulate the accessibility of proximal genes to the transcriptional machinery. Histone acetylation (via histone acetyltransferases) is associated with transcriptional activation; deacetylation (via HDACs) and citrullination (arginine deiminase) (Thompson and Fast, 2006) are associated with repression; and histone methylation via methyltransferases is associated with both activation and repression. DNA methylation is also associated with repression (Jaenisch and Bird, 2003). Epigenetic regulators are involved in encystation in *G. duodenalis*. The histone deacetylase HDAC-1 is required for transcription of cyst-specific genes (Sonda et al., 2010), and histone citrullination by arginine deiminiase is associated with preventing encystation (Touz et al., 2008). These data suggest that substantial epigenetic changes occur during encystation. Therefore, the transcriptional differences between WB-C4 and both its susceptible parent and excysted progeny can be inferred to be the product of epigenetic changes (Müller et al., 2008).

Evidence from both eukaryotes and drug-resistant bacteria suggests that elements of the epigenome are heritable (Adam et al., 2008; Richards, 2006). In this context, the transcriptional differences in laboratory-derived nitroheterocyclic-resistant lines could be attributed to the development of a resistant epigenotype whose replication during trophozoite division is selected for in the presence of MET. 1062ID10 was observed to revert to MET sensitivity over several weeks of drug-free culture, during which time PFOR, TrxR and peroxiredoxin activity returned to levels similar to the susceptible parent (Smith et al., 1988). Gradual reversion to sensitivity was also observed in WB-M1 in the absence of MET (Tejman-Yarden et al., 2011). Taken together, reports of reversion to drug sensitivity in *G. duodenalis* are fully consistent with a model of epigenetically-based resistance that is perpetuated in trophozoites in the presence of drug, and is reversed through epigenetic recalibration during encystation or when the drug is removed.

4.1. Redox-sensitive epigenetic regulators

Studies of MET exposure, encystation, epithelial cell co-culture, unfolded protein and heat-shock responses in *G. duodenalis* clearly demonstrate the ability of this protist to mount dynamic transcriptional responses to changing environmental conditions (Lindley et al., 1988; Ma'ayeh and Brook-Carter, 2012; Morf et al., 2010; Müller et al., 2007b; Ringqvist et al., 2011; Sonda et al., 2010; Spycher et al., 2013). In addition to HDAC-1, the WB genome encodes five putative Sir2 HDACs, five putative histone acetyltransferases and six histone methylases (Morrison et al., 2007; Sonda et al., 2010) which await specific functional characterization. Sir2 HDACs consume NAD in the process of histone deacetylation (Fig. 2) and their activity is proposed to increase as the intracellular ratio of NAD to NADH increases (Denu, 2003; Fulco et al., 2003; Guarente, 2000; Smith et al., 2000). Given the oxidative stress associated with exposure to nitroheterocyclics, Sir2 HDACs may be important regulators of the initial transcriptional response (Müller et al., 2007b) and the molecular phenotypes of resistant organisms. In *Candida glabrata*, a Sir2 homologue was shown to repress transcription of antioxidant and fluconidazole-resistance genes. This enzyme was inactivated when certain cysteine residues were ablated, indicating the possibility of multiple levels of redox-based functional regulation (Orta-Zavalza et al., 2013). The putative redox-sensitive cysteine motif is conserved in three *G. duodenalis* Sir2 HDACs (unpublished observation), and one of these (ORF 11679) is down-regulated in the NTZ/MET-resistant line WB-C4 (Müller et al., 2008). This may represent the first indication of an epigenetic regulator of nitroheterocyclic resistance. Further investigation of the kinetics of Sir2 HDACs in *G. duodenalis* and the scope of genes under their control, could substantially expand our understanding of drug resistance mechanisms.

5. A link between gut conditions and treatment failure?

Compared to laboratory-derived nitroheterocyclic-resistant *G. duodenalis*, little work has been undertaken on resistance in vivo. As reviewed above, both oxygen and nitroheterocyclic compounds (and their respective intermediates) interact with similar oxidoreductase enzymes in *G. duodenalis*. Crucially however, oxygen has a greater affinity for electrons than do nitroheterocyclics (Supplementary Table 1), and multiple lines of evidence suggest that the efficacy of these drugs are compromised by intracellular dO_2. Firstly, under atmospheric dO_2 concentrations, MET shows little effect against otherwise susceptible strains (Gillin and Reiner, 1982), which may be due to futile redox cycling and/or oxidative inactivation of metalloenzymes such as the MET-activating PFOR/ferredoxin couple. In addition, dO_2 concentrations that saturate enzymes such as NADH oxidase would be expected to exert maximal demand for NAD(P)H, and could limit the availability of reducing power to drug-activating enzymes (Ellis et al., 1993). Transient increases in dO_2 in the host intestine may enable trophozoites to evade nitroheterocyclics, while generating maximal ATP. Could more chronic in vivo exposure to oxidative stress induce, or select for, molecular phenotypes that also render trophozoites resistant to nitroheterocyclics? This hypothesis is informed by reports of increased gut oxidation in malnourished children with infectious diarrhea (Khaled, 1994), and systemic oxidative stress in children with giardiasis (Soto-Méndez et al., 2014). An inverse correlation between PFOR activity and MET-susceptibility is reported in isolates from diagnostic duodenal biopsies for which prior MET exposure is not reported (Smith et al., 1988). Interestingly, loss of PFOR may have relatively little cost for parasites in vivo, as artificial suppression of *pfor-1* in *G. duodenalis* correlated with more rapid growth in the presence of dO_2 (Dan et al., 2000), and the MET-resistant line 1062ID10 remains infective in suckling mice, despite lacking detectable PFOR activity (Leitsch et al., 2011; Tejman-Yarden et al., 2011). Whereas down-regulation of PFOR in response to oxidative stress may prime an infecting population for MET resistance, heightened thioredoxin-based antioxidant activity may

prime parasites for resistance to FUR (Smith et al., 1988). Indeed, children harboring isolates with high thioredoxin-associated FUR resistance in vitro, subsequently failed two courses of FUR treatment (Smith et al., 1988; Townson et al., 1994a). Taken together, these data are consistent with a model of oxygen-induced nitroheterocyclic resistance that stems from chronic gut oxidation attendant with gut dysregulation and decreased bile quality, which selects for (possibly via Sir2 HDACs) altered transcription of glycolytic and/or antioxidant enzymes. Molecular phenotypes that enable parasites to better manage oxidative stress may inadvertently confer resistance to certain nitroheterocyclics. In order to further investigate the potential for oxygen-induced nitroheterocyclic resistance, oxygen-tolerant lines could be produced in the laboratory, for example by culturing parasites under higher dO_2. Animal models of giardiasis (e.g. *Giardia muris* in mice) could also be harnessed to test for correlations between host nutritional status, infection chronicity and nitroheterocyclic efficacy.

6. Systems biology for understanding drug resistance

The variety of molecular phenotypes and cross-resistance profiles reported for nitroheterocyclic-resistant *G. duodenalis*, demonstrate the complex and polygenic nature of resistance and our incomplete understanding of the underlying mechanisms (Upcroft and Upcroft, 2001) (Table 2). This is partially due to technical limitations, and the fact that much of the previous work was conducted prior to the availability of genome sequences. Technical variation between laboratories (particularly in dO_2 concentrations in media), and the chemically undefined nature of TYI-S-33 medium itself, may affect the molecular phenotypes of resistant lines. A completely defined medium would be of great benefit for future research in this field. Given that key glycolytic enzymes are perturbed in nitroheterocyclic-resistant lines, alternative sources of energy for *G. duodenalis* are of interest. Drug resistant lines show lower, but highly variable, infectivity in suckling mice (strain C57BL/6), which may be explained in part by a defect in cyto-adherence (Tejman-Yarden et al., 2011). Cyto-adherence appears to be glucose-dependent but not dependent on intracellular ATP concentrations, and cannot be rescued by arginine, which is an alternative ATP source (Tejman-Yarden et al., 2011). In *E. histolytica*, oxidative inactivation of PFOR stimulates the conversion of glucose to glycerol, which is catabolized to yield both ATP and NADPH (Husain et al., 2012). The development of high-throughput metabolomics (Dunn et al., 2012) could be harnessed to provide detailed and comprehensive insights into the metabolic profiles of nitroheterocyclic-resistant *G. duodenalis*.

Knowledge gaps regarding the antioxidant network in *G. duodenalis* also present obstacles for nitroheterocyclic resistance research. Functional thioredoxins, and rubredoxin-like electron transport chains are yet to be demonstrated in *G. duodenalis* (Leitsch et al., 2011; Mastronicola et al., 2014; Testa et al., 2011; Vicente et al., 2009), and a widely assumed ferredoxin:NAD(P) reductase, which would transport electrons from reduced ferredoxin to NAD(P) (Brown et al., 1998; Ellis et al., 1993; Leitsch et al., 2011; Nixon et al., 2002; Upcroft and Upcroft, 2001), remains undiscovered (Müller, 2003) (Fig. 1). Affordable sequencing has provided four genomes to date (Adam et al., 2013; Franzén et al., 2009; Jerlström-Hultqvist et al., 2010; Morrison et al., 2007), leading to a well-defined *G. duodenalis* gene-set that is now supported by detailed RNA-seq data (Franzén et al., 2013; Tolba et al., 2013). However, genome-wide analyses are only as useful as the functional annotations available for genes of interest. Around 50% of the proteins predicted from the *G. duodenalis* WB genome currently lack functional annotation (Morrison et al., 2007). Despite the obvious challenges of manipulating a tetraploid genome (Davis-Hayman and Nash, 2002; Wampfler et al., 2014), the Cre/LoxP system has recently been adapted to *G. duodenalis* (Wampfler et al., 2014), and genome editing using targeted nucleases (Kim and Kim, 2014) should follow soon. In lieu of functional characterization in vitro, advances in three-dimensional structural homology search tools, such as I-TASSER (Roy et al., 2010), should provide considerable insight into functionally un-annotated gene products. More broadly, post-transcriptional and post-translational regulation of gene products is beginning to be investigated in parasitic protists, and may well be important for drug resistance. For example, mutations in a ubiquitin ligase are implicated in quinine-resistant *Plasmodium falciparum*, possibly by modifying the longevity or stability of the chloroquine-resistance transporter (Sanchez et al., 2014). Small non-coding RNA (Burroughs et al., 2014; Chen et al., 2011; Prucca et al., 2008) and histone modification (Sonda et al., 2010; Touz et al., 2008) are emerging as crucial mechanisms of transcriptional regulation in *G. duodenalis*, and await genome-wide investigation using proteomics (Bantscheff et al., 2012) and chromatin-linked immunoprecipitation-based sequencing (ChIP-seq) (Brinkman et al., 2012). The integration of these types of data sets into gene interaction networks is already elucidating the general biology and drug-resistance mechanisms of other parasitic protists (Burroughs et al., 2014; Chen et al., 2011; Clayton, 2014; Lewis et al., 2014), and similar approaches will soon be applied to *G. duodenalis*.

7. Nitroheterocyclic activation and resistance in other microaerophiles

Although the present review has focused on the antioxidant system and nitroheterocyclic resistance mechanisms in *G. duodenalis*, research in this area in other microaerophiles has contributed greatly to our understanding of the key themes and potential diversity of resistance mechanisms. As mentioned above, nitroheterocyclic drugs are also cytotoxic against microaerophiles including *T. vaginalis*, *E. histolytica* and *H. pylori* (Bachmann et al., 2011; Farthing, 2006; Urgesi et al., 2012). Like *G. duodenalis*, these organisms encode PFORs, ferredoxins and NAD(P)H-dependent oxidoreductases that are implicated in activating nitroheterocyclic drugs.

T. vaginalis colonizes the urogenital tract causing urethritis/vaginitis. This parasite also encodes a TrxR that is involved in activating MET and detoxifying H_2O_2 (Leitsch et al., 2009). Clinical MET resistance appears to rely on down-regulation of a dO_2 detoxification enzyme, flavin reductase, leading to futile redox cycling. The *T. vaginalis* flavin reductase produces H_2O_2 which must be further detoxified by thioredoxin-dependent peroxiredoxin (Chapman et al., 1999; Coombs et al, 2004; Linstead and Bradley, 1988). The coupling of thioredoxin cycling to dO_2 detoxification in *T. vaginalis*, is proposed to account for the continued activity of TrxR in clinically MET-resistant isolates (Leitsch et al., 2012b). Resistance involving down-regulation of TrxR is possible under low dO_2 conditions in the laboratory, and may be contingent upon prior flavin reductase down-regulation (Kulda, 1999; Leitsch et al., 2012b). However this type of resistance has not been observed in clinical isolates, likely due to the higher dO_2 conditions in vivo (Wagner and Levin, 1978). Conversely, clinical isolates of *G. duodenalis* exhibit a range of TrxR activities (Smith et al., 1988), and TrxR is not directly coupled to the major dO_2 detoxification system (i.e., NADH oxidase). Therefore TrxR down-regulation could theoretically precede, or occur independently of mechanisms that allow futile redox cycling in *G. duodenalis*, which may afford a greater variety of in vivo resistance mechanisms to this protist.

MET resistance mechanisms also appear to be hierarchical in the gastric ulcer-causing bacterium *H. pylori*. Mutations in a MET-activating nitroreductase (RdxA) typically occur early in the development of MET-resistance (Goodwin et al., 1998; Martinez-Julvez et al., 2012; Olekhnovich et al., 2009; Sisson et al., 2000; Sisson et al., 2002), and mutations in other genes subsequently confer greater levels of resistance (Albert et al., 2005). Secondary mutations in a FMN/FAD synthetase-coding gene are documented in a highly resistant line (Albert et al., 2005), lending further weight to the 'flavin starvation' hypothesis described above. Transcriptional modulation is also implicated in MET-resistant *H. pylori*. The *fur* gene that encodes an iron-dependent transcription factor, is mutated in both resistant clinical isolates (Albert et al., 2005) and laboratory strains (Tsugawa et al., 2011), and likely results in differential transcription

of oxidoreductases including superoxide dismutase (Carpenter et al., 2013).

Lastly, *E. histolytica* is a destructive parasite that can invade gut tissue (causing dysentery) and more oxygen-rich organs such as the liver (causing abscesses). Puzzlingly, clinical MET resistance is hardly documented, although resistant laboratory lines have been created and characterized (Duchêne, 2015). Two atypical NADPH-dependent oxidoreductases in *E. histolytica* exhibit ferredoxin:NADP reductase (FNR) activity, and also reduce ferric iron and activate MET (Jeelani et al., 2010). These enzymes may now provide a template for sensitive interrogation of the many hypothetical proteins in *G. duodenalis*, that will hopefully yield the elusive FNR.

8. Conclusion

G. duodenalis utilizes an elaborate antioxidant network to protect oxygen-sensitive metalloenzymes including PFOR, ferredoxin and ferredoxin-containing nitroreductases — enzymes that are implicated in the metabolism of nitroheterocyclics. Drug-resistant lines exhibit differential regulation of metalloenzymes, specifically, down-regulation of the PFOR-ferredoxin couple appears to lead to resistance against a number of nitroimidazoles, whereas lower nitroreductase-1 activity is implicated in resistance to a broader spectrum of nitroheterocyclics, including nitazoxanide. Functional inhibition of oxidoreductase enzymes may also be important for nitroheterocyclic resistance, and implicates the full complement of enzymes involved in the production and reduction of NAD(P) and flavin cofactors. The potential for oxygen-dependent transcriptionally-mediated nitroheterocyclic resistance is supported through multiple lines of evidence, including increased tolerance to both oxygen and metronidazole in PFOR-deficient lines; differential regulation of a redox-sensitive histone deacetylase in a multi-drug resistant laboratory line; and evidence in symptomatic children of both increased oxidative stress, and nitroheterocyclic-resistant *G. duodenalis* infections. Both genetic and epigenetic perturbations are implicated in nitroheterocyclic resistance, but the latter may be sufficient to produce resistance. Further investigation into redox signal transduction, and complete elucidation of the antioxidant system in *G. duodenalis* are required. In conjunction with advanced genome annotation strategies and advancing reverse genetic technologies, comprehensive genomic, transcriptomic, proteomic and metabolomic profiling of drug-resistant lines should greatly improve our understanding of drug resistance mechanisms in this, and other medically important microaerophilic pathogens.

Acknowledgments

BREA is supported by an Australian Post-graduate Award (Australian Government) and the Victorian Life Sciences Computation Initiative (Victoria, Australia). MJM and ARJ are partially supported by an Australian Research Council Linkage Grant (number LP120200122).

Appendix A. Supplementary data

Supplementary data to this article can be found online at http://dx.doi.org/10.1016/j.biotechadv.2015.04.009.

References

Abboud P, Lemée V, Gargala G, Brasseur P, Ballet JJ, Borsa-Lebas F, et al. Successful treatment of metronidazole- and albendazole-resistant giardiasis with nitazoxanide in a patient with acquired immunodeficiency syndrome. Clin Infect Dis 2001;32:1792–4.
Adagu IS, Nolder D, Warhurst DC, Rossignol J-F. In vitro activity of nitazoxanide and related compounds against isolates of *Giardia intestinalis*, *Entamoeba histolytica* and *Trichomonas vaginalis*. J Antimicrob Chemother 2002;49:103–11.
Adam RD. Biology of *Giardia lamblia*. Clin Microbiol Rev 2001;14:447–75.
Adam RD, Yang YM, Nash TE. The cysteine-rich protein gene family of *Giardia lamblia*: loss of the CRP170 gene in an antigenic variant. Mol Cell Biol 1992;12:1194–201.
Adam T, Murali B, Glenn NO, Potter SS. Epigenetic inheritance based evolution of antibiotic resistance in bacteria. BMC Evol Biol 2008;8:52.
Adam RD, Dahlstrom EW, Martens CA, Bruno DP, Barbian KD, Ricklefs SM, et al. Genome sequencing of *Giardia lamblia* genotypes A2 and B isolates (DH and GS) and comparative analysis with the genomes of genotypes A1 and E (WB and Pig). Genome Biol Evol 2013;5:2498–511.
Albert TJ, Dailidiene D, Dailide G, Norton JE, Kalia A, Richmond TA, et al. Mutation discovery in bacterial genomes: metronidazole resistance in *Helicobacter pylori*. Nat Methods 2005;2:951–3.
Alsford S, Eckert S, Baker N, Glover L, Sanchez-Flores A, Leung KF, et al. High-throughput decoding of antitrypanosomal drug efficacy and resistance. Nature 2013;482:232–6.
Arbo A, Pavía-Ruz N, Santos JI. Opsonic requirements for the respiratory burst of neutrophils against *Giardia lamblia* trophozoites. Arch Med Res 2006;37:465–73.
Argüello-García R, Cruz-Soto M, Romero-Montoya L, Ortega-Pierres G. In vitro resistance to 5-nitroimidazoles and benzimidazoles in *Giardia duodenalis*: variability and variation in gene expression. Infect Genet Evol 2009;9:1057–64.
Bachmann LH, Hobbs MM, Sena AC, Sobel JD, Schwebke JR, Krieger JN, et al. *Trichomonas vaginalis* genital infections: progress and challenges. Clin Infect Dis 2011;53:s160–72.
Bantscheff M, Lemeer S, Savitski MM, Kuster B. Quantitative mass spectrometry in proteomics: critical review update from 2007 to the present. Anal Bioanal Chem 2012;404:939–65.
Bartelt LA, Roche J, Kolling G, Bolick D, Noronha F, Naylor C, et al. Persistent *G. lamblia* impairs growth in a murine malnutrition model. J Clin Invest 2013;123:2672–84.
Biagini GA, Park JH, Lloyd D, Edwards MR. The antioxidant potential of pyruvate in the amitochondriate diplomonads *Giardia intestinalis* and *Hexamita inflata*. Microbiology 2001;147:3359–65.
Boreham PFL, Phillips RE, Shepherd RW. Altered uptake of metronidazole in vitro by stocks of *Giardia intestinalis* with different drug sensitivities. Trans R Soc Trop Med Hyg 1988;82:104–6.
Boreham P, Upcroft JA, Upcroft P. Biochemical and molecular mechanisms of resistance to nitroheterocyclic drugs in *Giardia intestinalis*. In: Coombs GH, editor. Biochemical Protozoology; 1991.
Brinkman AB, Gu H, Bartels SJJ, Zhang Y, Matarese F, Simmer F, et al. Sequential ChIP-bisulfite sequencing enables direct genome-scale investigation of chromatin and DNA methylation cross-talk. Genome Res 2012;22:1128–38.
Brown DM, Upcroft JA, Upcroft P. Cysteine is the major low-molecular weight thiol in *Giardia duodenalis*. Mol Biochem Parasitol Sep 1993;61(1):155–8.
Brown DM, Upcroft JA, Upcroft P. Free radical detoxification in *Giardia duodenalis*. Mol Biochem Parasitol 1995;72:47–56.
Brown DM, Upcroft JA, Upcroft P. A H_2O-producing NADH oxidase from the protozoan parasite *Giardia duodenalis*. Eur J Biochem 1996a;241:155–61.
Brown DM, Upcroft JA, Upcroft P. A thioredoxin reductase-class of disulphide reductase in the protozoan parasite *Giardia duodenalis*. Mol Biochem Parasitol 1996b;83:211–20.
Brown DM, Upcroft JA, Edwards MR, Upcroft P. Anaerobic bacterial metabolism in the ancient eukaryote *Giardia duodenalis*. Int J Parasitol Jan 1998;28(1):149–64.
Burroughs AM, Ando Y, Aravind L. New perspectives on the diversification of the RNA interference system: insights from comparative genomics and small RNA sequencing. WIREs RNA 2014;5. http://dx.doi.org/10.1002/wrna.1210.
Carpenter BM, Gilbreath JJ, Pich OQ, McKelvey AM, Maynard EL, Li ZZ, et al. Identification and characterization of novel *Helicobacter pylori* apo-fur-regulated target genes. J Bacteriol 2013;195:5526–39.
Chabriere E, Cavazza C, Contreras-Martel C, Fontecilla-Camps JC. Pyruvate-ferredoxin oxidoreductase. Chichester, UK: Encyclopedia of Inorganic and Bioinorganic Chemistry; 2011.
Chapman A, Linstead DJ, Lloyd D. Hydrogen peroxide is a product of oxygen consumption by *Trichomonas vaginalis*. J Biosci 1999;24:339–44.
Chen N, Upcroft JA, Upcroft P. Physical map of a 2 Mb chromosome of the intestinal protozoan parasite *Giardia duodenalis*. Chromosome Res 1994;2:307–13.
Chen XS, Penny D, Collins LJ. Characterization of RNase MRP RNA and novel snoRNAs from *Giardia intestinalis* and *Trichomonas vaginalis*. BMC Genomics 2011;12:550.
Clayton CE. Networks of gene expression regulation in *Trypanosoma brucei*. Mol Biochem Parasitol 2014;195:96–106.
Coombs GH, Westrop GD, Suchan P, Puzova G, Hirt RP, Embley TM, et al. The amitochondriate eukaryote *Trichomonas vaginalis* contains a divergent thioredoxin-linked peroxiredoxin antioxidant system. J Biol Chem 2004;279:5249–56.
Crozet MD, Botta C, Gasquet M, Curti C, REmusat V, Hutter S, et al. Lowering of 5-nitroimidazole's mutagenicity: towards optimal antiparasitic pharmacophore. Eur J Med Chem 2009;44:653–9.
Dan M, Wang AL, Wang CC. Inhibition of pyruvate-ferredoxin oxidoreductase gene expression in *Giardia lamblia* by a virus-mediated hammerhead ribozyme. Mol Microbiol 2000;36:447–56.
Davis-Hayman SR, Nash TE. Genetic manipulation of *Giardia lamblia*. Mol Biochem Parasitol 2002;122:1–7.
Denu JM. Linking chromatin function with metabolic networks: Sir2 family of NAD(+)-dependent deacetylases. Trends Biochem Sci 2003;28:41–8.
Di Matteo A, Scandurra FM, Testa F, Forte E, Sarti P, Brunori M, et al. The O2-scavenging flavodiiron protein in the human parasite *Giardia intestinalis*. J Biol Chem 2007;283:4061–8.
Duchêne M. Metronidazole and the redox biochemistry of *Entamoeba histolytica*. In: Nozaki T, Bhattacharya A, editors. Amebiasis: Springer; 2015.
Dunn LA, Burgess AG, Krauer KG, Eckmann L, Vanelle P, Crozet MD, et al. A new-generation 5-nitroimidazole can induce highly metronidazole-resistant *Giardia lamblia* in vitro. Int J Antimicrob Agents 2010;36:37–42.
Dunn WB, Erban A, Weber RJM, Creek DJ, Brown M, Breitling R, et al. Mass appeal: metabolite identification in mass spectrometry-focused untargeted metabolomics. Metabolomics 2012;9:44–66.

Eckmann L, Laurent F, Langford TD, Hetsko ML, Smith JR, Kagnoff MF, et al. Nitric oxide production by human intestinal epithelial cells and competition for arginine as potential determinants of host defense against the lumen-dwelling pathogen *Giardia lamblia*. J Immunol 2000;164:1478–87.
Edwards DI. Nitroimidazole drugs—action and resistance mechanisms. I. Mechanisms of action. J Antimicrob Chemother 1993a;31:9–20.
Edwards DI. Nitroimidazole drugs—action and resistance mechanisms. II. Mechanisms of resistance. J Antimicrob Chemother 1993b;31:201–10.
Ellis JE, Wingfield JM, Cole D, Boreham PF, Lloyd D. Oxygen affinities of metronidazole-resistant and-sensitive stocks of *Giardia intestinalis*. Int J Parasitol 1993;23:35–9.
Escobedo AA, Cimerman S. Giardiasis: a pharmacotherapy review. Expert Opin Pharmacother 2007;8:1885–902.
Espey MG. Role of oxygen gradients in shaping redox relationships between the human intestine and its microbiota. Free Radic Biol Med 2013;55:130–40.
Farthing MJ. Giardiasis. Gastroenterol Clin North Am 1996;25:493–515.
Farthing MJG. Treatment options for the eradication of intestinal protozoa Nat Clin Pract Gastroenterol Hepatol 2006;3:436–45.
Fraaije MW, Mattevi A. Flavoenzymes: diverse catalysts with recurrent features. Trends Biochem Sci 2000;25:126–32.
Franzén O, Jerlström-Hultqvist J, Castro E, Sherwood E, Ankarklev J, Reiner DS, et al. Draft genome sequencing of *Giardia intestinalis* assemblage B isolate GS: is human giardiasis caused by two different species? PLoS Pathog 2009;5:e1000560.
Franzén O, Jerlström-Hultqvist J, Einarsson E, Ankarklev J, Ferella M, Andersson B, et al. Transcriptome profiling of *Giardia intestinalis* using strand-specific RNA-Seq. PLoS Comput Biol 2013;28(9):e1003000.
Fulco M, Schiltz RL, Iezzi S, King MT, Zhao P, Kashiwaya Y, et al. Sir2 regulates skeletal muscle differentiation as a potential sensor of the redox state. Mol Cell Jul 2003;12:51–62.
Gardner TB, Hill DR. Treatment of giardiasis. Clin Microbiol Rev 2001;14:114–28.
Gillin FD, Diamond LS. *Entamoeba histolytica* and *Giardia lamblia*: effects of cysteine and oxygen tension on trophozoite attachment to glass and survival in culture media. Exp Parasitol Aug 1981;52(1):9–17.
Gillin FD, Reiner DS. Effects of oxygen tension and reducing agents on sensitivity of *Giardia lamblia* to metronidazole in vitro. Biochem Pharmacol 1982;31:3694–7.
Gillin FD, Hagblom P, Harwood J, Aley SB, Reiner DS, McCaffery M, et al. Isolation and expression of the gene for a major surface protein of *Giardia lamblia*. Proc Natl Acad Sci U S A 1990;87:4463–7.
Goncalves VL, Vicente JB, Pinto L, Romao CV, Frazão C, Sarti P, et al. Flavodiiron oxygen reductase from *Entamoeba histolytica*: modulation of substrate preference by tyrosine 271 and lysine 53. J Biol Chem 2014;289:28260–70.
Goodwin A, Kersulyte D, Sisson G, Veldhuyzen van Zanten SJO, Berg DE, Hoffman PS. Metronidazole resistance in *Helicobacter pylori* is due to null mutations in a gene (rdxA) that encodes an oxygen-insensitive NADPH nitroreductase. Mol Microbiol 1998;28:383–93.
Guarente L. Sir2 links chromatin silencing, metabolism, and aging. Genes Dev 2000;14:1021–6.
Guerrant RL, DeBoer MD, Moore SR, Scharf RJ, Lima AAM. The impoverished gut—a triple burden of diarrhoea, stunting and chronic disease. Nat Rev Gastroenterol 2013;10:220–9.
Halliez MC. Extra-intestinal and long term consequences of *Giardia duodenalis* infections. World J Gastroenterol 2013;19:8974.
Han J, Collins LJ. Reconstruction of sugar metabolic pathways of *Giardia lamblia*. Int J Proteomics 2012;2012:1–9.
Hausen MA, Freitas Jr JCM, Monteiro—Leal LH. The effects of metronidazole and furazolidone during *Giardia* differentiation into cysts. Exp Parasitol 2006;113:135–41.
Hoffman PS, Sisson G, Croxen MA, Welch K, Harman WD, Cremades N, et al. Antiparasitic drug nitazoxanide inhibits the pyruvate oxidoreductases of *Helicobacter pylori*, selected anaerobic bacteria and parasites, and *Campylobacter jejuni*. Antimicrob Agents Chemother 2007;51:868–76.
Horner DS, Hirt RP, Embley TM. A single eubacterial origin of eukaryotic pyruvate:ferredoxin oxidoreductase genes: implications for the evolution of anaerobic eukaryotes. Mol Biol Evol 1999;16:1280–91.
Husain A, Sato D, Jeelani G, Soga T, Nozaki T. Dramatic increase in glycerol biosynthesis upon oxidative stress in the anaerobic protozoan parasite *Entamoeba histolytica*. Kita K, editor. PLoS Negl Trop Dis 2012;6:e1831.
Jaenisch R, Bird A. Epigenetic regulation of gene expression: how the genome integrates intrinsic and environmental signals. Nat Genet 2003;33:245–54.
Jarroll EL, Paget TA. Carbohydrate and amino acid metabolism in *Giardia*: a review. Folia Parasitol 1995;42:81–9.
Jeelani G, Husain A, Sato D, Ali V, Suematsu M, Soga T, et al. Two atypical L-cysteine-regulated NADPH-dependent oxidoreductases involved in redox maintenance, L-cystine and iron reduction, and metronidazole activation in the enteric protozoan *Entamoeba histolytica*. J Biol Chem 2010;285:26889–99.
Jerlström-Hultqvist J, Franzén O, Ankarklev J, Xu F, Nohýnková E, Andersson JO, et al. Genome analysis and comparative genomics of a *Giardia intestinalis* assemblage E isolate. BMC Genomics 2010;11:543.
Jiménez-Cardoso E, Flores-Luna A, Pérez-Urizar J. In vitro activity of two phenylcarbamate derivatives, singly and in combination with albendazole against albendazole-resistant *Giardia intestinalis*. Acta Trop 2004;92:237–44.
Jiménez-Cardoso E, Eligio-García L, Cortés-Campos A, Flores-Luna A, Valencia-Mayoral P, Lozada-Chávez I. Changes in β-giardin sequence of *Giardia intestinalis* sensitive and resistant to albendazole strains. Parasitol Res 2009;105:25–33.
Khaled MA. Oxidative stress in childhood malnutrition and diarrhoeal diseases. J Diarrhoeal Dis Res 1994;12:165–72.
Kim H, Kim J-S. A guide to genome engineering with programmable nucleases. Nat Rev Genet 2014;15:321–34.
Knodler LA. Cloning and expression of a prokaryotic enzyme, arginine deiminase, from a primitive eukaryote *Giardia intestinalis*. J Biol Chem 1998;273:4470–7.
Kosek M, Bern C, Guerrant RL. The global burden of diarrhoeal disease, as estimated from studies published between 1992 and 2000. Bull World Health Organ 2003;81:197–204.
Krieg NR, Hoffman PS. Microaerophily and oxygen toxicity. Annu Rev Microbiol 1986;40:107–30.
Krupa A, Sandhya K, Srinivasan N, Jonnalagadda S. A conserved domain in prokaryotic bifunctional FAD synthetases can potentially catalyze nucleotide transfer. Trends Biochem Sci 2003;28:9–12.
Kulda J. Trichomonads, hydrogenosomes and drug resistance. Int J Parasitol 1999;29:199–212.
Kumar M, Adhikari S, Hurdle JG. Action of nitroheterocyclic drugs against *Clostridium difficile*. Int J Antimicrob Agents 2014;44:314–9.
Lane S, Lloyd D. Current trends in research into the waterborne parasite *Giardia*. Crit Rev Microbiol 2002;28:123–47.
Leitsch D, Kolarich D, Binder M, Stadlmann J, Altmann F, Duchêne M. *Trichomonas vaginalis*: metronidazole and other nitroimidazole drugs are reduced by the flavin enzyme thioredoxin reductase and disrupt the cellular redox system. Implications for nitroimidazole toxicity and resistance. Mol Microbiol 2009;72:518–36.
Leitsch D, Burgess AG, Dunn LA, Krauer KG, Tan K, Duchene M, et al. Pyruvate:ferredoxin oxidoreductase and thioredoxin reductase are involved in 5-nitroimidazole activation while flavin metabolism is linked to 5-nitroimidazole resistance in *Giardia lamblia*. J Antimicrob Chemother 2011;66:1756–65.
Leitsch D, Schlosser S, Burgess A, Duchêne M. Nitroimidazole drugs vary in their mode of action in the human parasite *Giardia lamblia*. Int J Parasitol Drugs Drug Resist 2012a;2:166–70.
Leitsch D, Drinić M, Kolarich D, Duchêne M. Down-regulation of flavin reductase and alcohol dehydrogenase-1 (ADH1) in metronidazole-resistant isolates of *Trichomonas vaginalis*. Mol Biochem Parasitol 2012b;183:177–83.
Lemée V, Zaharia I, Nevez G, Rabodonirina M, Brasseur P, Ballet JJ, et al. Metronidazole and albendazole susceptibility of 11 clinical isolates of *Giardia duodenalis* from France. J Antimicrob Chemother 2000;46:819–21.
Lewis IA, Wacker M, Olszewski KL, Cobbold SA, Baska KS, Tan A, et al. Metabolic QTL analysis links chloroquine resistance in *Plasmodium falciparum* to impaired hemoglobin catabolism. PLoS Genet 2014;10:e1004085.
Li L, Wang CC. A likely molecular basis of the susceptibility of *Giardia lamblia* towards oxygen. Mol Microbiol 2006;59:202–11.
Li Z, Kulakova L, Li L, Galkin A, Zhao Z, Nash TE, et al. Mechanisms of catalysis and inhibition operative in the arginine deiminase from the human pathogen *Giardia lamblia*. Bioorg Chem 2009;37:149–61.
Lindley TA, Chakraborty PR, Edlind TD. Heat shock and stress response in *Giardia lamblia*. Mol Biochem Parasitol 1988;28:135–43.
Lindmark DG. Energy metabolism of the anaerobic protozoon *Giardia lamblia*. Mol Biochem Parasitol 1980;1:1–12.
Linstead DJ, Bradley S. The purification and properties of two soluble reduced nicotinamide: acceptor oxidoreductases from *Trichomonas vaginalis*. Mol Biochem Parasitol 1988;27:125–34.
Liu SM, Brown DM, O'Donoghue P, Upcroft P, Upcroft JA. Ferredoxin involvement in metronidazole resistance of *Giardia duodenalis*. Mol Biochem Parasitol 2000;108:137–40.
Lloyd D. The plasma membrane of microaerophilic protists: oxidative and nitrosative stress. Microbiology 2004;150:1183–90.
Lloyd D, Coombs GH, Lloyd D, Coombs GH, Paget TAP. Aerotolerantly anaerobic protozoa: some unsolved problems. Biochemistry and molecular biology of 'anaerobic' protozoa. Harwood Academic Publishers; 1989. p. 267–86.
Lloyd D, Harris JC, Maroulis S, Biagini GA, Wadley RB, Turner MP, et al. The microaerophilic flagellate *Giardia intestinalis*: oxygen and its reaction products collapse membrane potential and cause cytotoxicity. Microbiology 2000;146:3109–18.
Lloyd D, Harris JC, Biagini GA, Maroulis S, Edwards MR, Turner MP, et al. Oxygen homeodynamics. In: Olson BE, Olson ME, Wallis P, editors. *Giardia*. CABI Publishing; 2002.
Lundström J, Holmgren A. Protein disulfide-isomerase is a substrate for thioredoxin reductase and has thioredoxin-like activity. J Biol Chem 1990;265:9114–20.
Ma'ayeh SY, Brook-Carter PT. Representational difference analysis identifies specific genes in the interaction of *Giardia duodenalis* with the murine intestinal epithelial cell line, IEC-6. Int J Parasitol 2012;42:501–9.
Maloney J, Keselman A, Li E, Singer SM. Macrophages expressing arginase 1 and nitric oxide synthase 2 accumulate in the small intestine during *Giardia lamblia* infection. Microbes Infect 2015. http://dx.doi.org/10.1016/j.micinf.2015.03.006. [in press].
Martínez-Júlvez M, Rojas AL, Olekhnovich I, Angarica VE, Hoffman PS, Sancho J. Structure of RdxA — an oxygen-insensitive nitroreductase essential for metronidazole activation in *Helicobacter pylori*. FEBS J 2012;279:4306–17.
Mastronicola D, Testa F, Forte E, Bordi E, Pucillo LP, Sarti P, et al. Flavohemoglobin and nitric oxide detoxification in the human protozoan parasite *Giardia intestinalis*. Biochem Biophys Res Commun Sep 3 2010;399(4):654–8.
Mastronicola D, Giuffrè A, Testa F, Mura A, Forte E, Bordi E, et al. *Giardia intestinalis* escapes oxidative stress by colonizing the small intestine: a molecular hypothesis. IUBMB Life 2011;63:21–5.
Mastronicola D, Falabella M, Testa F, Pucillo LP, Teixeira M, Sarti P, et al. Functional characterization of peroxiredoxins from the human protozoan parasite *Giardia intestinalis*. Dinglasan RR, editor. PLoS Negl Trop Dis 2014;8:e2631.
Mattevi A. A close look at NAD biosynthesis. Nat Struct Mol Biol 2006;13:563–4.
McArthur AG, Knodler LA, Silberman JD, Davids BJ, Gillin FD, Sogin ML. The evolutionary origins of eukaryotic protein disulfide isomerase domains: new evidence from the amitochondriate protist *Giardia lamblia*. Mol Biol Evol 2001;18:1455–63.

McCormick BJ. Frequent symptomatic or asymptomatic infections may have long-term consequences on growth and cognitive development. In: Heitdt PJ, Lang D, Riddle MS, Walker RI, Rusch V, editors. Old Herborn University Seminar Monographs. Herborn, Germany: Institute for Microbiology und Biochemistry; 2014.
McIntyre P, Boreham PF, Phillips RE, Shepherd RW. Chemotherapy in giardiasis: clinical responses and in vitro drug sensitivity of human isolates in axenic culture. J Pediatr 1986;108:1005–10.
Mendis AH, Thompson RC, Reynoldson JA, Armson A, Meloni BP, Gunsberg S. The uptake and conversion of L-[U^{14}C-] aspartate and L-[U^{14}C-] alanine to $^{14}CO_2$ by intact trophozoites of *Giardia duodenalis*. Comp Biochem Physiol B 1992; 102:235–9.
Monis PT, Caccio SM, Thompson RCA. Variation in *Giardia*: towards a taxonomic revision of the genus. Trends Parasitol Feb 2009;25(2):93–100.
Mørch K, Hanevik K, Rivenes AC, Bødtker JE, Næss HN, Stubhaug B, et al. Chronic fatigue syndrome 5 years after giardiasis: differential diagnoses, characteristics and natural course. BMC Gastroenterol 2013;13.
Morf L, Spycher C, Rehrauer H, Fournier CA, Morrison HG, Hehl AB. The transcriptional response to encystation stimuli in *Giardia lamblia* is restricted to a small set of genes. Eukaryot Cell 2010;9:1566–76.
Morrison HG, McArthur AG, Gillin FD, Aley SB, Adam RD, Olsen GJ, et al. Genomic minimalism in the early diverging intestinal parasite *Giardia lamblia*. Science 2007; 28(317):1921–6.
Müller M. Energy metabolism. Part I: anaerobic protozoa. In: Marr JJ, Nilsen TW, Komuniecki R, editors. Molecular medical parasitology. London: Academic Press; 2003. p. 125–39.
Müller J, Sterk M, Hemphill A, Müller N. Characterization of *Giardia lamblia* WB C6 clones resistant to nitazoxanide and to metronidazole. J Antimicrob Chemother 2007a;60: 280–7.
Müller J, Wastling J, Sanderson S, Müller N, Hemphill A. A novel *Giardia lamblia* nitroreductase, GlNR1, interacts with nitazoxanide and other thiazolides. Antimicrob Agents Chemother 2007b;51:1979–86.
Müller J, Ley S, Felger I, Hemphill A, Müller N. Identification of differentially expressed genes in a *Giardia lamblia* WB C6 clone resistant to nitazoxanide and metronidazole. J Antimicrob Chemother 2008;62:72–82.
Müller J, Schildknecht P, Müller N. Metabolism of nitro drugs metronidazole and nitazoxanide in *Giardia lamblia*: characterization of a novel nitroreductase (GlNR2). J Antimicrob Chemother 2013;68:1781–9.
Müller J, Rout S, Leitsch D, Vaithilingam J, Hehl A, Müller N. Comparative characterisation of two nitroreductases from *Giardia lamblia* as potential activators of nitro compounds. Int J Parasitol Drugs Drug Resist 2015;5:37–43.
Mustacich D, Powis G. Thioredoxin reductase. Biochem J 2000;346:1–8.
Nathan C, Shiloh MU. Reactive oxygen and nitrogen intermediates in the relationship between mammalian hosts and microbial pathogens. Proc Natl Acad Sci U S A 2000;97: 8841–8.
Nillius D, JJ M, Muller N. Nitroreductase (GlNR1) increases susceptibility of *Giardia lamblia* and *Escherichia coli* to nitro drugs. J Antimicrob Chemother 2011;66: 1029–35.
Nixon JEJ, Wang A, Field J, Morrison HG, McArthur AG, Sogin ML, et al. Evidence for lateral transfer of genes encoding ferredoxins, nitroreductases, NADH oxidase, and alcohol dehydrogenase 3 from anaerobic prokaryotes to *Giardia lamblia* and *Entamoeba histolytica*. Eukaryot Cell 2002;1:181–90.
Nolan MJ, Jex AR, Upcroft JA, Upcroft P, Gasser RB. Barcoding of *Giardia duodenalis* isolates and derived lines from an established cryobank by a mutation scanning-based approach. Electrophoresis 2011;32:2075–90.
Olekhnovich IN, Goodwin A, Hoffman PS. Characterization of the NAD(P)H oxidase and metronidazole reductase activities of the RdxA nitroreductase of *Helicobacter pylori*. FEBS J 2009;276:3354–64.
Orta-Zavalza E, Guerrero-Serrano G, Gutiérrez-Escobedo G, Cañas-Villamar I, Juárez-Cepeda J, Castaño I, et al. Local silencing controls the oxidative stress response and the multidrug resistance in *Candida glabrata*. Mol Microbiol 2013;88:1135–48.
Pacher P, Beckman JS, Liaudet L. Nitric oxide and peroxynitrite in health and disease. Physiol Rev 2007;87:315–424.
Paget TA, jarroll EL, Manning P, Lindmark DG, Lloyd D. Respiration in the cysts and trophozoites of *Giardia muris*. J Gen Microbiol 1989;135:145–54.
Paget TA, Kelly ML, jarroll EL, Lindmark DG, Lloyd D. The effects of oxygen on fermentation in *Giardia lamblia*. Mol Biochem Parasitol 1993;57:65–71.
Paget TA, Macechko PT, jarroll EL. Metabolic changes in *Giardia intestinalis* during differentiation. J Parasitol 1998;84:222–6.
Paget T, Maroulis S, Mitchell A, Edwards MR, Jarroll EL, Lloyd D. Menadione kills trophozoites and cysts of *Giardia intestinalis*. Microbiology 2004;150:1231–6.
Pal D, Banerjee S, Cui J, Schwartz A, Ghosh SK, Samuelson J. *Giardia*, *Entamoeba*, and *Trichomonas* enzymes activate metronidazole (nitroreductases) and inactivate metronidazole (nitroimidazole reductases). Antimicrob Agents Chemother 2009;53:458–64.
Park J-H, Schofield PJ, Edwards MR. *Giardia intestinalis*: characterization of a NADP-dependent glutamate dehydrogenase. Exp Parasitol 1998;88:131–8.
Paz-Maldonado MT, Argüello-García R, Cruz-Soto M, Mendoza-Hernández G, Ortega-Pierres G. Proteomic and transcriptional analyses of genes differentially expressed in *Giardia duodenalis* clones resistant to albendazole. Infect Genet Evol 2012;15:10–7.
Pineda E, Encalada R, Rodríguez-Zavala JS, Olivos-García A, Moreno-Sánchez R, Saavedra E. Pyruvate:ferredoxin oxidoreductase and bifunctional aldehyde-alcohol dehydrogenase are essential for energy metabolism under oxidative stress in *Entamoeba histolytica*. FEBS J 2010;277:3382–95.
Poxleitner MK, Carpenter ML, Mancuso JJ, Wang CJR, Dawson SC, Cande WZ. Evidence for karyogamy and exchange of genetic material in the binucleate intestinal parasite *Giardia intestinalis*. Science 2008;319:1530–3.
Prucca CG, Slavin I, Quiroga R, Elías EV, Rivero FD, Saura A, et al. Antigenic variation in *Giardia lamblia* is regulated by RNA interference. Nature 2008;456:750–4.
Rafferty S, Luu B, March RE, Yee J. *Giardia lamblia* encodes a functional flavohemoglobin. Biochem Biophys Res Commun 2010;399:347–51.
Richards EJ. Inherited epigenetic variation—revisiting soft inheritance. Nat Rev Genet 2006;7:395–401.
Ringqvist E, Palm JED, Skarin H, Hehl AB, Weiland M, Davids BJ, et al. Release of metabolic enzymes by *Giardia* in response to interaction with intestinal epithelial cells. Mol Biochem Parasitol 2008;159:85–91.
Ringqvist E, Avesson L, Söderbom F, Svärd SG. Transcriptional changes in *Giardia* during host–parasite interactions. Int J Parasitol 2011;41:277–85.
Robertson LJ, Hanevik K, Escobedo AA, Mørch K, Langeland N. Giardiasis—why do the symptoms sometimes never stop? Trends Parasitol 2010;26:75–82.
Roy A, Kucukural A, Zhang Y. I-TASSER: a unified platform for automated protein structure and function prediction. Nat Protoc 2010;25(5):725–38.
Sánchez LB. Aldehyde dehydrogenase (CoA-Acetylating) and the mechanism of ethanol formation in the amitochondriate protist, *Giardia lamblia*. Arch Biochem Biophys 1998;354:57–64.
Sánchez LB, Morrison HG, Sogin ML, Müller M. Cloning and sequencing of an acetyl-CoA synthetase (ADP-forming) gene from the amitochondriate protist, *Giardia lamblia*. Gene 1999;233:225–31.
Sánchez LB, Elmendorf H, Nash TE, Müller M. NAD(P)H:menadione oxidoreductase of the amitochondriate eukaryote *Giardia lamblia*: a simpler homologue of the vertebrate enzyme. Microbiology 2001;147:561–70.
Sanchez CP, Liu C-H, Mayer S, Nurhasanah A, Cyrklaff M, Mu J, et al. A HECT ubiquitin-protein ligase as a novel candidate gene for altered quinine and quinidine responses in *Plasmodium falciparum*. PLoS Genet 2014;10:e1004382.
Savioli L, Smith H, Thompson A. *Giardia* and *Cryptosporidium* join the 'Neglected Diseases Initiative'. Trends Parasitol 2006;22:203–8.
Schofield PJ, Costello M, Edwards MR, O'Sullivan WJ. The arginine dihydrolase pathway is present in *Giardia intestinalis*. Int J Parasitol 1990;20:697–9.
Schofield PJ, Edwards MR, Matthews J, Wilson JR. The pathway of arginine catabolism in *Giardia intestinalis*. Mol Biochem Parasitol 1992;51:29–36.
Sisson G, Jeong JY, Goodwin A, Bryden L, Rossler N, Lim-Morrison S, et al. Metronidazole activation is mutagenic and causes DNA fragmentation in *Helicobacter pylori* and in *Escherichia coli* containing a cloned *H. pylori* rdxA^{+} (nitroreductase) gene. J Bacteriol 2000;182:5091–6.
Sisson G, Goodwin A, Raudonikiene A, Hughes NJ, Mukhopadhyay AK, Berg DE, et al. Enzymes associated with reductive activation and action of nitazoxanide, nitrofurans, and metronidazole in *Helicobacter pylori*. Antimicrob Agents Chemother 2002;46: 2116–23.
Smith NC, Bryant C, Boreham PF. Possible roles for pyruvate:ferredoxin oxidoreductase and thiol-dependent peroxidase and reductase activities in resistance to nitroheterocyclic drugs in *Giardia intestinalis*. Int J Parasitol 1988;18:991–7.
Smith JS, Brachmann CB, Celic I, Kenna MA, Muhammad S, Starai VJ, et al. A phylogenetically conserved NAD^{+}-dependent protein deacetylase activity in the Sir2 protein family. Proc Natl Acad Sci U S A 2000;97:6658–63.
Solaymani-Mohammadi S, Genkinger JM, Loffredo CA, Singer SM. A meta-analysis of the effectiveness of albendazole compared with metronidazole as treatments for infections with *Giardia duodenalis*. PLoS Negl Trop Dis 2010;4:e682.
Sonda S, Morf L, Bottova I, Baetschmann H, Rehrauer H, Caflisch A, et al. Epigenetic mechanisms regulate stage differentiation in the minimized protozoan *Giardia lamblia*. Mol Microbiol 2010;76:48–67.
Soto-Méndez M, Aguilera C, Mesa M, Campaa-Martn L, Martn-Laguna V, Solomons N, et al. Relationship between oxidative stress biomarkers in urine and erythrocytes, and to estimates of fecal *Giardia intestinalis* intensity in Guatemalan preschool children with a common menu offering (639.3). FASEB J 2014;28.
Spycher C, Herman EK, Morf L, Qi W, Rehrauer H, Aquino Fournier C, et al. An ER-directed transcriptional response to unfolded protein stress in the absence of conserved sensor-transducer proteins in *Giardia lamblia*. Mol Microbiol 2013; 88:754–71.
Tako EA, Hassimi MF, Li E, Singer SM. Transcriptomic analysis of the host response to *Giardia duodenalis* infection reveals redundant mechanisms for parasite control. 2013;4: e00660-13.
Tejman-Yarden N, Millman M, Lauwaet T, Davids BJ, Gillin FD, Dunn L, et al. Impaired parasite attachment as fitness cost of metronidazole resistance in *Giardia lamblia*. Antimicrob Agents Chemother 2011;55:4643–51.
Tekwani BL, Mehlotra RK. Molecular basis of defence against oxidative stress in *Entamoeba histolytica* and *Giardia lamblia*. Microbes Infect 1999;1:385–94.
Testa F, Mastronicola D, Cabelli DE, Bordi E, Pucillo LP, Sarti P, et al. The superoxide reductase from the early diverging eukaryote *Giardia intestinalis*. Free Radic Biol Med 2011; 51:1567–74.
Thompson PR, Fast W. Histone citrullination by protein arginine deiminase: is arginine methylation a green light or a roadblock? ACS Chem Biol 2006;1:433–41.
Tolba MEM, Kobayashi S, Imada M, Suzuki Y, Sugano S. *Giardia lamblia* transcriptome analysis using TSS-Seq and RNA-Seq. PLoS One 2013;8:e76184.
Touz MC, Rópolo AS, Rivero MR, Vranych CV, Conrad JT, Svard SG, et al. Arginine deiminase has multiple regulatory roles in the biology of *Giardia lamblia*. J Cell Sci 2008;121:2930–8.
Townson SM, Laqua H, Upcroft P, Boreham PF, Upcroft JA. Induction of metronidazole and furazolidone resistance in *Giardia*. Trans R Soc Trop Med Hyg 1992; 86:521–2.
Townson SM, Boreham PF, Upcroft P, Upcroft JA. Resistance to the nitroheterocyclic drugs. Acta Trop 1994a;56:173–94.
Townson SM, Hanson GR, Upcroft JA, Upcroft P. A purified ferredoxin from *Giardia duodenalis*. Eur J Biochem 1994b;220:439–46.

Townson SM, Upcroft JA, Upcroft P. Characterisation and purification of pyruvate:ferredoxin oxidoreductase from *Giardia duodenalis*. Mol Biochem Parasitol 1996;79:183–93.
Trammell SA, Brenner CM. Targeted, LCMS-based metabolomics for quantitative measurement of NAD^+ metabolites. Comp Struct Biotechnol J 2013;4. http://dx.doi.org/10.5936/csbj.201301012.
Tsugawa H, Suzuki H, Satoh K, Hirata K, Matsuzaki J, Saito Y, et al. Two amino acids mutation of ferric uptake regulator determines *Helicobacter pylori* resistance to metronidazole. Antioxid Redox Signal 2011;14:15–23.
Upcroft P, Upcroft JA. Drug targets and mechanisms of resistance in the anaerobic protozoa. Clin Microbiol Rev 2001;14:150–64.
Upcroft JA, Upcroft P, Boreham PFL. Drug resistance in *Giardia intestinalis*. Int J Parasitol 1990;20:489–96.
Upcroft JA, Healey A, Murray DG, Boreham PF, Upcroft P. A gene associated with cell division and drug resistance in *Giardia duodenalis*. Parasitology 1992;104:397–405.
Upcroft JA, Mitchel R, Chen N, Upcroft P. Albendazole resistance in *Giardia* is correlated with cytoskeletal changes but not with a mutation at amino acid 200 in beta-tubulin. Microb Drug Resist 1996;2:303–8.
Urgesi R, Cianci R, Riccioni ME. Update on triple therapy for eradication of *Helicobacter pylori*: current status of the art. Clin Exp Gastroenterol 2012;5:151–7.
Uzlikova M, Nohýnková E. The effect of metronidazole on the cell cycle and DNA in metronidazole-susceptible and -resistant *Giardia* cell lines. Mol Biochem Parasitol 2015. http://dx.doi.org/10.1016/j.molbiopara.2015.01.005. [in press].
Verdu EF, Riddle MS. Chronic gastrointestinal consequences of acute infectious diarrhea: evolving concepts in epidemiology and pathogenesis. Am J Gastroenterol 2012;107:981–9.
Vicente JB, Testa F, Mastronicola D, Forte E, Sarti P, Teixeira M, et al. Archives of biochemistry and biophysics. Arch Biochem Biophys 2009;488:9–13.
Wagner G, Levin R. Oxygen tension of the vaginal surface during sexual stimulation in the human. Fertil Steril 1978;30:50–3.
Wampfler PB, Faso C, Hehl AB. The Cre/loxP system in *Giardia lamblia*: genetic manipulations in a binucleate tetraploid protozoan. Int J Parasitol 2014;44:497–506.
Wright JM, Dunn LA, Upcroft P. Efficacy of antigiardial drugs. Expert Opin Drug Saf 2003;2:529–41.